CONTENTS:

Survey of some Danish hpc containing microsilica and flyash.

Dirch H. Bager
Ph.D., Chief Concrete Technologist
Research and Development Centre, Aalborg Portland A/S
Rørdalsvej 44, P.O. Box 165, DK-9100 Aalborg
E-mail: db@aalborg-portland.dk

ABSTRACT
This paper presents information on some of the concrete constructions made in Denmark during the last 20 years. Focus has been put on the influence of secondary cementitious materials as fly ash and microsilica on the durability properties.

The survey concludes that use of such secondary cementitious materials is beneficial for durability of concrete in aggressive environments.

Key words: Durability, fly ash, microsilica, aggressive environment.

INTRODUCTION

In Denmark, the use of microsilica and flyash started in the mid 1970'ies. The ready mix concrete producer Færdigbeton (Since 1988 a part of Unicon) in North Jutland were the prime actor regarding microsilica, whereas the use of flyash mainly was introduced by the Copenhagen based ready mix company 4K.

After a few years, the two ideas for mix design merged, and since then high performance concrete in Denmark nearly always are three powder mixtures with cement, flyash and microsilica. The Danish Engineering Society produced an Advice for the use of MS & FA in concrete in 1987. /1987-1/

A lot of well-documented tests and full-scale constructions have been carried out since then. The paper presents a brief summary of the experience from some of these. The information collected in this paper also serves as part of the Danish input to the CONLIFE project /2001-3/ regarding experience of utilisation of flyash and microsilica for durable concrete in aggressive environments.

1 STRUCTURES

The structures dealt with are given in table 1. Most of the constructions are bridges and roads. The Danish Road Directorate has been very active and interested in the use of secondary cementitious materials, and therefore through the years offered full-scale test possibilities on some of their constructions.

Table 1: Tests and constructions

Year	Construction	Cement type	Mineral additives	28 days strength levels, MPa {Cylinders}	28 days strength levels, MPa {Cubes¤}
1979	Fishladder in Klokkerholm	CEM I 42.5 SR CEM I 42.5 CEM II 42.5/BV	MS FA	40 - 115	*48 – 133*
1980 *	Fiskebæk bridge – Edge Beams	CEM I 42.5 SR	MS	39 - 130	*45 – 150*
1981	Ryå bridge	CEM I 42.5 SR	MS	60	*70*
1984	Madum Å bridge	CEM I 42.5 SR	FA	33	*40*
1981-'84	Farø Bridges	CEM I 42.5 SR	FA	45	*54*
1983	Groyines, Thyborøn	CEM I 42.5	FA	38	*44*
1983 *	Test elements, Aalborg Portland	CEM I 42.5 SR CEM I 42.5 CEM II 42.5/BV	MS FA	25 - 62	*29 - 72*
1984	Bredal bridge, Vejle	CEM I 42.5 SR	MS		
1984	Road pavement, M30, Falster	CEM I 42.5 SR	MS		
1990	Road pavement, Slagslunde	CEM I 42.5 SR	MS	60	*70*
1992	Road pavement, Aalborg Portland	CEM I 42.5 SR	MS FA	100	*116*
1995	Road pavement, Hjørring	CEM I 42.5 SR	MS FA	95	*110*
1995	Gadholtroad bridge	CEM I 42.5 SR	MS	93	*108*

*: These constructions are dealt with in more details in other papers in the proceeding.
¤: Cube strengths calculated in accordance with the introductory remarks

2 MATERIALS

The constructions dealt with in this paper are all situated in outdoor aggressive environments. Therefore all aggregates fulfil requirements for such environments. For what concerns the cement, the Danish low alkali, sulphate resistant cement CEM I 42.5 – SR is the one mostly used since the Danish Road Directorate prefer this cement. Typical compositions of the different types of cement are given in table 2.

Table 2: Typical compositions of the Danish cement types used.

	CEM I 42.5 SR	CEM I 42.5	CEM II 42.5/BV
C_3S, %	65	55	55
C_{2S}, %	22	20	20
C_3A, %	1 – 2	9	10
C_4AF, %	5	8	9
$CaSO_4$, %	2.5 – 3.0	2.5 – 5.0	3.0 – 5.0
Eqv. Na_2O, %	0.3	0.7	0.6
Blaine, m/kg	300	420	440
Fly-ash content, %	-	< 5	20 – 25

The flyash and microsilica used normally have fulfilled the requirements set up in the Advice on use of flyash and microsilica from the Danish Engineering Society /1987-1/, see table 3

Table 3: Chemical compositions of flyash and microsilica according to /1987-1/

	Fly ash	Micro Silica
SiO_2, %	48 – 56	85 – 99.8
Al_2O_3, %	14 – 34	0.02 – 3.5
Fe_2O_3, %	4 – 10	0.1 – 3.0
CaO, %	4 – 8	0.08 – 0.7
MgO, %	1 – 4	0.3 – 3.0
SO_3, %	0.4 – 2	0.1 – 1.0
Total $K_2O + Na_2O$ %	1 - 3	0.3 – 3.5
Soluble Eqv. Na_2O, %	0.2 - 1	-
Cl^-, %	< 0.1	-
LOI, %	-	0.8 - 3
Density, kg/m_3	2100 - 2300	2200

3 FISHLADDER IN KLOKKERHOLM

In 1979 Aalborg Portland initiated a project in order to document the durability of concrete containing secondary cementitious materials as fly ash and microsilica. /1994-1/

The project was primarily focused on the use of microsilica. 9 different concrete mixes are included in the project. The test site is a fish ladder connecting a small stream and a lake in the northern part of Jutland at the city of Klokkerholm. The fish ladder has been exposed to ground water since 1979.

The project has been carried out in close co-operation with companies from the Danish concrete industry, including producers of precast-elements, contractors, consultants as well as additive producers or agents.

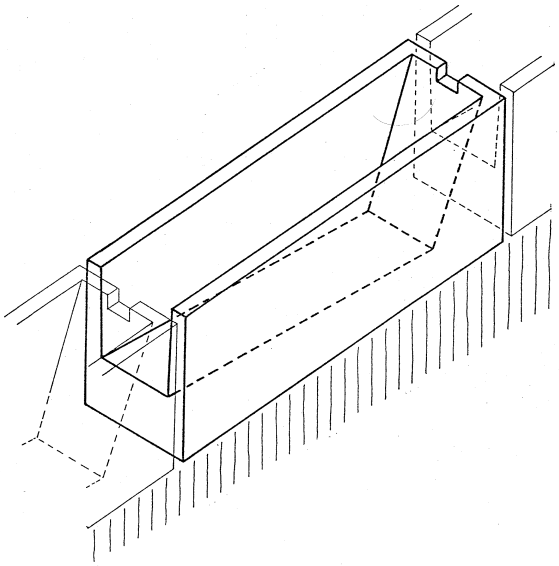

Figure 1: Isometric drawing of the individual precast steps in the fish ladder.

Figure 2: Photo of the fishladder (July 2001)

3.1 Materials

Table 4: Concrete mix-design

Concrete type		F2	F3	F4	F5	F6	F7	F8	F9	F10
Cement type ¤		RP	SR	BC	RP	RP	RP	RP	RP	RP
Cement	kg/m^3	330	330	310	290	400	330	530	415	294
Flyash	kg/m^3	-	-	-	125	-	-	-	-	-
	%/cement	-	-	-	43	-	-	-	-	-
	%/binder	-	-	-	30	-	-	-	-	-
Micro silica	kg/m^3	-	-	-	-	-	-	42	125	209
	%/cement	-	-	-	-	-	-	8,0	30	71
	%/binder	-	-	-	-	-	-	7,3	23	42
Water	kg/m^3	160	160	150	160	115	102	120	113	105
Sand	kg/m^3	710	800	722	664	772	772	698	705	714
Gravel, 8 /12 mm	kg/m^3	535	533	541	498	579	579	524	530	536
Gravel 12 / 16 mm	kg/m^3	535	445	541	498	579	579	523	530	536
Air entraining		+	+	+	+	-	+	-	-	-
Plastizising		-	-	-	+	+	+	+	+	+
w/c –ratio [#)]	-	0.48	0.48	0,48	0.47	0.29	0.31	0.20	0.17	0.15
Slump	mm	25	0	20	15	25	0	145	70	115
Vebe	sec	2.2	4.7	3.3	3.2	5.2	8-10	1	3.5	4.9
Density	kg/m^3	2280	2330	2300	2280	2450	2420	2470	2420	2440
Air content	%	4.9	3.8	3.8	4.0	2.0	3.6	1.5	2.2	1.9

¤: RP: CEM I 42.5. SR: CEM I 42.5 – SR. BC: CEM II 42.5 BV
[#)]: w/(c+2MS+0.4FA)

Table 5: Strength development – laboratory water cured specimens

Concrete type		F2	F3	F4	F5	F6	F7	F8	F9	F10
1 day		12	14	10	11	30	31	51	50	36
7 days		30	35	30	28	58	55	75	85	82
28 days		38	44	40	45	72	66	95	115	114
28 days ¤		*44*	*51*	*46*	*52*	*84*	*77*	*110*	*133*	*132*
90 days	MPa	42	50	52	56	82	78	115	135	133
1000 days		48	60	59	65	94	83	116	137	147
2280 days		52	65	60	71	102	94	125	143	158
5000 days A)		46	62	52	51	76	80	100	118	117
5000 days B)		58	78	65	64	99	100	125	148	146

¤: Cube strengths calculated in accordance with the introductory remarks
A): 100 mm drilled cores from the fish ladder
B): Recalculated from A) by multiplying with the conservative cast cylinder/drilled core correction factor of 1.25

3.2 Durability judgement in 2001

The construction has been exposed to inland condition and ground water since erection. No de-icing agents have been applied. No visual signs of deterioration are seen. A comprehensive study is undertaken by I. A. Juel /2002-1/

4 FISKEBÆK BRIDGE – EDGE BEAMS

These elements were produced in 1980 – 1981. Nine different types of concrete were used. /1981-1/

The aim of the project was to investigate the influence of microsilica on the durability of concrete. Edge beams are located in very severe environment.

4.1 Materials

Ordinary Danish sulphate resistant, low alkali cement CEM I 42.5 was used for all the concrete elements. No special analysis was performed.

Table 6: Concrete mix-design

		1	4	5	A	B	C	D	E	F
Cement	kg/m^3	331	505	222	300	345	296	295	241	347
	kg/m^3	0	102	11	30	70	49	30	48	0
Micro silica	%/cement	0	20	5	10	20	17	10	20	0
	%/binder	0	17	5	9	17	14	9	17	0
0/4 mm	kg/m^3	760	670	745	615	660	600	695	625	680
4/8 mm	kg/m^3	1135	1100	1335	1210	1205	1200	1250	1245	1140
8/16 mm	kg/m^3									
Water	kg/m^3	125	112	99	125	120	129	128	115	145
Air		+	-	+	+	-	+	-	+	+
Plast		+	-	-	+	-	+	-	-	+
SPT		-	+	+	-	+	-	+	+	-
w/c–ratio #)	-	0.38	0.16	0.22	0.35	0.25	0.33	0.36	0.34	0.42
Slump	Mm	40	>220	200	60	80	80	80	70	80
Air content	%	6.9	1.9	1.2	6.3	1.7	5.7	1.7	4.8	6.6

#): w/(c+2MS+0.4FA)

Table 7: Compressive strength. 20 °C watercured specimens

Concrete type		1	4	5	A	B	C	D	E	F
28 days	MPa	67	132	104	55	74	55	59	54	39
28 days ¤	*MPa*	*78*	*153*	*121*	*64*	*86*	*64*	*68*	*63*	*45*

¤: Cube strengths calculated in accordance with the introductory remarks

Performance of the elements has been studied in 1986 and 1994. /1995-1/

4.2 Durability judgement in 2001

The elements have been removed in 2000 and a detailed inspection has been carried out. See /2001-1/

5 RYÅ BRIDGE

Ryå Bridge is a small 14 m wide bridge crossing the 7.5 m wide Ryå rivulet in the northern part of Jutland, situated at the main road No. 447 from Aalborg to Hjørring. The bridge is made with dense microsilica containing concrete. No membranes have been used hence the traffic is driving directly on the structural concrete. /1982-1/

Since construction in 1981, the annual daily traffic load has increased from 9000 vehicles to 15000 vehicles in year 2000. Today a new highway has been opened (October 2001), and the traffic load has decreased.

Figure 3: Photo of the Ryå bridge (July 2001)

Figure 4: Sideview of the bridge

5.1 Materials

For this construction, chemical composition of the cement and the microsilica have been measured, see table 7

Table 7: Cement and mineral additives

	CEM I 42.5 SR	Micro Silica
SiO_2, %	24	89
Al_2O_3, %	2	0.4
Fe_2O_3, %	2	0.6
CaO, %	66	-
MgO, %	0.7	2.5
SO_3, %	2	-
LOI, %	1.2	3
Eqv. Na_2O, %	0.3	3.8
Blaine, m/kg	280	2000
Density, kg/m^3	3150	2200

Table 8: Concrete mix-design

		Bridge deck
Cement	kg/m^3	301
	kg/m^3	46
Micro silica	%/cement	15
	%/binder	13
0/4 mm	kg/m^3	674
4/8 mm	kg/m^3	1175
8/16 mm	kg/m^3	
Water	kg/m^3	120
w/c–ratio #)	-	0.30
Slump	mm	65
Air content	%	5,6

#): w/(c+2MS+0.4FA)

Table 9: Development of compressive strength, MPa. {Cylinders}

Age	Comp. strength
7 days	37.4
28 days	57.8
28 days ¤	*67*
56 days	62.5
12 years, drilled cores A)	49.9
12 years, drilled cores B)	62.4

¤: Cube strengths calculated in accordance with the introductory remarks
B): Recalculated from A) by multiplying with the conservative cast cylinder/drilled core correction factor of 1.25

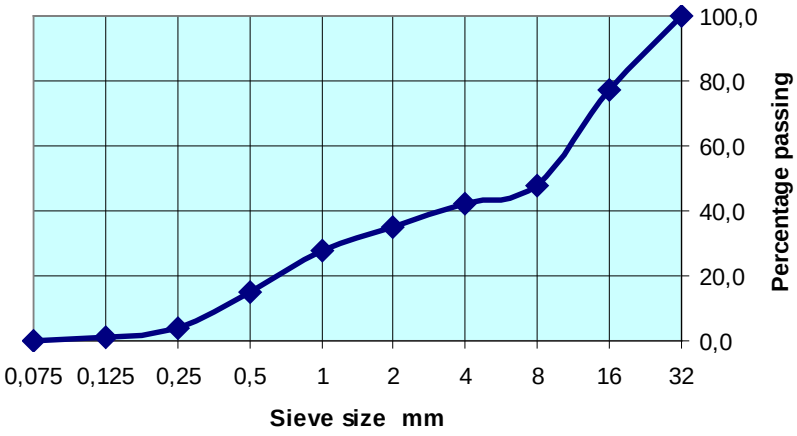

Figure 5: Aggregate grading for the concrete in the Ryå Bridge

5.2 Description of the construction

The bridge deck was cast November 27'th, 1981 between 7 am. and 2 pm.. A tent covering the whole construction secured good working conditions. Air temperature: 6 deg. C. Concrete temperature: 11 deg. C. Relative humidity in the tent close to 100%. The concrete was mixed at a 2 m^3 free fall mixer and transported 20 km to the site. A pump was used for delivering the concrete. Compaction was carried out with 3 56 mm poker vibrators. The surface was levelled with a vibrator beam and brushed perpendicular to the direction of the road. 4 hours after brushing, the surface was covered with plastic for the following 19 days.

Before the bridge was opened for traffic a silicone solution was applied to the surface in order to reduce the possibility for water and chlorides to penetrate the concrete.

5.2.1 Exposure conditions during the first 10 years

During the first 10 years of exposure, the bridge has been exposed to climatic conditions as shown in table 10.

Table10: Climatic conditions during the first 10 years exposure

	1982	1983	1984	1985	1986	1987	1988	1989	1990	1991	1992
Days with precipitation	170	188	157	181	166	143	164	155	182	137	157
Days with frost	86	92	83	136	113	100	99	50	60	84	71
Lowest temperature	-25	-12	-12	-24	-19	-26	-9	-11	-6	-13	-10
No. of deicings	70	68	85	81	98	81	63	52	66	114	67

5.3 Chloride penetration

In 1991 measurement of the chloride profile was measured on cores drilled from the surface on the bridge deck. /1993-1/

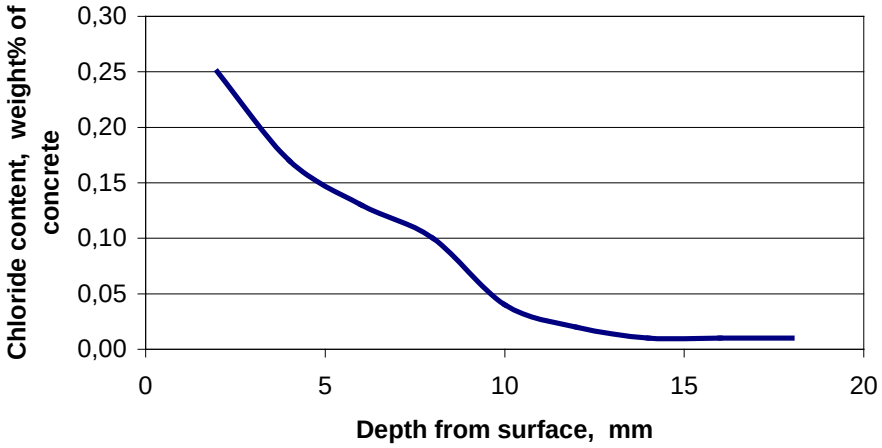

Figure 6: Chloride profile in bridge deck after 10 years exposure /1993-1/

5.4 Durability judgement in 2001

In 2001 only a visual inspection has taken place. No indication of damage was observed. The photo in figure 7 shows the surface.

Figure 7: Exposed aggregate in the wheel path on the Ryå Bridge after 20 years exposure. In the bottom of the picture, the original brushed surface texture can be seen

6 MADUM Å BRIDGE

As the Ryå Bridge was used for testing the influence of microsilica, then the Madum Å Bridge was used for testing the influence of flyash. Traffic is driving directly on the concrete. /1985-1/

Figure 8 : Madum Å Bridge (Photo: November 2001)

6.1 Materials

Table 11: Concrete mix-design of the bridge deck

CEM I 42.5 SR	kg/m^3	320
	kg/m^3	80
Flyash	%/cement	25
	%/binder	20
0/4 mm	kg/m^3	490
4/8 mm	kg/m^3	354
8/16 mm	kg/m^3	402
16/32 mm	kg/m^3	501
Water	kg/m^3	138
Air		+
Plast		+
SPT		-
w/c–ratio [#)]	-	0.39
Slump	mm	< 80
Air content	%	5.6

[#)]: w/(c+2MS+0.4FA)

Table 12: Development of compressive strength, MPa. {Cylinders}

Age	Comp. strength
1 day	7.5
7 days	23.1
28 days	33.1
28 days ¤	*38*
56 days	41.9
112 days	44.4
3 years	50.0

¤: Cube strengths calculated in accordance with the introductory remarks

The concrete was mixed in a 1½ m^3 free fall mixer, and transported 85 km to the site in truck mixers. The concrete was pumped in the forms.

In November 2001, the pavement still functioned without problems. The surface can be seen in figure 9

Figure 9: Surface of Madum Å bridge deck, November 2001

7 THE FARØ BRIDGES

The Farø bridges are two bridges connecting the Danish islands of Zealand and Falster, crossing the small island of Farø. The bridges carry the motorway, connecting Copenhagen with Germany and the rest of Europe. The bridges have a total length of 3.3 km supported on 33 columns directly exposed to seawater. /1985-2/

The bridges were constructed in the period from 1980 to 1985. The substructure is a reinforced concrete structure; the superstructure is a steel structure. Different types of concrete have been used for underwater concrete, concrete for the foundation, for the columns and for the pylons. With respect to durability, the columns are the most interesting parts of the structure.

Table 13: Concrete mix-design for the columns

CEM I 42.5 SR	kg/m^3	330
	kg/m^3	40
Flyash	%/cement	12
	%/binder	11
0/2 mm	kg/m^3	622
2/8 mm	kg/m^3	285
8/25 mm	kg/m^3	920
Water	kg/m^3	140
Air		+
Plast		+
SPT		-
w/c–ratio #)	-	0.40
Slump	mm	70
Air content	%	6.6

#): w/(c+2MS+0.4FA)

The average 28 days compressive strength (150/300mm cylinders) measured on 1200 tests was: 45.2 MPa, corresponding to a 150 mm cube strength of 54 MPa, according to the introduction.

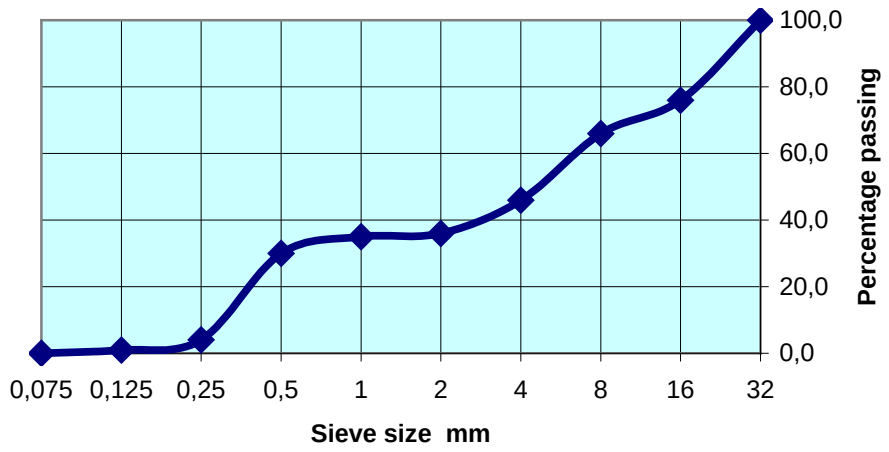

Figure 10: Aggregate grading for the Farø Bridges

Chloride penetration rate has been estimated on basis of measurements from 1988 to 1997 /1997-1/. In 50 mm depth, the specified thickness of the cover layer, the chloride content was zero in 1997. The chloride diffusion coefficient is between 5 and 10 m^2/sec * 10^{-13}.
Assuming a critical chloride content of 0.05 to 0.10 % Cl^- by mass of concrete, corrosion of reinforcement is expected to initiate after 15 – 40 years in the tidal zone. This assumption is verified over time allowing different repair strategies to be considered.

At present, no corrosion is considered ongoing.

8 GROYINES AT THYBORØN

In 1983 the Danish Coast Inspection Authorities initiated a project concerning improvement of the durability of the concrete dolos blocks in the groyines at the West Coast of Jutland. Aalborg Portland and Danaske participated in this project concerning the concrete mix design and the use of flyash. /1988-1/

Table 14: Concrete mix-design

CEM I 42.5	kg/m^3	280
	kg/m^3	80
Flyash	%/cement	29
	%/binder	22
0/4 mm	kg/m^3	640
4/8 mm	kg/m^3	
8/16 mm	kg/m^3	1165
16/32 mm	kg/m^3	
Water	kg/m^3	148
Air		+
Plast		-
SPT		-
w/c–ratio #)	-	0.47

#): w/(c+2MS+0.4FA)

Table 15: Air pore characteristics in hardened concrete

Total air	%	4.7
Spec. surface	mm^{-1}	42
Spacing factor	mm	0.12

28 days strength: 38 MPa. The corresponding cube strength calculated according to the introductory remarks is 44 MPa.

The concrete tend to be so durable, that fly ash has been used in production of these Dolos blocks since**.**

Figure 11: Dolos blocks at Thyborøn. Photographed in November 2001

9 TEST ELEMENTS AT AALBORG PORTLAND

In 1983 Aalborg Portland initiated a project in order to document the durability of concrete containing secondary cementitious materials as fly ash and microsilica. /1994-1/

Three different qualities of concrete are included in the project. The quality is characterised by the cement content, which is 260, 340 and 390 kg/m^3 respectively. With an approximately constant water demand of 140 l/m^3 for the various concrete mixes, this corresponds to w/c-ratios in the range of 0.35 to 0.55. The concrete types with 390 kg/m3 are generally judged as high performance types of concrete.

The project focused on different mix designs exposed to seawater and natural weather as well as exposure to de-icing chemicals in the same amount as is used on the main roads in North Jutland. The test was initiated in 1983, and comprises both exposure sites in the harbour of Hirtshals and on Aalborg Portland's area. In this test series, 16 different concrete mixes are included. Three types of cement have been used: CEM I 42.5 SR, CEM I 42.5 and CEM II 42.5 B/V

The project is further described in /2001-2/

10 BREDAL BRIDGE

In 1984 a bridge crossing the Highway near Vejle was constructed.

For this construction, the experience from the Ryå bridge was adopted. Thus approximately the same concrete mix design and design of the bridge was used. This includes that traffic is driving directly on the concrete.

The traffic load on this bridge is far much lower than on Ryå, and the abrasion therefore also less pronounced. Figures 12 & 13 shows the appearance of the bridge in 2001 after 15 years of service. It is remarkable, that no cores have been taken from the structure, indicating that the responsible authorities fully believe in the quality of the concrete (CEM 42.5 SR + MS), and the design of the bridge.

Figure 12: Bredal Bridge

Figure 13: Surface of Bredal Bridge after 15 years exposure

11 ROAD PAVEMENT, M30, FALSTER

In the autumn of 1984, 7 km of highway M30 was constructed in concrete. Width 8 m, thickness 200 mm. Paving was carried out with a normal slipform paver, operated by a German company.

Table 16: Concrete mix-design

CEM I 42.5 SR	kg/m^3	300
Flyash	kg/m^3	-
Micro silica slurry (50% water)	kg/m^3	30
Micro silica	%/cement	5
	%/binder	5
0/4 mm	kg/m^3	710
5/18 mm	kg/m^3	840
18/25 mm	kg/m^3	360
Water	kg/m^3	108
Air		+
Plast		+
SPT		-
w/c–ratio #)	-	0.37
Air	%	6.9

#): w/(c+2MS+0.4FA)

Table 17: Air pore characteristics in hardened concrete

Total air	%	5.2
Spec. surface	mm^{-1}	43
Spacing factor	mm	0.12

The concrete had a compressive strength of 33 MPa after 7 days (150/300 mm cylinders).

No problems have been reported regarding the durability of the concrete today.

12 SLAGSLUNDE ROAD

This 6 m wide small road in the northern part of Sealand was made in October 1990. The road serves both for normal traffic between some small villages, and as the main road for transport to a foodstuff factory.

Figure 14: Slagslunde Road

12.1 Materials

Table 18: Concrete mix-design

CEM I 42.5 - SR	kg/m^3	330
	kg/m^3	33
Micro silica	%/cement	10
	%/binder	9
0/4 mm	kg/m^3	660
4/8 mm	kg/m^3	204
8/25 mm	kg/m^3	996
Water	kg/m^3	140
Eqv. w/c ratio[#)]	-	0.35
Air		+
Plast		+
SPT		-
Slump	mm	65
Air content	%	7.0

[#)]: w/(c+2MS+0.4FA)

Grading of the aggregates can be seen in figure 15.

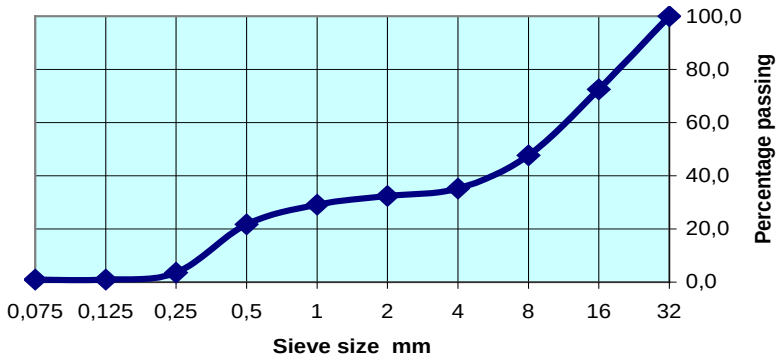

Figure 15: Aggregate grading for the Slagslunde Road

Table 19: Development of compressive strength. 20 °C watercured specimens

8 hours		1.2
12 hours		9.4
1 day		20.0
2 days		29.1
3 days	MPa	38.0
7 days		44.4
14 days		53.1
28 days		58.6
28 days ¤		*70*

¤: Cube strengths calculated in accordance with the introductory remarks

The concrete was paved with a Biddwell paver. It showed up, that the workability was too high for this paving operation on an inclined ground. This led to a mortar rich uneven surface that had to be bumpcutted in the summer of 1991.

Air pore structure as measured on 4 drilled cores from the road: Air content: 3.4%, Specific surface: 28 mm^{-1} and spacing factor: 0.21 mm

Freeze/thaw testing has been carried out, both on laboratory cast specimens during the pretesting of the concrete, and on cores drilled from the road. The latter cores was drilled before the surface was bumpcutted, hence a mortar rich layer tend to be vulnerable to freeze/thaw. On half the cores, this layer was removed before testing. These specimens represent therefore better the properties the actual bumpcutted surface. The scaling can be seen on figure 16.

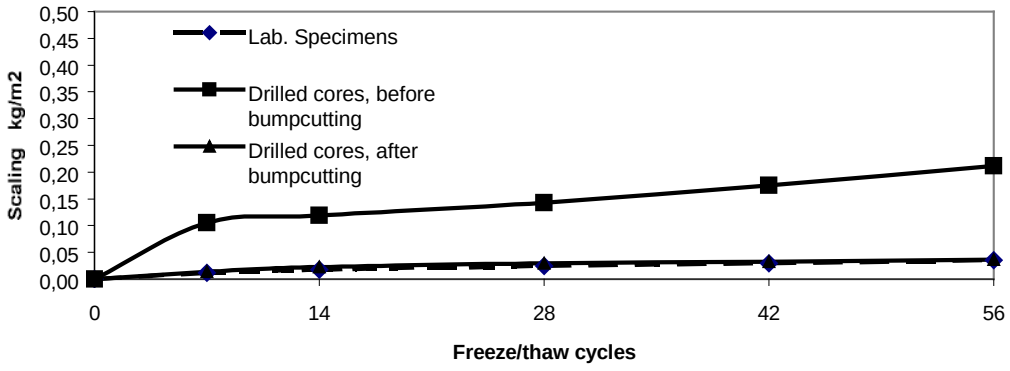

Figure 16: Scaling of concrete samples from Slagslunde Road. Tested shortly after construction in 1990

12.2 Durability judgement in 2001

Figure 17: Surface of the Slagslunde Road. In the bottom of the picture the original exposed surface, in the top the bump-cutted surface. Photograph taken in October 2001

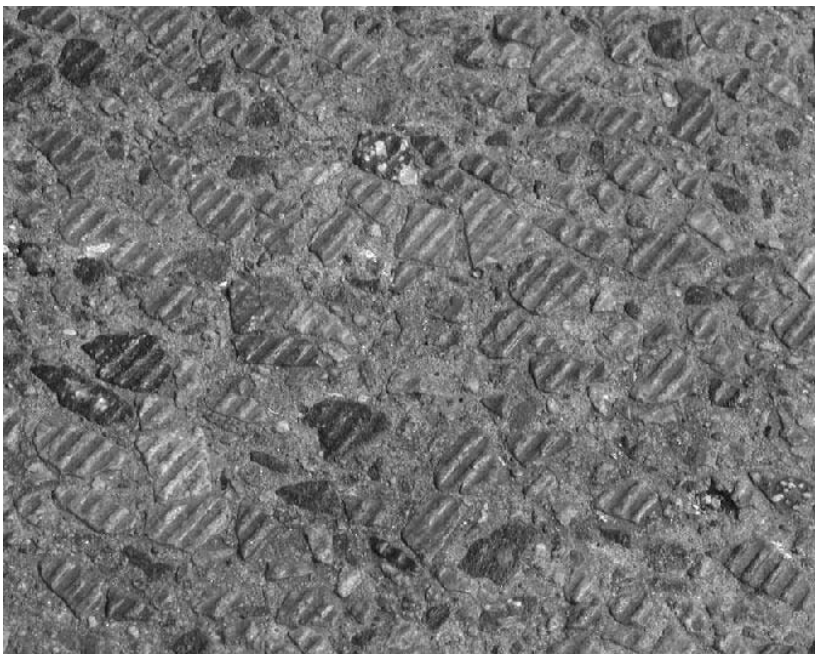

Figure 18: Surface of the Slagslunde Road in the wheelpath in front of the foodstuff factory. The bumpcutted grooves can still be seen in the aggregates, while abrasion has polished the grooves away from the mortar phase

13 INTERNAL ROAD AT AALBORG PORTLAND

The road, which is used for heavy vehicles and dumpers op to 40 tonnes axle load, was made in august 1992.

The construction was a three-layer construction.

- A base layer of 100 mm, with cement treated gravel material. 28 days compressive strength: 12 MPa. *{Corresponding cube strength: 14 MPa}*
- A layer of no-fines concrete, 140 mm, compressive strength 40 MPa {*Corresponding cube strength: 48 MPa}*
- An 80 mm wearing course of high strength concrete, compressive strength 99 MPa *{Corresponding cube strength: 119 MPa}*

The road was constructed as part of Aalborg Portland's development project on Paver Compacted Concrete for roads. Paving was done with a large asphalt paver with a high-compacting screed. (See figure 22). This paver fully compacted the very dry type of concrete.

Figure 19: The 6 m wide road at Aalborg Portland

13.1 Materials

Table 20: Concrete mix-design

CEM I 42.5 SR	kg/m^3	275
	kg/m^3	80
Flyash	%/cement	29
	%/binder	21
	kg/m^3	28
Micro silica	%/cement	10
	%/binder	7
0/2 mm	kg/m^3	565
4/8 mm	kg/m^3	1480
8/16 mm	kg/m^3	-
Water	kg/m^3	80
w/c–ratio #)	-	0.22
Slump	mm	0
Air content	%	1.5

#): w/(c+2MS+0.4FA)

The reason for not having larger aggregates than 8 mm in the top layer was that the texture of the surface should be made by exposed aggregates. Having such small aggregates exposed in the surface can result in noise reduction on the same level as open graded asphalt.

Table 21: Development of compressive strength, MPa {Cast cylinders}

Age	Comp. strength
2 days	43
7 days	65
28 days	99
28 days ¤	*115*

¤: Cube strengths calculated in accordance with the introductory remarks

On drilled cores compressive strength of 71 MPa was measured in 2001, ie. after 9 years exposure. Recalculation by multiplying with the conservative cast cylinder/drilled core correction factor of 1.25 gives a compressive strength of 89 MPa.

Freeze/thaw test according to SS137244, the Scandinavian Slab Test was made on drilled cores. The average scaling after 56 cycles was 0.11 kg/m^2.

13.2 Durability judgement in 2001

Figure 20: Surface of the road. No damage at the sawn joint or the edge can be seen.

During the years, some cracks have appeared in the top layer. It is believed that movements in the underlying layers cause these cracks. This high strength concrete tends to be very brittle, and therefore very sensitive to such movements.

Besides these cracks, no degradation can be found on the surface.

14 ROAD PAVEMENT, HJØRRING

This road, 8-m wide and 1750 m long road was made in the autumn of 1995. The pavement built up was a result of a 4-year European project; ECOPAVE (Economic Pavement system) carried out between 1988 and 1992. /1997-1/

The idea was to pave the concrete with an asphalt-paver with a high compaction screed, and to establish transverse cracks closely. With a distance of 1.5 m between active cracks, the shrinkage of the individual flags are so small, that full load bearing capacity is kept across the cracks. In this way the costly dowels are avoided.

There have only been constructed two roads according to this technique in Denmark. A three km long highway in the Southern part of Jutland paved with a traditional slip-form paver, and the small section close to Hjørring described in this paper. The actual paving- and transverse crack forming techniques did, unfortunately, result in an uneven surface.

Figure 21: View of the Hjørring ECOPAVE road

Figure 22: Concrete paving on the Hjørring ECOPAVE section

14.1 Materials

Table 22: Concrete mix-design

Cement	kg/m^3	260
	kg/m^3	55
Fly Ash	%/cement	21
	%/binder	16
	kg/m^3	20
Micro silica	%/cement	8
	%/binder	6
0/2 mm	kg/m^3	673
4/8 mm	kg/m^3	388
8/11 mm	kg/m^3	1055
Water	kg/m^3	87
Air		-
Plast		-
SPT		+
w/c–ratio #)	-	0.27
Slump	mm	0
Air content	%	1,5

#): w/(c++2MS+0.4FA)

Table 23: Development of compressive strength, MPa

Age	Comp. strength
1 day	29
7 days	69
28 days	94
28 days ¤	*109*

¤: Cube strengths calculated in accordance with the introductory remarks

Freeze/thaw test according to SS137244, the Scandinavian Slab Test, has been carried out on drilled cores from the road. Average scaling from 16 cores representing 7 different production day, was 0.25 kg/m^2 after 56 cycles. (Minimum 0.04 and maximum 0.54 kg/m^2)

Figure 23 shows a part of the surface, photographed in October 2001.

Figure 23: Surface and a transverse sawn crack of the ECOPAVE road after 6 years of service.

As for the internal road at Aalborg Portland, the high strength concrete tends to be so brittle that small movements of the underlying layers gives rise to cracks.

15 GADHOLTROAD BRIDGE

This bridge was constructed in 1995. One idea behind the design was to utilise high strength concrete in construction. This is not covered by the Danish codes of practise, so the Norwegian code NS 3473 was used for the design. The bridge was designed for a characteristic compressive strength of 75 MPa. /1996-1/

Figure 24: The high-strength concrete bridge, " Gadholtvej Bridge"

15.1 Materials

Table 24: Concrete mix-design

Cement	kg/m^3	426
	kg/m^3	30
Micro silica	%/cement	7
	%/binder	7
0/4 mm	kg/m^3	625
2/8 mm	kg/m^3	276
8/16 mm	kg/m^3	934
Water	kg/m^3	128
Air		+
Plast		+
SPT		+
w/c–ratio #)	-	0.26
Slump	mm	130
Air content	%	3,5

#): w/(c+2MS+0.4FA)

Table 25: Development of compressive strength. MPA (Cylinders)

	Cast cylinders	Drilled cores
28 days	93	79
28 days ¤	*111*	-
½ year	96	81
1 year	93	89

¤: Cube strengths calculated in accordance with the introductory remarks

Freeze/thaw testing after 28 days according to the Swedish Standard SS137244, the Scandinavian slab test, resulted in scaling after 56 cycles of 0.38 kg/m^2. However, the acceleration rate of the scaling was >2, and by definition the concrete was not frost resistant. Another freeze/thaw test was prolonged to 112 cycles, resulting in a scaling of 0.82 kg/m^2, and a judgement of "acceptable freeze/thaw durability".

15.2 Durability judgement in 2001

No special investigation has been made in 2001. Figures 24 & 25 have been photographed in the autumn of 2001. No signs of deterioration of the concrete are to be seen.

Figure 25: Surface of the arch

16 GREAT BELT CONNECTION AND ØRESUND LINK

The huge amount of tests and investigations during the previous years have lead to the general acceptance that use of secondary cementitious materials as fly ash and microsilica improves the durability properties of concrete in aggressive environments. Therefore the large Danish infra structure constructions as the Great Belt connection as well as the Øresund link both utilised these mineral additives in the concrete.

Table 26: Concrete mix-design for the Great Belt connection

		Great Belt - East bridge
CEM I 42.5 SR	kg/m^3	320
	kg/m^3	47
Flyash	%/cement	15
	%/binder	12
	kg/m^3	20
Micro silica	%/cement	6
	%/binder	5
0/2 mm	kg/m^3	618
28 mm	kg/m^3	396
4/8 mm	kg/m^3	
8/16 mm	kg/m^3	476
16/25 mm	kg/m^3	336
Water	kg/m^3	133
Air		+
Plast		+
SPT		+
Retarder		-
w/c–ratio #)	-	0.35

#): w/(c+2MS+0.4FA)

Table 27: Development of compressive strength. MPa (Cylinders)

Concrete type	Great Belt
28 days	56
28 days ¤	*65*

¤: Cube strengths calculated in accordance with the introductory remarks

It is interesting to note, that it is stated in /1999-1/ that "After 10 years' testing and investigation of frost resistance it was concluded that a suitable air void structure is probably needed in high performance concrete with low water/cement ratio and that the Swedish standard test method is probably the best method on the market for testing these types of concrete, although there is a wide variability in results when used on hardened concrete".

17 FINAL REMARKS

This paper presents experience from some of the well-documented Danish tests of mineral admixtures as fly ash and microsilica in concrete exposed to aggressive climate.

The survey covers a wide range of concrete types

- equivalent w/c-ratios in the range 0.16 – 0.47.
- compressive strengths (150 cube) between 30 MPa and 150 MPa.
- three types of cement.
- cement content between 222 and 505 kg/m^3.
- workability from 0 mm to >220 mm slump.

Many years of experience have demonstrated the necessity for use of air-entraining agents in concrete exposed to freezing and de-icing chemicals. Hence, nearly all the concrete presented in this survey is air-entrained.

To the opinion of the author, these examples demonstrates, that durable high performance concrete can be produced utilising secondary cementitious materials as flyash and microsilica.

REFERENCES

1981-1 Forsøg med kantelementer af silicabeton, 1981
Vejdirektoratet 1981 (In Danish)

1982-1 Betons holdbarhed. Rapport no 4: Ryå-broen – Forsøg med silicabeton.
Vejdirektoratet 1982 (In Danish)

1985-1 Betons Holdbarhed. Rapport no. 5: Madum Å-broen. Forsøg med flyveaskebeton
Vejdirektoratet 1985 (In Danish)

1985-2 The Concrete of the Farø Bridge
Vejdirektoratet 1985

1987-1 Dansk Ingeniørforenings Anvisning for Anvendelse af Flyveaske og Mikrosilika i Beton. Normstyrelsens publikationer NP-188-R, April 1987 (In Danish)

1988-1 Mouritzen, J., "Dolosblokke – Beton med flyveaske"
Durable concrete with industrial by-products
VTT Symposium 89 – Espoo 1988

1993-1 Betons holdbarhed. Rapport no 6: Ryå-broen – Forsøg med silicabeton.
Egenskabsudvikling 1981 – 1993
Vejdirektoratet 1993 (In Danish)

1994-1 Nepper-Christensen, P., Kristensen, B.W., Rasmussen, T.H., "Long-Term Durability of Special High Strength Concretes". Proceedings from the Third International on Durability of Concrete. Nice 1994. ACI Publication P-145

1995-1 Erfaringer med anvendelse af mikrosilicabeton - Fiskebækbroens kantelementer
Vejdirektoratet, Driftsområdet Rapport 20, 1995 (In Danish)

1996-1 Buebro i højstyrkebeton – Projektering, forprøvning og udførelse.
Vejdirektoratet, Rapport nr 32, 1996 (In Danish)

1997-1 Stoltzner, E., Buhr, B., Engelund, S.: The Faroe Bridges – Chloride Penetration rate Estimated on a Basis of Measurements from 1988 to 1997.
Fifth CANMET/ACI International Conference on "Durability of Concrete", Barcelona, Spain June 2000
ACI SP-192-29

1997-2 Bager, D.H., Krarup, P., "New Technologies for Concrete pavement Construction"
Sixth International Purdue Conference on Concrete Pavement Design and Construction, 1997

1999-1 Concrete Technology. The Storebælt Publications, A/S Storebæltsforbindelsen 1999

2001-1 Larsen, E.S., "Long Term Experience of Micro Silica Concrete – Edgebeams of the Fiskebæk Bridge", ibid.

2001-2 Bager, D.H., “Aalborg Portland Durability Project – 18 Years Survey”, ibid.

2001-3 Setzer, M.J., Palecki, S., “Life-time prediction of high performance concrete with respect to durability (CONLIFE). ibid

2002-1 Juel, I.A., Ph.D. thesis regarding sea water durability of concrete. To be submitted summer 2002.

High Performance Road Concrete in Norway

Trine Tveter
Ph.D., Head of Department Materials and Construction
Norwegian Building Research Institute,
Forskningsveien 3B, P.O.Box 123 Blindern, 0314 OSLO
E-mail: trine.tveter@byggforsk.no

Tom Farstad
Engineer, Scientist
Norwegian Building Research Institute,
Forskningsveien 3B, P.O.Box 123 Blindern, 0314 OSLO
E-mail: tom.farstad@byggforsk.no

ABSTRACT

High Performance Concrete (HPC) has been proven to give 3 times better resistance towards wear from studded tyres than asphalt. These results are from accelerating testing. Since Norway is one of the very few countries using studded tyres these results lead to a massive campaign to promote concrete paving. As a result a number of test roads (up to 8000 m) were produced, mainly in the 1980s.

The EU-project "Life time prediction of high-performance concrete with respect to durability", CONLIFE, has one activity on state of the art of HPC structures.

The paper presents from testing pavements that have been exposed to freezing/thawing and de-icing salt for 10-15 years.

Key words: High Performance Concrete, wear, studded tyres

1. INTRODUCTION

In Norway there is no tradition for using concrete as road paving. It has to a certain extent been used on bridges and in tunnels, but asphalt has been the only road paving up to the late 1970s.

Norway is one of very few countries still using studded tyres. Over the last years the use has been restricted, but in the early 80s there were no restriction in the winter season (1. October – 15. April). The interest in and the use of High Performance Concrete developed in Norway through 1980 and 1981. Together with the knowledge about this material started research activities on the use of HPC in road paving. The Norwegian cement and concrete industry made big investments to succeed with this concept.

2. ACCELERATED TESTING

NORCEM, the Norwegian cement producer developed a road wear simulator (Veislitern) that first operated in the period 1986-1991. A comprehensive test program was carried out in that period. The aim was to test the wear resistance of HPC against studded tyres. A total of 96 series was carried out.
The test rig was a circular road with diameter 6 m (speed 60 km/h, axle load 5 tons, contact pressure 7 bar). In the test machine 12 elements of concrete were mounted, pairs of which were identical. Four truck wheels with studded tyres were driving around the carrousel at a maximum speed of 60 km/h. Part of the test is carried out on dry surface and part of it on wet surface. The dept of the wear is measured every 10000 circles.

Figure 1: Road wear simulator ("Veislitern")

Some of the conclusions from the test program were:

The compressive strength is the one parameter of most importance with respect to wear resistance against studded tyres.

With the right choice of coarse aggregate the wear resistance can be improved up to 50 %. This also leads to an increase in compressive strength hence the improvement is a combination of the two factors.

The result from this sections and scanning electron microscopy also showed great importance of mixing and paving equipment.

The test results show that concrete has 3 times better wear resistance than asphalt under these test conductions.

2.1 Mix-design

The volume of paste in all mix-designs is in the region 30-33 %. (Cement, silica fume, water, admixtures, air content)
Different kinds of rock types in the coarse aggregate tractions.
Different kinds of fine aggregates.
Maximum aggregate size in the range 8-32 mm.
Different kinds of cement:

Normal Portland Cement – CEM I
Low alkali high strength Portland Cement – CEM I
Portland Cement containing 20 % fly ash – CEM II/A-D

Silica fume (added as compacted powder) was used in all mixes in the range

$$\frac{s}{c+s} = 0.01 \qquad (1)$$

to

$$\frac{s}{c+s} = 0.13 \qquad (2)$$

The compressive strength varied from 70 MPa to 100 MPa (strength after 28 days on 100x100x100 mm cubes). {These compressive strengths corresponds to compressive strengths of 150 mm cubes on 78 – 114 MPa, according to the introduction in the proceeding}

No air entrained concretes were tested.

Fly ash (as part of the cement) and silica fume were the only cementitious constituents that were included.

The tests carried out only included different mix-design of plastic concrete (workability 10-20 mm slump). Roller compacted concrete were not testing in “Veislitern”.

The results showed that it was not possible to produce a HPC that totally resisted wear from studded tyres.

3. TEST ROADS

Partly on basis of the results from the test program carried out in “Veislitern” some test roads were produced around Norway. The specified compressive strength was in the range C75-C85 MPa (28 days 100 mm cubes as mentioned above) {150 mm cube: 84 – 96 MPa}. The thickness of the pavements was from 180-260 mm. There were mainly two production procedures used:

- Slip form paving
  Fresh concrete with a slump 10-20 mm

- Roller compacted concrete
  Fresh concrete with “no” slump

The mix-designs were based on a low alkali, low heat developing Portland Cement (type CEM I), initially developed for the platform production in the North Sea.

The sources of fine and coarse aggregates varied. Addition of ca. 5 % micro silica (mostly added as compacted powder) was used in most cases.

Admixtures used was plastiziser, super plastiziser and in some cases air entrainer.

The complete mix design will be maid available in the final report from the Conlife project.

4. DURABILITY OF TEST ROADS

Some of the test roads have shown excellent durability. However a number of the test roads gave more sever wear than expected and needed repair after few years. There is no sufficient repair or maintenance procedures, so many of the test roads are today covered with asphalt.

The situation in Norway today is so that asphalt has taken over the whole marked again. There were to few projects and the experiences mixed. The contractors could not keep updated equipment and trained workmen.

5. CONLIFE PROJECT

Norway, with Norwegian Building Research Institute is a partner in the EU-project “Life-time prediction of high-performance concrete with respect to durability” with Aalborg–Portland. The University of Essen is the scientific co-ordinator of the project.

One of the work packages contains state of the art of existing HPC structures.

Together with the Norwegian Road Authorities we have drilled cores from a number of roads, tunnels and bridges. We have defined a test program.

5.1 Test program

The drilling of cores were planned to cover most places where HPC structures have been built. The different places are shown on the map, figure 2.

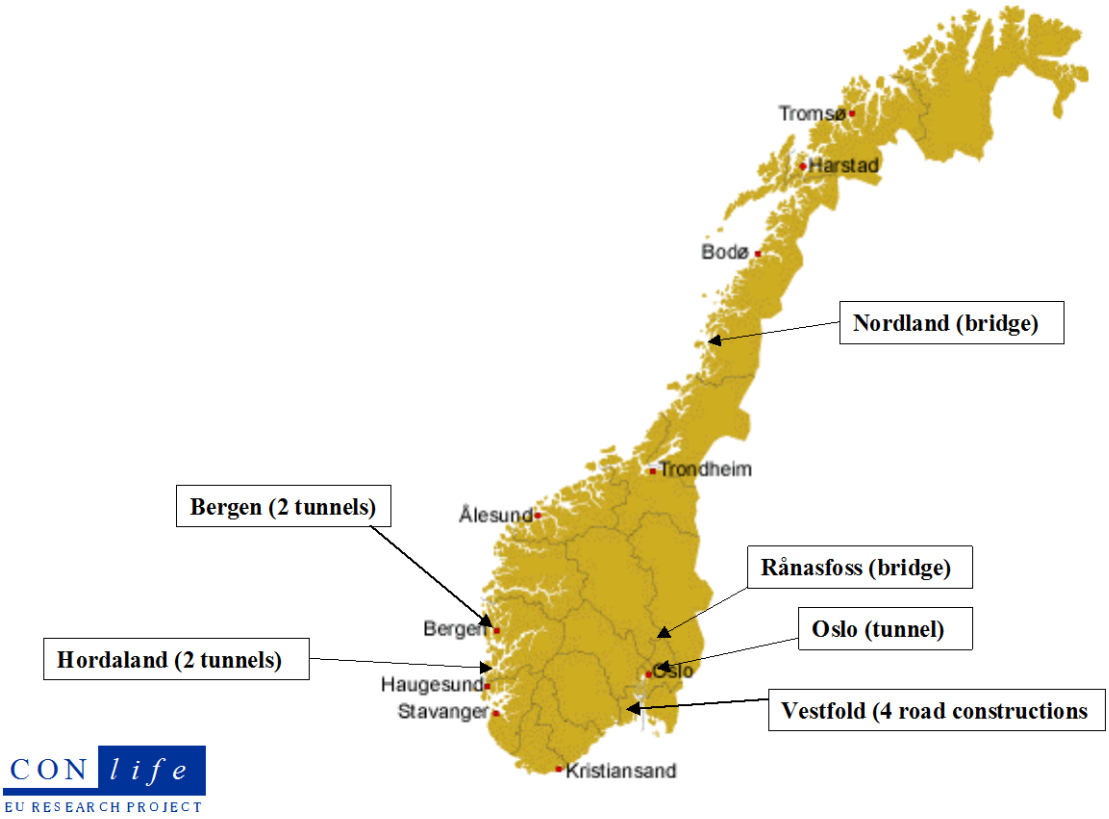

Figure 2: Plan for drilling of cores

5.2 Sampling

The cores were drilled with a diameter of the cylinder of 100 mm. The cores were drilling all through the concrete layer i.e. 170-220 mm.

No cores were drilled in the worn track of the surface.

When there was an asphalt layer on top of the concrete surface the asphalt was removed before testing.

Figure 3 shows from what part of the cores the different samples were taken.

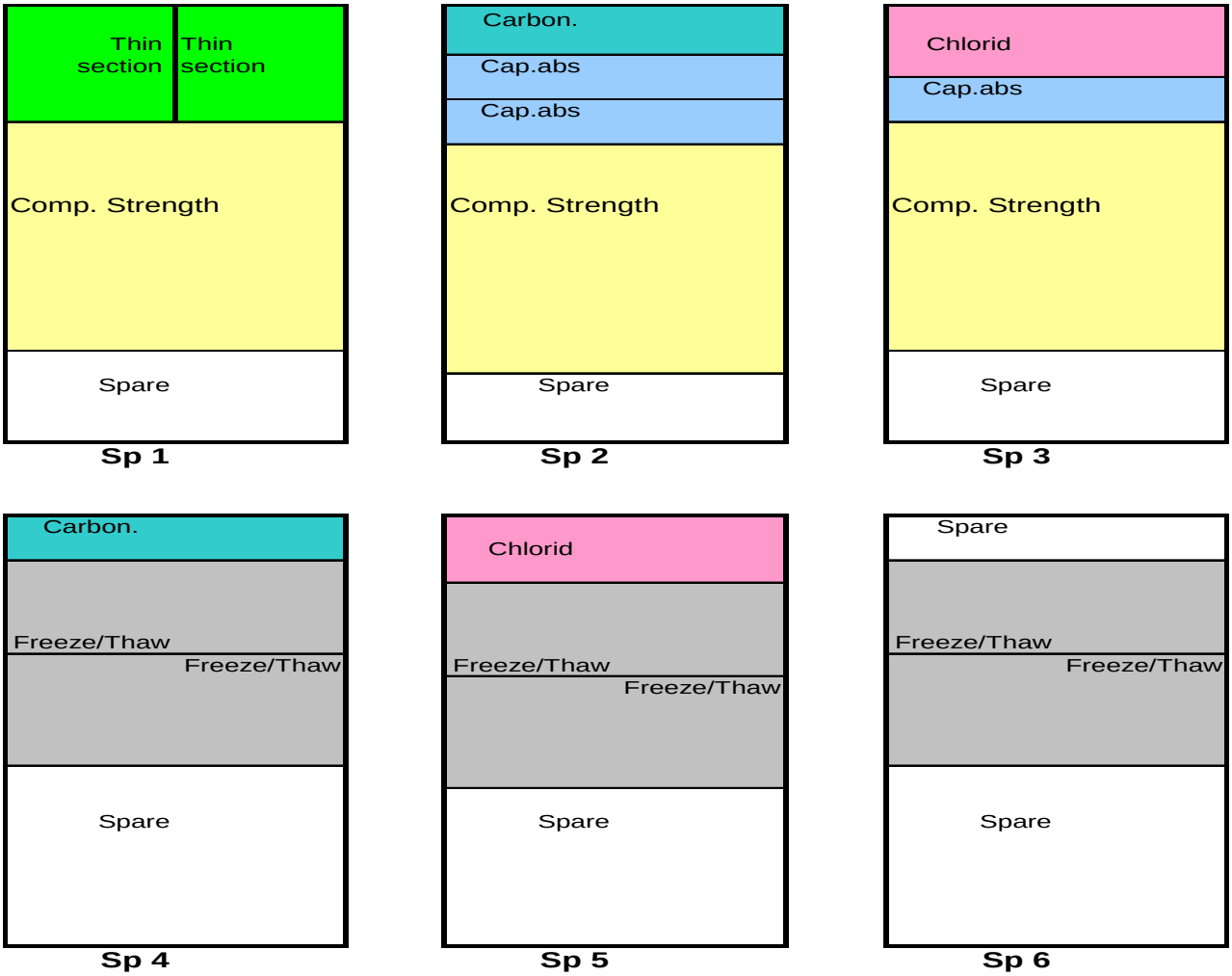

Figure 3: Sampling of cores

Table 1: The test methods used

Property/method	Test-standard (procedure)
Thin sections	NBI procedure (FLR-technique)
Capillary absorption/Porosity	Nordtest NT Build 368
Compressive strength/Density	NS 3668/NS 3673
Chloride content	NS 3671
Freeze thaw	SS 13 72 44
Carbonation	NBI procedure (Phenolphthalein)

Table 2: Sampling of HCP cores

Location	Construction type	Concrete	Spec. strength	Year of casting	Cores drilled	No. of Cores
Akershus	Road pavement –E 6 Jessheim	Wet -cast	C 75	1991	June 01	6
Bergen	Road pavement –E 16 Damsgård tunnel	Wet -cast	C 75	1990	Sept. 01	6
--«--	Road pavement –E 16 Sætre tunnel	PCC	C 75	1990	Sept. 01	6
Hordaland	Road pavement –E 16 Fjæra tunnel	PCC	C 75	1990	Okt. 01	6
--«--	Road pavement –E 16 Eljavik tunnel	PCC	C 75	1990	Okt. 01	6
Vestfold	Road pavement –E 18 Gulli A	Wet- cast	C 75	1980	Sept. 01	6
--«--	Road pavement –E 18 Gulli B	Wet- cast	C 75	1985	Sept. 01	6
--«--	Road pavement –E 18 Klinestad	Wet -cast	C 75	1989	Sept. 01	6
--«--	Road pavement –E 18 Tassebekk	Wet -cast	C 75	1989	Sept. 01	6
--«--	Road pavement –E 18 Sem	Wet -cast	C 75	1989	Sept. 01	6
Oppland	Bridge pavement –E 6 Rånåsfoss	Wet -cast w/fiber	C 75	1992	Okt. 01	3
Oslo	Road pavement –RV 160 Smestad tunnel	Wet -cast	C 90	1990	Okt. 01	6
Nordland	Bridge pavement –RV 17 Helgeland bridge	Wet -cast	C 75	1990	Okt. 01	3
	No. of sites: 13				Tot. no. of cores:	72

Figure 4: Akershus – Jessheim E 6, Drilling of cores June 2001

Figure 5: Bergen – Damsgård tunnel, Drilling of cores September 2001

Figure 6: Bergen – Sætre tunnel, Drilling of cores September 2001

5.3 Test results

Visual inspection
Both on the roller compacted and on the slip form paved concrete it could be seen a better compaction on the top part than of the lower part of the core.

On some cores could be seen air voids in the surface.

Compressive strength
E 6 Jessheim

The specific strength was C 75.

Chloride penetration, total porosity

Table 3: Porosity

Sample	PF %
SK 1	22.9
SK 2	26.3
SK 2	27.5
mean	25.6
Std. div.	2.4

Figure 7: Chloride content, two specimens drilled from Jessheim

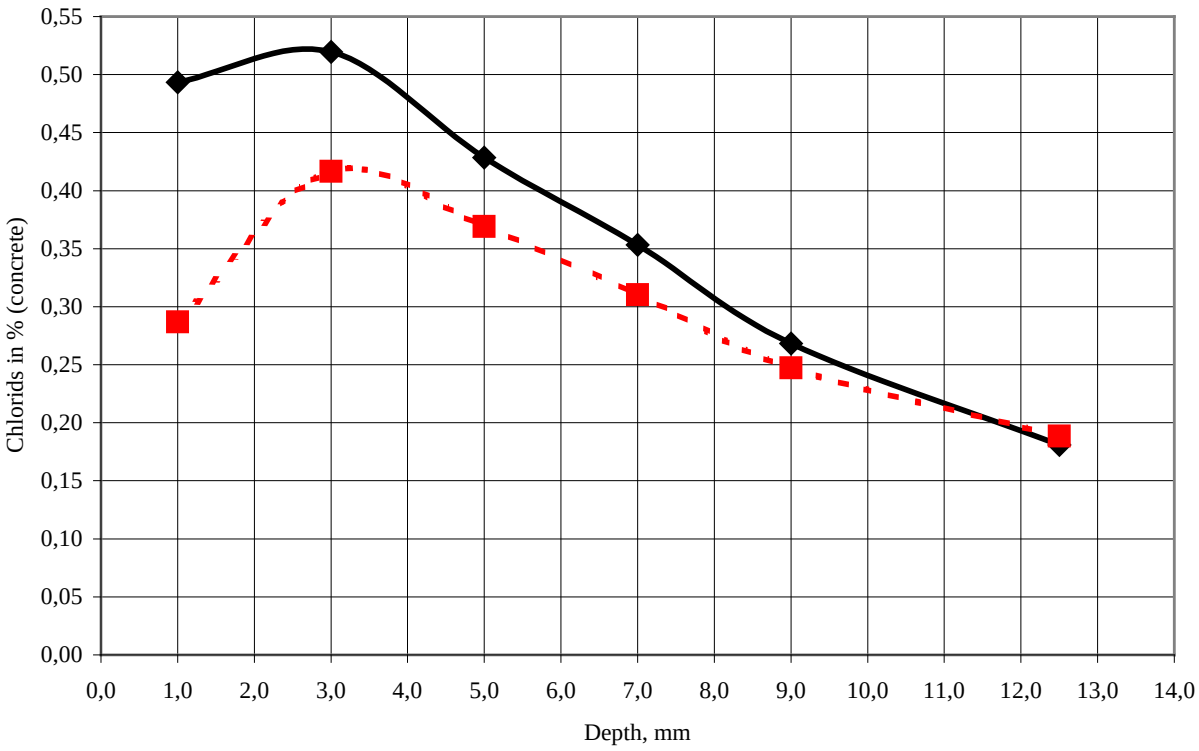

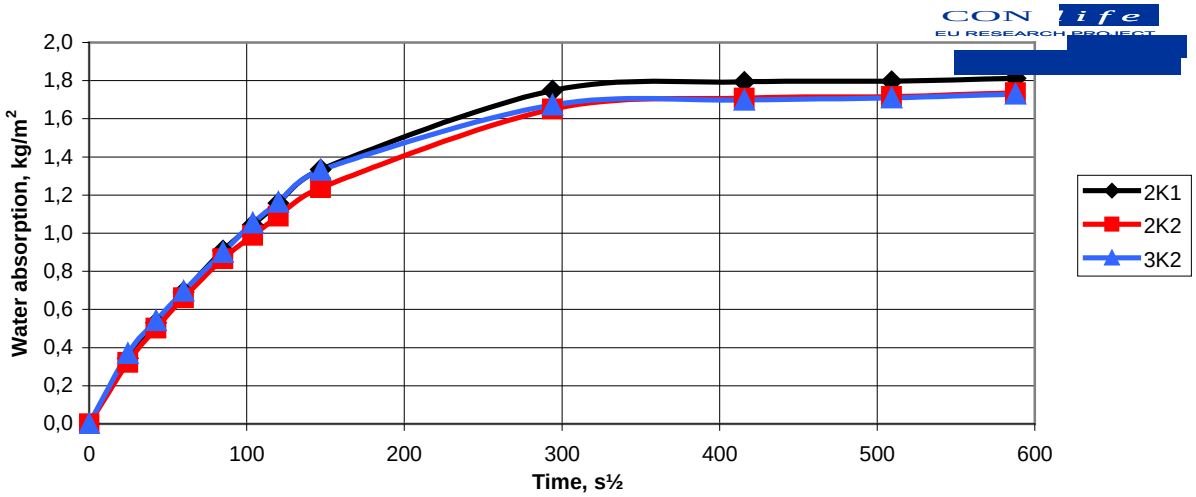

Figure 8: Capillary absorption Jessheim

Table 4: Compressive strength (drilled cores 100x100 mm) – NS 3668

Samples	Density (kg/m^3)	Compressive strength (MPa)	Samples	Density (kg/m^3)	Compressive strength (MPa)
V 101 [1]	2452	109.3	D 1 [5]	2449	98.9
V 102 [1]	2436	105.1	D 2 [5]	2466	103.7
V 103 [1]	2486	100.1	D 3 [5]	2463	113.1
Mean value	2458	104.8	Mean value	2459	105.2
V 201 [2]	2466	105.3	F 1 [6]	2412	35.5
V 202 [2]	2465	115.6	F 2 [6]	2394	27.2
V 203 [2]	2459	113.8	F 3 [6]	2410	27.4
Mean value	2464	111.6	Mean value	2405	30.0
V 301 [3]	2536	104.6	E 1 [7]	2468	44.8
V 302 [3]	2521	97.5	E 2 [7]	2512	72.9
V 303 [3]	2541	106.3	Mean value	2490	58.9
Mean value	2533	102.8	S 1 [8]	2315	36.4
V 401 [4]	2485	110.4	S 2 [8]	2287	32.1
V 402 [4]	2496	114.2	S 3 [8]	2295	26.4
V 403 [4]	2473	113.4	Mean value	2299	31.6
Mean value	2485	112.7	1 [9]	2368	95.1
			2 [9]	2365	99.0
			3 [9]	2385	101.7
			Mean value	2373	98.6

[1] E 18 Gulli
[2] E 18 Sem
[3] E 18 Ramsum
[4] E 18 Fokserød
[5] Damgaardstunnelen
[6] Fjæratunnelen
[7] Eljarviktunnelen
[8] Sætretunnelen
[9] Jessheim

6. FURTHER WORK

All the drilled cores will be tested according to the test program described in chapter 5.1. In addition cores will be drilled in the north of Norway.

Comprehensive reports with conclusions will be part of the CONLIFE project.

Silica Fume to Enhance Concrete Quality, Icelandic Experience Concerning Alkali-Silica Reactions

Gisli Gudmundsson
Ph.D., Research specialist
The Icelandic Building Research Institute, Rb-Keldnaholt, IS-112 Reykjavik, Iceland
E-mail: gudmundsson.g@rabygg.is

Hakon Olafsson
director
The Icelandic Building Research Institute, Rb-Keldnaholt, IS-112 Reykjavik, Iceland
E-mail: olafsson.h@rabygg.is

ABSTRACT

Silica fume has been intermilled with Icelandic cement since 1979. The main reason why silica fume is utilised in this way is to reduce or eliminate alkali-silica reactions in concrete. Now after more than 20 years of service there are no signs of alkali-silica reactions in concrete in Iceland. These findings are supported by standardised alkali silica test methods.

However, the homogeneity of silica fume both in cement and hardened concrete is not always as good as expected since small clusters of silica fume can be found in hardened concrete and test results have shown these lumps to be alkali silica reactive.

Key words: Alkali-silica reactions, silica fume, durability.

1. INTRODUCTION

Silica fume has been utilised in concrete for some decades now. Initially it was used as a cement replacement material, but in recent years silica fume is used more and more as a solid additive (micro filler) in concrete (1). Increased strength and improved durability are the main benefits. Incorporation of superplastizicers and silica fume offers flowable concrete with low w/c - ratio. In other words silica fume affects concrete quality in many ways and when properly proportioned it will greatly improve the quality of both fresh (green) and hardened concrete. Moreover, the utilisation of silica fume in concrete effects the environment in a very beneficial way. Silica fume is a by- or a waste product, mainly from ferrosilicium plants. As a cement replacement material, its usage will lower the cement consumption hence, less carbon dioxide will be emitted into the

atmosphere. Generally for each ton produced of cement clinker, one ton of carbon dioxide is emitted into the atmosphere.

As a cement replacement material silica fume is highly effective as a possolan. In Iceland silica fume has been used now for almost 20 years and virtually eliminated all alkali-silica reactions (ASR) in concrete (2). Prior to this ASR caused serious problem in domestic houses in Iceland in the years from 1961 to 1979. Today, about 7.5 % of silica fume is added to the ordinary Portland cement. About 1-3 % rhyolite (a natural possolan) is also added to the OP-cement. Upon grinding the cement clinker, the silica fume and the rhyolite are inter ground with the clinker.

In this paper we will give an overview of the experience regarding the utilisation of silica fume in concrete in Iceland, more detailed review can be found elsewhere (3).

2. EFFECTIVENESS OF SILICA FUME AGAINST ALKALI-SILICA REACTIONS

Serious damages were caused by alkali-aggregate reactions (AAR) in domestic houses in Iceland in the years from 1961 to 1979. Preventive actions (possolan cement - non reactive aggregates) were taken for larger concrete structures. For houses no such actions were taken during this period. At that time, houses were not considered in any danger (3). Icelandic Portland cement has extremely high alkali content, currently about 1.65 % wt. as $Na_2O_{eq.}$ with the sodium to potassium oxide ratio of about 3:1 by weight (2). The aggregates used in concrete are mostly volcanic and some of which are very reactive in terms of AAR. The high reactivity is mostly due to high content of rhyolitic material, altered basalt and sea dreaded material was commonly used unwashed. In 1979 preventive measures were taken to fight AAR in concrete, those were: 1) blending silica fume into cement, 2) changing the criteria on reactive materials, 3) sea dredged material must be washed, and the use of reactive material was limited. Since then, there have been no reported cases of AAR in concrete.

2.1 Laboratory testing

In order to evaluate the long term performance of silica fume blended concrete ASTM C 227 tests were carried out over long period of time. The test it self is controversial and the results can be misleading, since leaching of alkalies out of the mortar bars can take place (4). Apparently the leaching of alkalies, which reduces expansions, is only serious when the mortar bars are stored in wicks. In all ASTM C 227 tests carried out in Iceland the samples are never stored in wicks. Leaching should therefore be minimised in these tests. In Figure 1 is shown results of 4 independent studies. In these studies the samples were tested in the ASTM C 227 test for 11 to 14 years. The source of aggregate is the same in all the runs, Hvalfjordur material, which is considered very reactive material, in terms of AAR. The cement type is the same in all the studies, Icelandic Portland cement. In study number 1 the cement does not contain any silica fume, but in all the others it contains 7.5 % intermilled silica fume. As expected the measured expansion is highest in the samples from study 1. The measured expansion is similar and much lower in the others studies. The expansion rate is highest during the first 2 years, then is decreases for a while. After some 4 to 6 years it seems that the expansion increases over a period of few years and then the expansion levels out.

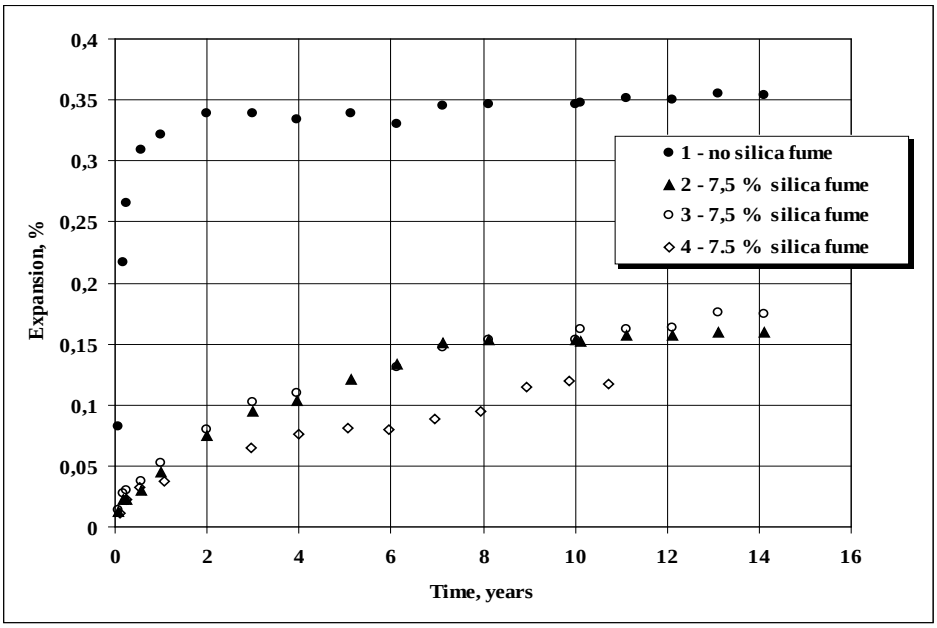

Figure 1 - Measured ASTM C 227 expansion in sample which have been tested for 11 to 14 years (5).

The interpretation of this increased expansion after 4 to 6 years is not simple and controversial. One could suggest that at this time the silica fume is used up and therefore the silica fume does only prolong the ASR for some years, but it does not fully prevent it. The general conclusions which can be drawn from these tests results is that the silica fume reduced AAR expansion in mortar bars considerably.

In Figure 2 are given test results from the ultra accelerated test method ASTM C 1260 (6). The aggregates used in these samples are classified as non-reactive based on the ASTM C 227 test method. Three types of cement were used: Icelandic ordinary Portland cement without any silica fume, Icelandic ordinary Portland cement with 7.5 % silica fume and finally a Danish low alkali ($Na_2O_{eq.}$ less than 0.4 % wt) ordinary Portland cement without silica fume. In the ASTM C 1260 standard, expansions of less than 0.1 % after 14 days are indicative of innocuous behaviour. The highest expansion is produced in the reference sample, without any silica fume, much less when 7.5 % silica fume is used and well within the 0.1 % expansion limits. It is interesting that the samples made with the Danish cement produces similar expansion as the Icelandic cement with 7.5 % silica fume.

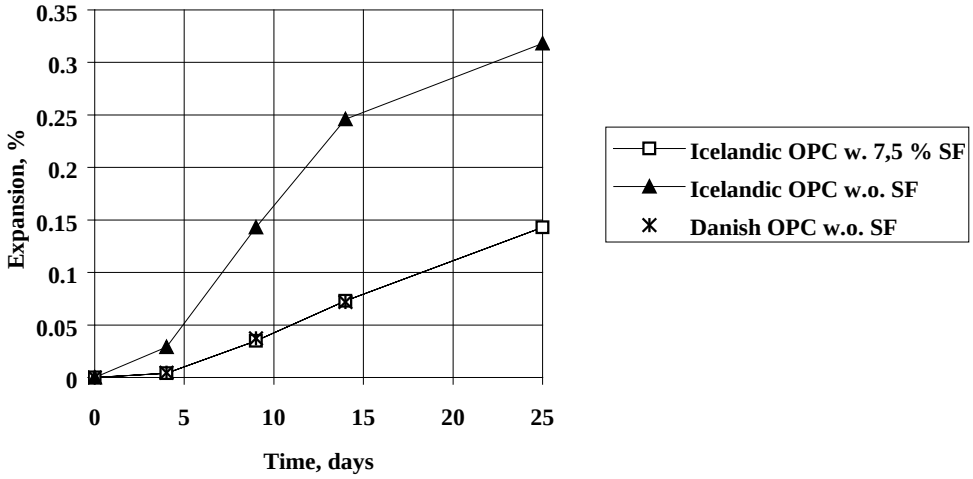

Figure 2 - Test results of ASTM C 1260 test method. Average percentage expansion of mortar bars made with "innocuous" basaltic aggregates. From (6).

2.2 Conditions surveys

Many conditions surveys have been carried out on houses build after 1979. In these surveys the structures are observed visually and cores are taken for laboratory inspection. No signs of AAR have been reported. Furthermore, all aggregates intended for concrete must be tested with the ASTM C 227 mortar bar test method. The aggregates must be tested with Icelandic OP-cement without any possolanic addition. Such cement has not been on the market since 1972, but it is produced for IBRI for this test. The measured expansion can not exceed 0.1 % after 12 months, if it does the aggregate is rejected and is not utilised in concrete.

In (5) houses from 1981, 1982 and 1983 were inspected. In this period the Icelandic ordinary Portland cement contained 5 % silica fume. The aggregates are all from the same source and are classified as alkali silica reactive. Measured ASTM C 227 expansion was more than 0.15 % after one year and measured ASTM C 1260 expansion was about 0.2 % after 14 days, when tested with non silica fume blended cement (CEM I). Cores were taken from the houses and a full petrographic examination was made on the cores to determine the presence and extent of ASR.

The concrete in all the houses can be considered in good conditions after 14 to 16 years of service. In general no visual cracks were observed on the concrete walls, except for one wall, where map cracking was detected. Some gel formation was observed in two houses. The gel formation was only found in voids and often close to rhyolitic or altered basaltic aggregates. There were no cracks observed in the samples, which can be associated with the alkali-gel formation. In Figure 3 is shown an example of alkali-silica gel formation. The gel was formed in a void adjacent to rhyolitic aggregate. There is no sign of any crack formation associated with this gel formation.

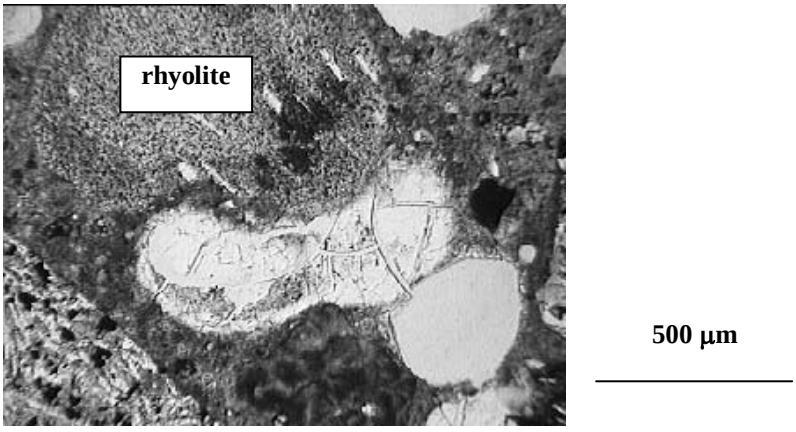

Figure 3 - An example of alkali-silica gel formation in a 18 year old silica fume concrete. The gel was formed in a void adjacent to rhyolitic aggregate.

Based on the test results, shown in 2.1 and many other ASTM C 227 and 1260 test results (3, 7, 8, 9, 10, 11, 12, 13, 14, 15, 16), combined practical experience in Iceland it is safe to say that after 20 years of service, inter-grinded silica fume in cement is very effective against AAR in concrete.

3. SILICA FUME LUMPS IN CEMENT AND HARDENED CONCRETE

It is a common misunderstanding in the literature that all silica fume used in mortars and concrete is as very fine powder. Recently, is has been shown that some of the silica fume is in relatively large lumps in hardened concrete (2, 17, 20, 21). These lumps are typically from 50 up to 100 μm in diameter, but much larger lumps have been observed (18). If the bulk density of the densified silica fume is too high it may be difficult disperse the silica fume in the concrete, poorly dispersed silica fume larger than 30 μm could act as alkali silica reactive aggregates (19), and obviously large amounts of lumps will reduce the beneficial filling role of silica fume in concrete.

Raw undensified silica fume collected from the filters at production sites, consists mainly of spherical particles, smaller than 10^{-6} m in diameter and with a relatively low bulk density. Silica fume is either supplied as such to concrete producers, but more commonly, to gain more workability, it is compacted to a bulk density from >500 kg/m^3 (air-densified silica fume) to about 1000 kg/m^3 (moist-pelletised silica fume). It is also common to make a liquid suspension of silica fume particles, slurry. Usually the dry content of silica fume in slurries is about 50 % by mass.

The silica fume utilised in Icelandic cement is a by-product from a ferrosilicium plant (Icelandic Alloys, Ltd.), located within 10 km from the cement plant. The silica fume is compacted at the ferrosilicium plant in two different ways. It is either compacted with air, which results in a relatively small grains (up to few mm in diameter); or it is pelletised with water, which results in relatively large and hard (dense) silica fume pellets. In the grinding process some relatively large and dense silica fume grains manage to escape through it without being crushed down. Figure 4 is a photomicrograph of such cement with some of the silica fume as relatively large lumps. In this case the silica fume lump is much larger than the clinker grains and therefore it does not have any possolanic activity, it must be at least 100 times smaller than the clinker to possess any possolanic activity.

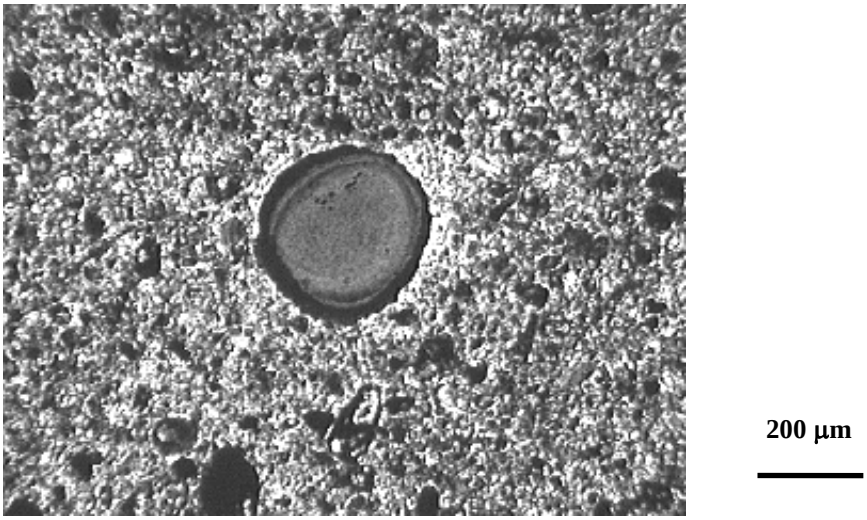

Figure 4 - Photomicrograph of silica fume cluster in an unhydrated ordinary Portland cement.

In Figure 5 is shown a grain size distribution chart of densified and undensified silica fume and for comparison a CEM I cement. From the Figure it can be see that the densified silica fume contains about 10 % of relatively large lumps and that its particle size distribution is relatively similar to the cement. The undensified silica fume has much finer particle size distribution.

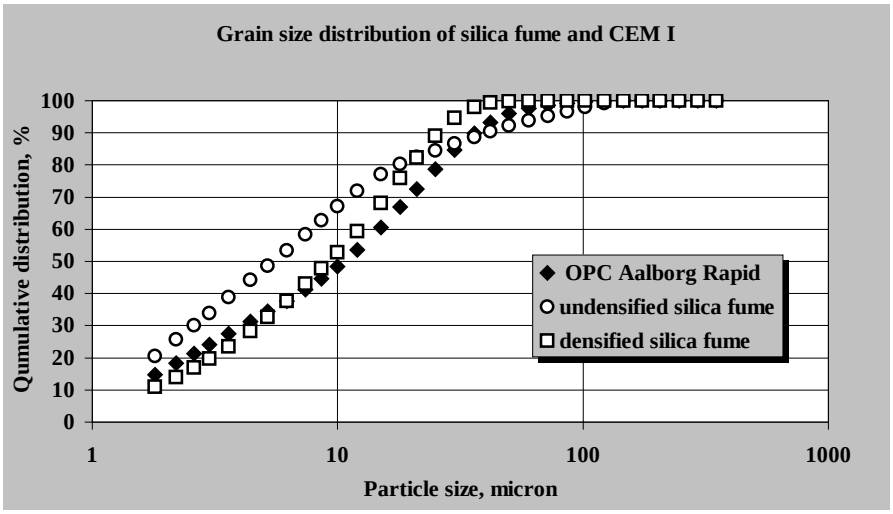

Figure 5 - Particle size distribution of silica fume and CEM I cement

Although there are no field evidence of alkali silica reactions in concrete since 1979, we have found evidence of alkali silica reactions in experimental samples. These reactions involve the silica fume lumps. In Figure 6 is shown a mortar bar sample, which was tested in the ASTM C 227 test. The concrete contained some silica fume lumps and during the test some of the lumps were reactive and produced alkali silica gel. The measured expansion was 0.123, 0.188, and 0.245 % after 6 months, 1 and 2 years, respectively. The expansion limits in this test method are 0.05 and 0.1 % after 6 months and 1 year, respectively. Therefore this sample is indeed very alkali-silica reactive.

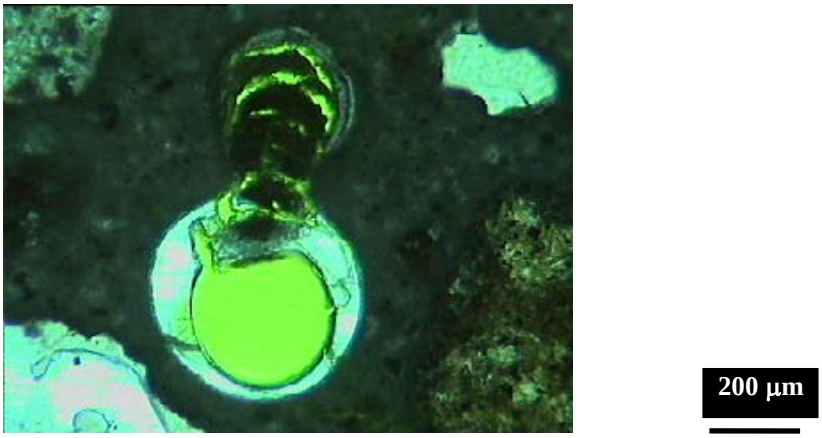

Figure 6 - Photomicrograph of silica fume lump and an alkali-silica gel in an air void.

4. CONCLUSIONS

The purpose of utilising silica fume in Icelandic cement was to reduce or eliminate the risk for damaging alkali silica reactions in concrete. The experience after 20 years shows this main goal has been achieved. Many conditions surveys, which have been carried out since 1979 have shown no deterioration due to alkali-silica reactions.

The homogeneity of silica fume in cement is not always as good as expected, since small lumps of silica fume are found in hardened concrete. There is some concern that these lumps may reduce the beneficial effect silica fume has against AAR in concrete. The alkali content of Icelandic cement is very high and the climate in Iceland is favourable for AAR (high humidity and many freeze/thaw cycles, which will promote AAR). Therefore, the risk of AAR to take place is always imminent. However 20 years of experience have proven silica fume very useful in the fight against AAR in concrete.

REFERENCES

1. Lewis, R., "Microsilica," Concrete, 1996, pp. 23-25.
2. Gudmundsson, G., Olafsson, H., "Silica fume in concrete - 16 years of experience in Iceland." In: Alkali-aggregate reaction in concrete, ed: Shayan, A., Proc. of the 10th International Conference, Melbourne, 1996, pp. 562-569.
3. Gudmundsson, G. and Asgeirsson, H., "Parameters affecting alkali expansion in Icelandic concrete," 6th Int. Conf. on Alkalis in Concrete, eds. Idorn, G.M.. Rostam, S., DBF, Copenhagen, Denmark, 1983, pp. 217-221.
4. Rogers, C.A., Hooton, R.D. "Reduction in Mortar and Concrete Expansion with Reactive Aggregates Due to Alkali Leaching," Cement, Concrete and Aggregates, 1991, vol. 13, pp. 42-49.
5. Gudmundsson, G., Ólafsson, H., "Alkali-silica reactions and silica fume: 20 years of experience in Iceland," Cement and Concrete Research, 1999, pp. 29, 1289-1297.
6. Gudmundsson, G., Moller, J., "Intermilled silica fume in cement and concrete." In: Proc. of the 19th International Conference on Cement Microscopy, eds: Jany, L., Nisperos, A., Bayles, 1997, J., pp. 86-92.

7. Gudmundsson, G., “Investigation on Icelandic pozzolans. Proc. on AAR,” ed. O.P. Haldorsson, Reykjavik, Iceland, IBRI-publication, 1975, pp. 65-77.
8. Gudmundsson, G. and Asgeirsson, H., “Some investigations on alkali aggregate reaction,” Cement and Concrete Research, 1975, vol. 5, pp. 211-220.
9. Gudmundsson, G. and Asgeirsson, H., “Pozzolanic activity of silica dust,” Cement and Concrete Research, 1979, vol. 9, pp. 249-252.
10. Olafsson, H., “Effect of silica fume on alkali-silica reactivity of cement. Condensed silica fume in concrete,” Division of Building Materials, the Institute of Technology, Trondheim, Norway, 1982.
11. Olafsson, H. and Helgason, Th., “Reactivity of Icelandic aggregates and effect of NaCl and pozzolans on AAR in concrete,” IBRI-publication (in Icelandic), 1983.
12. Asgeirsson, H., Kristjansson, R. and Olafsson, H., “The effect of silica fume on the properties of cement and concrete,” IBRI-publication (in Icelandic), 1985.
13. Asgeirsson, H., “Silica fume in cement and silane for counteracting of alkali-silica reactions in Iceland,” Cement and Concrete Research, 1986, vol. 16, pp. 423-428
14. Olafsson, H., ”AAR problems in Iceland - Present state. Proceedings 8th ICAAR,” ed.: Okada, K., Nishibayashi, S., Kawamura, M., 1989, pp. 65-70
15. Olafsson, H., “Alkali-silica reactions - Icelandic experience,” In: The Alkali-Silica Reactions in Concrete, ed: Swamy, R.N., Blackie, London, 1992, pp. 208-222
16. Gudmundsson, G. and Möller, “Influence on intermilling silica fume and rhyolite in Icelandic cement on alkali-silica reaction”. The 9th Int. Cong. Chem. Cement, New Delhi, India, 1992, pp.167-173.
17. St John, D.A., “The dispersion of silica fume”. In: Mechanisms of chemical degradation of cement-based systems, eds: Scrivener, K.L., Young, J.F., E&FN Spoon, 1997, pp. 58-66.
18. Marusin, S.L., Shotwell, L.B., “Alkali-silica reactions in concrete caused by densified silica fume lumps - A case study,” 5th CANMET/ACI International conference on fly ash, silica fume, slag and natural pozzolans in concrete, Milwaulkee, 1995, pp. 45-59
19. St John, D.A., Freitag, S.A., “Fifty years of investigation and control of AAR in New Zealand”. In: Alkali-aggregate reaction in concrete, ed: Shayan, A., Proc. of the 10th International Conference, Melbourne, 1996, pp. 150-157
20. Sveinsdottir, E.L. and Gudmundsson, G., “Condition of hardened Icelandic concrete. A microscopic investigation”. In: Proceedings of the 4th Euroseminar on Microscopy Applied to Building Materials, 1993, 11 pages
21. Lagerblad, B. and Utkin, P., “Undispersed granulated silica fume in concrete - Chemical system and durability problems,” Mat. Res. Soc. Symp. Proc., 1995, vol. 370, pp. 89-97.

Long Term Performance of Micro Silica Concrete - Edge Beams of the Fiskebæk Bridge

Erik Stoklund Larsen
Ph.D., M.Sc., Senior Project Manager
COWI Consulting Engineers and Planners AS
Parallelvej 2, 2800 Kongens Lyngby
E-mail: esl@cowi.dk

Birit Buhr
B.Sc. Senior Concrete Specialist
COWI Consulting Engineers and Planners AS
Parallelvej 2, 2800 Kongens Lyngby
E-mail: bbu@cowi.dk

Kirsten Eriksen
M.Sc. Senior Concrete Specialist
COWI Consulting Engineers and Planners AS
Parallelvej 2, 2800 Kongens Lyngby
E-mail: kie@cowi.dk

ABSTRACT

The present paper summarises 20 years of results on performance and durability of silica fume concrete. The edge beams of the Fiskebæk Bridge, cast in 1980-81, consist of a number of concrete types with varying contents of silica fume, fly ash and polypropylene fibres. Petrographic investigations showed complex changes in microstructure. It is seen a tendency of increased micro cracking with increased addition of silica fume and decreased water cement ratio. Investigation of chloride penetration showed that silica fume addition result in very dense concrete. The chloride ingress does not seem to follow the classic chloride diffusion.

Key words: chloride, edge beams, silica fume, fly ash, polypropylene fibres, long term performance, durability.

1 INTRODUCTION

1.1 General

The edge beams of the Fiskebæk Bridge was cast and placed in 1980-81, at the same time as the experimental bridge crossing the stream Ryå was planned. Experience from the Fiskebæk Bridge was used in proportioning the concrete to the Ryå bridge.

This article describes the results on durability and performance of different concrete mixes with various silica fume contents (from 10 to 50 % by weight of cement), air content and water/cement ratios. In addition, two reference mixes without silica fume were cast for comparison of the results.

From each type of concrete, 3-4 edge beams, 4.5 m long, were cast. After hardening, the beams were placed in position on the Fiskebæk Bridge (both on the east and west bridge), where they up until spring 2001 have been exposed to natural weathering and water spray containing de-icing salt during the winter time. In 2001, due to comprehensive rehabilitation and changes of the bridge superstructure, the edge beam elements were replaced by in-situ cast edge beams. Apart from 8 edge beam elements, 4 kept by COWI and 4 kept by The Technical University of Denmark, the remainder of the experimental elements was demolished.

Two major investigations have been carried out during the time since placing of the elements. The first study was in 1994 and reported in [11], and the second is the present study.

1.2 Objective

The objective of the investigation has been to

- evaluate the long term ingress of chloride over time using different concrete types with varying amounts of silica fume and fibers compared with concrete without silica fume and fibers
- evaluate the microstructure and development in microstructure over time

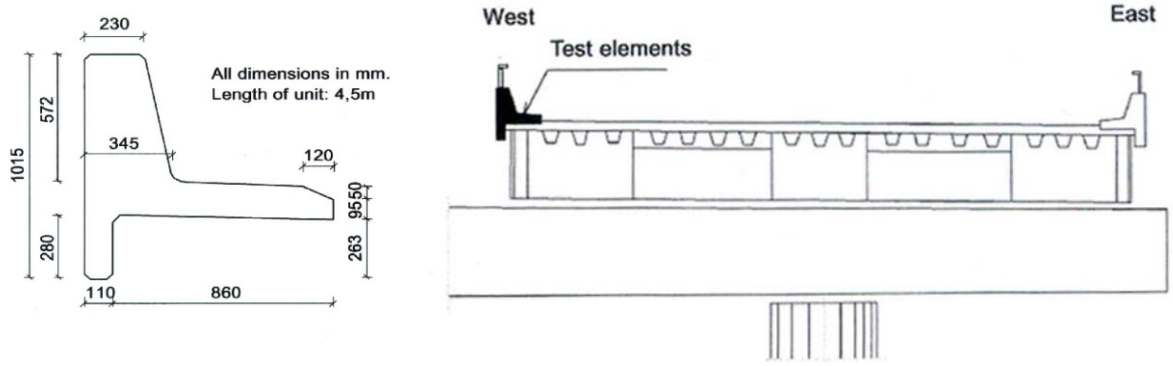

Figure 1 - Dimensions and placing of edge beam elements on the Fiskebæk (East) bridge.

Figure 2 - Eight experimental edge beam elements from the Fiskebæk bridges are still kept for further studies.

1.3 Test Programme

The Fiskebæk Bridge consists of an East bridge where the experimental edge beam elements were placed in 1980 and a West bridge where edge beam elements were placed in 1981. The elements had a similar geometry as the well-known New Jersey element. The test elements were all placed near the overtaking lane of the highway. This type of environment is normally considered as extremely aggressive (chloride, drying, water and freeze-thaw exposure).

When producing the 36 elements, 11 different concrete types were used with a varying amount of cement, air entrainment, silica fume, fly ash and fibers.

In table 1 the overall test program can be seen. Both in 1993 and 2001 cores were drilled. One Ø100 mm core was drilled from each of the 36 edge beams approx. 30 cm above ground level.

The concrete cores were sawn perpendicular to the surface allowing for a thin section to be prepared from part of the core and chloride profiles from the remainder of the core. The thin sections were placed perpendicular to the surface from 0-45 mm below the surface. In 1993 the rest of the core, approximately 100 - 200 mm long, was tested for compressive strength.

The chloride profile was obtained by profile grinding and sawing the core to varying depth below the surface. The chloride content was then determined on the dust collected according to COWI Concrete laboratory procedures which for all practical purposes correspond to DS 423.28 [8].

Table 1 - Overview of selected investigations.

	1980/81	1982	1983	1984	1986	1993	2001
Mechanical properties							
- Compression strength	!					!	
- E-modulus						!	
Petrographic investigations	!		!		!	!	!
Chloride intrusion							
- Profiles						!	!
- Bulk diffusion						!	
Freeze-thaw test	!						
Visual inspection	!	!		!	!	!	!

2 COMPOSITION OF CONCRETE

In Table 2 and 3, the concrete composition can be seen for the series cast in 1980 and 1981.

Ordinary low-alkali sulphate resistant Portland cement (CEM I) was used in all mixes. In all series silica fume from Norway was added as dry powder. Special investigations on the cement and silica fume were not carried out.

The content of alkali-reactive material in the fine aggregate was determined partly by mortar prism tests, partly by petrographic analysis. Both investigations showed that the content of alkali-reactive material was insignificant. Preliminary investigations of the stone aggregate proved that it was free from alkali-reactive particles.

Table 2 - Composition of edge beams cast in 1980 and placed on the East Bridge of the Fiskebæk Bridge [1], [2]. Average of three values.

Series		1	2	3	4	5
Silica fume per cement content		0 %	0 %	15 %	20 %	50 %
Cement (c)	[kg/m^3]	331	450	499	505	222
Fly ash (FA)	[kg/m^3]	0	180	224	0	0
Silica fume (SF)	[kg/m^3]	0	0	73	102	111
Fibre	[vol.%]	0	1.75	1.25	0	0
Water (w)	[kg/m^3]	125	259	180	112	99
Sand	[kg/m^3]	757	746	748	671	745
Aggregates 4/18 mm	[kg/m^3]	1135	319	499	1102	1335
Air entrainment	+/-	+	+	-	-	-
Air, measured	[%]	6.9	6.7	3.5	1.9	1.2
Plasticiser	+/-	-	-	+	+	+
Super plasticiser	+/-	-	+	-	-	-
Slump	mm	36	54	78	> 220	196
w/c		0.38	0.58	0.36	0.22	0.45
w/(c + FA + SF)		0.38	0.41	0.23	0.18	0.30
eq. w/c = w/(c + 0.4FA + 2SF)		0.38	0.50	0.25	0.16	0.22

Table 3 - Composition of edge beams cast in 1981 and placed on the West Bridge of the Fiskebæk Bridge [1], [2].

Series		A	B	C	D	E	F
Silica fume per cement content		10 %	20 %	17 %	10 %	20 %	0 %
Cement (c)	[kg/m^3]	300	345	296	295	241	347
Silica fume (SF)	[kg/m^3]	30	70	50	30	48	0
Water (w)	[kg/m^3]	125	120	129	128	115	145
Sand	[kg/m^3]	615	660	600	695	625	680
Aggregates 4/18 mm	[kg/m^3]	1210	1205	1200	1250	1245	1140
Air entrainment	+/-	+	-	+	-	+	+
Air, measured	[%]	6.3	1.7	5.7	1.7	4.8	6.6
Plasticiser	+/-	+	-	+	-	-	+
Super plasticiser	+/-	-	+	-	+	+	-
Slump	mm	64	79	80	59	65	80
w/c		0.42	0.34	0.44	0.43	0.48	0.42
w/(c + FA + SF)		0.38	0.29	0.37	0.39	0.40	0.42
eq. w/c = w/(c + 0.4FA + 2SF)		0.35	0.25	0.33	0.36	0.34	0.42

3 MECHANICAL PROPERTIES

Compressive strength was tested on all concrete types after 28 days of water curing on cast cylinders Ø 150 x 300 mm. The results are presented in table 4.

In 1993 an investigation on drilled cores was carried out on the Danish Technical University. Three drilled cores (Ø 100 mm x 200 mm) from each type of concrete were tested in a deformation controlled testing machine and consecutive data on compression and deformation of the test specimen were recorded. The idea was to obtain information of the material ductility and elasticity.

The results showed stress-strain curves with indications on crack formation during the test [11]. These indications of cracking were noise, different form normal testing and slightly curved (and scattered) stress-strain relationships. However, it was possible to determine the maximum compressive strength and modulus of elasticity from the results. The strength results from the 1993-test were adjusted according to [12] for comparison to the compressive strength results (28-day) from 1981/82.

*Table 4 - Compressive strength and E-modulus. Average values of three test specimens (standard deviation in brackets). * Indicates that only two specimens were tested.*

	Series	1	2	3	4	5	A	B	C	D	E	F
	Silica fume content	0 %	0 %	15 %	20 %	50 %	10 %	20 %	17 %	10 %	20 %	0 %
1981/82 Cylinders	28-day compressive strength (MPa)	67 (2)	25 (3)	83 (10)	132 (6)	104 (4)	54 (2)	74 (2)	55 (1)	59 (2)	54 (3)	39 (2)
	Cube strengths ¤	*80*	*30*	*100*	*158*	*125*	*65*	*89*	*66*	*71*	*65*	*47*
1993 Cores	Compressive strength (MPa)	70 (16)	41 (8)	89 (3)	79* (13)	95 (17)	37* (8)	53 (8)	46 (3)	60* (6)	56 (10)	49 (11)
	E-modulus (GPa)	50 (6)	33 (6)	37 (2)	57* (10)	51 (5)	56* (7)	36 (11)	36 (11)	44* (9)	51 (10)	31 (6)

¤: Converted from the measured cylinder strength according to the introduction in the proceedings.

4 MICRO CRACKS

Micro cracks defined as cracks of width less than 10 μm in the paste or in the adhesion zones along aggregate were counted on thin sections. In each section, 10 visual fields of 5.8 mm^2 each were counted, where aggregate accounted for less than 50 % of the field. The magnification used was 63, and fluorescent light was used.

The coefficient of variation for repeated counts on a section is typically 20-25% with 10 fields per repetition. This relatively high value results from the uneven distribution of cracks and the variation in the proportion of the field taken up by aggregate. To reduce the variation coefficient it would be necessary to count a greater number of fields per section.

In the investigated sections from 1993, which included one section from each unit and 3 units per series, variation coefficients within a series (3 sections, one count per section) were found to be practically the same as those found by repeated measurements on the same section. It can therefore be assumed that each series can be considered as uniform with respect to number of micro cracks. However, the counting in 2001 showed large variations in the counting when compared to the counting in 1993. Also deviations between the personal and the used equipment is seen. These errors are still under discussion and improvement of the method is necessary. But the counting can be used as an relative measure when personal and equipment used is the same.

The counting of micro-cracks has the limitation, that the lengths and pattern of micro-cracks are not registered, i.e. the same result for the number of micro-cracks in two concrete types does not necessarily mean that they have the same micro crack pattern. In one case the cracks may be short and isolated, in the other longer and connected. An adequate method of describing the crack pattern is still lacking. In figure 4, examples are presented on the crack patterns of the different silica concrete types is shown.

In figure 3 the number of paste cracks (average values) is plotted against the silica content. It can be seen that the number of cracks is roughly proportional to the silica content. The number of cracks in series 4 and 5 (not shown in the figure) are at a lower level than the other mixes, but differ from them in having an extremely low water/powder ratio. For these mixes, the rate of crack development is lower than for the others. This can be interpreted as an effect of the low water/powder ratio, resulting in the formation of many micro cracks soon after casting, while free water was still available. It is anticipated that the reactions almost came to a standstill later, due to lack of water in the concrete.

A tendency of development of paste cracks with time has also be seen. For instance the concrete types with silica addition, all with air entrainment have approximately 0.5 cracks/mm^2 at 28 days. After 5 years (or earlier) the number of cracks have increased and there is some indication of a linear development with age in the first few years, but this is still unclear. After 20 years the development of cracks seems to have stopped at a level of 3-5 cracks/mm^2. The number of cracks in silica fume concrete is approximately twice the number of cracks in concrete without silica fume addition.

The number of paste cracks also seems to be dependent of the water/powder ratio. The results show a tendency for the number of paste cracks to decline with increasing equivalent water cement ratio.

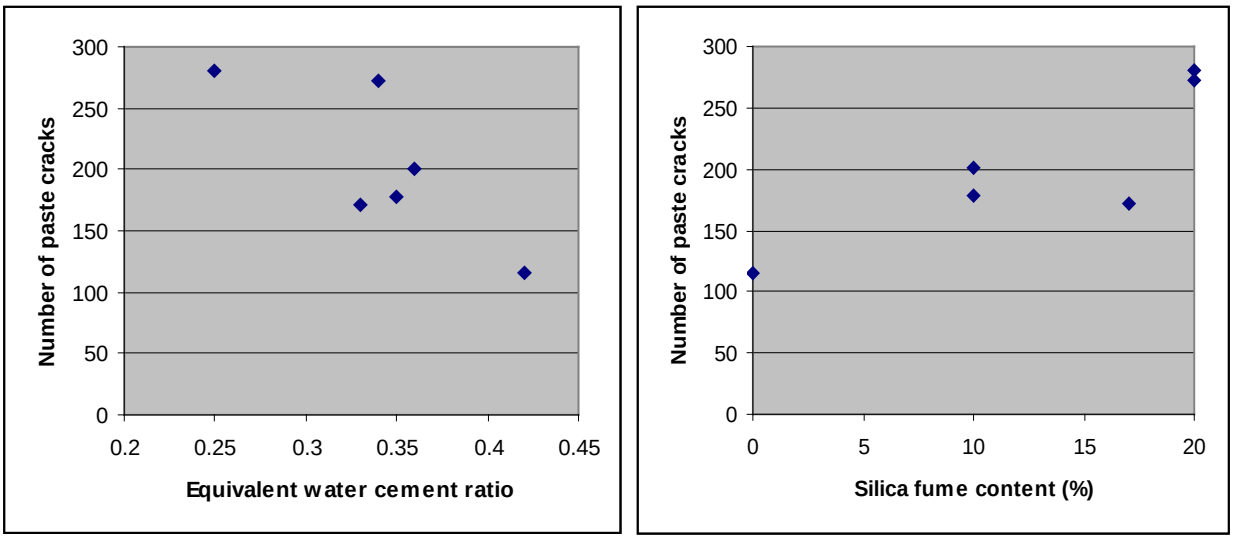

Figure 3 - The number of paste cracks as function of silica content and the equivalent water cement ratio. Series A - F are shown. The number of cracks is measured per 58 mm^2 concrete area. The counting is an average of three thin sections.

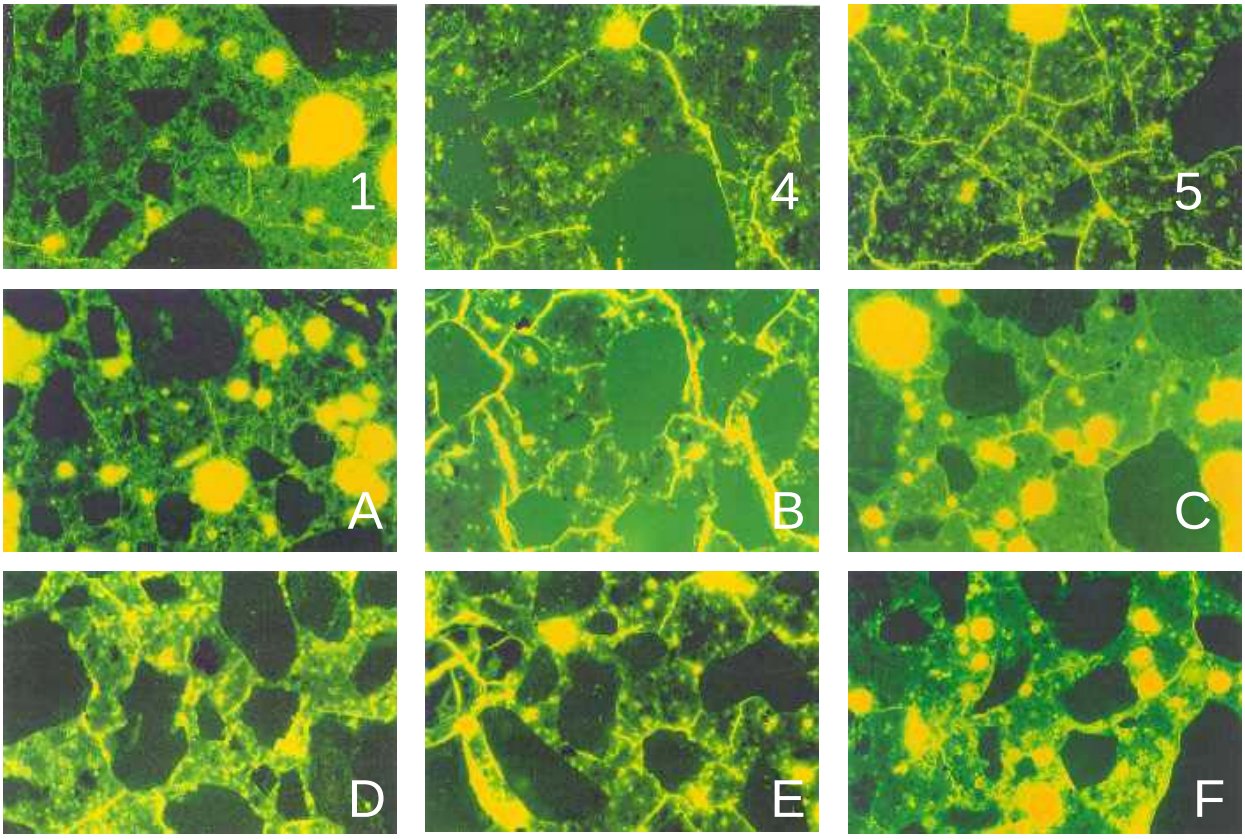

Figure 4 - Examples on crack patterns of the different silica concrete types.

5 CHLORIDE INGRESSION

5.1 "The Block"

The general impression is that very few chloride profiles show even approximate agreement with Fick's second law. In series A to F, all cores have a lower chloride content in the outermost mm of the concrete than at greater depths. Examples are shown in figure 6.

Cores from all the series in both 1993 and 2001 showed a chloride content that was quite low. The silica concretes showed a tendency to have a relatively high chloride content in the first few millimetres below the concrete surface; with increasing depth, the content rapidly fall to zero.

Comparing the calculated apparent surface chloride concentration for the concrete is compared with the measured surface concentration reveals the error that arises in approximating Fick's second law. The modification of Fick's second law involves the outermost chloride measurement, usually being omitted, when calculating the chloride diffusion coefficient.

Diffusion coefficients compared with the water/powder ratio show that the magnitude of the chloride diffusion coefficient depends on the paste porosity which is hardly surprising. A lower water/powder ratio gives a lower diffusion coefficient, but also the addition of silica reduces the chloride penetration. The classical dependence of permeability on the water/powder ratio is shown most clearly when the activity factor for silica is in the range 1 to 3.

The extent of the micro-cracks may have a weak influence on chloride penetration in a given cross-section. In figure 5 a comparison of series 4 and 5, which have much the same water/powder ratio and are very dense concrete types, shows that series 5 has three times as many micro-cracks as series 4. The cracks in series 5 form a continuous network, unlike those in series 4; series 5 has a chloride diffusion coefficient approx. 5-10 times that of series 4. Although the chloride contents are quite low, the penetration depth in series 5 is significantly deeper than in series 4. The chloride profiles for series 4 shows that there is practically no chloride below a depth of 5 mm. The chloride content in the outermost few millimetres, however, is much higher for series 4 than for series 5. It seems likely that the higher cement content and the lower silica content in series 4 are the causes of the greater extent of chloride binding near the surface.

The general impression from a review of the chloride profiles is that the silica concrete types show an almost "block like" uptake of chlorides in the outermost millimetres. The chloride content then falls rapidly to zero, typically over a distance of 10-15 mm. The outer part of the concrete (the "block") is the zone directly affected by moisture from the surroundings (e.g. capillary suction and/or adsorption), with or without salt, wash-out, drying out, liquid and salt transport in cracks etc. The concrete below this surface block typically has a more uniform environment with a relative humidity dependent on the distribution of pore sizes in the paste and the humidity of the surroundings. The chlorides are transported in the fine water-filled pores (adsorbed water-film) in the cement paste, the rate of transport depending on the given relative humidity. Below the surface block, micro cracks, fine cracks or large pores in the paste will have no significant effect, as they will be empty. Furthermore, their surface area is small in relation to that of the fine paste pores.

As an example, series A, C, D and F that have approximately the same w/(c + 2s) ratio, show the same chloride penetration pattern after the estimated depth of the block has been deducted. The depth of the block appears to vary inversely with the amount of silica added to the concrete.

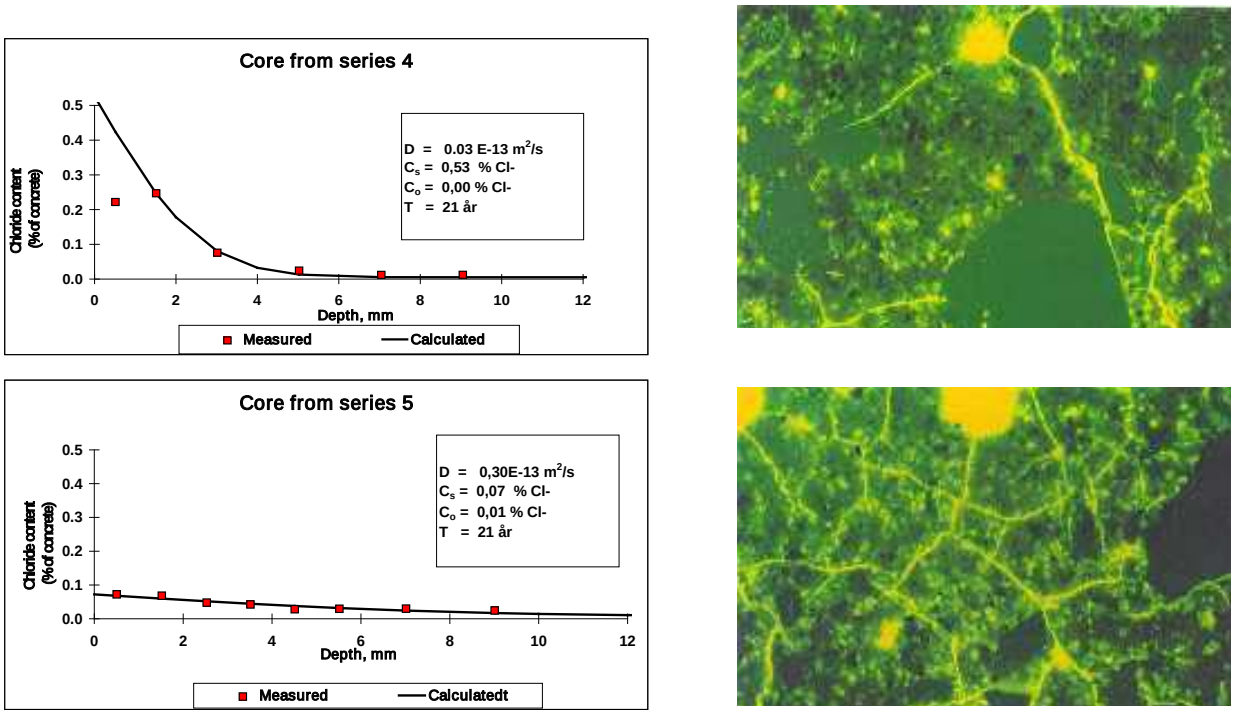

Figure 5 - The influence of cracks on the penetration depth of the chlorides.

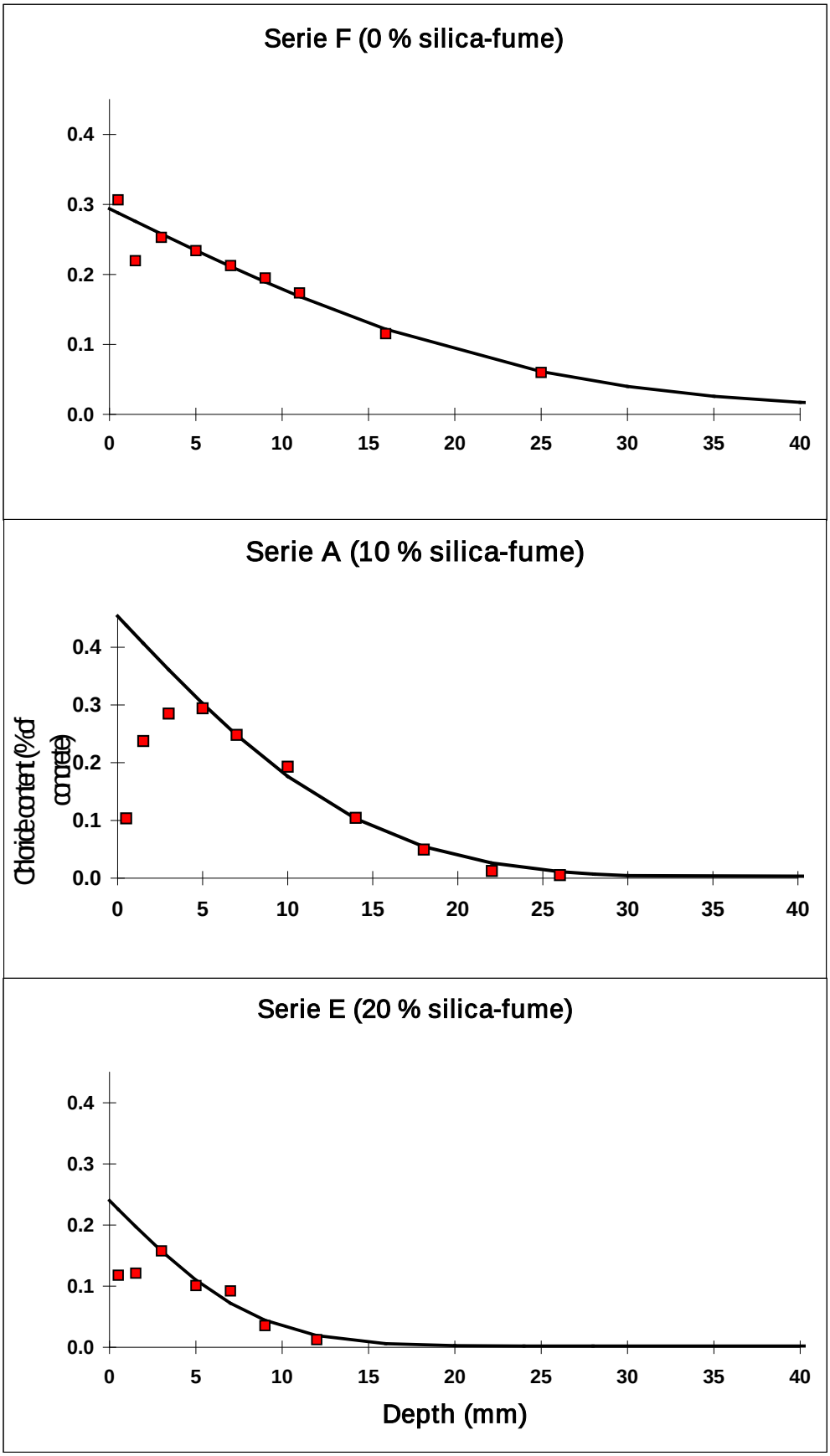

Figure 6 - Examples on chloride profiles after 21 years of natural exposure of weathering and de-icing salt at winter time.

5.1 Diffusion Properties

Despite the reservation with respect to Fick´s 2nd law of diffusion the diffusion parameters were calculated using Fick´s 2nd law of diffusion [9] expressing the chloride ingress mathematically. The initial chloride content, C_0 has been fixed corresponding to the actual measured background chloride content in the core in question (varying between 0.002 and 0.012 % Cl^- by weight of concrete). Two, one or no chloride content results have been omitted when performing the calculations. The best curve fit has been used for the reported diffusion properties.

In Table 5 the average diffusion parameters given by the diffusion coefficient, D, and the surface chloride concentration, C_s, can be seen after 21 years (West Bridge) of exposure and after 14 years of exposure [6]. In Table 6 the average diffusion parameters given by the diffusion coefficient, D and the surface chloride concentration, C_s, can be seen both after 20 years (East Bridge) of exposure and after 13 years of exposure [6].

In Figure 7 the depth corresponding to 0.10 % Cl- by weight of concrete can be seen versus the silica fume content in %.

In Figure 8 the diffusion coefficient, D versus the silica fume content can be seen.

In Figure 9 the surface concentration Cs versus the silica fume content can be seen.

For most Portland cements, the diffusion coefficient is expected to decrease in time. However the low-alkali-sulphate-resistant cement, as used in the Fiskebæk edge beams, is expected to have a low chloride binding capacity and thus a limited decrease in expected diffusion coefficient with time. Previous investigations show that the decrease in chloride diffusion over time is limited when compared to the random variation in concrete characteristics for bridges older than approx. 15 years where low alkali sulphate resistant cement has been used [10].

Table 5 - Diffusion properties for concrete types exposed since 1980 on the East Bridge of the Fiskebæk Bridge. Average values of three measurements given.

Series	Micro Silica per cement content	eq. w/c	Air (+/-), Fibre (%vol), Fly Ash (%)	Exposure time (Years)	Diffusion coefficient, (Factor 10^{-14} m^2/s)	Surface concentration, (% Cl^- by weight of concrete)	Depth corresponding to 0.10% Cl^- by weight of concrete (mm)
1 [1)]	0 %	0.38	+, 0, 0	14	8 +/- 2 [1)]	0.32 +/- 0.18	7 +/- 6
				21	19 +/- 11	0.33 +/- 0.09	16 +/- 6
2	0 %	0.50	+, 1.75, 40	14	20 +/- 8	0.51 +/- 0.14	16 +/- 4
				21	26 *	0.54 *	27 *
3	15 %	0.25	-, 1.25, 45	14	1 +/- 0	0.46 +/- 0.25	3 +/- 1
				21	2 +/- 1	0.42 +/- 0.12	5 +/- 2
4	20 %	0.16	-, 0, 0	14	0 +/- 0	0.38 +/- 0.09	2 +/- 0
				21	1 +/- 2	0.43 +/- 0.30	2 +/- 2
5	50 %	0.22	-, 0, 0	14	2 +/- 2	0.09 +/- 0.06	1 +/- 1
				21	4 *	0.10 *	2 *

** Indicates average of two values only*

1) Calculations omitting one and two results from one of the three chloride profiles result in calculated diffusion coefficients of 12 and 23 10^{-14} m^2/s, respectively. Omitting two results yield a better curve fit than not omitting any results

Table 6 - Diffusion properties for concrete exposed since 1981 on the West Bridge of the Fiskebæk Bridge.

Series	Micro Silica per cement content	eq. w/c	Air (+/-)	Exposure time (Years)	Diffusion coefficient, (Factor 10^{-14} m^2/s)	Surface concentration, (% Cl- by weight of concrete)	Depth corresponding to 0.10% Cl- by weight of concrete (mm)
A	10 %	0.35	+	13	18 +/- 4	0.51 +/- 0.07	16 +/- 1
				20	15 +/- 3	0.40 +/- 0.08	16 +/- 2
B	20 %	0.25	-	13	3 +/- 1	0.46 +/- 0.09	6 +/- 1
				20	4 +/- 2	0.42 +/- 0.03	8 +/- 3
C	17 %	0.33	+	13	18 +/- 11	0.34 +/- 0.14	11 +/- 2
				20	14 +/- 5	0.39 +/- 0.03	15 +/- 2
D	10 %	0.36	-	13	14 +/- 3	0.48 +/- 0.06	14 +/- 2
				20	15 +/- 5	0.40 +/- 0.11	15 +/- 2
E	20 %	0.34	+	13	9 +/- 4	0.39 +/- 0.09	10 +/- 3
				20	7 +/- 4	0.26 +/- 0.07	7 +/- 4
F	0 %	0.42	+	13	36 +/- 16	0.33 +/- 0.01	18 +/- 4
				20	55 +/- 39	0.31 +/- 0.03	26 +/- 9

The thin section analysis of the C-series show that the silica fume formation of lumps in the paste. This poor dispersion of the silica fume may be an explanation of the relative high diffusion coefficient compared to series E.

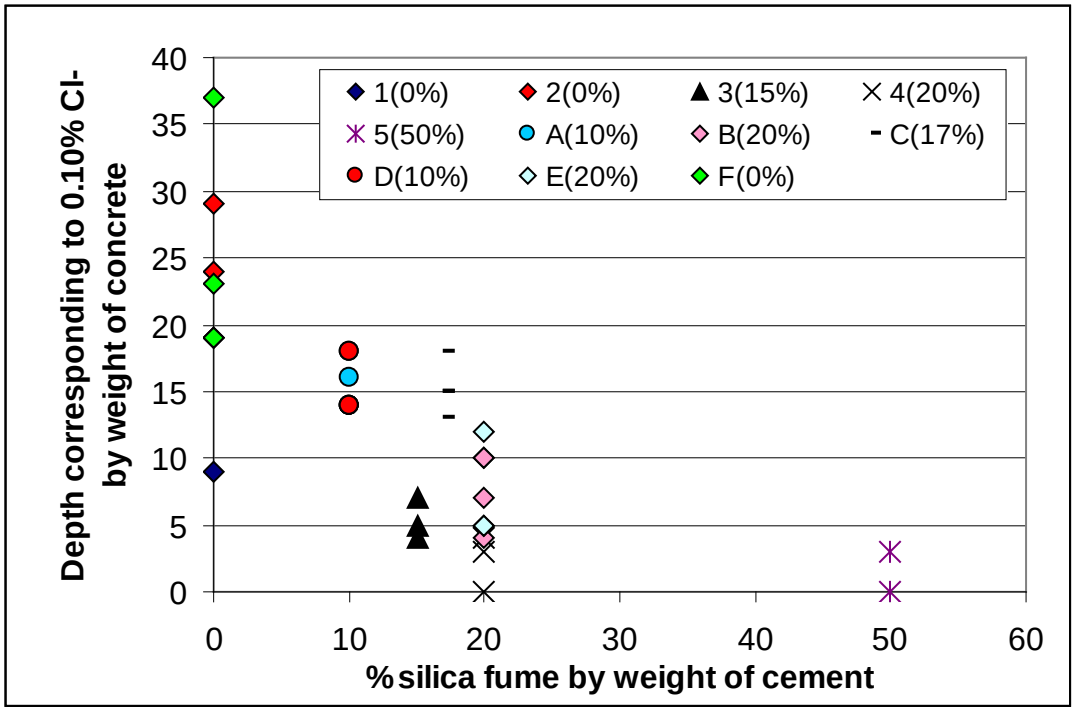

Figure 7 - The depth corresponding to 0.10 % Cl- by weight of concrete versus the silica fume content in % by weight of cement. It shall be noted that series 2 and 3 contain 1.75 and 1.25 % vol. of fibres and series 3 also fly ash.

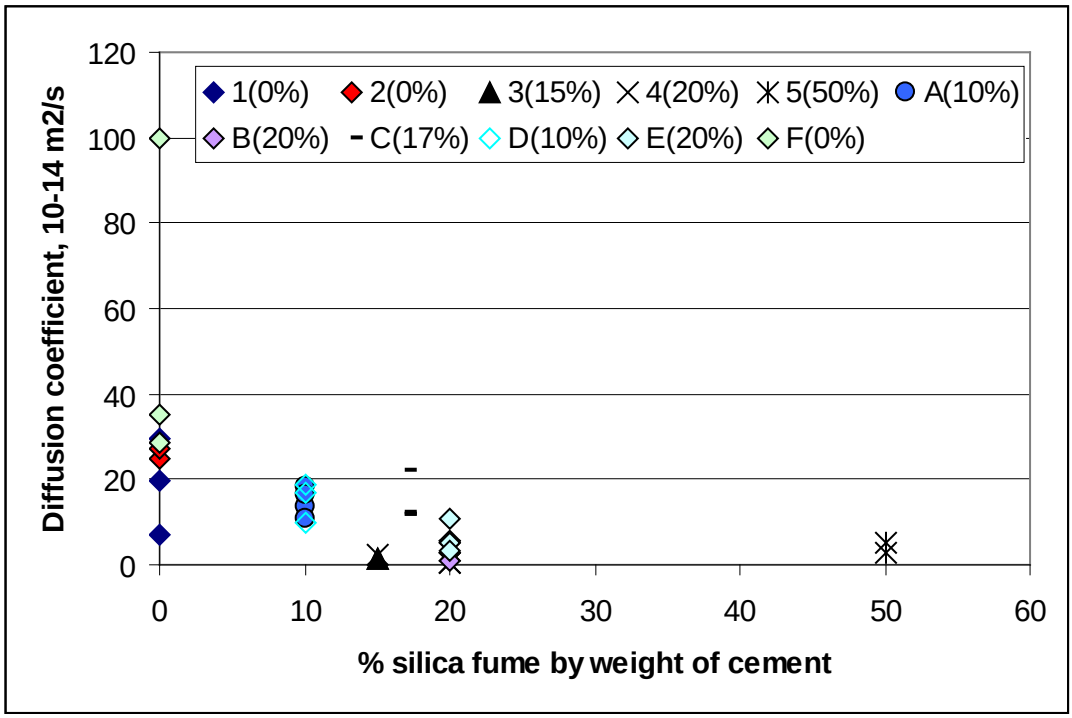

Figure 8 - The diffusion coefficient, D versus the silica fume content by weight of cement. It shall be noted that series 2 and 3 contain 1.75 and 1.25 % vol. of fibres and series 3 also fly ash.

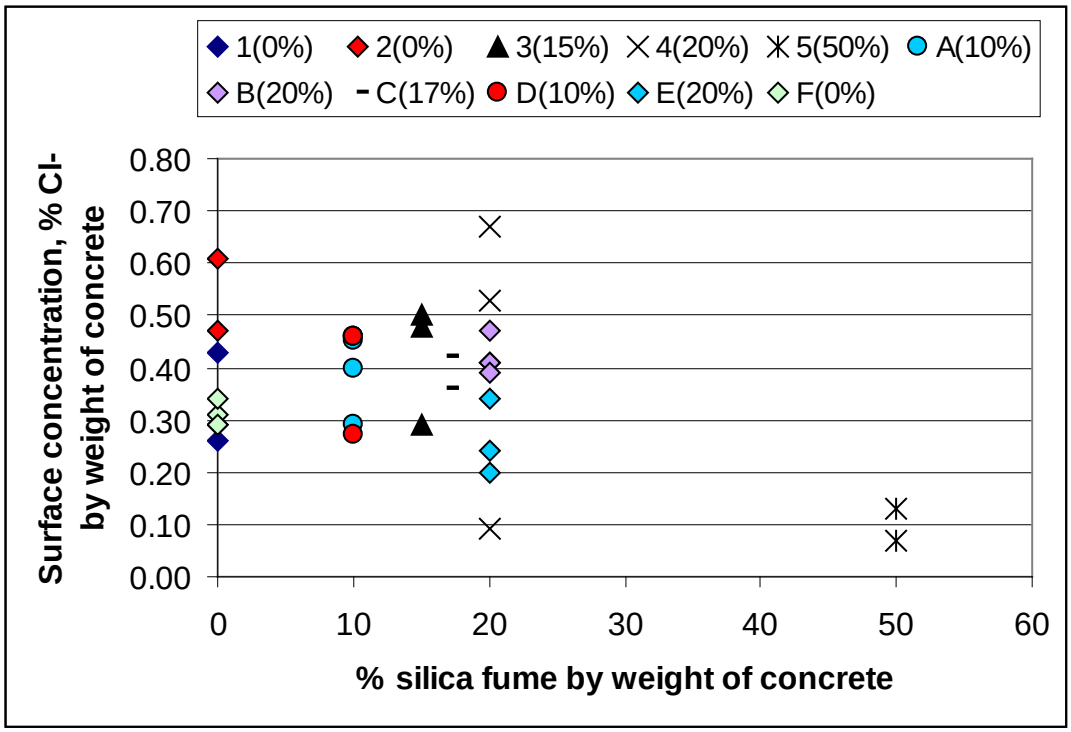

Figure 9 - The surface concentration, Cs, versus the silica fume content by weight of cement. It shall be noted that series 2 and 3 contain 1.75 and 1.25 % vol. of fibres and series 3 also fly ash.

5.3 Bulk Diffusion Test

Bulk diffusion tests (according to [13]) were carried out in 1993 on drilled cores from series A, E and F, with 10%, 20% and 0% silica fume respectively; all had entrained air. The tests were carried out at such a depth in the cores that they were chloride-free at the start.

The chloride profiles for the three cores after chloride bulk diffusion exposure show that the addition of silica fume and low paste porosity has a beneficial influence on chloride penetration. The bulk diffusion tests show diffusion coefficients from 4 to 60 times higher than those of the specimens subjected to natural exposure. This is probably related to the fact that it is not strictly chloride diffusion (water saturated condition) that occurs under natural exposure without water saturation, but a composite and much more complex form of chloride penetration. The bulk diffusion coefficients for series F are 35 times higher than those for series A and E. The in-situ coefficients for series F are 2-4 times higher than those for series A and E.

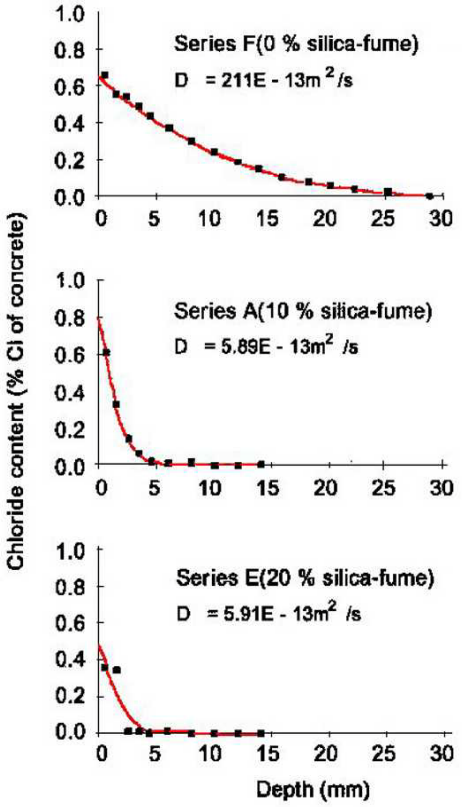

Figure 10 - Chloride intrusion profiles after bulk diffusion.

It is this difference that should be stressed. In the bulk diffusion tests the concrete types were water saturated, and chloride ions can be transported by all pores and cracks. The in-situ concrete types were saturated only occasionally in the outermost 5-10 mm (the "block"). In addition, as mentioned above, a fairly constant environment presumably exists with a relative humidity determined by the surroundings and the pore-size distribution (w/c ratio, self-desiccation, etc.). For the in-situ specimens, there is no great difference between series F and series A and E, where small pores are water- filled (by adsorption), while any large pores are empty. The transport of chlorides into the concrete took place in the small water-filled pores in series A, E and F, and can easily be of the same order of magnitude in the three cases. But it is practically certain that series F had larger pores than A and E due to higher capillary porosity. But as long as these pores are empty they do not affect the transport. It is only when the concrete is brought into water saturated condition that the influence of the large pores in F is marked.

Table 7 - The results of chloride intrusion in-situ compared with bulk diffusion.

	In-situ						Bulk Diffusion		
	D_{Cl} 10^{-14} m²/s		$C_{S,\ Calculated}$ (% Cl)		$C_{S,\ Measured}$ (% Cl)		D_{Cl} 10^{-14} m²/s	$C_{S,\ Calculated}$ (% Cl)	$C_{S,\ Measured}$ (% Cl)
Series	1993	2001	1993	2001	1993	2001			
F (s/c = 0%)	35	35	0.3	0.3	0.2	0.3	2100	0.6	0.6
A (s/c = 10%)	15	19	0.6	0.4	0.2	0.1	60	0.8	0.6
E (s/c = 20%)	9	11	0.5	0.3	0.2	0.1	60	0.5	0.4

5 VISUAL INSPECTION

The edge beam elements on Fiskebæk Bridge were visually inspected immediately after casting in 1980/81, and again in 1981, 1982, 1983, 1984, 1986, 1994 and 2001.

The units of series A to F were inspected after erection in December 1981. No signs of deterioration were observed. The units were again inspected in April 1982, after one winter exposure. Surface spalling was observed on several units, but was confined to the thin paste layer over the aggregate.

The general conclusion is that after 14 years of exposure in a highly aggressive environment, none of the concrete types investigated have developed sufficient signs of deterioration to justify describing it as non-durable.

6 CONCLUSIONS

After the first winter exposure, several edge-beam units showed minor surface spalling, which was confined to the paste layer over the aggregate; more severe signs of deterioration was not observed. The spalling increased only slightly subsequently, and the durability of the units is therefore considered satisfactory.

The results of the petrographic investigations show a highly complicated micro-structure with regard to paste homogeneity as well as extent and pattern of micro-cracking. The investigations of the silica-fume concrete types point to the following tendencies: The extent of micro cracking continues to increase with time and the silica content is correlated with number of micro cracks.

The investigations also show that silica-concrete is highly impervious to chloride penetration. Fick's second law does not account for the chloride profiles in the cores drilled after 14 and 21 years exposure, indicating that a more complex penetration mechanism has operated. Very low diffusion coefficients for silica concrete are obtained when the calculation is based on Fick's second law.

The results of the accelerated bulk diffusion tests also show that there is a much higher difference in chloride penetration in a water saturated environment between concrete with silica fume addition and a reference concrete than found under in-situ conditions without water saturation.

ACKNOWLEDGEMENT

The present study has been funded by the Danish Road Directorate and Elkem A/S.

A special thank is given to Dr. Per Fidjestøl for fruitful discussions during the project.

REFERENCES

1. COWIconsult, "Forsøg med kantelementer af fiber- og silicabeton, Rapport over forundersgøelser og udførelse", Vejdirektoratet, 1980
2. COWIconsult, "Forsøg med kantelementer af silicabeton, 1981 - Rapport over founrdersøgelser og udførelse", Vejdirektoratet, 1982
3. Teknologisk Institut, "Fiberbetonelementer m.v. sag nr. 251.3536, Teknologisk Institut, 1980
4. Larsen et al. Vejdirektoratet, "Rapport nr. 6, Ry Å broen - Forsøg med silicabeton - egenskabsudvikling 1981-1993, Vejdirektoratet, 1993
5. Afdelingen for Bærende konstruktioner "Deformationsstyret trykprøvning af udborede betoncylindre - vejdirektoratet"
6. COWIconsult, "Firskebækbroen - chloridindtrængning i kantelementer - datarapport", 1994, Vejdirektoratet
7. Dansk Teknologisk Institut, "Beregning af temperatur og spændinger for kantelementer til Fiskebækbroen". Brev dateret 25/11-1994
8. DS 423.28. Betonprøvning. Hærdnet beton. Chloridindhold.
9. HETEK report no. 53. Chloride penetration into concrete - State of the Art, The Danish Road Directorate, 1997.
10. E. Stoltzner, B. Buhr, S. Engelund: The Faroe Bridges. Chloride Penetration rate estimated on a basis of measurements from 1988 to 1997, Fifth CANMET/ACI International conference on Durability of concrete, Barcelona, Spain, June 2000
11. E. S. Larsen, K. Eriksen: Erfaringer med anvendelse af mikrosilikabeton - Fiskebækbroens kantelementer. Rapport 20, Vejdirektoratet, 1995.
12. Beton Bogen, Aalborg Portland/Cto, 2nd edition, 1985.
13. NT BUILD 443 Concrete Testing - Hardened Concrete - Chloride Penetration (APM 302).

A Comparison of Chloride Ingress in Densit® Materials and Traditional Cement Based Materials.

Bjarne W. Mikkelsen
Ph.D., Project manager
R & D Department, Densit A/S
Rørdalsvej 44, DK-9100 Aalborg.
E-mail: bwm@densit.dk

ABSTRACT

In relatively porous materials like spraying mortar the chloride diffusion coefficient in Densit® products is roughly half the diffusion coefficient in comparable spraying products. In less porous materials the difference between Densit® products and conventional products becomes more pronounced and in pure pastes the chloride diffusion coefficient is approximately 2,5 order of magnitude (350 times) higher in conventional ordinary Portland paste than in Densit® paste.

Key words: Case stories, Chloride, Densit®

1. INTRODUCTION

The most common causes of corrosion of reinforcing steel are carbonation and chloride attack. Generally, all high quality concrete based on Portland cement can provide excellent corrosion protection for steel because of the inherent high pH of the cement pore water solution.

In general reinforcing steel enclosed in concrete is not exposed to corrosion because the pH value in the local environment is high enough to prevent corrosion from taking place. One exception is when chloride ions are present. Even though a passive film protects the steel a sufficient high concentration of chloride ions (at the pitting potential) can (and will) break through the film and attack the steel. To obtain long durability and avoid failure of a concrete construction in environment where chloride ions are present it is beneficial to use concrete with a high resistance against chloride ion diffusion in order to protect the reinforcing steel from corrosive attack.

Based on case stories this paper deals with comparisons of conventional high quality cement products and Densit® products with respect to chloride diffusion. Densit® products are characterised by a binder consisting of Portland cement (type CEM I according to EN 197-1) Silica fume and a superplasticizer. Silica fume and superplasticizer reduce the water demand (water-binder ratio is always below 0,3) with the consequence that harden material posses a very dense structure with high density and a compressive strength in the range 100 –350 MPa. Actually, the weakest part of Densit® mortar is the aggregate.

2. CASE STORIES

In the following five cases are presented. All case stories deals with chloride diffusion in Densit® materials compared to other more conventional cement based materials. Different types of materials (Spraying mortars, castable mortars and pastes) and different methods (profile grinding, double cell technique and Electron Probe Micro Analysis) are used in the selected case stories. Also, The case stories represent a span in time since the oldest case story is dated 1983 and the latest is dated 1998.

2.1 Tests at the Danish Corrosion Centre in 1983.

In 1983 Carolyn M. Hansson, The Danish Corrosion Centre [1] published a report where chloride penetration was investigated in a Densit®-like material and a Sulphate resistant Portland cement (SRPC) (type CEM I according to EN 197-1). The Densit®-like material was composed using the same SRPC as the one used as reference.

Table 1. - The recipes used for the test at the Danish Corrosion Centre in 1983.
** $w/c = w/(c + 2*SiO_2)$.*

	Densit®-like paste	Densit®-like mortar	SRPC paste	SRPC mortar
SRPC	1,00	1,00	1,00	1,00
Microsilica	0,20	0,24	-	-
Superplasticizer	0,025	0,03	-	-
Water	0,18	0,18	0,30	0,30
w/c *	0,129	0,129	0,30	0,30
Quartz sand 0-4 mm	-	1,80	-	3,0

Densit®-like cement pastes with w/c ratios of 0,129 and SRPC paste with w/c ratio of 0,300 was used for the investigation of chloride penetration by means of the double cell technique. Slices, 2-3 mm in thickness were placed as a “membrane” to separate the two cells. One cell was filled with 22,5 ml saturated $Ca(OH)_2$ solution, while the second cell contained a 1 M NaCl solution saturated with $Ca(OH)_2$. Periodically, 0,1 ml of solution was removed from the first cell and analysed for chloride ion content.

Two sets of samples were tested at room temperature. One set was prepared seven weeks after casting having been kept under water the whole time. The second set was kept in the laboratory atmosphere for additionally two weeks.

The test was monitored during four month. While measurable chloride concentrations penetrated the SRPC within a few days, the chloride ions penetrating through the Densit®-like samples remain within the level of uncertainty of the analysis method (approx. 50 ppm) for the whole period.

Additional tests was performed at 40 °C and 50 °C with no effect on the Densit®-like samples while an increased chloride ion penetration was observed in the SRPC samples as shown in figure 1.

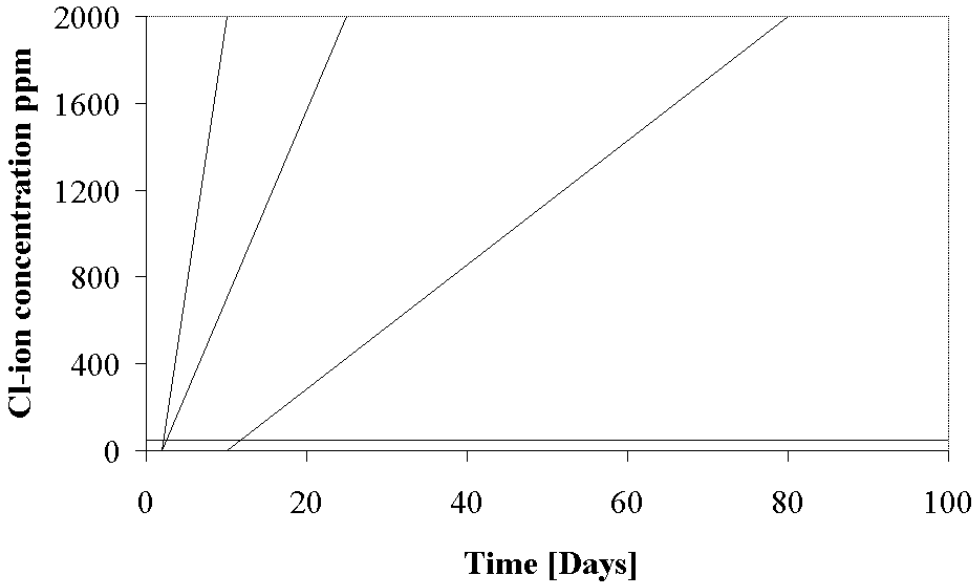

Figure 1 – Concentration of Chloride ions penetrating SRPC and Densit®-like paste at the temperatures shown.

To determine whether the sand/cement interface could be an easy path for chloride diffusion, tests were made at 60 °C on mortar (for the recipes see table 1) samples of Densit®-like material and SRPC. After 13 month the chloride ion concentration in three of five measuring cells with Densit®-like samples was just detectable (20 – 60 ppm). In the last two measuring cells with Densit®-like sample chloride ions was not detected.

From the obtained measurements, approximate values of the maximum limit of the effective diffusion coefficient of chloride ions through Densit®-like material and SRPC have been calculated and are given in table 2.

Table 2. – Effective chloride ion diffusion coefficients obtained by the double cell method.

Material	w/c	Temp. °C	D m^2/sec
Densit®-like paste	0,129	22	$< 0{,}2\ 10^{-13}$
Densit®-like paste	0,129	40	$< 0{,}2\ 10^{-13}$
Densit®-like paste	0,129	50	$< 0{,}2\ 10^{-13}$
Densit®-like mortar	0,129	60	$< 0{,}1\ 10^{-13}$
SRPC paste	0,3	22	$11\ 10^{-13}$
SRPC paste	0,3	40	$34\ 10^{-13}$
SRPC paste	0,3	50	$80\ 10^{-13}$
SRPC mortar	0,3	60	$120\ 10^{-13}$

2.2 Tests at Force Institute in 1992.

In 1992 Force Institute [2] made an investigation of chloride ingress and carbonation in two materials a Densit® material and a reference material based on Ordinary Portland Cement (OPC) (type CEM I according to EN 197-1). The recipes for the two materials are shown in table 3.

Table 3 – The recipes and some properties for the Densit® material used in the Force Institute Case.

	Densit® material	OPC
Densit® Tix binder	30,0 kg	
OPC		30,0 kg
Quarts sand 0-2,2 mm	70,0 kg	70,0 kg
Water	7,5 kg	12,0 kg

After casting the test specimens was stored under water at 20 °C for 28 days. Hereafter chloride penetration measurements were performed in accordance with NT BUILD 443.

Two Densit® material test specimens and one reference test specimens were exposed at 23 °C in water containing 165 g NaCl per litre water for 84 days. After exposure the surface was milled in steps of 1 mm until a depth of 10 mm was milled away and powder milled away in each step was analysed. Also a single step at the depth of approximately 45 mm was analysed. The results are shown in figure 2.

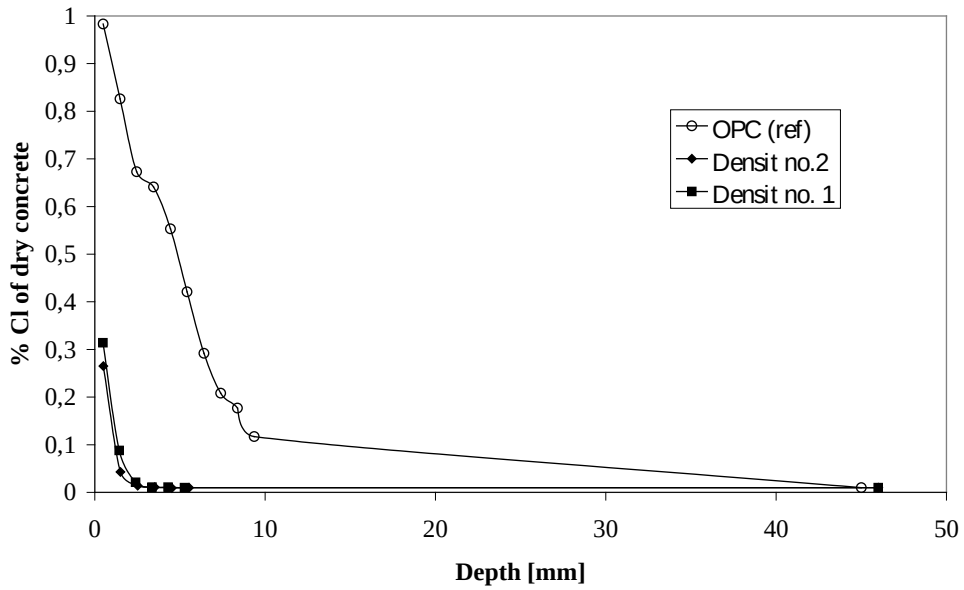

Figure 2 – Measured values of chloride content in Densit® samples and OPC (ref) at different depths.

Based on the measurements the diffusion coefficients are calculated (shown in table 4).

Table 4 – The calculated Diffusion coefficients for the Densit® material and OPC used.

Specimens	D [m^2/sec]	C_S [%]	C_0 [%]
Densit® No 1	$7{,}4\ 10^{-14}$	0,48	0,01
Densit® No 2	$4{,}8\ 10^{-14}$	0,48	0,01
OPC (ref)	$255\ 10^{-14}$	1,04	0,01

2.3 Tests at Force Institute in 1998.

In 1998 Force Institute made an investigation of chloride ingress in a Densit® material. As reference the data from the test performed on Ordinary Portland cement (OPC) (type CEM I according to EN 197-1) in 1992 was used. The composition of the Densit® material is shown in table 5. The chloride diffusion coefficient was determined in accordance to the Nortest method NT BUILD 443.

Table 5 – Composition and some data of the material used in the tests.

	Densit® material
Densit® binder	19,5 kg
Quarts sand 0-2 mm	31,1 kg
Granite 2-5 mm	49,4 kg
Water	4,8 kg
Air content	2,5 %
Density	2507 kg/m^3
Slump	40 mm
Vebe	6 sec.
Comp. Strength 23h@80°C	148 ± 2 MPa

Two Densit® material test specimens was exposed at 23 °C in water containing 165 g NaCl per litre water for 84 days. After exposure thin layers were ground stepwise and parallel with the exposed surface (10 steps of 0,5 mm). Additionally two samples were taken from the bulk concrete. The results are shown in figure 3.

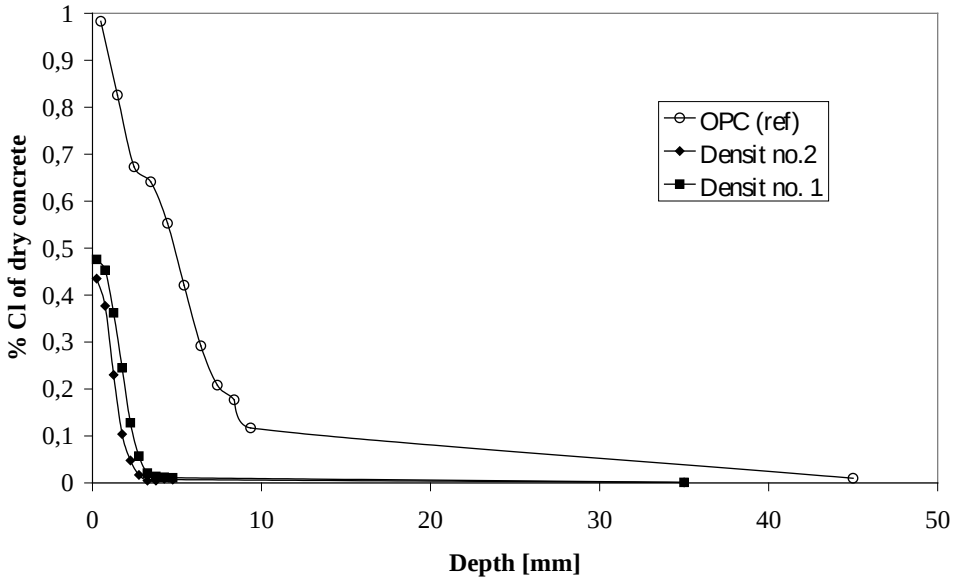

Figure 3 – Measured values of chloride content in Densit® samples and OPC (ref) at different depths.

Based on the measurements the diffusion coefficients are calculated (shown in table 6).

Table 6 – The calculated Diffusion coefficients for the Densit material and OPC used.

Specimens	D [m^2/sec]	C_S [%]	C_0 [%]
Densit® No 1	20,0 10^{-14}	0,72	0,001
Densit® No 2	10,6 10^{-14}	0,70	0,001
OPC (ref)	255 10^{-14}	1,04	0,01

2.4 Mandal City Bridge, Norway.

In 1997 Kjell Løland et. al. [4] reported test results from a pilot project where three different products were compared with respect to chloride diffusion. The aim of the pilot project was to give the necessary facts to decide which product should be used for rehabilitation of the Mandal City Bridge. The three products were Ducorit® Spraying Mortar 1000, Rescon DS and Betokem C25.
Ducorit® Spraying Mortar 1000, manufactured by Densit A/S, is a very high performance spraying concrete applied by wet spraying.
Rescon DS, manufactured by Rescon A/S, is a high performance spraying concrete applied by dry spraying.
Betokem C25, manufactured by A/S Oslo Mørtelverk, is a spraying concrete applied by dry spraying.
All products were mixed in accordance with the prescription from the respective producers. Chloride bulk diffusion performed on prepared concrete cores was measured after an exposure of 35 days in 165 g NaCl /1000 ml water solution. The results are shown in figure 4.

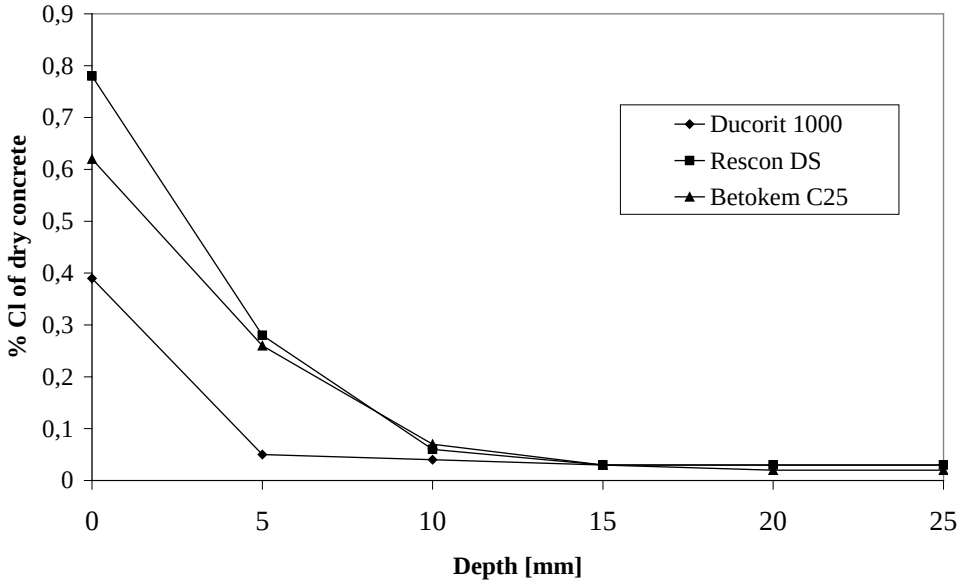

Figure 4 – Measured values of chloride content at different depths in the three spraying products used for the Mandal City Bridge pilot project.

From these measurements the diffusion coefficients for the three products was calculated. See table 7.

Table 7 – The calculated Diffusion coefficients for the three products used.

Specimens	D [m^2/sec]	C_S [%]	C_0 [%]
Ducorit® 1000	117 10^{-14}	0,27	0,03
Rescon DS	307 10^{-14}	0,76	0,015
Betokem C25	493 10^{-14}	0,65	0,15

2.5 The Electron Probe Micro Analysis.

In 1998 Ole Mejlhede Jensen published a report entitled ”Chloride ingress in cement paste and mortar measured by Electron Probe Micro Analysis”. This report deals with modelling chloride ingress due to exposure of synthetic seawater where the measurements are based on Electron Probe Micro Analysis (EPMA) as well as on more traditional methods.

EMPA is a technique where a cross section of an exposed test specimen is scanned by an electron beam like in a scanning electron microscope. A small volume (approximately 1-2 μm^3) is analysed. In this way a line scan can be performed or alternatively a selected area can be mapped with respect to the presence of chloride ions. A very high spatial resolution can be achieved by this technique.

I this work 19 mixtures (paste and mortar) with different water/cement ratio and different content of silica fume and with or without superplasticizer where investigate at up to 7 different exposure times (1 to 180 days). One of these mixtures is similar to a Densit® binder, which typically have a water/cement ratio of 0,3 or less and a silica fume content of more than 10%. The cement used was type CEM I according to EN 197-1.

For comparison the following two pastes are selected from [5]:
Densit®-like paste:

w/c = 0,3
silica fume 20%
superplasticizer

Conventional paste:

w/c = 0,3
silica fume 0%
superplasticizer

The results of a comparison of a Densit®-like paste and a more conventional paste are shown in figure 5 and 6.

The diffusion coefficients for chloride ions were calculated to 0,009 10^{-12} m^2/s and 3,4 10^{-12} m^2/s for Densit®-like paste and the more conventional paste respectively. A remarkably difference.

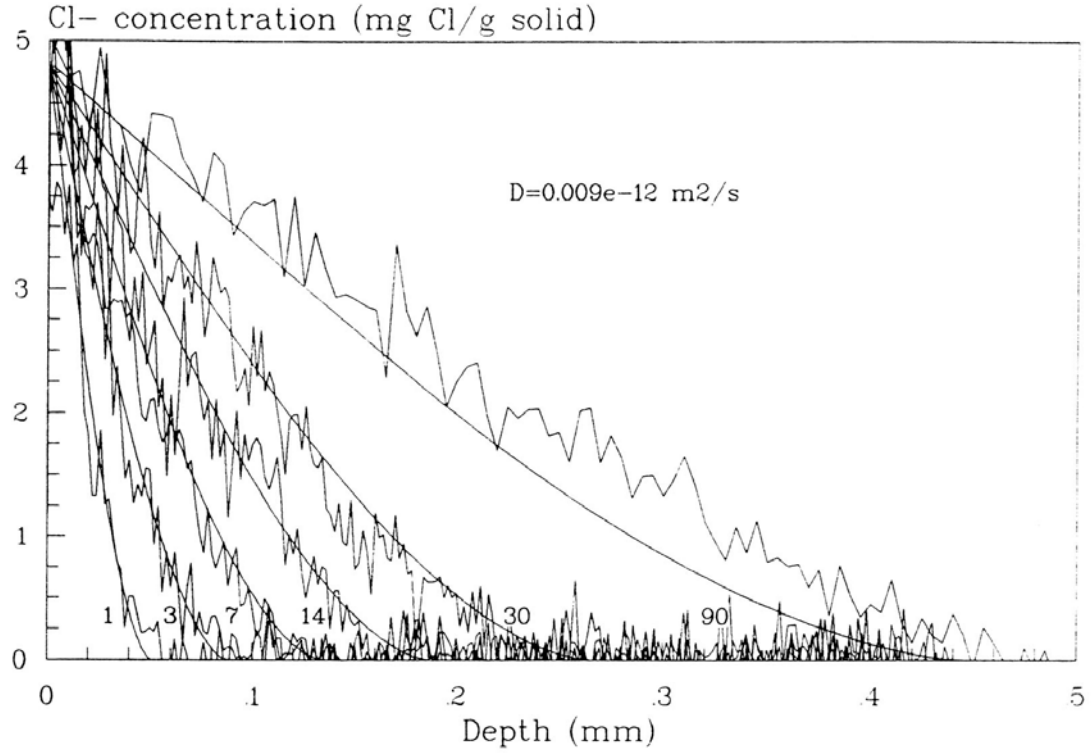

Figure 5 – From [5]. Influence of exposure time (marked on the curves) on chloride ingress in a Densit®-like paste. The fluctuating curves are measurement based on EPMA mapping.

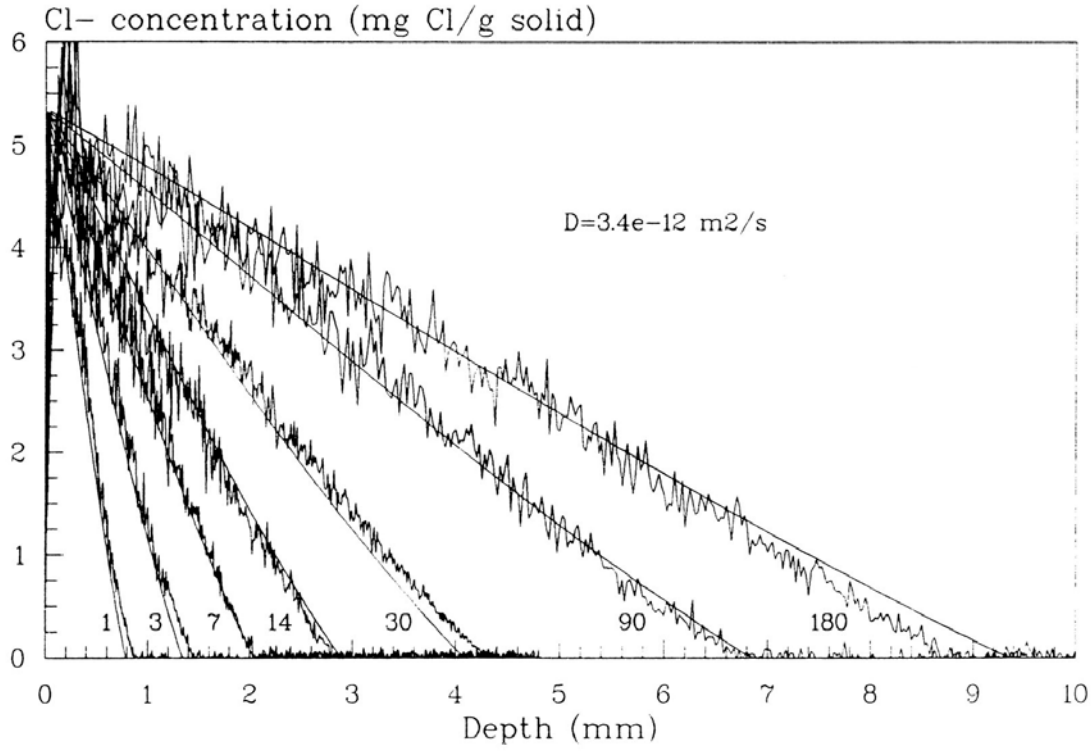

The smooth curves are calculated profiles with diffusion coefficient of D = 0,009 10^{-12} m^2/s.
Figure 6 – From [5]. Influence of exposure time (marked on the curves) on chloride ingress in a conventional paste. The fluctuating curves are measurement based on EPMA mapping. The smooth curves are calculated profiles with diffusion coefficient of D = 3,4 10^{-12} m^2/s.

3. CONCLUSION

From the presented case stories it is concluded that Densit®-like materials posses a much higher resistance against chloride ion diffusion than more conventional cement based materials. Typically, the diffusion coefficient, D, in Densit®-like materials is one magnitude of order (or even more) less than the diffusion coefficient in comparable products. An exception from this is spraying mortars, which generally gives less diffusion resistance than castable mortars. It is known [6] that the magnitude of the diffusion coefficient depends highly on porosity and porous structure. Densit® spraying mortar (and spraying mortars in general) is known to be more porous than castable products.
The overall conclusion is that the coefficient for chloride ion diffusion in Densit® paste is several orders of magnitude less than the diffusion coefficient for an ordinary Portland cement paste. The diffusion coefficient in a Densit® mortar is at least on order of magnitude less than the diffusion coefficient in a comparable ordinary Portland mortar.
In spraying mortars the bulk diffusion is controlled by the porosity and porous structure and the high diffusion resistance in the Densit® binder will therefore only improve the bulk resistance with a factor 2 – 4.

REFERENCES.

1. Carolyn M. Hansson, “Characterization of Densit for Protection of Steel Reinforcement”, The Danish Corrosion Centre, October 1983.
2. Force Institute, Corrosion Department, “Measurement of Chloride penetration and Carbonisation in Densit Material”, December 1992. In Danish.
3. Force Institute, Concrete Inspection and Analysis Department, “Bulk Diffusion Test on Densitop®-100”, June 1998.
4. Kjell Løland et. al., “Very High-Performance, Wet Sprayed Concrete for the Rehabilitation of Mandal City Bridge”, 1997.
5. Ole Mejlhede Jensen, “Chloride Ingress in Cement and Mortar Measured by Electron Probe Micro Analysis”. DTU, December 1998.
6. Birgit Sørensen, “Kloridtransport i beton”, Beton-Teknik no. 3/17/1990. In Danish.

Long term experience with microsilica concrete in a marine environment.

Per Fidjestøl,
Elkem ASA Materials,
Box 8126, Kristiansand, Norway
e-mail: per.fidjestol@elkem.no

Harald Justnes,
Chief Research Engineer
SINTEF Civil and Environmental Engineering
Cement and Concrete, N-7034 Trondheim, Norway
e-mail: harald.justnes@civil.sintef.no

ABSTRACT

23 years ago sections of wharves in Gothenburg were cast in silica fume concrete of three different qualities, one with admixed chloride. At the same time parallel sections were cast in conventional concrete with similar target mechanical properties. The paper summarizes the results from an investigation of the four concrete qualities without admixed chloride. The main observations are that all concretes continue to gain strength, that silica fume concrete is very resistant to chloride penetration, that error function type curve fitting is of dubious value for normal concrete, and that silica fume content appears very important in controlling chloride ingress.

Key words: silica fume, microsilica, chloride, marine, field, strength.

1. INTRODUCTION

In 1977 to 1978 three sections of wharf was built in Gothenburg, Sweden. The wharf was previously described in a paper by Sellevold and Maage (1987), with descriptions of microstructure and mechanical properties. In 2000 a new set of samples were retrieved, taken from the same locations as in the previous investigation. The investigations this time also included characterisation of chloride resistance properties and porosity. It further turned out that the results for strength and chloride resistance indicated that the nominal mixes reported in (1), from the reports during construction, were incorrect, and fairly extensive analysis had to be performed in order to establish the mixtures actually used – which were significantly different from the nominal mixtures reported.

Figure 1: The maps on this page show the location of Gothenburg

The wharves are located at the mouth of the Gotha river on the west coast of Sweden. They form the outermost part of the massive port facilities of Gothenburg, and are situated in slightly brackish water due to the dilution caused by the river. The wharves are massive structures, more than 600 meters long altogether for the investigated section.

In the wharves, altogether five different concrete qualities are used, only four are reported here. “Low” quality concrete was used in the lower part of the structure, while higher quality concrete was used in the upper part. Two separate mixtures were used for each of the situations, with and without microsilica (silica fume). Thus, there is parallel exposure of otherwise (nominally) comparable concretes, giving unique opportunity to study the effect of microsilica addition.

2. COLLECTION OF SAMPLES

2.1 Location of sampling areas.

The wharf has huge rubber bumpers to provide absorption of kinetic energy of ships arriving at the wharf. As can be seen from the photos the bumpers are fixed by brackets. Such brackets have been sampled as also indicated in the photo.

Figure 2: The pictures on this page show overview and details of wharves and bumper

The lower part of the bracket is in K350 (35 MPa characteristic cube strength), while the upper part is in K500 – 50MPa.

2.2 Cores and their use

The cores that were drilled varied in length from 330 to 430 mm. After drilling, they were shipped to SINTEF in Trondheim, who performed the investigations.

Typical use of the cores was (SINTEF report 70161/1):

- Outer 120 mm from two cores: Chloride profile according to Internal SINTEF procedure

- The outer 120-mm from the third core was used for SEM.

- The next 100 mm from all cores were used for density and compressive strength (NS 3673 (density), NS3668 (compressive strength)

- The next 60-mm from each core was used for determination of chloride bulk diffusion according to Nordtest method NT Build 443

The final pieces were used for samples to determine capillary absorption, internal SINTEF procedure

3. CONCRETE MIXTURE COMPOSITIONS

The nominal mixtures, given in reference (1) based on reports from the construction period, were incompatible with the test results; especially for such basic properties as strength and chloride ingress. It was therefore decided to attempt to determine the recipes

The procedure was extensive and involved DTG, wet chemistry and microstructure investigations. Fortunately the cement was known and the chemical composition at the time of construction was known. The silica fume that was likely to be used at this location typically had a SiO_2 content of 92%, which value was used in the analysis.As it turned out the differences between the stated mixture designs and those determined by analysis were significant, and the ones determined in this testing are used in the rest of this report. The method used to determine the real mix can be inaccurate, but the existing knowledge of the composition of component materials makes the determination more reliable.

Table 1. Nominal and estimated concrete composition; nominal in italics.

	1 {17/5 - 77}	2 {20/6 - 77}	3 {8-9/12 - 76}	5 {13-19/9 - 78}
Cement	*370*	*445*	*270*	*315*
	409	455	216	348
Microsilica	*46 (12%)*	*0*	*40 (15%)*	*0*
	22 (5.4%)	0	30 (13.7%)	0
Water	166	187	181	185
w/c	*0.45*	*0.42*	*0.67*	*0.59*
w/(c+s)	*0.40*	*0.42*	*0.58*	*0.59*
w/b	0.45	0.42	0.68	0.56

Table 1 gives the relevant details concerning the composition of the binder. The figures in italics represent the nominal compositions.

4. OBSERVATIONS

4.1 Compressive strength

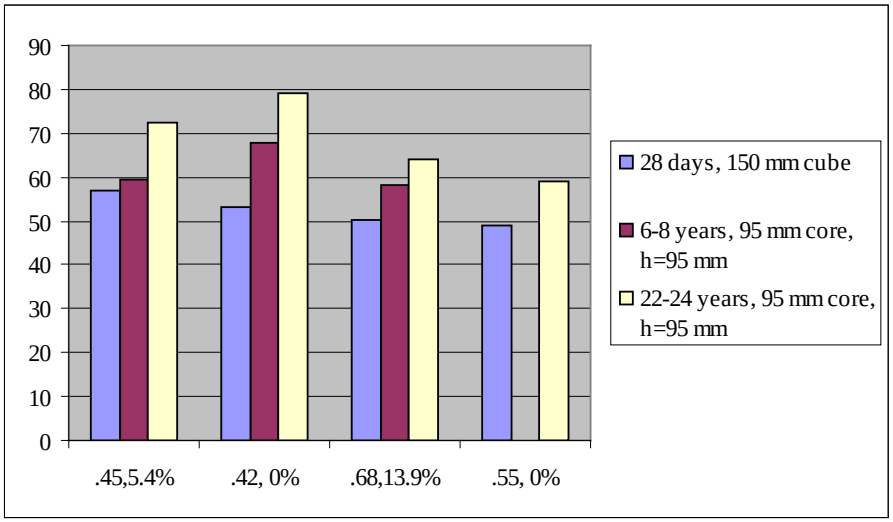

Figure 3: Development of compressive strength

The figure shows that all concretes show consistent gain of strength over time, the effect of microsilica being approximately as expected.

4.2 In-situ chloride profile.

In situ profiles are given in the figure 4 below.

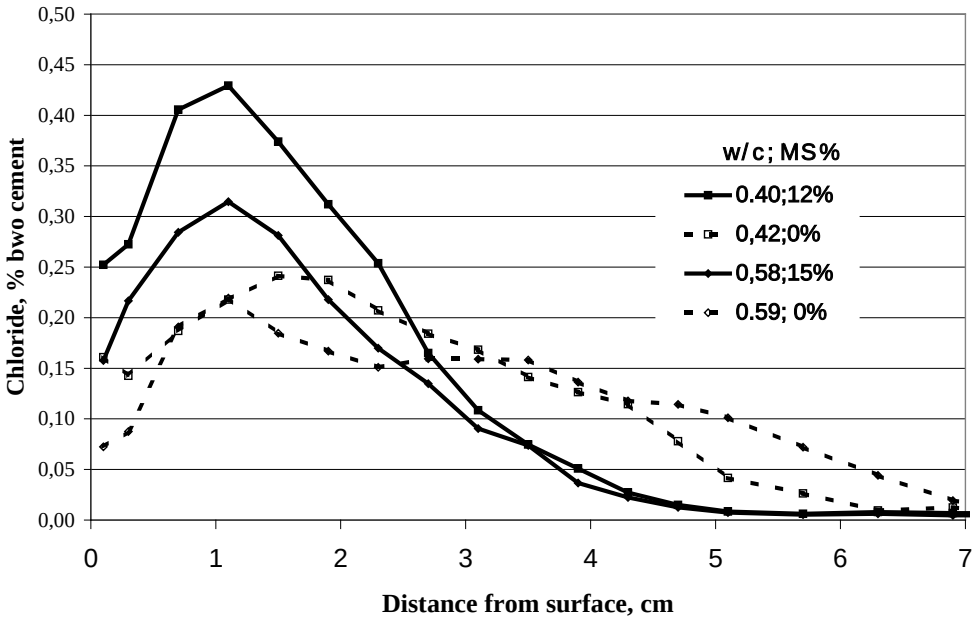

Figure 4: Observed chloride profiles

The most striking features are:

- Differences in shape between regular and microsilica concrete
- The efficiency of microsilica in reducing chloride ingress
- The probable effect of 3-7 mm carbonation on the chloride profile near the surface.

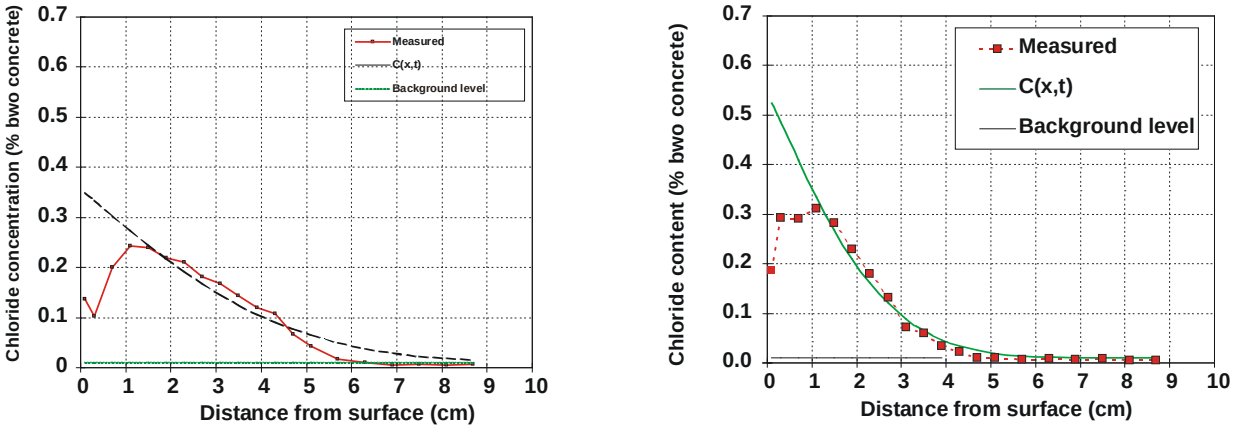

Figure 5: Fitting of the error function

Also shown are the fitted curves for determination of diffusion coefficient and surface concentration profile for two of the mixes.

The table gives estimated curve fitting parameters and corresponding regression coefficients for the two specimens used for each series.

Table 2. Transport parameters by curve fitting to "Fick's 2nd law"

Recipe	"Surface Concentration" C_0 (%)	Diffusion coefficient D_0 (10^{-12} m^2/s)	Regression coefficients
w/cm=0.45, 5.4% microsilica	0.74	0.32	0.99, 0.97
w/cm=0.42, no microsilica	0.37	0.90	0.95, 0.96
w/cm=0.68, 13.8% microsilica	0.53	0.33	0.99, 0.99
w/cm=0.56, no microsilica	0.26	1.9	0.92, 0.85

4.3 Laboratory chloride profiles (NT Build 443)

From the centre of the cores (i.e. most distant from the surface), specimens of 60 mm height were made. For all but one of the series, three parallels were tested. For the last series, two parallels were available. Determination of chloride resistance was performed according to NT Build 443.

Table 3. Average transport coefficients from NT-Build 443

Recipe	"Surface Concentration" C_0 (%)	Diffusion coefficient D_0 (10^{-12} m^2/s)
w/cm=0.45, 5.4% microsilica	0.97	3.5
w/cm=0.42, no microsilica	0-99	17
w/cm=0.68, 13.8% microsilica	0.95	3.2
w/cm=0.56, no microsilica	0.73	31

4.4 Electrical resistivity

The electrical resistivity was determined using en internal SINTEF procedure where water saturated cylinders were coated with a conductive, water-based gel on the ends. Then the conductivity was determined at 1kHz. The results (mean of three samples) are in table 4.

Table 4. Electrical resistivity at 1kHz

Recipe	Specific resistance Ωm
w/cm=0.45, 5.4% microsilica	156
w/cm=0.42, no microsilica	52
w/cm=0.68, 13.8% microsilica	301
w/cm=0.56, no microsilica	62

5. MICROSTRUCTURE INVESTIGATIONS

5.1 Plane and thin section

These investigations showed that there were no signs of concrete deterioration for any of the samples. The microscopy indicated slightly lower w/cm than the nominal mix specifications stated. The use of silica fume gave reduced portlandite content.

Carbonation was found in all samples, from 3.2 mm in the sample with 5% microsilica to a maximum of 6.7 mm in the sample from concrete with w/cm=0.68 and 14% microsilica.

5.2 SEM

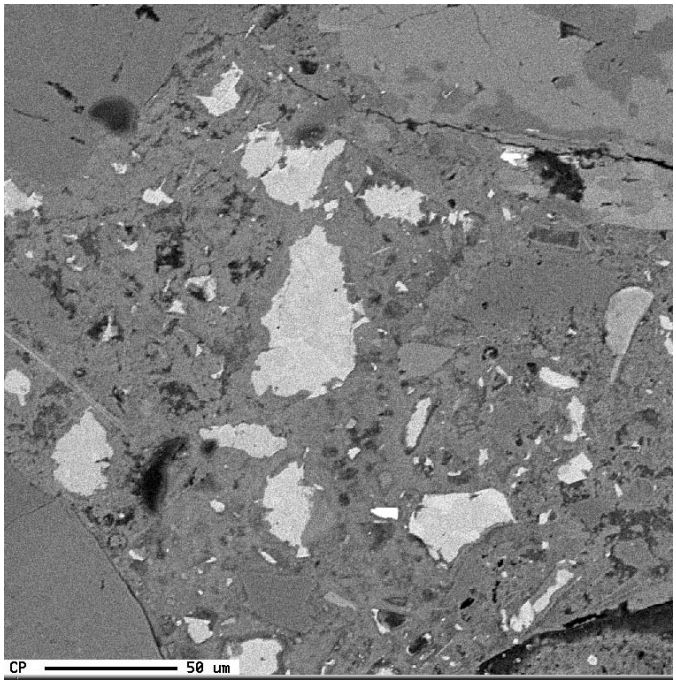

Fig.6. Unhydrated cement in low w/p, 5% MS

The investigation showed that the concrete with low w/cm and 5% microsilica had significant amounts of unhydrated cement, indicating dry conditions inside the concrete. Such unhydrated cement was found close to the surface of the concrete. In this concrete, portlandite could not be identified, even if there should be a significant amount present, indicating that the portlandite is distributed throughout the matrix. Some microsilica agglomerates (about 10 microns diameter or less) were identified)

In the low w/cm concrete without microsilica, portlandite was very visible, especially in the paste/aggregate transition zone. The presence of ettringite in air voids indicates moist conditions.

The high w/cm with 14% microsilica concrete showed no portlandite (due to pozzolanic reaction) The cement was fully hydrated.

In the high w/cm concrete without microsilica, much portlandite was found, both in the matrix and in pores.

5.3 Porosity and capillary absorption

Capillary suction and porosity were tested using internal SINTEF procedure KS 70 110. The table gives average results (average of four parallel samples)

Table 5. Capillarity and porosity

Recipe	Resistance number (x 10^7 s/m^2)	Capillary number x 10^2 kg/$m^2s^{0.5}$	Suction porosity %	Open macropores, %	Closed macropores %
w/cm=0.45, 5.4% microsilica	4.1	2.06	13.9	0.2	1.4
w/cm=0.42, no microsilica	3.7	2.01	12.9	0.1	2.4
w/cm=0.68, 13.8% microsilica	6.1	1.69	13.7	0.2	3.5
w/cm=0.56, no microsilica	3.0	2.29	13.2	0.2	2.7

6. CONCLUSIONS AND SUMMARY

The main lesson to be learned is that old information should be checked as carefully as possible. The problems experienced here related to mix design show this to be absolutely necessary.

The concrete has been exposed close to water, but protected from rain. Chloride exposure has been from airborne chlorides and possible splashing.

The results show a dramatic effect of microsilica on the resistance to chloride penetration; otherwise the most important observations are:

- Strength has increased for all concrete qualities since the last measurements 15 years ago.
- Chloride profiles for non-microsilica concrete indicate convection type chloride transport.
- Carbonation is likely to have influenced shape of chloride profile at the surface.
- After 22 years, the concrete with low w/cm and microsilica still had unhydrated cement.
- Nominal and real mixture compositions were very different – especially for the microsilica concretes.
- Low chloride transport and high electrical resistivity of the microsilica concretes indicate that the corrosion protection of the steel reinforcement should be very good.

REFERENCES

1. Magne Maage and Erik J. Sellevold. Effect of microsilica on the durability of concrete structures Concrete International, Volume: 9, Issue: 12 . 1987

2. SINTEF reports 70161/1 through 70161/8. Various authors, Reports on various investigations on drilled cores from Älvsborgshamn wharf in Gothenburg (In Norwegian)

3. Society for Technical and Industrial Research, Trondheim, Norway

Prevention of Deleterious Alkali Aggregate Reactions by use of Norwegian Portland-Fly Ash Cement

Knut O. Kjellsen
PhD, Project Manager
Norcem A.S, R&D Dept.
N-3950 Brevik, Norway
E-mail: knut.kjellsen@norcem.no

Terje F. Rønning
PhD, R&D Manager
Norcem A.S, R&D Dept.
N-3950 Brevik, Norway
E-mail: terje.ronning@norcem.no

Inger Meland,
Research Engineer
SINTEF Civil and Environmental Engineering,
Cement and Concrete
N-7465 Trondheim, Norway
E-mail: inger.meland@sintef.civil.no

ABSTRACT

Different Norwegian cements have been tested with respect to alkali aggregate reactions (AAR). The main objective of the investigation was to verify the efficiency of fly ash and Portland-fly ash cement to suppress expansion due to AAR in concrete containing Norwegian alkali reactive aggregates. The concrete specimens were tested according to the Canadian Standard (A23.2-14A). Length change and changes in weight were measured up to 4 years. The results were compared with the acceptance limits for length change given in the Norwegian guidelines for avoiding detrimental AAR. The results indicate that concrete based on Norwegian Portland-fly ash cement and alkali reactive aggregates is durable even though the total alkali content in the concrete mix exceeds 5.0 kg/m^3.

Key words: Concrete, alkali reactive aggregates, expansion, fly ash, cement

1 INTRODUCTION

The recognition of deleterious alkali aggregate reactions (AAR) in concrete is of relatively recent date in Norway. Over the last ten years research programs have been conducted in order

to evaluate Norwegian aggregates, whether they are alkali reactive or not, and to adopt test methods suitable for Norwegian aggregates [e.g.1-2]. The Norwegian reactive aggregates are of the slow/late-expansive type [1]. Today, Norwegian Portland-fly ash cement, or low-alkali Portland cements, are used in concrete containing potentially alkali reactive aggregates. One objective of the Norwegian research has been to establish recommendations for the production of durable concrete by use of alkali reactive aggregates. Based on national and international experience and research results the Norwegian Concrete Association has given recommendations for avoiding detrimental AAR in concrete [3]. According to these guidelines Portland cement (CEM I) can be used with potentially reactive aggregates provided the total content of alkalis (Na_2O_{eqv}) is less than 3.0 kg/m^3 concrete. Norwegian Portland-fly ash Cement (CEM II/A-V), or Portland cement (CEM I) with at least 10 % silica fume, can also be used. In this case up to 5.0 kg alkalis (Na_2O_{eqv}) pr m^3 concrete is accepted, alkalis in fly ash or silica fume not included. Concrete mixes not fulfilling these requirements can be accepted provided they are shown to be durable by field experience or laboratory testing.

Supplementary cementing materials, such as fly ash, can be used to minimize expansion from AAR. Numerous laboratory test reports, including long-term expansion measurements, have shown fly ash to be effective in preventing detrimental AAR [e.g. 4-11]. Field studies of mass concrete dams, in Britain and Canada, made of Portland cement concrete with reactive aggregates and fly ash as a mineral admixture revealed no deleterious AAR after several decades in service [12-13]. Comparable structures made with the same aggregates and similar concrete compositions, except they did not contain fly ash, showed severe distress due to AAR. Use of supplementary materials to eliminate deleterious AAR is now recommended in several National codes and guidelines [3, 14-17]. The effectiveness of fly ash to prevent deleterious effects of AAR depends on factors such as amount of fly ash used, chemical composition of the ash, content of alkalis in the concrete, and reactivity of the aggregate [e.g. 11, 18-19].

One important mechanism by which fly ash suppress expansion due to AAR seems to be associated with its ability to reduce the alkalinity of the pore solution. Probably because the lower C/S-ratio C-S-H gel produced by the pozzolanic reaction enables greater incorporation of alkali ions. Thus, less alkali and hydroxyl ions will be dissolved in the pore solution and made accessible for AAR [e.g. 5, 20, 21]. Fly ash reduces the content of CH through its pozzolanic reaction. Lowered CH contents have been ascribed an additional mechanism to why fly ash effectively reduce AAR [22]. It is also possible that the presence of fly ash modify the composition of alkali gel in such a way that it expands less [23]. It has also been suggested that fly ash reduces AAR expansion because it leads to reduced moisture transport and lowered electrical conductivity [24].

The objectives of the present study were to investigate:

- The capability of Norwegian Portland-fly ash cement to prevent deleterious AAR in concrete of high alkali contents, up to 7 kg Na_2O_{ekv}/m^3 concrete. (Series 1)
- The effect of different Norwegian cements with respect to AAR in concrete containing 5 kg Na_2O_{ekv} /m^3 and reactive aggregates. (Series 2)
- The minimum content of fly ash needed to prevent deleterious AAR in concrete containing 5 kg Na_2O_{ekv}/m^3 and reactive aggregates. (Series 3)

2 MATERIALS AND EXPERIMENTAL PROCEDURES

2.1 Materials

The various types and trading names of the Norwegian cements adopted in this study are provided in Table 1. The chemical and physical characteristics of the cements and the fly ash (FA) are given in Table 2. Three Series of concrete mixes were made. In Series 1 (Table 3), three mixes were made with the Norwegian Portland-fly ash cement (STD FA). Total alkali contents of the three mixes were kept at 3.5, 5, and 7 kg/m^3 concrete, respectively. Alkalis in the fly ash are not included. The five concrete mixes of Series 2 (Table 4) were made of the different Norwegian cements given in Table 2. The total alkali content was kept at 5 kg/m^3 concrete. In Series 3 (Table 5), parts of the Portland cement were replaced by fly ash. Replacements levels were 5, 10, 20, and 35 % (as percentage of binder).

Table 1. Types (EN 197-1/NS 3086) and names of the NORCEM cements

General notation	Cement types	Trading names	Trading names, abbreviated
Portland-fly ash cement	CEM II / A - V- 42, R	Standard FA	STD FA
Ordinary Portland cement	CEM I - 42,5 R	Standard	STD
Low alkali Portland cement	CEM I - 52,5 LA	Anlegg	ANL
Rapid hardening Portland cement	CEM I - 42,5 RR	Industri	IND
Sulphate resisting Portland cement	CEM I - 42,5 R - SR - LA	Sulfatresistent	SR

Table 2. Characteristics of the cements and the fly ash (The different cements are denoted by the abbreviated trading names)

Oxides	STD FA	STD	ANL	IND	SR	FA
SiO_2 (%)	-	20.3	21.2	19.6	21.5	55.4
Al_2O_3 (%)	-	4.6	4.1	4.6	3.7	27.4
Fe_2O_3 (%)	-	3.4	3.3	3.3	4.8	3.9
CaO (%)	-	62.8	64.4	62.4	63.9	3.6
MgO (%)	-	2.3	1.7	2.6	1.9	1.0
SO_3 (%)	2.7	2.6	2.9	3.3	2.5	-
K_2O (%)	1.22	0.93	0.43	1.18	0.53	1.06
Na_2O (%)	0.41	0.30	0.22	0.43	0.19	0.28
Na_2O_{eqv} (%)	1.22*	0.91	0.50	1.21	0.54	0.98
Free lime (%)		0.9	0.5	1.9	1.0	-
Ignition loss (%)	1.4	2.1	2.5	2.6	0.4	-
Blaine (m^2/kg)	420	358	373	556	304	620
Free carbon (%)	-	-	-	-	-	3.0

*) Including alkalis in fly ash.

The total alkali content was kept at 5 kg/m^3 concrete (alkalis in the fly ash not included). Sodium hydroxide (NaOH) was added to many of the concrete mixes to achieve constant total alkali content in kg pr m^3 concrete. The sodium hydroxide was dissolved in the mix water and added to

the concrete during mixing. A low-calcium fly ash (ASTM type F/EN 450) is used in the Norwegian Portland-fly ash cement.

Table 3. Mix proportions and properties of fresh mixes - Series 1

Mix		STD FA - 3.5	STD FA - 5	STD FA - 7
Total Na_2O eqv (from cement – fly ash + added NaOH) (kg/m^3)		3.5	5	7
Cement	STD FA (kg/m^3)	410	410	410
Sand 0 - 5 mm (kg/m^3)		770	770	770
Aggregates	5 - 10 mm (kg/m^3)	333	333	333
	10 - 14 mm (kg/m^3)	"	"	"
Cataclasite	14 - 20 mm (kg/m^3)	"	"	"
NaOH addition (kg/m^3)		0	2.0	4.5
Total water (kg/m^3)		197	197	197
w/c		0.48	0.48	0.48
Slump (mm)		70	65	75
Air content (%)		1.5	1.8	2.0
Density (kg/m^3)		2411	2410	2401
Compressive strength (MPa) 28 d. ¤		57.9	53.2	42.4

¤: 150 mm cube strength

Table 4. Mix proportions and properties of fresh mixes - Series 2

Mix		STD FA 5	ANL - 5	STD - 5	IND - 5	SR - 5
Total Na_2O eqv (from cement – fly ash + added NaOH) (kg/m^3)		5	5	5	5	5
Cement	STD FA (kg/m^3)	410				
	ANL (kg/m^3)		410			
	STD (kg/m^3)			410		
	IND (kg/m^3)				410	
	SR (kg/m^3)					410
Sand 0 - 5 mm (kg/m^3)		770	787	787	787	787
Aggregates	5 - 10 mm (kg/m^3)	333	337	337	337	337
Cataclasite	10 -14 mm (kg/m^3)	"	"	"	"	"
	14 - 20 mm (kg/m^3)	"	"	"	"	"
NaOH addition (kg/m^3)		2.0	3.8	1.6	-	3.6
Total water (kg/m^3)		197	197	197	197	197
w/c		0.48	0.48	0.48	0.48	0.48
Slump (mm)		70	80	75	70	90
Air content (%)		1.8	2.0	1.8	1.6	2.1
Density (kg/m^3)		2410	2412	2120	2439	2422
Compressive strength (MPa) 28 d. ¤		53.2	59.2	50.9	68.0	52.5

¤: 150 mm cube strength

The fly ash is inter-ground with the clinker in the production of this cement. The fly ash that was added to the concrete mixes (Series 3) was ground separately ahead of concrete mixing. The sand (0-5 mm) was a non-reactive natural sand of granitic origin. The coarse aggregate was an alkali reactive rock (cataclasite). The coarse aggregate was crushed, and then fractioned into three fractions; 5-10, 10-14, and 14-20 mm.

Table 5. Mix proportions and properties of fresh mixes - Series 3

Mix		STD - 0 % FA	STD - 5 % FA	STD - 10 % FA	STD - 20 % FA	STD - 35 % FA
Total Na_2O eqv (from cement – fly ash + added NaOH) (kg/m^3)		5	5	5	5	5
Cement	3 parts STD 1 part ANL (kg/m^3)	408	390	369	329	265
Fly ash addition (kg/m^3)		-	20.4	41.2	82.3	143
Sand 0 - 5 mm (kg/m^3)		788	793	793	796	788
Aggregates Cataclasite	5 - 10 mm (kg/m^3)	337.7	339.7	339.7	341	337.3
	10-14 mm (kg/m^3)	"	"	"	"	"
	14-20 mm (kg/m^3)	"	"	"	"	"
NaOH addition (kg/m^3)		2.17	2.40	2.61	3.05	3.65
Total water (kg/m^3)		193	195	190	191	189
w/(c + FA)		0.47	0.47	0.46	0.46	0.46
w/(c+0.4·FA)		0.47	0.49	0.49	0.53	0.59
w/c		0.47	0.50	0.51	0.58	0.71
Slump (mm)		80	70	80	80	80
Air content (%)		2.2	1.5	1.5	1.5	1.7
Density (kg/m^3)		2405	2420	2415	2425	2400
Compressive strength (MPa) 28 d ¤		48.7	47.1	49.9	45.1	39.5

¤: 150 mm cube strength

2.3 Test method

The Canadian Standard Method 'Potential Expansivity of Aggregates (Procedure for Length Change due to Alkali-Aggregate Reaction in Concrete)' [25] has been used for testing concrete prisms with respect to AAR. This test method should be used according to the Norwegian guidelines [3] when measurement of expansion is to be performed. The prisms (100x100x450 mm) were stored above water in closed 50 liters polyethylene boxes lined with wet cloths, 3 prisms in each box. Changes in length and weight of the prisms have been measured up to 4 years. The presented results are the average of three test results.

3 RESULTS AND DISCUSSION

The results of Series 1 are provided in Figure 1, and in the Appendix (Table A1). According to the Norwegian guidelines [3] a concrete with the Norwegian Portland-fly ash cement can be regarded as non-reactive without further testing provided the alkali content is below 5 kg/m^3 (alkalis from the fly ash not accounted for). For a Portland cement concrete the maximum alkali content is 3 kg/m^3. However, concrete mixes with higher alkali contents than these can be considered non-reactive if measurements show less than 0.03% expansion at 1 year. If the mix contains supplementary cementing materials the measured expansion should be less than 0.03% at 1 year, or 0.04% at 2 years.

The results of this study indicate that the 5 kg alkali limit for Norwegian Portland-fly ash cement is conservative as the mix with this alkali content expands only 0.017% at 2 years, whereas the acceptance limit is 0.04%. Even for the very high content (7 kg/m^3), the expansion is below the limit given in the Norwegian recommendations. For the mixes with 3 or 5 kg alkalis pr m^3 concrete there is practically no increase in expansion beyond about 2 years (130 weeks). The

length change is well below the 2 years limit (0.04%) even after 4 years (0.031%) for the mix with 5 kg/m^3 alkalis. The expansion of the mix with 7 kg alkalis pr m^3 increases steadily between 2 and 4 years. After 4 years the expansion is 0.058%.

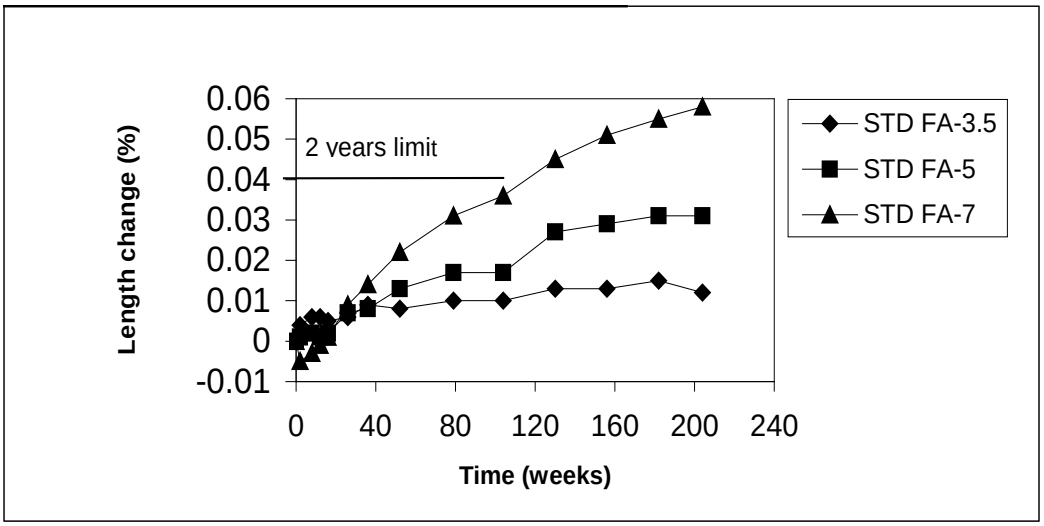

Figure 1. Measured length change of Series 1. The concrete mixes contain Portland-fly ash cement (STD FA) and different content of alkalis (3.5, 5 or 7 kg Na_2O_{eqv}/m^3).

The results of Series 2 are provided in Figure 2 and in the Appendix (Table A2). It can be observed that the expansion of the mixes with Portland cement (ANL, STD, IND, and SR) and 5 kg alkalis pr m^3 exceeds the acceptance limit (0.03% at 1 year) provided in the guidelines [3] after 12 weeks. The mix with Portland-fly ash cement and 5 kg alkalis is, as previously discussed, well below the acceptance limit. The increase in expansion of the Portland cement concrete prisms is rapid, and becomes around 0.3% at one year and 0.4% at 2 years. This is about 6 times the expansion measured with the Portland-fly ash cement and 7 kg alkalis pr m^3 after 4 years. Obviously, increasing the alkali content by 2 kg/m^3 beyond the limits given in the guidelines causes much greater expansion when the Portland cements are used than when the Portland-fly ash cement is used. Visual inspection of the exterior of the concrete prisms made with the Portland-fly ash cement and 7 kg alkalis revealed no cracks or other signs of deterioration after 4 years, whereas those with Portland cement and 5 kg alkalis were severely cracked after 2 years.

From these results one may deduce that a concrete based on the Portland-fly ash cement can be much more robust than a low-alkali Portland cement concrete towards AAR if the concentration of alkalis increases due to ingress of alkalis. Indeed, there have been cases where low-alkali cement was used in pavements and damage occurred. It was found that water from the base moved up to the top of the slabs and evaporated, leaving behind dissolved alkalis and causing the top of the slabs to be effectively high-alkali [26]. Alkalis originating from seawater or deicing agents may also accumulate in the surface of concrete structures.

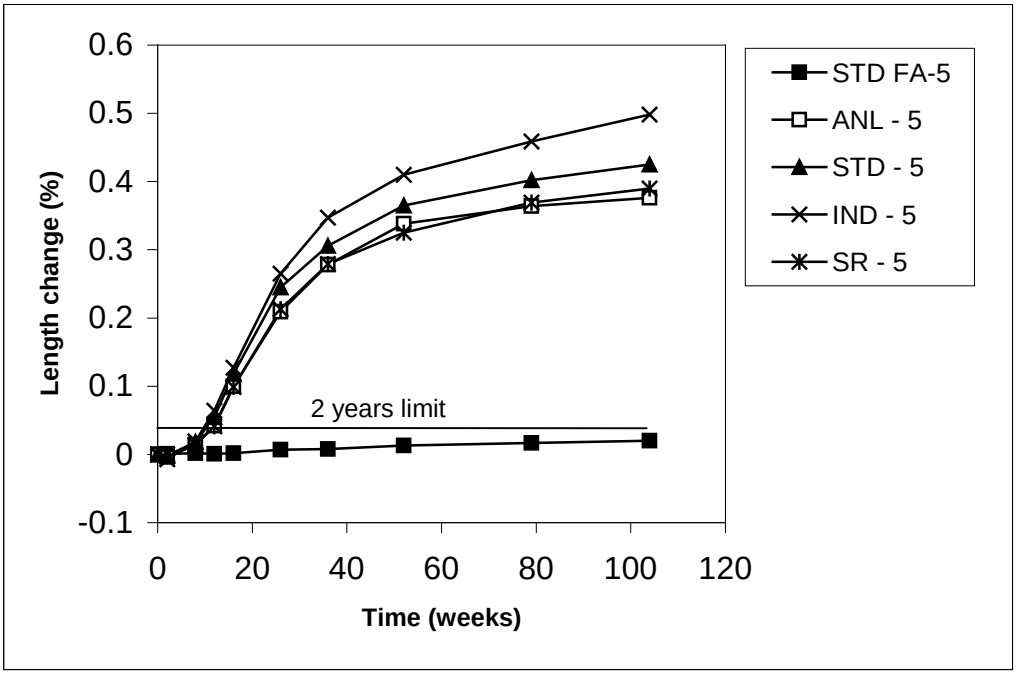

Figure 2. Measured length change of Series 2. The concrete mixes contain different types of cement (STD FA, ANL, STD, IND, or SR) and 5 kg Na_2O_{eqv} / m^3.

Figure 3 shows the results of Series 3. The numerical results are tabulated in Table A3 in the Appendix. It can be seen from Figure 3 that the measured expansion is beyond the limits given in the Norwegian guidelines (i.e. 0.03% at 1 year or 0.04% at 2 years) for the mixes with 0, 5 or 10% fly ash and 5 kg alkalis. With the particular fly ash and clinker adopted in this study a fly ash level of about 20% is necessary to fulfill the requirement in the guidelines. The expansion gradually decreases when the fly ash content is increased. Increasing the fly ash content from 20 to 35% reduces the expansion, but the absolute effect is small since the expansion of the 20% fly ash mix is small.

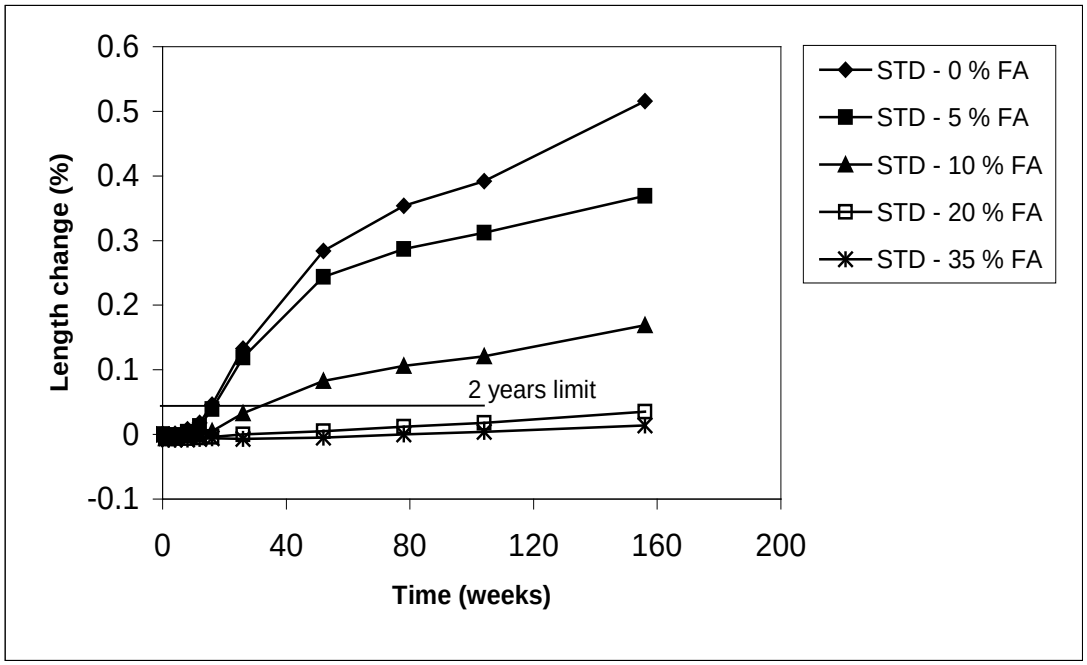

Figure 3: Measured length change of Series 3. The concrete mixes contain STD and ANL in proportion 3:1, and different contents of fly ash (0, 5, 10, 20 or 35 %). Total alkali content 5 kg Na_2O_{eqv}/m^3.

5 CONCLUSIONS

Different Norwegian cements, four Portland cements (CEM I) and one Portland-fly ash cement (CEM II/A-V), have been tested with respect to expansion due to alkali aggregate reaction (AAR). A Norwegian slowly reacting aggregate was used as the coarse aggregate in the concrete mixes. The concretes were tested according to the Canadian Standard Test Method A23.2-14A (Procedure for Length Change due to Alkali-Aggregate Reaction in Concrete Prisms). Testing was performed up to 4 years. Three test series were conducted. In Series 1 the capability of Norwegian Portland-fly ash cement to prevent deleterious AAR in concretes with differing alkali contents (up to 7 kg/m^3, alkalis in fly ash not included) were tested. In the second test Series the length change of mixes containing the various Portland cements were measured. In the third Series various contents of fly ash were tested with respect to length change. The alkali content was kept at 5 kg/m^3 concrete in Series 2 and 3, alkalis in fly ash not included. The results were considered on the basis of the Norwegian recommendations for avoiding detrimental AAR [3].

Use of Norwegian Portland-fly ash cement (CEM II/A-V) was found to be very effective in preventing deleterious AAR at alkali contents up to 5 kg/m^3 concrete. An alkali content of 7 kg/m^3 in the mix with Portland-fly ash cement caused greater expansion, but the expansion was still below the acceptance limits given in the guidelines. Close to 20% fly ash is necessary to fulfill the requirement for maximum expansion given in the recommendations, with the particular fly ash and clinker adopted in this study. Ten percent fly ash is too little.

Increasing the alkali content by 2 kg/m^3 above the maximum alkali content given in the Norwegian recommendations caused severe expansion and cracking of the specimens with Portland cement. However, the specimens with Portland fly-ash cement behaved much better. The length change was several times smaller and no cracking was observed by visual

examination of the specimens. This indicate that concrete based on the Portland-fly ash cement can be more robust against detrimental AAR if the alkali content becomes higher than the limits given in the recommendations, for example by ingress of alkalis from the exterior.

REFERENCES

1. Jensen, V., 'Alkali Aggregate Reaction in Southern Norway', Doctor technicae thesis, Norwegian Institute of Technology, Trondheim, 1993. 262 p.
2. 'NORMIN 2000: Alkali Aggregate Reactions in Concrete' Report, Norwegian Aggregates Producers Association, Oslo, March 1999. 166 p. (In Norwegian).
3. 'Durable Concrete With Alkali Reactive Aggregates', Publication No. 21, Norwegian Concrete Association, Oslo, April 1996. 27p. (In Norwegian).
4. Pepper, L. & Mather, B., 'Effectiveness of Mineral Admixtures in Preventing Excessive Expansion of Concrete due to Alkali-Aggregate Reaction', *Proceedings* of the American Society for Testing Materials, American Society for Testing Materials, Philadelphia, Vol. 59, 1959. pp. 1178-1203.
5. Nixon, P.J., Page, C.L., Bollinghaus, R. & Canham, I., 'The Effect of a Pfa with a High Total Alkali Content on Pore Solution Composition and Alkali silica Reaction', *Magazine of Concrete Research*, Vol. 38, No. 134, March 1986. pp. 30-35.
6. Chatterji, S. & Nepper-Christiansen, P., 'Evaluation of Portland Flyash Cement as a Preventive Against Alkali-Silica Reaction', *Nordic Concrete Research*, No. 6, 1987. pp. 51-56.
7. Oberholster, R.E., 'Alkali-Aggregate Reaction and Mineral Admixtures', *Proceedings* of an Engineering Foundation Conference 'Advances in Cement Manufacture and Use', Engineering Foundation, New York, 1988. pp. 155-173.
8. Alasali, M.M. & Malhotra, V.M., 'Role of Concrete Incorporating High Volumes of Fly Ash in Controlling Expansion due to Alkali-Aggregate Reaction', *ACI Materials Journal*, Vol. 88, No. 2, 1991. pp. 159-163.
9. Blackwell, B.Q., Thomas, M.D.A., Nixon, P.J. & Pettifer, K., 'The use of Fly Ash to Suppress Deleterious Expansion due to AAR in Concrete Containing Greywacke Aggregate', *Proceedings* 9th International Conference on Alkali-Aggregate Reaction in Concrete, London, July 1992. pp. 102-109.
10. Shayan, A., Diggins, R. & Ivanusec, I., 'Effectiveness of Fly Ash in Preventing Deleterious Expansion due to Alkali-Aggregate Reaction in Normal and Steam-Cured Concrete', *Cement and Concrete Research*, Vol. 26, 1996. pp. 153-164.
11. Durchesne, J. & Bérubé, M-A., 'Long-Term Effectiveness of Supplementary Cementing Materials Against Alkali-Silica Reaction', *Cement and Concrete Research*, Vol. 31, 2001. pp. 1057-1063.
12. Thomas, M.D.A, Blackwell,B.Q & Pettifer, K., 'Suppression of Damage from Alkali Silica Reaction by Fly-Ash in Concrete Dams', *Proceedings* of the 9th International Conference on Alkali-Aggregate Reaction in Concrete, London, 1992. pp. 1059-1066.
13. Thomas, M.D.A, 'Field Studies of Fly-Ash Concrete Structures Containing Reactive Aggregates', *Magazine of Concrete Research*, Vol. 48, No. 177, 1996. pp. 265-279.
14. Concrete Society, 'Alkali Silica Reaction, Minimizing the Risk of Damage to Concrete', Concrete Society Technical Report No 30, Concrete Society, London, 1992.
15. Thomas, M.D.A, Hooton, R.D & Rogers, C.A., 'Prevention of Damage Due to Alkali-aggregate Reaction (AAR) in Concrete Construction – Canadian Approach', *Cement, Concrete, and Aggregates*, Vol. 19, No. 1, 1997. pp. 26-30.

16. ‘Standard Practice to Identify Degree of Alkali-Reactivity of Aggregates and to Identify Measures to Avoid Deleterious Expansion in Concrete’, Methods of Test for Concrete, A23.2-27A, Canadian Standards Association, Toronto, 2000. pp. 251-259.
17. ACI Manual of Concrete Practice, Materials and General Properties of Concrete, Part 1, American Concrete Institute, Farmington Hills, 2000.
18. Thomas, M.D.A, Blackwell, B.Q. & Nixon, P.J., ‘Estimating the Alkali Contribution from Fly Ash to Expansion due to Alkali-Aggregate Reaction in Concrete’, *Magazine of Concrete Research*, Vol. 48, No. 177, 1996. pp. 251-264.
19. Thomas, M.D.A. & Blackwell, B.Q., ‘Summary of BRE Research on the effect of Fly-Ash on Alkali-Silica Reaction in Concrete’, *Proceedings* of the 10th International Conference on Alkali-Aggregate Reaction in Concrete, Melbourne, 1996. pp. 554-561.
20. Hobbs, D.W., ‘Effect of Mineral and Chemical Admixtures on Alkali-Aggregate Reduction’, *Proceedings* of the 8th International Conference on Alkali-Aggregate Reaction in Concrete, Kyoto, 1989. pp. 173-186.
21. Durchesne, J. & Bérubé, M-A., ‘The Effectiveness of Supplementary Cementing Materials in Suppressing Expansion due to ASR: Another Look at the Reaction Mechansims Part 2: Pore Solution Chemistry’, *Cement and Concrete Research*, Vol. 24, No. 2, 1994. pp. 221-230.
22. Thomas, M.D.A., ‘Microstructural Studies of Alkali-Silica Reaction in Fly Ash Concrete’, *Proceedings* of the 17th International Conference on Cement Microscopy, Calgary, 1995. pp. 242-256.
23. Thomas, M.D.A., Nixon, P.J. & Pettifer, K., ‘The Effect of Pulverised-Fuel Ash with a High Total Alkali Content on Alkali Silica Reaction in Concrete Containing Natural UK Aggregate’, *Proceedings* of the 2nd International Conference on the Durability of Concrete, Montreal, 1991. pp. 919-940.
24. Hu, Z. & Hooton, R.D., ’Migration of Alkali Ions in Mortar due to Several Mechanisms’, *Cement and Concrete Research*, Vol. 23, 1993. pp. 951-961.
25. ‘Potential Expansivity of Aggregates (Procedure for Length Change due to Alkali-Aggregate Reaction in Concrete Prisms)’, Methods of test for Concrete, A23.2-14A, Canadian Standards Association, 1994.
26. Personal communication, Professor R.D. Hooton, University of Toronto, Canada.

APPENDICES

Table A1.Changes in length and weights of the test prisms - Series 1

Time (weeks)	STD FA - 3.5		STD FA - 5		STD FA - 7	
	changes in length (%)	changes in weights (%)	changes in length (%)	changes in weights (%)	changes in length (%)	Changes in weights (%)
2	0.004	0.09	0.001	0.15	- 0.005	0.11
8	0.006	0.26	0.002	0.27	- 0.003	0.23
12	0.006	0.31	0.001	0.28	- 0.001	0.25
16	0.005	0.33	0.002	0.31	0.001	0.27
26	0.006	0.36	0.007	0.32	0.009	0.29
36	0.009	0.40	0.008	0.36	0.014	0.36
52	0.008	0.43	0.013	0.43	0.022	0.46
78	0.010	0.48	0.017	0.46	0.031	0.52
104	0.010	0.50	0.017	0.46	0.036	0.56
130	0.013	0.50	0.027	0.49	0.045	0.57
156	0.013	0.50	0.029	0.50	0.051	0.63
182	0.015	0.51	0.031	0.52	0.055	0.66
208	0.012	0.52	0.031	0.52	0.058	0.69

Table A2. Changes in length and weights of the test prisms - Series 2

Time weeks	STD FA - 5		ANL - 5		STD - 5		IND – 5		SR - 5	
	chs. in length (%)	chs. in weight (%)	chs. in length (%)	chs. in weight (%)	chs. in length (%)	chs. in weight (%)	chs. in length (%)	chs. in weight (%)	chs. in length (%)	chs. in weight (%)
2	0.001	0.15	-0.004	0.08	-0.002	0.09	-0.007	0.18	0	0.07
8	0.002	0.27	0.014	0.28	0.018	0.33	0.019	0.46	0.014	0.23
12	0.001	0.28	0.042	0.39	0.055	0.44	0.064	0.64	0.041	0.26
16	0.002	0.31	0.100	0.58	0.118	0.62	0.127	0.80	0.099	0.47
26	0.007	0.32	0.209	0.74	0.245	0.83	0.265	0.98	0.213	0.71
36	0.008	0.36	0.278	0.88	0.306	0.91	0.347	1.11	0.279	0.82
52	0.013	0.43	0.338	1.05	0.365	1.06	0.410	1.27	0.325	0.93
78	0.017	0.46	0.364	1.05	0.402	1.02	0.459	1.33	0.369	0.99
104	0.020	0.46	0.376	1.06	0.425	1.06	0.498	1.43	0.390	1.30

Table A 3. Changes in length and weights of the test prisms - Series 3

Time weeks	STD 0 % FA		STD 5 % FA		STD 10 % FA		STD 20 % FA		STD 35 % FA	
	chs. in length (%)	chs. in weight (%)	chs. in length (%)	chs. in weight (%)	chs. in length (%)	chs. in weight (%)	chs. in length (%)	chs. in weight (%)	chs. in length (%)	chs. In weight (%)
2	-0.003	0.101	-0.003	0.108	-0.005	0.091	-0.005	0.155	-0.008	0.018
4	0.001	0.156	-0.001	0.144	-0.004	0.127	-0.006	0.200	-0.008	0.054
8	0.008	0.257	0.004	0.216	-0.001	0.182	-0.006	0.237	-0.008	0.091
12	0.018	0.313	0.013	0.270	0.000	0.209	-0.005	0.255	-0.007	0.127
16	0.046	0.395	0.039	0.279	0.005	0.237	-0.004	0.282	-0.006	0.136
26	0.133	0.588	0.119	0.577	0.033	0.337	0.000	0.310	-0.007	0.154
52	0.248	0.855	0.244	0.811	0.083	0.525	0.005	0.358	-0.005	0.200
78	0.354	0.990	0.287	0.920	0.106	0.616	0.012	0.395	0.000	0.227
104	0.392	1.080	0.312	1.000	0.121	0.682	0.018	0.446	0.004	0.266
156	0.516	-	0.369	-	0.169	-	0.035	-	0.014	-

Frost Resistance of Concrete Containing Secondary Cementitious Materials - Experience from Three Field Exposure Sites

Peter Utgenannt
Doctoral candidate
SP Swedish National Testing and Research Institute
Box 857, SE-501 15 Borås, Sweden
e-mail: peter.utgenannt@sp.se

Per-Erik Petersson
Professor, Head of the Department of Building Technology
SP Swedish National Testing and Research Institute
Box 857, SE-501 15 Borås, Sweden
e-mail: pererik.petersson@sp.se

ABSTRACT

Concrete samples made from different cement/binder types, including secondary cementitious materials, have been exposed at three different field test sites for five years. All the sites are situated in Sweden, one in a highway environment, one in a marine environment and one in an environment without salt exposure. The resistance to internal and external frost damage has been regularly evaluated by measurements of change in volume and ultrasonic pulse transmission time. The results after five years' exposure clearly indicate the highway environment as being the most aggressive with regard to external frost damage. The influence of the climate on the internal frost damage is less pronounced. Results show that concretes containing large amounts of slag in the binder have the severest scaling, whether with or without entrained air. For concrete without entrained air, qualities containing OPC + 5 % silica as binder seems to be more susceptible to internal damage than do the other qualities.

Key words: Freeze/thaw, Field test, Laboratory test, Secondary cementitious materials

1. INTRODUCTION

Frost resistance is one of the most important properties determining the durability of concrete in the Scandinavian countries, as well as in other European countries with cold climates. To be able to prove concrete qualities to be frost-resistant a number of test methods have been developed: for example, Swedish Standard SS 13 72 44 for scaling resistance [1], Finnish Standard SFS 5448 for dilation [2] and the measurement for critical degree of saturation [3].
These test methods have been developed primarily on the basis of experience of traditional concrete. When new types of concrete are introduced - for example, with new types of binders, filler

materials, admixtures etc. - we do not know how to evaluate the test results or even if the freeze/thaw test methods used are relevant. More knowledge and experience of the salt/frost resistance of these new concrete qualities in the field is needed. One way to acquire this experience is to expose concrete specimens to representative outdoor environments. Such an investigation was started in Sweden in the mid-nineties. Three field exposure sites were established in the south-west of Sweden: one in a highway environment beside highway 40 (60 km east of Gothenburg), one in a marine environment at Träslövsläge harbour (80 km south of Gothenburg) and one in an environment without salt exposure on SP's premises in Borås (70 km east of Gothenburg). The air temperature and relative humidity ranges are the same at the highway exposure site and at SP's premises, with minimum temperatures between –15 °C and –20 °C, and with a precipitation of about 900 mm per year. The temperatures at the marine exposure site at Träslövsläge harbour are somewhat milder, and the precipitation is about 700 mm per year. The micro-climates surrounding the test specimens, however, vary significantly between the three sites, with the highway microclimate being the most moist and saline, and the climate at SP being the 'mildest', with no salt and only pure precipitation.

A large number of concrete mixtures of varying quality with different binder types/combina-tions, varying water/binder ratios and air contents were produced and placed at the field exposure sites. The frost damage has been regularly evaluated by measurements of the volume change of the specimens and the change in ultrasonic transmission time through each specimen. This paper presents results after five winter seasons for concrete qualities produced with four different binder combinations: one with Ordinary Portland Cement (OPC), one with a CEM III cement type and two with OPC and secondary cementitious materials.

2. MATERIALS AND SPECIMENS

The binder types/combinations studied in this investigation are shown in Table 1. For chemical composition, see [4].

Table 1 - Binder types/combinations investigated

Binder type/combination	Comments
1 OPC[1)] (CEM I)	Low alkali, sulphur-resistant
2 OPC[1)] + 5 % silica by binder weight	Silica in the form of slurry
3 OPC[1)] + 30 % slag by binder weight	Ground blast furnace slag added in the mixer
4 CEM III/B	Dutch slag cement, ~70 % slag

[1)] OPC = Ordinary Portland Cement (Degerhamn standard [5] is a low-alkali, sulphur-resistant cement)

Ten different concrete qualities were produced for each of the binder types/combinations. Concrete qualities with five different water/binder (w/b) ratios (0.30, 0.35, 0.40, 0.50, 0.75), and with and without entrained air, were produced for all binder combinations. 0-8 mm natural and 8-16 mm crushed aggregate was used for all mixes. A naphthalene-based plasticizer, Melcrete, was used for mixtures with w/b-ratio of 0.40 and lower. The air-entraining agent used, L16, is a tall-oil derivative. A summary of concrete constituents and properties is presented in Table 2 below, for a complete presentation see [4].

Table 2 - Concrete qualities used in this investigation.

Binder type	w/b-ratio	Eqv. w/c-ratio[1]	Cement (kg/m^3)	SCM[2] (kg/m^3)	AEA[3]	Air content fresh (%)	Slump (mm)	Compressive strength (MPa) SS[4]	Recalc[5]	Scaling (kg/m^2)[6] 28	56
OPC	0.30	0.30	500	-	Yes	4.8	240	95	87	0.024	0.035
	0.35	0.35	450	-	Yes	4.8	190	95	87	0.054	0.085
	0.40	0.40	420	-	Yes	4.6	125	67	60	0.014	0.023
	0.50	0.50	370	-	Yes	4.6	90	49	44	0.017	0.022
	0.75	0.75	260	-	Yes	4.7	100	21	18	0.127	0.141
	0.30	0.30	500	-	No	1.1	120	102	93	0.156	0.256
	0.35	0.35	450	-	No	1.2	140	91	83	1.94	4.39
	0.40	0.40	420	-	No	0.8	130	87	79	3.11	7.92
	0.50	0.50	385	-	No	0.8	70	56	50	5.09	14.5
	0.75	0.75	265	-	No	0.9	60	31	27	4.34	>15
OPC+5% silica	0.30	0.29	475	25	Yes	4.6	100	103	94	0.041	0.119
	0.35	0.33	427.5	22.5	Yes	4.5	90	91	83	0.022	0.041
	0.40	0.38	399	21	Yes	4.8	105	72	65	0.023	0.035
	0.50	0.48	361	19	Yes	4.6	70	57	51	0.020	0.026
	0.75	0.71	237.5	12.5	Yes	4.3	70	25	22	0.19	0.20
	0.30	0.29	475	25	No	1.1	125	121	111	0.12	0.20
	0.35	0.33	427.5	22.5	No	1.1	90	105	96	0.36	0.89
	0.40	0.38	399	21	No	0.5	100	84	76	1.67	3.25
	0.50	0.48	370.5	19.5	No	1.2	60	67	60	1.86	4.61
	0.75	0.71	256.5	13.5	No	0.3	75	35	31	3.45	6.58
OPC+30% slag	0.30	0.34	350	150	Yes	4.8	230	90	82	0.031	0.045
	0.35	0.40	315	135	Yes	4.8	130	86	78	0.086	0.139
	0.40	0.45	294	126	Yes	4.4	110	65	58	0.041	0.067
	0.50	0.57	259	111	Yes	4.8	80	49	44	0.021	0.033
	0.75	0.85	175	75	Yes	4.4	100	20	17	0.490	0.538
	0.30	0.34	350	150	No	0.7	220	101	92	0.097	0.128
	0.35	0.40	315	135	No	1.1	140	91	83	1.78	3.61
	0.40	0.45	294	126	No	0.9	120	78	71	1.78	3.83
	0.50	0.57	273	117	No	1.3	80	52	46	0.864	1.94
	0.75	0.85	185.5	79.5	No	0.5	80	25	22	1.58	4.37
CEM III (~70% slag)	0.30	0.30	520	-	Yes	4.8	200	78	71	0.245	0.356
	0.35	0.35	460	-	Yes	4.7	200	74	67	0.434	0.615
	0.40	0.40	420	-	Yes	4.3	120	61	55	0.568	0.845
	0.50	0.50	380	-	Yes	4.5	70	46	41	0.993	1.66
	0.75	0.75	255	-	Yes	4.4	90	26	23	2.05	3.16
	0.30	0.30	520	-	No	0.8	200	99	90	0.221	0.281
	0.35	0.35	470	-	No	0.7	200	80	72	0.490	0.653
	0.40	0.40	420	-	No	0.9	125	68	61	0.837	1.14
	0.50	0.50	400	-	No	1.0	65	54	48	1.21	1.61
	0.75	0.75	265	-	No	0.1	100	31	27	3.94	6.89

[1] Eqv. w/c-ratio= water/(cement + 2∗silica + 0.6∗slag). Not applicable for CEM III cement.
[2] SCM – Secondary Cementitious Materials
[3] AEA – Air Entraining Agent
[4] Dry stored cubes tested according to SS 13 72 10 at the age of 28 days
[5] Recalculated to wet stored cubes according to $f_{wet,cube}=0.76*(f_{dry,cube})^{1.04}$
[6] According to the 'Slab test', SS 13 72 44, freeze/thaw started at the age of 31 days

All concrete batches were produced in the autumn of 1996, and a number of 150 mm cubes were cast from each batch. The cubes were demoulded 24 hours after casting, and stored in lime-saturated water for six days. They were then stored in a climate chamber (50 % RH / 20 °C) for a period of between one and a half and three months. Between eight and twelve days before the specimens were placed at the field test sites, the cubes were cut, resulting in two specimens

with the shape of a half 150 mm cube with one cut surface and the rest mould surfaces. After cutting, the specimens were stored in a climate chamber (50 % RH / 20 °C) until placed at the test site. During this second conditioning period, the volume of, and transmission time through, each specimen were measured. Two specimens of each mixture were then placed at each test site.

At the highway environment test site, the specimens were placed in steel frames close to the road, so that they were splashed by the passing traffic. At the marine test site, the specimens were mounted on top of a pontoon, thus exposing them to the saline marine environment but with no direct contact with the sea water, except when splashed over them by storms. The specimens at the test site without salt exposure were placed on top of loading pallets: here, they were exposed only to water from precipitation. At all sites, the specimens were exposed with the cut surface turned upwards.

3. TEST PROCEDURES

In order to be able to detect both internal and external frost damage, the change in volume and ultrasonic pulse transmission time was measured regularly. The first measurement was carried out before placing the specimens at the test sites. The specimens at the highway site have subsequently been measured once a year, and the specimens at the other two sites after two, four and five years.

The volumes of the specimens are calculated from results obtained from measuring the weight of the specimens in water and in air respectively. The ultrasonic pulse transmission time through the specimen is measured as a mean of three measurement positions, where possible, on each specimen.

The following laboratory tests were carried out on each concrete mix in order to determine the concrete characteristics:

Testing the fresh concrete:

- Air content
- Density
- Slump
- Remoulding test

Testing the hardened concrete:

- Compressive strength in accordance with Swedish standard (SS) 13 72 10.
- Salt/frost resistance in accordance with SS 13 72 44 ('the slab test').
- Microscopical determination of the air void system, in principal in accordance with ASTM C 457.

Results from these tests are given partly in Table 2 above, and fully in Reference 4.

4. RESULTS

Figures 1-4 present results from measurements of the volume change after five years of exposure at the three field exposure sites. The reference value is the initial volume before exposure. Figures

1-3 show the results for concrete produced without entrained air, exposed at the three exposure sites, while Figure 4 shows the results for concrete with entrained air (4-5 %) exposed at the test site in a highway environment. Each point is a mean value of measurements on two specimens.

Figures 5-7 show the relative transmission time after five years' of exposure at the three field exposure sites. The reference value is that of measurements before exposure. Each point is a mean value of up to three measurements on each two test specimens, i.e. a mean value of up to six measurements. For some qualities with w/b-ratio 0.75, no value is presented. This is because damage to the concrete surfaces was so severe that measurements were not possible.

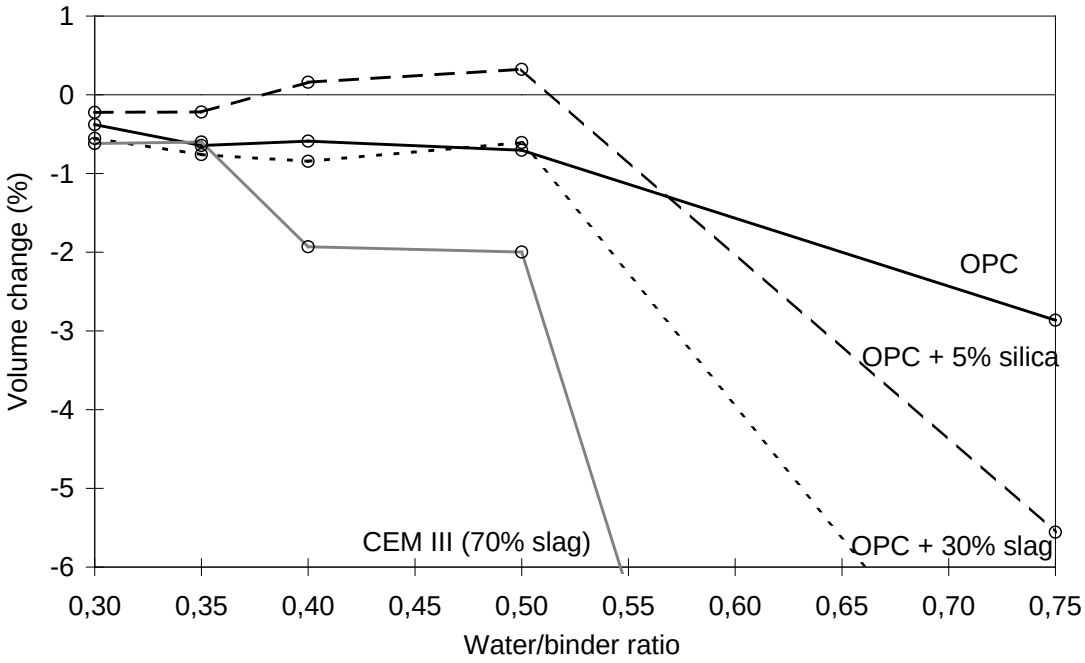

Figure 1 - Volume change after five winter seasons at the highway exposure site (Highway 40). Concrete with different binder combinations and water/binder ratios. No entrained air.

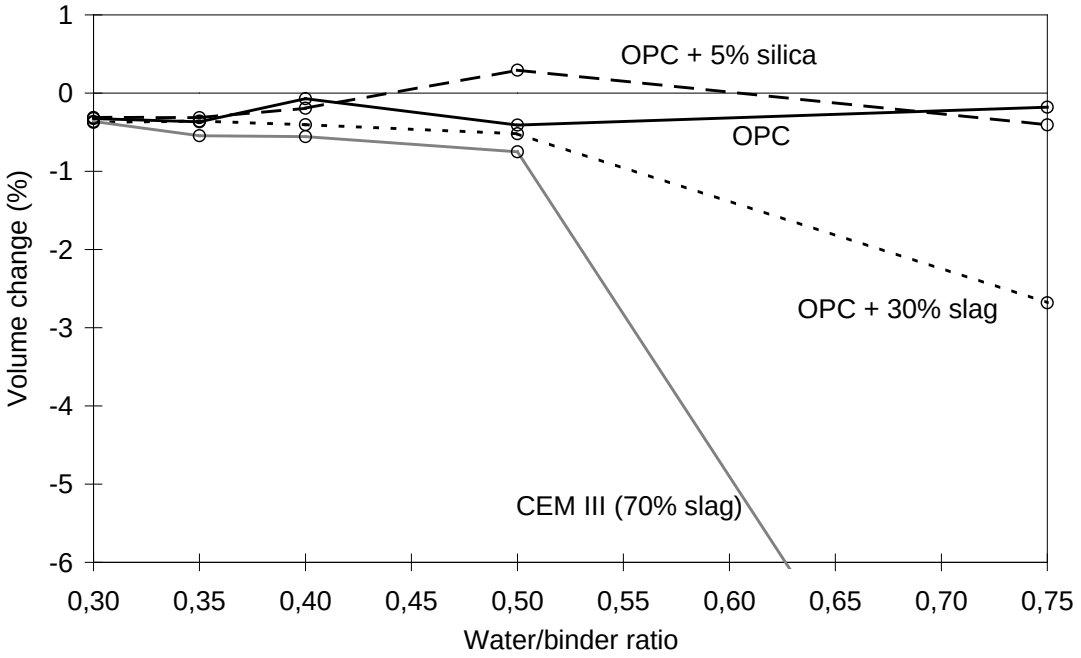

Figure 2 - Volume change after five winter seasons at the marine exposure site (Träslövsläge harbour). Concrete with different binder combinations and water/binder ratios. No entrained air.

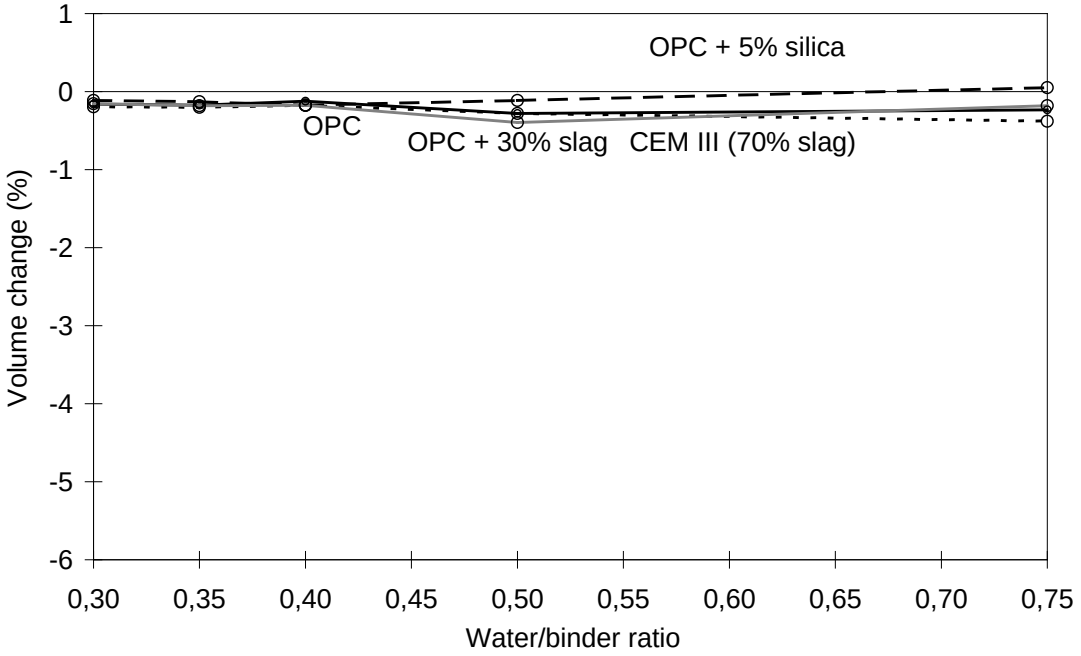

Figure 3 - Volume change after five winter seasons at the no-salt exposure site (SP in Borås). Concrete with different binder combinations and water/binder ratios. No entrained air.

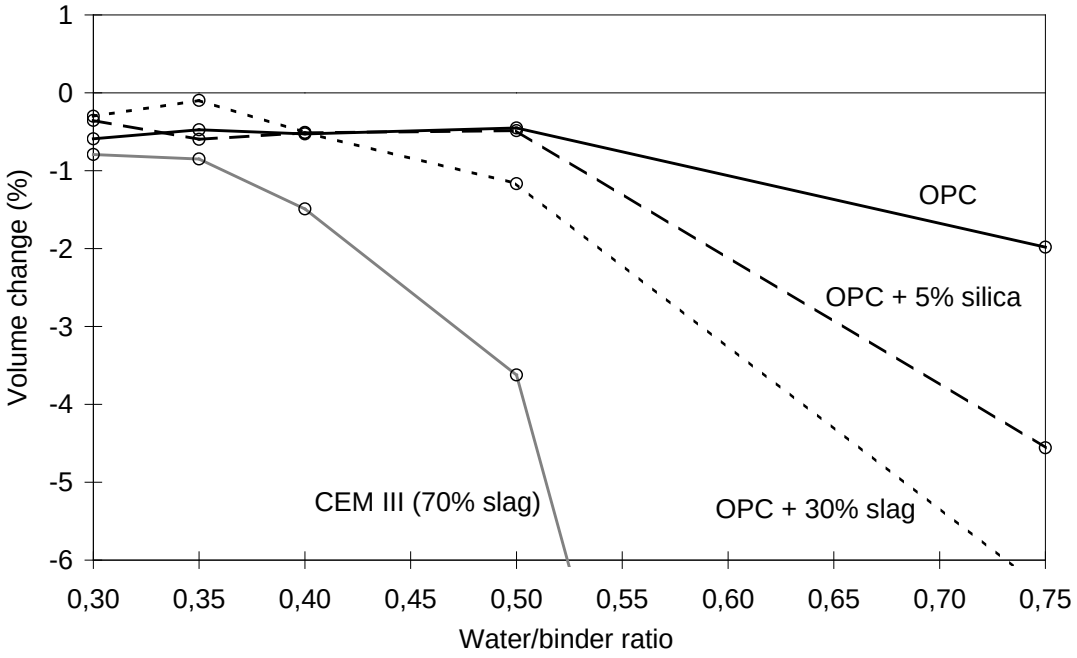

Figure 4 - Volume change after five winter seasons at the highway exposure site (Highway 40). Concrete with different binder combinations and water/binder ratios. With entrained air (4-5 %).

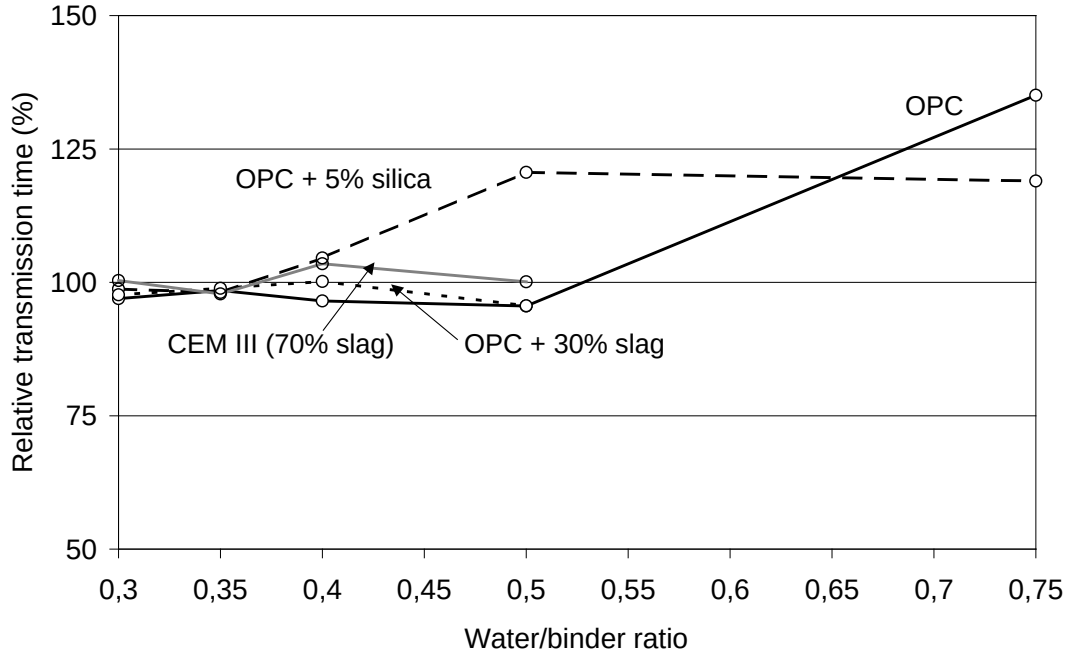

Figure 5 - Relative transmission time after five winter seasons at the highway exposure site (Highway 40). Concrete with different binder combinations and water/binder ratios. No entrained air.

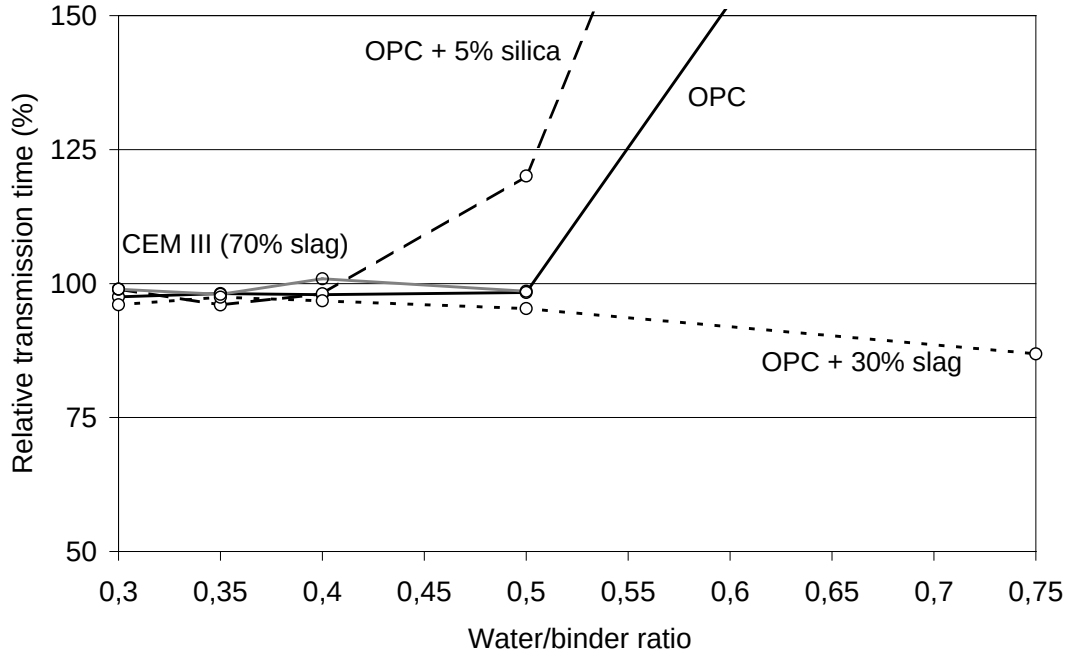

Figure 6 - Relative transmission time after five winter seasons at the marine exposure site (Träslövsläge harbour). Concrete with different binder combinations and water/binder ratios. No entrained air.

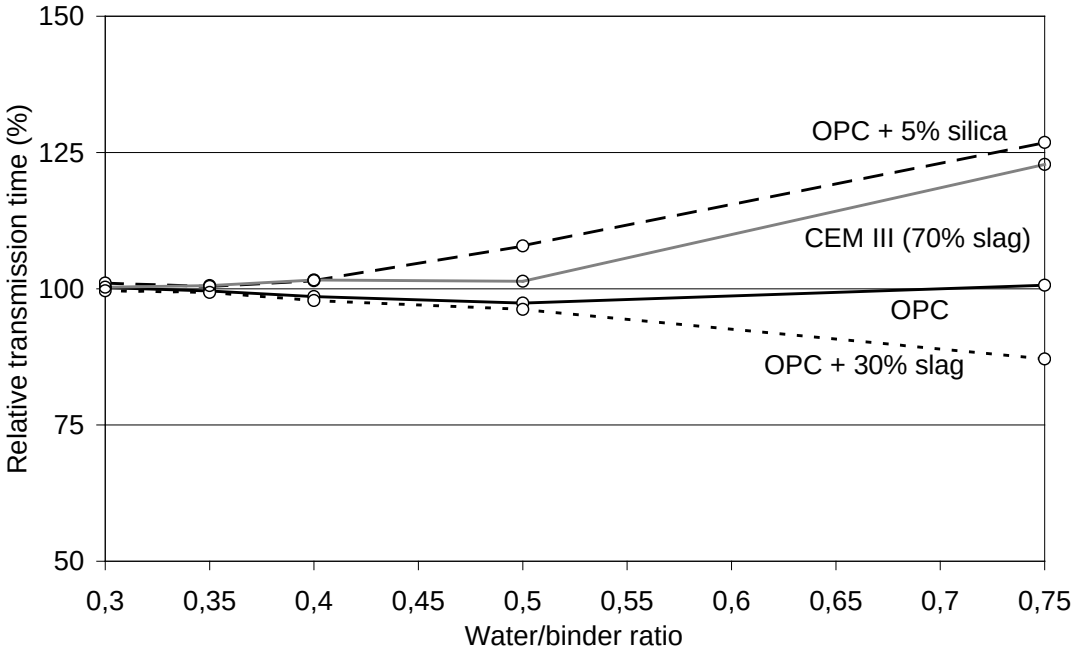

Figure 7 - Relative transmission time after five winter seasons at the no-salt exposure site (SP in Borås). Concrete with different binder combinations and water/binder ratios. No entrained air.

5. DISCUSSION

5.1 External frost damage

Figures 1, 2 and 3 show the external damage in the form of volume change after five winter seasons for different concrete qualities, all without entrained air, exposed in three different climates. Without comparing results from the different concrete qualities, it is clear that the climate has a large influence on the amount of external frost damage, i.e. surface scaling. Concrete exposed in a saline highway environment, Figure 1, shows much more extensive surface scaling than does concrete exposed in a salt-free environment. Concrete exposed in the marine environment shows external damage, but not as severe as concrete exposed in the highway environment, at least for qualities with w/b-ratios of 0.40 and over. These considerable differences in resistance to surface scaling can probably be explained by differences in:

- **Temperature**. The temperature in the marine environment is milder and fluctuates less than the temperature at the highway environment or the salt-free exposure site. However, the air temperature at these two latter sites is about the same.
- **Moisture conditions**. The moisture conditions at the different exposure sites vary significantly. During the winter months, the specimens at the highway site are subjected to a very moist environment, being constantly splashed by passing traffic. The specimens at the SP test site, however, are exposed only to natural precipitation.
- **Salt concentration**. The salt concentration in the water splashed over the samples at the highway site is, at least occasionally, much higher than the salt concentration in the marine environment. At the SP test site there is no exposure to salt.

Some significant differences with regard to surface scaling can be seen when comparing the different concrete qualities. For example, qualities with slag as part of the binder (CEM III and OPC + 30 % slag) show more severe external damage than mixtures with OPC and OPC + 5 % silica concrete, at least for qualities with w/b-ratio of 0.75. This is seen both at the highway and the marine exposure site. Concrete exposed at the salt-free test site, however, shows only small volume changes, irrespective of binder combination. Another significant difference is the increase in volume for some concrete qualities with OPC + 5 % silica as binder and with a w/b-ratio over 0.35. This increase is seen primarily at the highway and marine test sites. An increase in volume is probably caused by internal damage, i.e. micro-cracks: see further discussion below. A limitation of the volume measurements is that the measured volume is a net volume of both a negative and a positive element, in the respective forms of a volume loss due to surface scaling and a possible increase in volume due to internal cracking. Concrete qualities with an apparent volume loss might, therefore, also have a small increase in volume caused by internal cracking without this being observed. It is therefore important to complement volume measurements with other techniques in order to detect possible internal damage, e.g. ultrasonic pulse transmission time measurements.

Figure 4 shows the volume change after five winter seasons for concrete mixtures with entrained air exposed to the saline highway environment. In general, the volume changes for concrete with high water/binder ratios and entrained air are less than for concrete without entrained air (Figure 1). However, this is not valid for concrete qualities with CEM III as the binder. The volume change for qualities with CEM III as the binder and with entrained air is of the same order as (and sometimes even greater than) that for concrete without entrained air (w/b-ratios 0.50 and 0.75). For these qualities, entrained air does not seem to improve the scaling resistance. This

behaviour is confirmed by freeze/thaw testing in the laboratory, see Table 2. For concrete with CEM III as the binder, the air entrained qualities show damage of the same order as for concrete without air. For concrete with other binder types in this investigation, as expected, a significant improvement in scaling resistance is seen for qualities with entrained air compared to qualities without entrained air.

Comparing the results for concrete with and without entrained air after five years of exposure show in general only small differences in volume change for concrete with w/b-ratio 0.5 and below. However, the increases in volume for concrete qualities with OPC + 5 % silica that were observed in samples without entrained air are, as expected, not observed when entrained air is used.

5.2 Internal frost damage

Figures 5, 6 and 7 show the relative transmission time after five years of exposure for different concrete qualities, all without entrained air, exposed in three different climates. A relative transmission time over 100 indicates possible internal damage. Values over about 110 are more certain indications of internal damage. The results presented in Figures 5-7 show that a number of concrete qualities probably have internal damage and that there does not seem to be any significant difference between the different exposure climates. Table 3 shows the concrete qualities with possible internal damage at each test site.

Table 3 - Concrete qualities with potential internal damage at the three test sites. Detected by ultrasonic pulse transmission time.

Concrete quality	Highway	Marine	No salt exposure
OPC no air w/b 0.75	Damaged	Damaged	No D. indication
OPC+5 % silica no air w/b 0.75	Damaged	Damaged	Damaged
OPC+5 % silica no air w/b 0.50	Damaged	Damaged	Damaged
OPC+5 % silica no air w/b 0.40	Damaged	No D. indication	No D. indication
CEM III (70 % slag) no air w/b 0.75	Not measured	Not measured	Damaged

Combining the results from volume measurements with the transmission time measurements gives clear indications of internal damage for the concrete qualities with OPC + 5 % silica as binder shown in Table 3. Both an increase in volume and an increase in transmission time clearly indicate internal damage, probably micro-cracking. The surfaces of the qualities that show increased transmission time but no detectable increase in volume are too severely damaged to permit the detection of an increase in volume due to internal cracking. Microscopic techniques, such as analysis of polished sections or thin sections, could be used for finding further evidence of internal damage.

Polished sections were cut from each concrete quality listed in Table 3 to confirm and show possible internal cracking. The sections confirmed that the qualities judged as having internal damage when tested with ultrasonic pulse transmission time all showed internal cracking. Figure 8 show pictures of polished samples impregnated with epoxy resin and fluorescent dye for the three qualities with OPC + 5 % silica as binder listed in Table 3, exposed at the highway test site. The pictures show internal cracking in all three qualities, which increases in severity with increasing w/b-ratio.

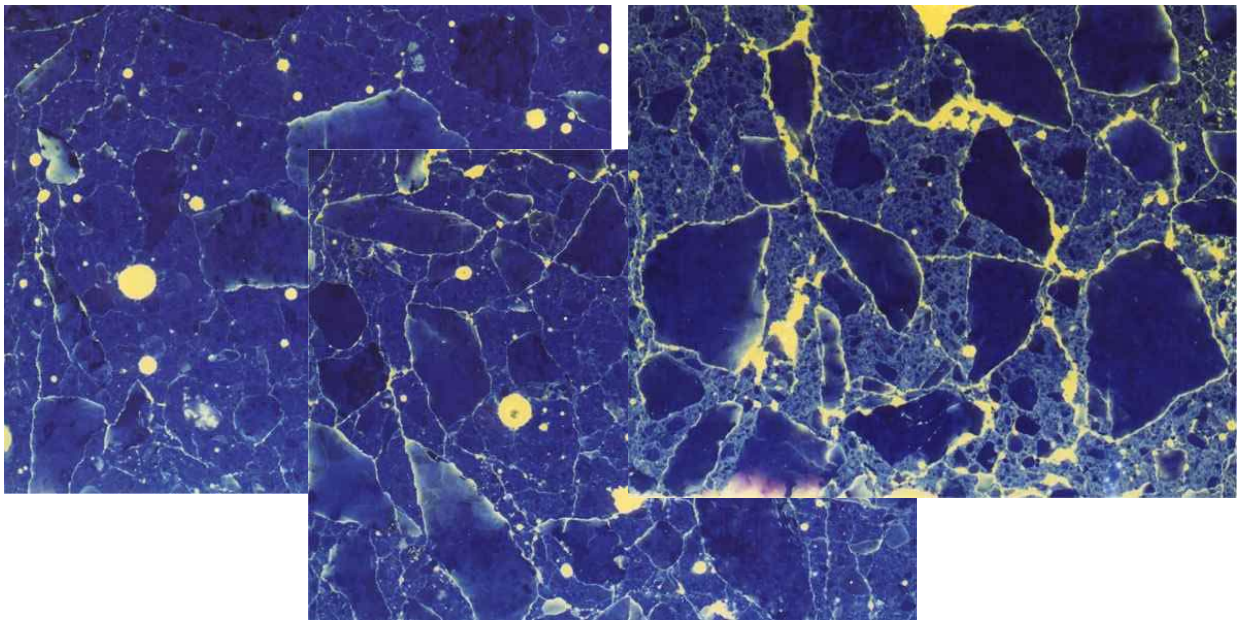

Figure 8 - Pictures of polished samples impregnated with epoxy resin and fluorescent dye of three concrete qualities exposed for five years at the highway exposure site. All with OPC + 5 % silica as binder and no air. From left: w/b 0.40; w/b 0.50; w/b 0.75.

The results from this investigation indicate that the concrete qualities with OPC + 5 % silica as binder and without entrained air seem more susceptible to internal frost damage than the other concrete qualities.

For the concrete quality with CEM III as binder in Table 3 it was not possible to measure the transmission time because of excessive surface damage. Microscopic analyses, however, show that the amount of internal damage, if any, is limited, see Figure 9. From the results discussed above, it seems as if the concrete qualities containing slag as part of the binder and without entrained air in this investigation are somewhat more resistant to internal damage than at least the concrete qualities with OPC + 5 % silica as binder. On the other hand, the concrete qualities with large amounts of slag as part of the binder seem to be more susceptible to scaling.

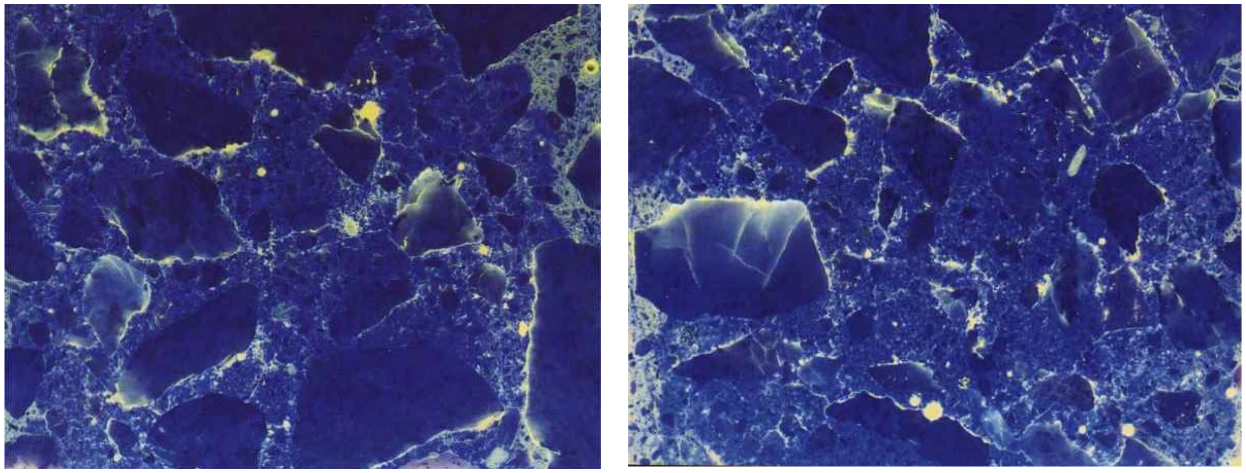

Figure 9 - Pictures of polished samples, impregnated with epoxy glue and fluorescent dye, of two concrete qualities exposed for five years at the highway and the marine exposure sites. From left: CEM III, no air and w/b 0.75, highway climate; CEM III, no air and w/b 0.75, marine climate.

A certain degree of 'healing' of specimens exposed at the highway site has been noted during the yearly measurements. Figure 10 shows results from yearly measurements of ultrasonic pulse transmission time on the three damaged concrete qualities with OPC + 5 % silica as binder.

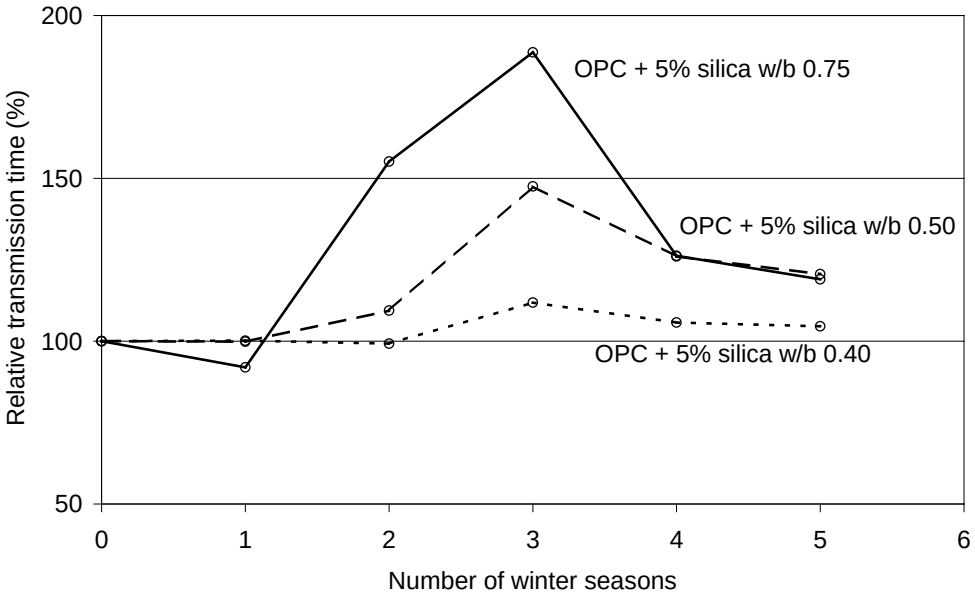

Figure 10 - Relative transmission time during five years of exposure at the highway exposure site.

The results in Figure 10 indicate a 'healing' effect after the third year, leading to reduced relative transmission time. Even though the reduction in relative transmission time or 'healing' seem substantial, the reduction can be caused by relatively limited healing. Only a few healing points are needed for an ultrasonic pulse to find a faster, shorter way through damaged material: see Figure 11. The healing can be explained by reaction between unhydrated cement and moisture transported in to the cracks, forming barriers of hydration products in the cracks and enabling the ultrasonic pulse to find a shorter way through the material.

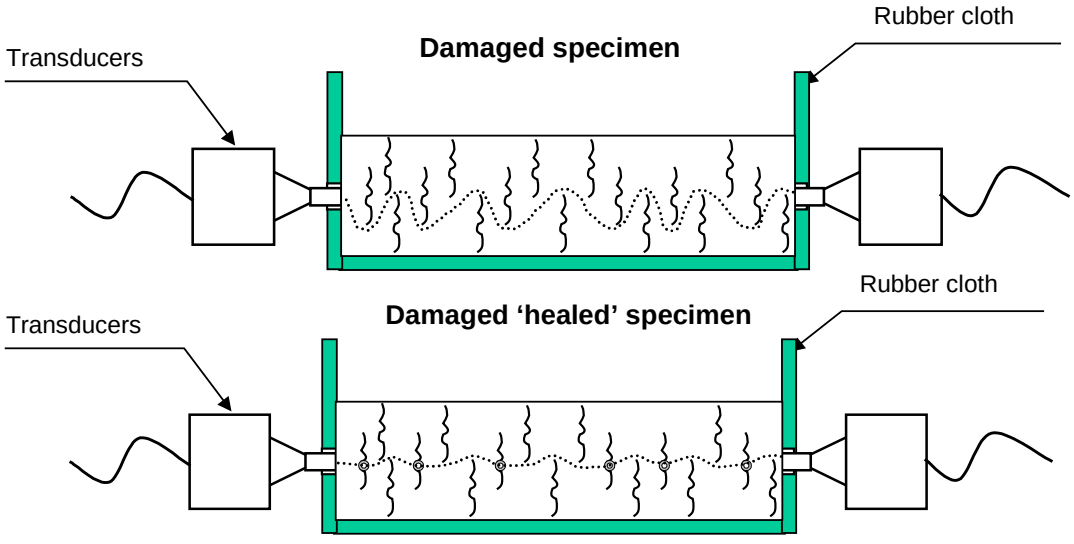

Figure 11 - Sketches of an ultrasonic pulse during transmission time measurements in a damaged specimen (top) and a specimen that has 'healed' (bottom).

This type of healing, where the hydration products form local barriers between cracks, gives no substantial healing in form of increased strength, durability or resistance to moisture or chlorides. Most of the network of micro cracks will probably still be open to an infiltration of moisture and chlorides, even though local healing creates a short cut for the ultrasonic pulse, resulting in a significantly shorter transmission time. This healing effect makes it hazardous to draw conclusions from single or even regular (if at long intervals) measurements of transmission time. A single measurement, after five year, on the concrete qualities shown in Figure 10 would lead to the conclusion that there might be some internal damage but not particularly severe. Evaluating results from yearly measurements and microscopic analysis (Figure 8) gives an indication of more severely damaged concrete. This is important knowledge when evaluating results not only from measurements in the laboratory but especially also when evaluating results from measurements in the field. From practical and economic points of view, it might be difficult to make measurements on building structures in the field on a more regular basis.

From the results described above, it can be noted that concrete with OPC or OPC + 5 % silica, with entrained air and a water/binder ratio of 0.50 or lower, seems to be salt/frost resistant in an aggressive highway environment, at least after five years' of exposure. Concrete qualities containing large amounts of slag as binder, however, seem to be less resistant to external salt/frost damage than concrete with OPC or OPC with some silica, at least when exposed to aggressive climates such as the highway or marine climate. These results are in agreement with results from an extensive field exposure investigation presented in [6]. In that investigation, a large number of concrete qualities with different amounts of slag and fly ash in the binder were exposed to the marine climate at the Treat Island exposure site, Canada. Results from that investigation clearly show that salt/frost resistance decreases with increasing amounts of slag as part of the binder; a result that is confirmed by the present investigation. As in the present investigation, the investigation at Treat Island also showed the positive effect of low water/binder ratio on the salt/frost resistance of concrete. The negative effects of high slag contents in the binder on the salt/frost resistance of concrete have been reported by several researchers, see [7, 8, 9, 10]. One probable explanation for this negative effect is the coarsening of the pore structure found in the carbonated skin of concrete containing slag [7, 9, 11]. Another probable explanation, presented in [9], is the existence of metastable carbonates in the carbonated zone of concrete rich in slag.

5.3 Correlation between laboratory and field tests

When testing the durability in the laboratory, e.g. salt/frost resistance, results are wanted that are relevant to durability in the actual field conditions. In the present investigation, each concrete quality was tested in the laboratory at the prescribed age of 28 days in accordance with the Swedish Standard for salt/frost resistance, SS 13 72 44 (the 'slab test'). Comparing the laboratory results with results from the field exposure site at SP's site (no salt exposure) is not relevant, since salt/frost resistant concrete are not prescribed in this climate. Concrete exposed at the marine and highway test sites is, however well suited for 'calibration' of the laboratory test method. Since the climate at the highway has proven to be most aggressive with regard to salt/frost resistance, the laboratory results are compared with results from this test site.

Figure 12 shows results from the laboratory tests and the volume change after five years of highway exposure. The diagram shows the scaling (kg/m²) after 56 freeze/thaw cycles as a function of the volume loss (%) after five years' highway exposure. The acceptance criterion in the laboratory test is 1 kg/m^2 (illustrated by a horizontal line). An acceptance criterion of 1.5 vol-

ume % (shown by the vertical line) after five years' exposure has been chosen for the field exposure specimens, corresponding to scaling of approximately 0.6 kg/m^2. Filled symbols represent concrete without entrained air. Symbols with a white centre represent concrete with entrained air. Enlarged symbols represent qualities with internal damage.

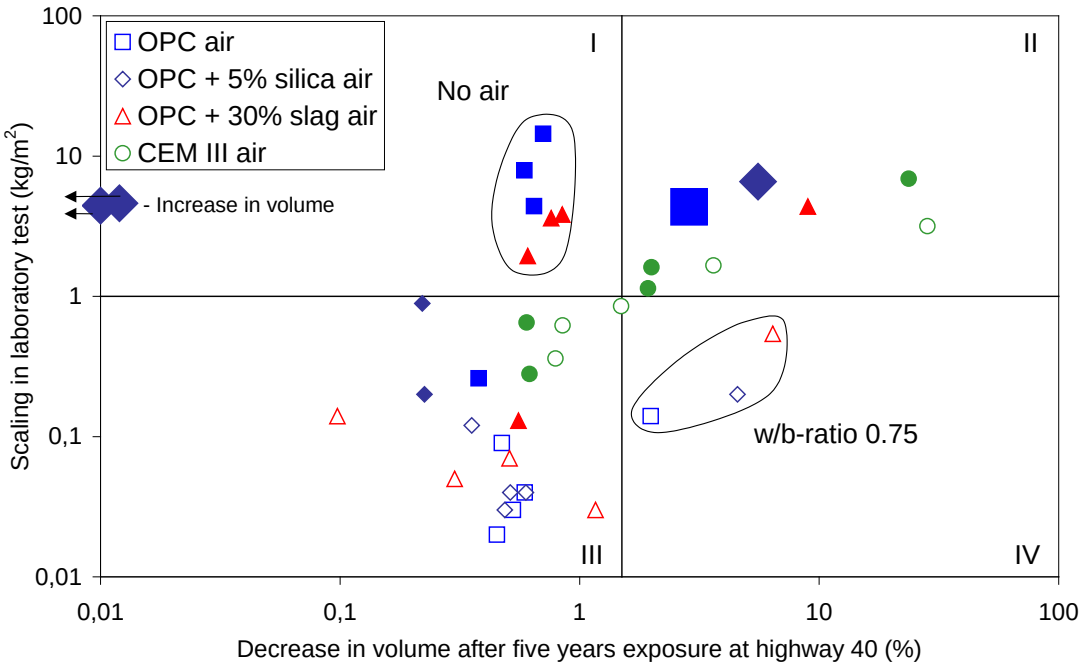

Figure 12 - Scaling resistance (tested in the laboratory) as a function of the decrease in volume for specimens exposed in the highway environment for five winter seasons. Filled symbols represent concrete without entrained air. Symbols with a white centre represent concrete with entrained air. Large symbols represent internal damage.

From the results presented in Figure 12, it can be seen that only three qualities fall into the IV quadrant, which is the worst case, and means that they are accepted by the test method, but fail in field exposure. These are air entrained qualities, however, with high water/binder ratios (0.75). The standard test method is primarily intended to be used for bridge concrete, with entrained air and with a w/b-ratio below 0.5.

Most qualities falls into quadrants II or III, which means that the test method and 'reality' correspond. Some concrete qualities fall into quadrant I, which means that the test method rejects them. However, as the concrete in quadrant I show only limited damage in the field, the test method results are on the safe side. None of these qualities has any entrained air, which makes them especially susceptible to frost damage. During the first five years, the climate has not been aggressive enough significantly to damage these qualities. However, one winter season with a more aggressive climate might cause internal damage as well as scaling on these qualities without entrained air, moving them into quadrant II. Two concrete qualities show an increase in volume and an increased transmission time, indicating internal frost damage. These qualities also fail the acceptance criterion when tested in the laboratory.

One explanation for the limited scaling in the field for the concrete qualities in quadrant I might be a positive effect of ageing. In a field investigation reported in [12], it was found that concrete aged and exposed in a marine climate showed better scaling resistance when tested in the labo-

ratory after aging than did virgin concrete. This increase in scaling resistance was especially apparent for concrete without entrained air, as was also found in this investigation. One effect of ageing that markedly improves the scaling resistance for OPC concrete is carbonation see [10].

On the whole, the results for concrete with w/b-ratio equal to or below 0.5 and with entrained air, shown in Figure 12, indicate that the slab test classifies these concrete qualities as could be expected. This is true for all binder combinations tested.

The results presented here are valid only for the materials, e.g. cement and binder types, used in this investigation. Other materials may lead to different results.

6. CONCLUSIONS

The following conclusions can be drawn after five years' exposure at the field exposure sites in a highway environment, a marine environment and a salt-free environment:

- There are substantial differences in external frost damage, depending on the environment. The most extensive external frost damage is observed on concrete specimens exposed in the highway environment. Concrete exposed in the salt-free environment shows only small changes in volume after five winter seasons.

- For all concrete qualities, scaling takes place only when exposed to salt. Internal damage, however, is observed on concrete qualities exposed at all three test sites, even when no salt is present.

- Concrete with OPC or OPC + 5 % silica as binder, with entrained air and a water/binder ratio of 0.5 or below, has good resistance to internal and external damage. Concrete with CEM III, however, suffers from severe scaling even with w/b-ratio below 0.5 and with entrained air.

- Internal damage is observed only for concrete qualities without entrained air and, furthermore, in most cases for concrete qualities with high water/binder ratios. However, for concrete qualities with OPC + 5 % silica as binder, internal damage is found at lower w/b-ratios, down to w/b 0.4.

- A 'healing' effect is observed on specimens with internal damage (cracking), making results from ultrasonic transmission time measurements hazardous to interpret. Interpreting results from single measurements can therefore lead to incorrect conclusions.

- Comparing results from laboratory testing in accordance with SS 13 72 44 (the 'slab test'), with results after five years of exposure at the field exposure sites, shows that the laboratory standard classifies most concrete qualities correctly.

7. ACKNOWLEDGEMENTS

This project is financially supported by FORMAS, the Development Fund of the Swedish Construction Industry and the cement producer Cementa AB.

REFERENCES

1. SS 13 72 44, 'Concrete testing- Hardened concrete- Frost resistance', Swedish Standards Institution (SIS, Stockholm), 3rd edition, 1995.
2. SFS 5448, 'Concrete, Durability, Freezing dilation', Finnish Standardisation Association (SFS), Helsinki, 1988.
3. Fagerlund, G., 'The critical degree of saturation method of assessing the freeze/thaw resistance of concrete', *Materials and Structures*, Vol.10, No.51, pp.217-229, 1977.
4. Utgenannt, P., 'The effect of binder on the frost resistance of concrete - Test specimens produced in 1996 - Material and production data and results from life testing in the laboratory', Swedish National Testing and Research Institute, BTB report no 1, 1997, (in Swedish).
5. Malmström, K., 'Cementsortens inverkan på betongs frostbeständighet' [The effect of cement type on the frost resistance of concrete], Swedish National Testing and Research Institute, Rapport 1990:07, 1990, (in Swedish).
6. Bremner, T.W. et.al., 'Role of supplementary cementing materials in concrete for the marine environment', in 'Durability of concrete – Aspects of admixtures and industrial by-products', Proceedings from the 2nd International seminar on - Some aspects of admixtures and industrial by-products, (Swedish council for building research, Gothenburg), 1989, pp. 23-32.
7. Gunter, M. et.al., 'Effect of curing and type of cement on the resistance of concrete to freezing in deicing salt solutions', ACI, SP 100, vol. 1, 1987, pp. 877-899.
8. Vesikari, E., 'The effect of ageing on the durability of concrete including by-products', in 'Durable concrete with industrial by-products', Proceedings from VTT Nordic research symposium 89, (Technical research center of Finland, Espoo), 1988, pp. 104-112.
9. Stark, J. et.al., 'Freeze-thaw and freeze-deicing salt resistance of concretes containing cement rich in granulated blast furnace slag', *ACI Materials Journal*, Vol. 94, No.1, 1997, pp. 47-55.
10. Utgenannt, P., 'Influence of carbonation on the scaling resistance of OPC concrete', Proceedings from the RILEM Workshop on Frost Damage in Concrete, Minneapolis, USA, 1999.
11. Matala, S., 'Effects of carbonation on the pore structure of granulated blast furnace slag concrete', Helsinki University of Technology, Faculty of Civil Engineering and Surveying, Concrete Technology, Report 6, Espoo, 1995.
12. Petersson, P.-E., 'Scaling resistance of concrete – Field exposure tests', Swedish National Testing and Research Institute, SP-report 1995:73, Borås, Sweden, 1995, (in Swedish).

AALBORG PORTLAND's durability project – 18 years judgement.

Dirch H. Bager
Ph.D., Chief Concrete Technologist
Research and Development Centre, Aalborg Portland A/S
Rørdalsvej 44, P.O. Box 165, DK-9100 Aalborg
E-mail: db@aalborg-portland.dk

ABSTRACT

Most of the information from 18 years exposure of 16 different types of concrete is presented in this paper. Three types of cement as well as secondary cementitious materials as fly ash and microsilica have been used.

The results demonstrate clearly, that fly ash and microsilica can improve the durability and the mechanical properties of concrete.

The paper present a huge amount of data. Only very general conclusions are drawn.

The behaviour of new types of concrete mixes, utilising new cements and new types of secondary cementitious materials might be judged on basis on a few tests carried out according to the test scheme used in the reported project.

Key words: Mineral additives, Flyash, microsilica, seawater, outdoor exposure, durability, mechanical properties

1 INTRODUCTION

Aalborg Portland initiated in 1983 a project to document the durability of concrete containing secondary cementitious materials as fly ash and microsilica.

Three different qualities of concrete are included in the project. The quality is characterised by the cement content, which is 260, 340 and 390 kg/m^3 respectively. With an approximately constant water demand of 140 l/m^3 for the various concrete mixes, this corresponds to w/c-ratios in the range of 0.35 to 0.55. The concrete types with 390 kg/m3 are generally judged as high performance types of concrete.

The project focused on exposure to seawater and natural weather as well as exposure to de-icing chemicals in the same amount as is used on the main roads in North Jutland. The test was initiated in 1983, and comprises both exposure sites in the harbour of Hirtshals and on Aalborg Portlands area. In this test series, 16 different concrete mixes are included. As reference, specimens have been stored in water at 20 ^{o}C. The test is designed to cover 25 years, hence the 18 years judgement does not include strength measurements or other destructive tests on the laboratory stored specimens.

The project was initiated in close co-operation with companies from the Danish concrete industry, including ready mix producers, contractors, consultants as well as additive producers.

2 DESCRIPTION OF THE FULL SCALE TESTS

The elements were cast in-situ at the in-land exposure site at Aalborg Portland, figure 2. The elements of comprised 1.0x1.0x0.2-meter flags to be exposed at the inland exposure site, as well as some 1.0x2.0x0.2 meter elements to be exposed in the splash zone in Hirtshals harbour. Some 1.0x2.0x0.2 m elements have also been exposed at the inland exposure site in order to judge on the influence of horizontal versus vertical casting and exposure. In addition, more than 60 cylinders, beams and cubes for laboratory measurements were cast for each concrete type.

Experimental set-up for measuring corrosion of the reinforcement was planned. Reinforcement mesh with varying cover thickness was placed in some of the elements. However, neither the set-up nor the actual measuring technique did result in consistent and reliable results, and the very time consuming measurements have been stopped. Hence, no information regarding reinforcement corrosion is available for the time being. (At 25 years age, a visual judgement might be carried out on drilled cores).

Figure 1 shows the arrangement of the test specimens at the inland test site at Aalborg Portland.

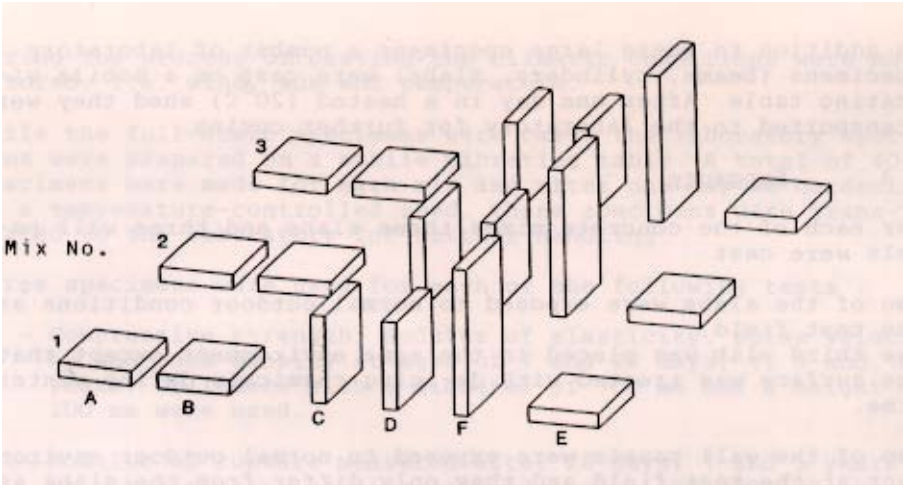

Figure 1. Arrangement of the test specimens at the inland test site at Aalborg Portland. Elements B, D & E have reinforcing mesh. Element E is exposed to de-icing salt during the winter season (3% NaCl solution, technical grade). Element F is the element situated in Hirtshals Harbour, only situated at the test area during casting of the elements /1/.

Figure 2A & 2B shows the actual test sites.

Figure 2A: Inland test exposure site at Aalborg Portland. Elements E to the left (Photographed in July 2001)

For the exposure to seawater in Hirtshals Harbour, a special rig of galvanised steel was made and mounted on the quay. The elements are placed in a depth so they are totally immersed during tide, and the upper ½ meter is exposed to air during ebb tide, as seen on figure 2.

Figure 2B. Elements in Hirtshals Harbour, ebb tide. (Photographed in July 2001)

3 MATERIALS

Chemical composition of the cement and the mineral additives are given in table 1. The mix design for the 16 different concrete types are presented in table 2.

Table 1: Cement and mineral additives

		CEM I 42.5	CEM I 42.5 SR	CEM II 42.5 / B-V	Fly ash	Micro Silica
SiO_2, %		21	24	27	53	92
Al_2O_3, %		5.2	2.5	10.3	31	2.2
Fe_2O_3, %		3.0	3.1	3.6	7.4	0.3
CaO, %		63	66	52	4.9	0.4
MgO, %		1.0	0.7	1.1	1.4	1.0
SO_3, %		2.9	1.8	2.3	0.7	0.7
LOI, %		1.5	0.9	2.3	2.4	3.0
Eqv. Na_2O, %		0.6	0.3	0.8	1.8	2.6
Fly-ash content, %		< 5	-	20 - 25	-	-
Blaine, m^2/kg		430	310	450	-	-
Boque composition of clinker	C_3S	55	60	55	-	-
	C_2S	20	26	20	-	-
	C_3A	10	2	10	-	-
	C_4AF	9	10	9	-	-
28 days strength, MPa		54	50	51	-	-

When mineral additions were used, activity factors of 3 and 0.3 respectively for microsilica and flyash were used in the mix-design. These activity factors are related to the strength giving properties of the products.

In 1987, the Danish Engineering Society published an Advice on the Use of Flyash and Microsilica in Structural Concrete /4/. In this advice, a conservative judgement on the activity factors with respect to durability lead to activity factors of 2 and 0.5. Since then these activity factors have been used in the Danish codes of practise for structural concrete, when calculating the equivalent w/c-ratio. In this paper an activity factor of 0.4 are used for fly ash, in accordance with EN 206.

Table 2: Concrete mix-design

		1	2	3	4	5	6	7	8	9	10	11	12	13	14	15	16
		260 kg cement					340 kg cement						390 kg cement				
Cement ¤)		BC	RP	SR	RP	BC	BC	RP	SR	BC	SR	RP	BC	RP	SR	SR	BC
Cement	kg/m^3	261	200	264	261	199	333	256	340	260	327	334	397	300	390	300	300
Flyash	kg/m^3	-	-	-	-	-	-	-	-	-	65	-	-	-	-	-	-
Micro silica	kg/m^3	-	20	-	-	21	-	26	-	26	-	-	-	30	-	30	32
0/4 mm	kg/m^3	718	780	732	725	775	630	725	653	703	600	635	565	640	592	670	635
4/8 mm	kg/m^3	125	125	125	125	125	125	125	125	125	125	125	125	125	125	125	125
8/16 mm	kg/m^3	1100	1100	1100	1100	1100	1100	1100	1100	1100	1100	1100	1100	1100	1100	1100	1100
Water	kg/m^3	141	125	138	140	143	146	141	142	140	141	144	165	140	142	136	143
w/c–ratio #)	-	0.54	0.52	0.52	0.54	0.59	0.44	0.46	0.42	0.45	0.40	0.43	0.42	0.39	0.36	0.38	0.39
Slump	mm	60	50	45	50	40	55	60	60	55	65	50	50	70	60	50	40
Air content	%	5.8	5.6	5.7	5.8	5.5	5.6	5.5	6.0	5.9	5.8	5.8	5.4	5.8	5.4	5.6	5.5

¤): Cement – types: RP: CEM I 42.5. SR: CEM I 42.5 – SR. BC: CEM II 42.5 B-V
#): w/(c+2MS+0.4FA)

Originally it was planned to use absolutely sound aggregates in order to avoid aggregate related durability problems. However, at too late stage it appeared, that the sand fraction did contain alkali reactive materials in the form of porous opaline flint. Thus problems related to alkali silica

reactions (ASR) must be foreseen. The coarse aggregates consisted of sound sea dredged rounded granite particles.

The concrete was mixed in a 3 m^3 free fall mixer, and transported in a truckmixer to the test area at Aalborg Portland, where al the elements were cast. The concrete for the slabs was vibrated with a screed-vibrator, trowelled by hand and finally broomed with a fibre broom to achieve a uniform grooved surface. Immediately after finishing, a curing membrane was sprayed onto the surface to prevent loss of water from the concrete. The wall panels were cast vertically and vibrated with a poker vibrator, and the formwork made of plywood resulted in a smooth surface. Loss of water could not take place until the formwork was stripped after 7 maturity days. Immediately after removal of the formwork the concrete surfaces was sprayed with a curing membrane.

For different practical reasons, casting of the elements of some of the different concrete types was not carried out on the same day. Only weather conditions for casting the large elements for Hirtshals Harbour will be reported here (Table 3)

Table 3: Weather conditions during casting of elements for exposure in Hirtshals Harbour.

Mix No.	Date	Air temp. deg. C	Concrete Temp. deg. C	Vind velocity m/sec	Relative humidity %	Sun
1	4/8 – 83	18	20	0-2	75	Clouded
2	14/4 – 83	7	9	2-3	90	Overcast
3	19/4 – 83	9	10	1-3	80	Clouded
4	21/4 – 83	9	10	3-4	80	Hazed
5	26/4 – 83	7	12	1-3	95	Overcast
6	2/5 – 83	9	12	3-5	80	Clouded
7	4/5 – 83	6	12	1-3	95	Overcast
8	7/6 – 83	16	16	4-6	60	Clear sun
9	9/6 – 83	17	17	3-4	75	Hazed
10	14/6 – 83	19	17	1-3	60	Clear sun
11	16/6 – 83	15	17	2-3	85	Clouded
12	21/6 – 83	23	24	6-8	50	Clear sun
13	16/8 – 83	19	19	1-3	95	Overcast
14	18/6 – 83	16	20	2-4	60	Clouded
15	30/6 – 83	15	19	1-2	85	Clouded
16	2/8 – 83	15	20	0-2	80	Overcast

4 PROPERTIES OF THE HARDENED CONCRETE

A comprehensive amount of investigations on the 16 types of concrete have been carried out, both initially and during the succeeding years. The tests and measurements involves:

a) Macro analysis on drilled cores.
b) Structural analysis on thin sections.
c) Measurements of air void characteristics on plane polished sections.
d) Freeze/thaw resistance according the former Nordic method.
e) Measurement of strength developments, both on samples stored in water at 20 deg. C, and on drilled cores.
f) Measurement of drying shrinkage.
g) Measurements of chloride profiles on the elements in Hirtshals Harbour.

h) Carbonation depths.

Survey reports for 1, 5 and 10 years exposure are published in /1/, /2/ & /3/ respectively.

4.1 Structural analysis, ad. a) & b).

Results from these measurements will not be reported here, because the technique and the way of judging the results have been changed since, meaning that it will be difficult to compare former results with measurements carried out today. Furthermore, a reason for not presenting the results is, that the author in 1987 concluded, that there could not be found any relation between the structural data and the abrasion on the surface on the elements in Hirtshals Harbour. Only some subjective remarks as "Increased capillary porosity in the outer few mm", or "The outer few mm do not contain artificial air bubbles" gave some relationship to the abrasion. /2/

In 1993 new thin sections from cores from the elements in Hirtshals Harbour was made. A summary of the findings is presented in table 4

Table 4: Summary of thin section analysis on concrete exposed 10 years in Hirtshals Harbour

Type	Binder comp.	Microcracks pr mm^2	Portlandite filled cracks	Portlandite filled pores	Alkali silica reaction	Ettringite filled pores	Ettringite filled cracks	Max. Carbonation depth, mm
1	BC	0.10	-	-	gel	some	-	1.3
2	RP+MS	0.24	minor	-	-	-	-	1.0
3	SR	0.32	advan.	Minor	-	-	-	2.5
4	RP	0.30	some	-	gel	some	some	1.6
5	BC+MS	0.30	-	-	-	minor	-	0.6
6	BC	0.58	minor	-	-	advan.	-	1.6
7	RP+MS	-	minor	-	-	minor	-	1.6
8	SR	0.52	some	Minor		minor	-	0.5
9	BC+MS	1.63	-	-	-	some	-	1.1
10	SR+FA	0.26	some	-	-	some	-	1.3
11	RP	0.07	some	-	gel	some	minor	1.5
12	BC	0.19	minor	-	-	some	-	1.3
13	RP+MS	6.07	minor	-	-	some	-	0.4
14	SR	0.10	some	-	-	-	-	1.8
15	SR+MS	4.74	some	-	-	minor	-	0.4
16	BC+MS	2.16	-	-	-	minor	-	0.6

RP: CEM I 42.5. SR: CEM I 42.5 – SR. BC: CEM II 42.5 B-V

4.2 Air void characteristics, ad. c)

Air void characteristics were measured on plane polished sections from cores from the hardened concrete elements. The data are presented in table 5

Table 5: Air void characteristics, hardened concrete (1983)

Concrete type		1	2	3	4	5	6	7	8	9	10	11	12	13	14	15	16
Air content	%	2.8	2.8	4.7	4.5	2.6	1.9	1.6	5.6	4.7	4.0	4.3	4.7	5.6	3.5	4.7	2.8
Spec. surface	mm^{-1}	50	41	28	52	32	59	35	29	37	36	30	32	29	36	30	42
Spacing factor	Mm	0.13	0.16	0.18	0.10	0.20	0.13	0.23	0.16	0.14	0.15	0.17	0.15	0.16	0.16	0.17	0.15

4.3 Freeze/Thaw resistance, ad. d)

Freeze/thaw resistance was judged with the former Nordic method. This method was withdrawn in 1985, after a recommendation from a Nordic Miniseminar "Beton & Frost" held in Køge 1983. /5/. The temperature control as well as the multidirectional temperature gradients made the method so in exact, that the results are meaningless. Hence they are not presented here.

4.4 Development of mechanical properties, ad. e)

For the 16 different types of concrete, measurement of the development of strength properties have been made at laboratory water stored specimens as well as on drilled cores from the exposed elements. The following tables 6 - 12 present the results.

Table 6: Development of compressive strength, MPa. 20 °C watercured specimens

Concrete type	1	2	3	4	5	6	7	8	9	10	11	12	13	14	15	16
7 days	20	21	17	21	16	24	30	31	21	33	30	28	30	38	39	29
28 days	27	36	25	28	27	32	51	40	34	44	38	38	49	48	62	46
28 days ¤	*32*	*43*	*30*	*34*	*32*	*38*	*61*	*48*	*41*	*53*	*46*	*46*	*59*	*58*	*74*	*55*
1 year	44	49	35	36	40	50	64	57	47	70	47	54	57	67	69	57
5 years	44	46	38	31	46	49	65	63	54	75	48	58	64	73	73	60
10 years	43	44	37	30	44	47	59	63	50	72	47	59	62	77	74	62

¤: Cube strengths calculated in accordance with the introductory remarks

Table: 7: Compressive strength (MPa) of concrete watercured 7 days, successively stored in air at 20 °C and relative humidity of 60% for 10 years

Concrete type	1	2	3	4	5	6	7	8	9	10	11	12	13	14	15	16
10 years	25	31	23	29	24	35	39	36	32	42	37	41	44	38	56	41

Table 8: Development of compressive strength, MPa. Vertical drilled cores from element B and E. (Elem. E has been salted during winter season)

Concrete type	1	2	3	4	5	6	7	8	9	10	11	12	13	14	15	16
28 days	26	38	19	20	29	28	48	33	38	40	35	-	-	52	61	46
1 year	39	49	36	28	38	44	69	47	43	52	46	43	57	65	69	52
1year, elem. E	39	39	43	28	42	44	50	48	44	65	43	53	54	58	65	50
10 years	36	44	35	18*	37	44	60	47	42	55	**	43	46	65	59	50
18 years	37	47	37	20*	48	45	69	53	52	66	38*	51	60	76	76	55

*: Cracks from ASR

**: Disintegrated from ASR

Table 9: Development of compressive strength, MPa. Horizontally drilled cores, element D

Concrete type	1	2	3	4	5	6	7	8	9	10	11	12	13	14	15	16
28 days	32	31	28	24	28	33	50	38	36	43	40	-	-	51	67	52
1 year	42	41	36	36	36	46	62	48	67	62	52	51	47	64	68	55
10 years	44	37	32	31	38	47	61	46	51	60	41*	55	56	59	61	61

*: Cracks from ASR

Table 10: Development of compressive strength, MPa. Drilled cores from elements in Hirtshals Harbour

Concrete type	1	2	3	4	5	6	7	8	9	10	11	12	13	14	15	16
1 year	39	39	43	28	42	44	49	48	44	65	43	53	54	58	65	50
10 years	47	43	48	12*	50	48	56	58	44	70	35*	59	56	71	67	57

*: Cracks from ASR

Table 11: Development of static modulus, Gpa. 20 °C watercured specimens. For 28 days even cores from elements B (vertical) and D (horizontal)

Concrete type	1	2	3	4	5	6	7	8	9	10	11	12	13	14	15	16
7 days	26	25	24	25	26	28	27	30	25	30	29	29		33		29
28 days	30	33	28	27	30	29	32	34	32	31	31	30		34		32
28 days, el. B	27	29	27	23	28	24	27	28	27	28	27	33	32	36	43	34
28 days, el. D	29	29	25	25	27	26	30	28	30	28	26	31	31	36	46	34
1 year	34	36	32	31	36	38	40			38	35	39	36	38	37	35
5 years	37	38	38	27	38			42	37	42	33	38	39	41	39	
10 years	35	33	34	30	35	32	32	37	30	42	36	34	33	48	39	38

Table 12: Development of dynamic modulus, GPa. 20 °C watercured specimens

Concrete type	1	2	3	4	5	6	7	8	9	10	11	12	13	14	15	16
7 days	45	46	42	42	43	45	49	52	44	51	47	48	48	55	43	47
28 days	50	51	57	47	51	51	54	56	51	53	53	53	52	56	49	50
1 year	54	58	48			54	57	56	50	52	57	54	56	59	57	57
5 years	57	59	50	48	59	59	61	64	56	61	55	58	60	64	63	58
10 years	49	50	46	42	49	49	53	53	47	52	48	51	49	55	54	50

4.5 Measurement of drying shrinkage, ad. f)

For each of the 16 concrete types, 100x100x600 mm beams were cast for measurement of drying shrinkage. The beams were stored in water for 28 days before exposure to relative humidity of 60 %, and temperature of 20 deg. C. The shrinkage data are listed in table 13.

Table 13: Drying shrinkage, % (relative humidity 60%, 20 deg. C)

Type:.	Binder comp.	Age, Days						
		7	14	28	56	112	365	1095
1	BC	0,142	0,231	0,337	0,425	0,464	0,507	0,538
2	RP+MS	0,159	0,234	0,365	0,411	0,465	0,534	0,549
3	SR	0,111	0,211	0,346	0,483	0,510		
4	RP	0,221	0,319	0,467	0,574	0,603	0,694	0,729
5	BC+MS	0,190	0,306	0,408	0,503	0,559	0,682	0,728
6	BC	0,218	0,314	0,413	0,515	0,531	0,632	0,655
7	RP+MS	0,169	0,232	0,308	0,375	0,398	0,487	0,510
8	SR	0,170	0,219	0,298	0,385	0,418	0,500	0,550
9	BC+MS	0,170	0,207	0,267	0,329	0,351	0,438	0,502
10	SR+FA	0,112	0,202	0,268	0,354	0,400	0,485	0,531
11	RP	0,132	0,222	0,302	0,377	0,425	0,495	0,534
12	BC	0,133	0,223	0,289	0,350	0,387	0,493	0,535
13	RP+MS	0,130	0,182	0,250	0,303	0,330	0,439	0,492
14	SR	0,143	0,200	0,278	0,365	0,427	0,514	0,569
15	SR+MS	0,080	0,143	0,198	0,223	0,263	0,382	0,446
16	BC+MS	0,102	0,147	0,203	0,267	0,302	0,370	0,468

RP: CEM I 42.5. SR: CEM I 42.5 – SR. BC: CEM II 42.5 B-V

In figure 3 the drying shrinkage up to 112 days for the five high performance types of concrete is shown.

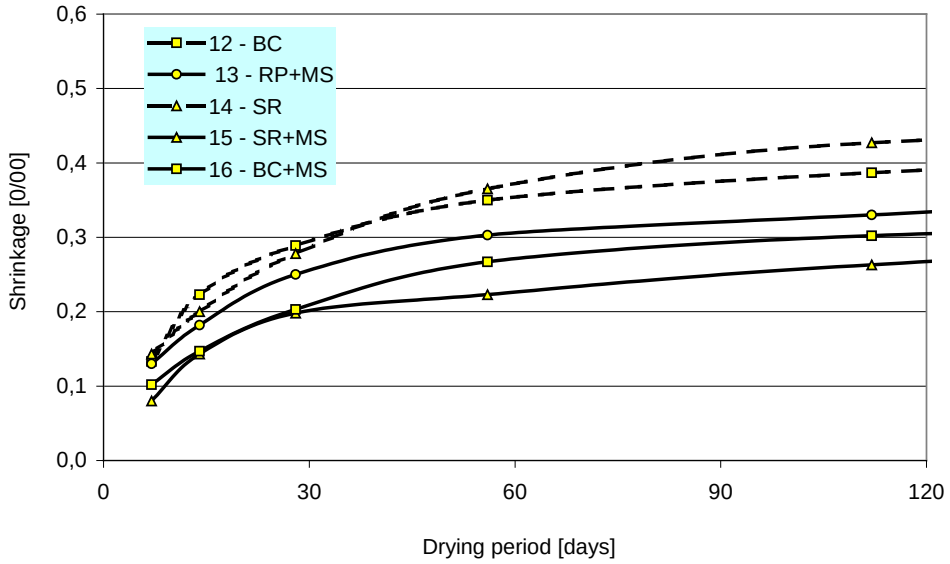

Figure 3: Drying shrinkage of the five high performance types of concrete

4.6 Measurement of chloride profiles, ad. g).

After 8½ year, chloride profiles in the elements exposed in Hirtshals Harbour were measured. Table 14 lists the results.

Table 14: Chloride profiles (weight pct. of concrete) after 8½ year's exposure in Hirtshals Harbour

		Depth from surface [mm]				
Element	Binder	2.5	7.5	12.5	17.5	32.5
1	BC	0.32	0.40	0.33	0.31	0.00
2	RP+MS	0.18	0.26	0.18	0.17	0.00
3	SR	0.24	0.22	0.21	0.18	0.00
4	RP	0.40	0.27	0.31	0.25	0.00
5	BC+MS	0.25	0.22	0.20	0.16	0.00
6	BC	0.39	0.47	0.34	0.26	0.00
7	RP+MS	0.31	0.28	0.26	0.17	0.00
8	SR	0.28	0.24	0.24	0.15	0.02
9	BC+MS	0.25	0.24	0.22	0.16	0.00
10	SR+FA	0.44	0.39	0.22	0.21	0.00
11	RP	0.22	0.28	0.17	0.16	0.00
12	BC	0.47	0.45	0.31	0.15	0.00
13	RP+MS	0.53	0.41	0.31	0.23	0.00
14	SR	0.35	0.26	0.19	0.16	0.00
15	SR+MS	0.31	0.28	0.21	0.14	0.00
16	BC+MS	0.27	0.31	0.31	0.21	0.00

RP: CEM I 42.5. SR: CEM I 42.5 – SR. BC: CEM II 42.5 B-V

4.7 Carbonation depth, ad. h)

After 10 years indoor exposure, 60% relative humidity, 20 deg. C, the depth of carbonation was measured with phenolphthalein, se table 15. In table 4, carbonation depths after 10 year for the elements in Hirtshals Harbour are shown.

Table 15: Depth of carbonation after 10 years indoor exposure

Concrete type		1	2	3	4	5	6	7	8	9	10	11	12	13	14	15	16
Carbonation depth	mm	27	28	41	30	34	24	18	20	25	16	18	16	16	15	14	17

5 DURABILITY JUDGEMENT AFTER 18 YEARS

In 2001, i.e. after 18 years exposure, a comprehensive study of the elements in Hirtshals Harbour have been carried out in relation to a Ph.D. study on seawater attack. See /6, 7/.

In figures 4 – 19, surfaces of the inland exposed concrete flags are shown, as well as microscopic structure and the chloride profile (table 16) for the 16 elements in Hirtshals Harbour. For what concerns the chloride profiles, the chloride profiles after 8½ year (table 14) are shown as well.

Table 16: Chloride profiles (weight pct. of concrete) after 18 year's exposure in Hirtshals Harbour. The chloride content in the seawater is 19 g/l. /12/

		Depth from surface [mm]					
Element	Binder	2.5	7.5	12.5	17.5	32.5	37.5
1	BC	0.29	0.43	0.38	0.33	0.20	0.16
2	RP+MS	0.27	0.33	0.33	0.25	0.17	0.13
3	SR	0.13	0.16	0.18	0.17	0.13	0.12
4	RP	-	-	-	-	-	-
5	BC+MS	0.20	0.24	0.25	0.18	0.12	0.08
6	BC	0.45	0.47	0.43	0.34	0.21	0.15
7	RP+MS	0.34	0.35	0.28	0.30	0.17	0.13
8	SR	0.46	0.37	0.35	0.30	0.21	0.20
9	BC+MS	0.24	0.31	0.25	0.20	0.07	0.04
10	SR+FA	0.39	0.35	0.31	0.22	0.06	0.01
11	RP	0.29	0.30	0.33	0.30	-	-
12	BC	0.44	0.46	0.37	0.31	0.04	0.02
13	RP+MS	0.41	0.36	0.34	0.28	0.12	0.07
14	SR	0.30	0.31	0.24	0.23	0.18	0.18
15	SR+MS	0.36	0.31	0.30	0.24	0.13	0.10
16	BC+MS	0.27	0.36	0.33	0.25	0.02	0.00

RP: CEM I 42.5. SR: CEM I 42.5 – SR. BC: CEM II 42.5 B-V

Photographs of the microstructure (epoxy impregnated thin sections) shows areas of 3.0 mm x 3.9 mm. The thin sections have been taken close to the surface of the elements. The dark areas are sand particles; the circular light areas are artificial entrained air. Narrow light lines are cracks and variation in color of the cement paste matrix between the sand particles is due to variation in w/c-ratio. The lighter the color, the larger the w/c-ratio.

In the current Danish Code of Practice – DS411 / 1999, a coverlayer to the reinforcement of at least 45 mm is prescribed for concrete exposed to sea water. Assuming a critical content of chlorides of 0.1 % Cl^- by mass of concrete, the time for expected initiation of reinforcement corrosion can be estimated by extrapolation of the chloride profiles in figures 4 to 19. [The extrapolation is not shown on the figures]. It has to be emphasized that such value of the critical Cl^- content is a very rough assumption. Different types of binders will not have the same chloride binding capacity. Thus, identical Cl^- contents do not necessarily mean the same amount of free harmful Cl^- ions. Furthermore, the pH value of the pore solution influences the passivation of the

reinforcement steel. Hence different cements and binders might give rise to different degrees of resistance to corrosion of the reinforcement.

a) Surface of concrete exposed to natural weathering

b) Surface of concrete exposed to natural weathering + deicing salts

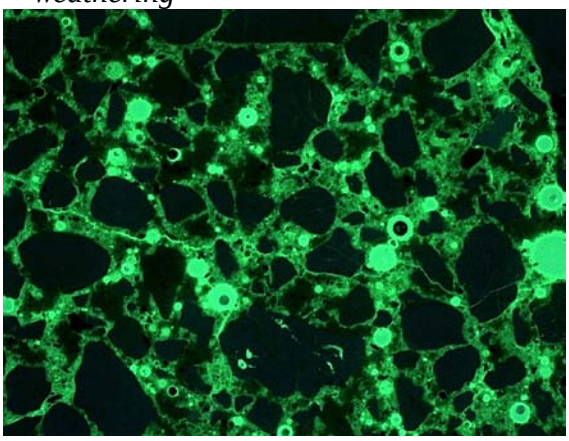

c) Microstructure of concrete exposed to sea water in Hirtshals Harbour

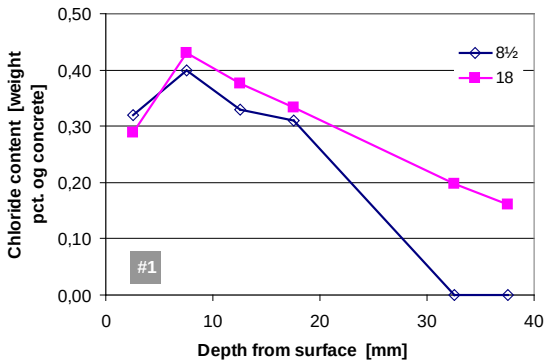

d) Chloride profile for concrete exposed to sea water in Hirtshals Harbour

Figure 4: Concrete type 1 after 18 years exposure

Figure 4 shows, that:

- The concrete surface is vulnerable for freeze/thaw and deicing salt. The cracks might be due to ASR, since thin sections from the tidal zone in Hirtshals reveals such reactions /7/.
- The paste matrix is homogeneous, and only few cracks have appeared.
- The air-content is low.
- Corrosion of reinforcement can be expected after app. 18 years.

a) Surface of concrete exposed to natural weathering

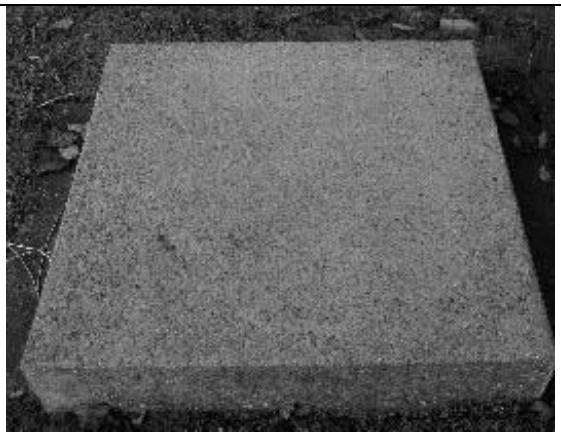

b) Surface of concrete exposed to natural weathering + deicing salts

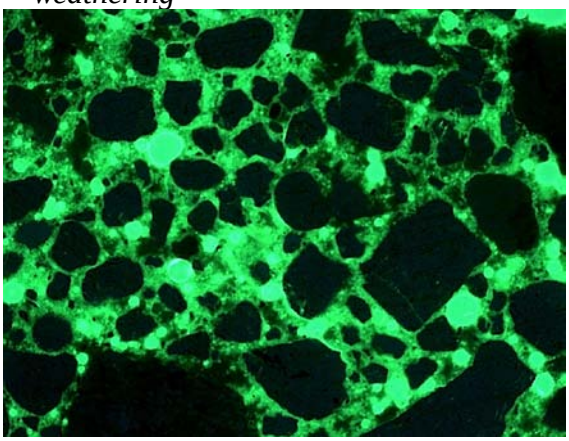

c) Microstructure of concrete exposed to sea water in Hirtshals Harbour

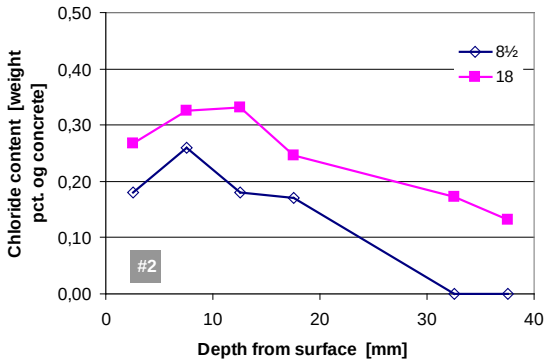

d) Chloride profile for concrete exposed to sea water in Hirtshals Harbour

Figure 5: Concrete type 2 after 18 years exposure

Figure 5 shows, that:

- The concrete surface is resistant to freeze/thaw and deicing salt.
- The paste matrix is fairly homogeneous.
- The air-content is low.
- Corrosion of reinforcement can be expected before 18 years age.

a) Surface of concrete exposed to natural weathering

b) Surface of concrete exposed to natural weathering + deicing salts

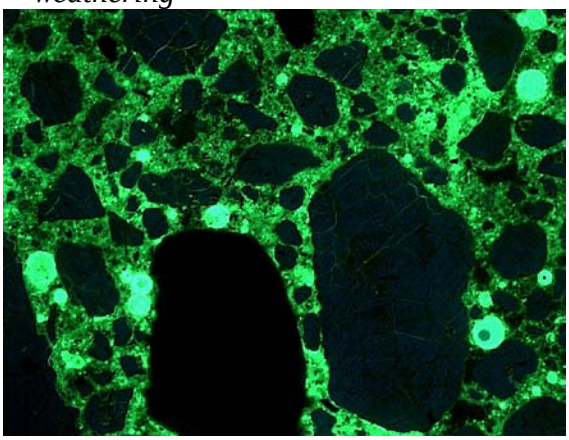

c) Microstructure of concrete exposed to sea water in Hirtshals Harbour

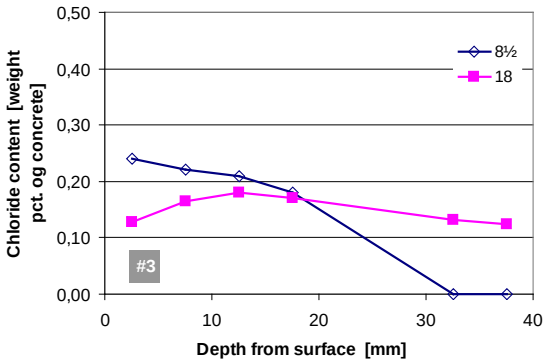

d) Chloride profile for concrete exposed to sea water in Hirtshals Harbour

Figure 6: Concrete type 3 after 18 years exposure

Figure 6 shows, that:

- The concrete surface is slightly vulnerable for freeze/thaw and deicing salt.
- The paste matrix is homogeneous.
- The air-content is fairly low and uneven distributed.
- Corrosion of reinforcement can be expected before 18 years age.
- The chloride content after 18 years is almost constant from the surface to the measured depth of 40 mm.
- Weak ASR can be seen, mainly in the outer layers of the submerged zones of the element in Hirtshals /7/.

a) Surface of concrete exposed to natural weathering

b) Surface of concrete exposed to natural weathering + deicing salts

It was not possible to make a representative thin section of this concrete.

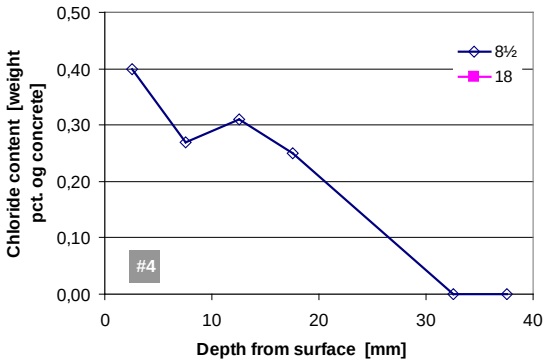

c) Microstructure of concrete exposed to sea water in Hirtshals Harbour

d) Chloride profile for concrete exposed to sea water in Hirtshals Harbour

Figure 7: Concrete type 4 after 18 years exposure

Figure 7 shows, that the concrete has been totally disintegrated by alkali silica reactions.

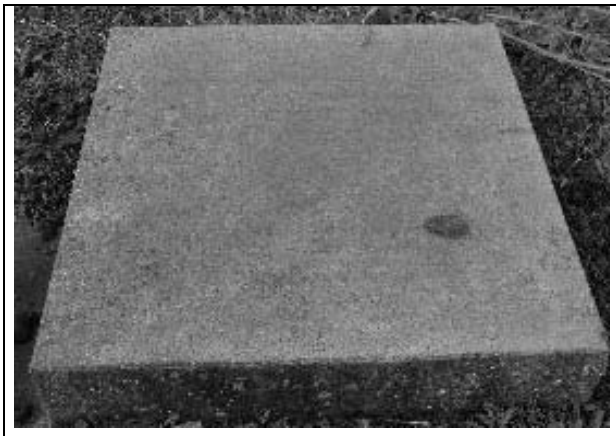

a) Surface of concrete exposed to natural weathering

b) Surface of concrete exposed to natural weathering + deicing salts

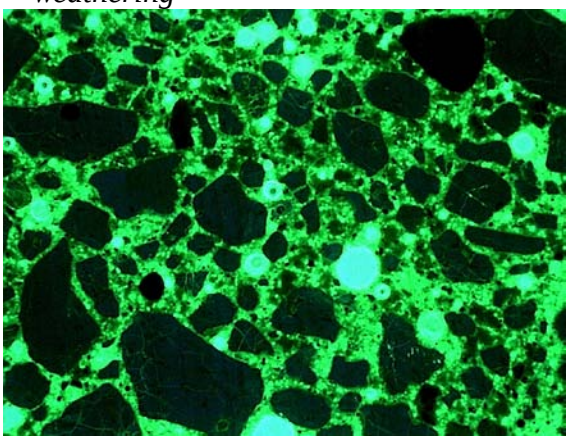

c) Microstructure of concrete exposed to sea water in Hirtshals Harbour

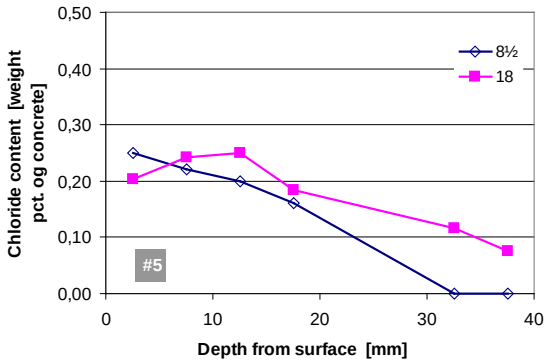

d) Chloride profile for concrete exposed to sea water in Hirtshals Harbour

Figure 8: Concrete type 5 after 18 years exposure

Figure 8 shows, that:

- The concrete surface is vulnerable for freeze/thaw and deicing salt.
- The paste matrix is homogeneous.
- The air-content is low.
- Corrosion of reinforcement can be expected after > 18 years.

a) Surface of concrete exposed to natural weathering

b) Surface of concrete exposed to natural weathering + deicing salts

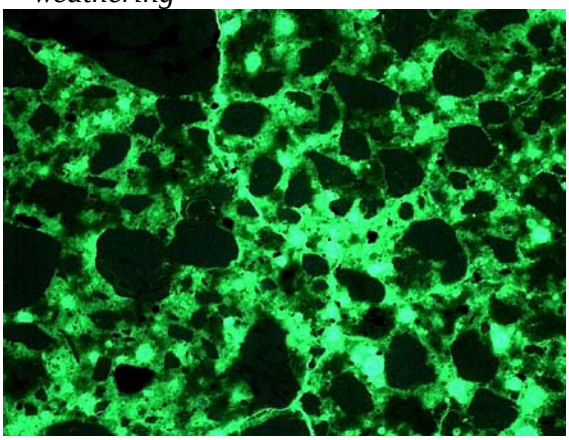

c) Microstructure of concrete exposed to sea water in Hirtshals Harbour

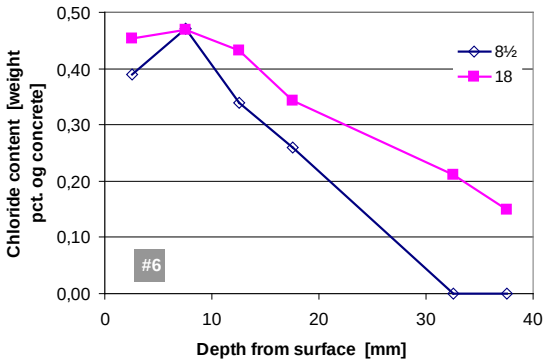

d) Chloride profile for concrete exposed to sea water in Hirtshals Harbour

Figure 9: Concrete type 6 after 18 years exposure

Figure 9 shows, that:

- The concrete surface is slightly vulnerable for freeze/thaw and deicing salt.
- The paste matrix is inhomogeneous, and few cracks have appeared.
- The air-content is low.
- Corrosion of reinforcement can be expected before 18 years age.

a) Surface of concrete exposed to natural weathering

b) Surface of concrete exposed to natural weathering + deicing salts

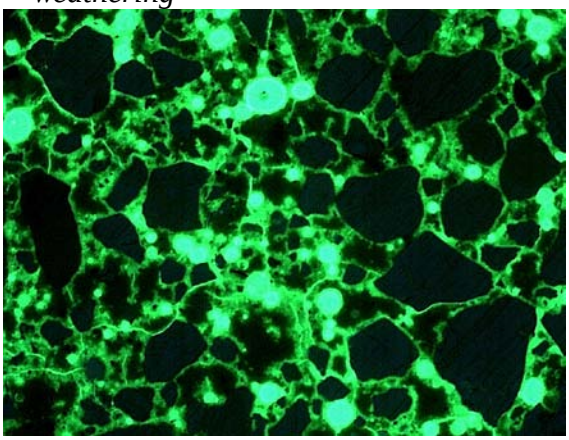

c) Microstructure of concrete exposed to sea water in Hirtshals Harbour

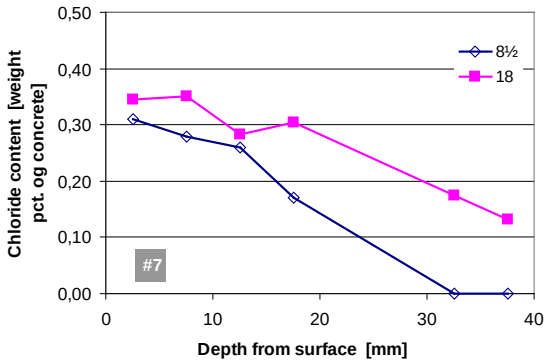

d) Chloride profile for concrete exposed to sea water in Hirtshals Harbour

Figure 10: Concrete type 7 after 18 years exposure

Figure 10 shows, that:

- The concrete surface is slightly vulnerable for freeze/thaw and deicing salt.
- The paste matrix is homogeneous, and cracks have appeared.
- The air-content is low.
- Corrosion of reinforcement can be expected before 18 years age.

a) Surface of concrete exposed to natural weathering

b) Surface of concrete exposed to natural weathering + deicing salts

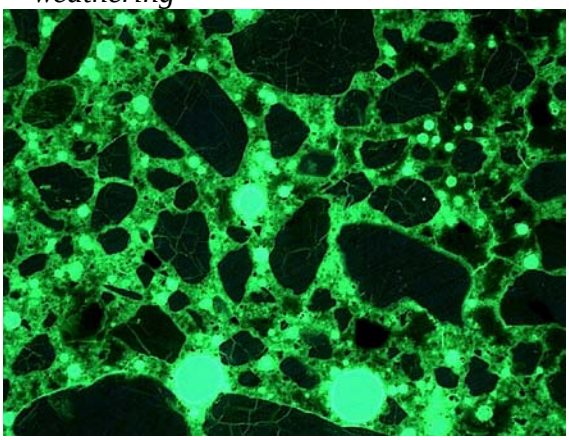

c) Microstructure of concrete exposed to sea water in Hirtshals Harbour

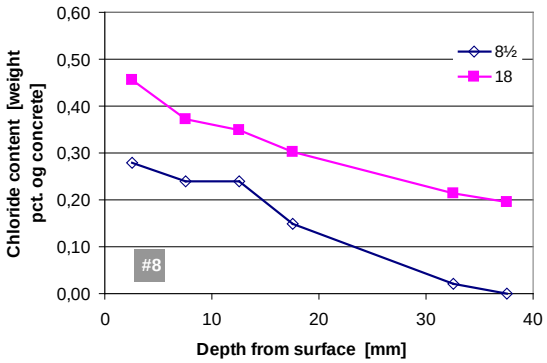

d) Chloride profile for concrete exposed to sea water in Hirtshals Harbour

Figure 11: Concrete type 8 after 18 years exposure

Figure 11 shows, that:

- The concrete surface is vulnerable for freeze/thaw and deicing salt.
- The paste matrix is fairly homogeneous.
- The air is uneven distributed.
- Corrosion of reinforcement can be expected before 18 years age.

a) Surface of concrete exposed to natural weathering

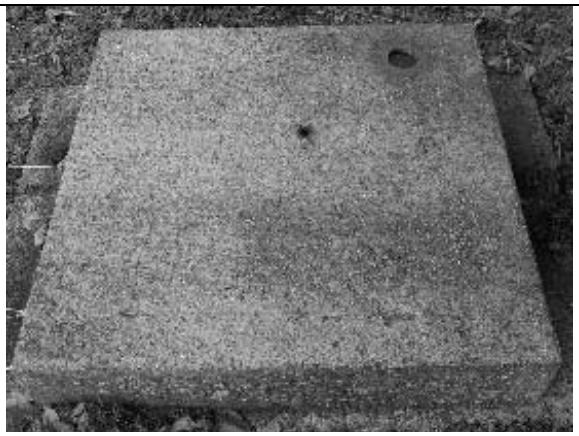

b) Surface of concrete exposed to natural weathering + deicing salts

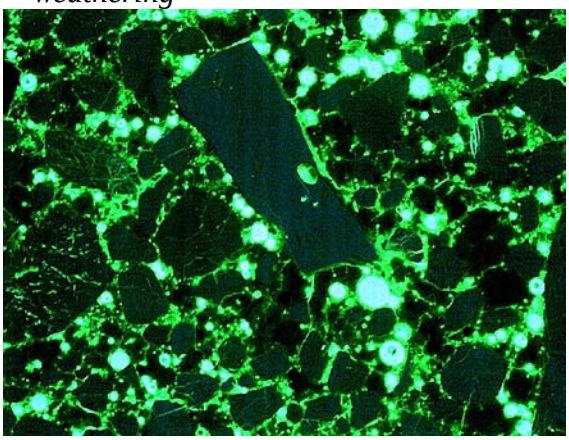

c) Microstructure of concrete exposed to sea water in Hirtshals Harbour

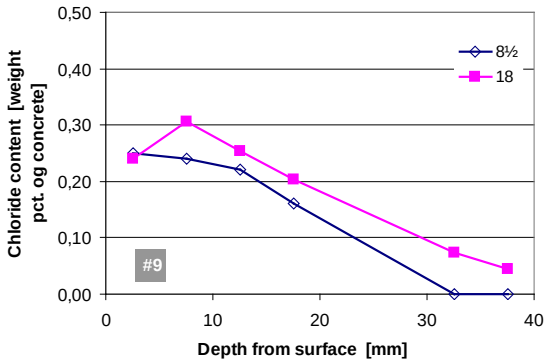

d) Chloride profile for concrete exposed to sea water in Hirtshals Harbour

Figure 12: Concrete type 9 after 18 years exposure

Figure 12 shows, that:

- The concrete surface is resistant to freeze/thaw and deicing salt.
- The paste matrix is homogeneous. There are cracks around the aggregates.
- There is a proper air-content.
- Corrosion of reinforcement can be expected after >> 18 years.

a) Surface of concrete exposed to natural weathering

b) Surface of concrete exposed to natural weathering + deicing salts

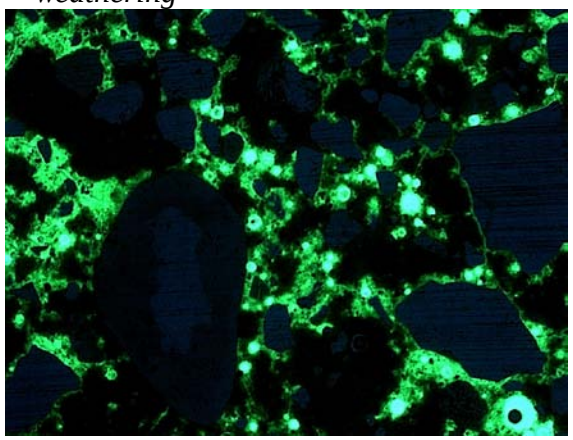

c) Microstructure of concrete exposed to sea water in Hirtshals Harbour

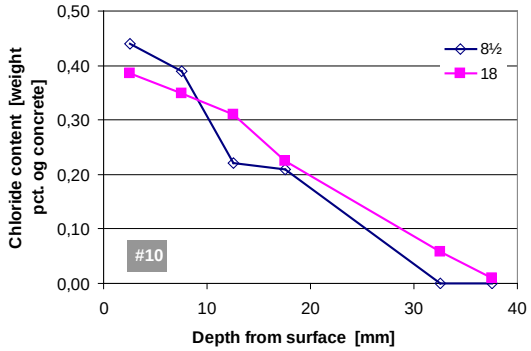

d) Chloride profile for concrete exposed to sea water in Hirtshals Harbour

Figure 13: Concrete type 10 after 18 years exposure

Figure 13 shows, that:

- The concrete surface is resistant to freeze/thaw and deicing salt.
- The paste matrix is fairly homogeneous.
- There is a high content of $Ca(OH)_2$ and only little pozzolan reaction have taken place /7/.
- The air-content is uneven distributed.
- Corrosion of reinforcement can be expected after >> 18 years.

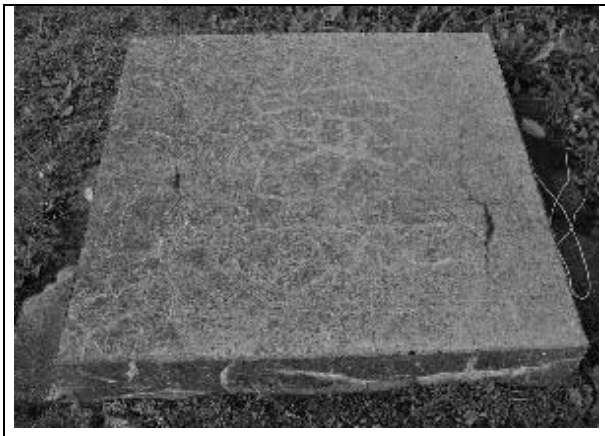

a) Surface of concrete exposed to natural weathering

b) Surface of concrete exposed to natural weathering + deicing salts

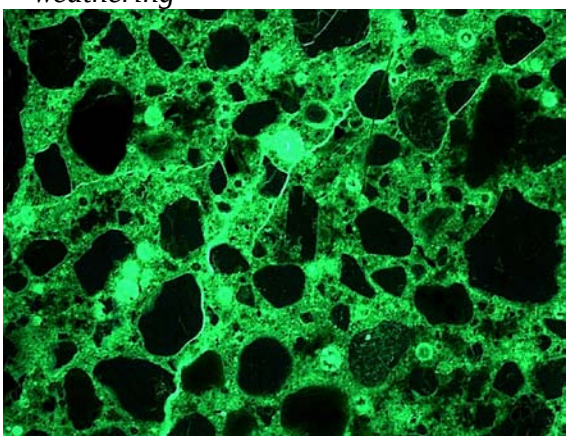

c) Microstructure of concrete exposed to sea water in Hirtshals Harbour

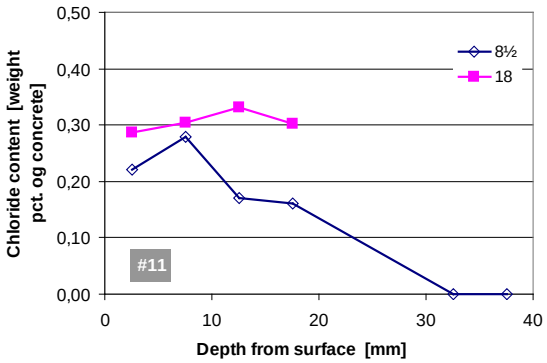

d) Chloride profile for concrete exposed to sea water in Hirtshals Harbour

Figure 14: Concrete type 11 after 18 years exposure

Figure 14 shows, that, the concrete has been disintegrated by alkali silica reactions. It was not possible to measure a chloride profile to a depth of 40 mm.

a) Surface of concrete exposed to natural weathering

b) Surface of concrete exposed to natural weathering + deicing salts

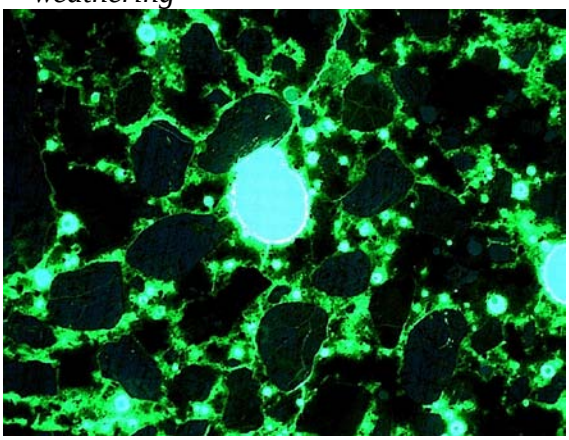

c) Microstructure of concrete exposed to sea water in Hirtshals Harbour

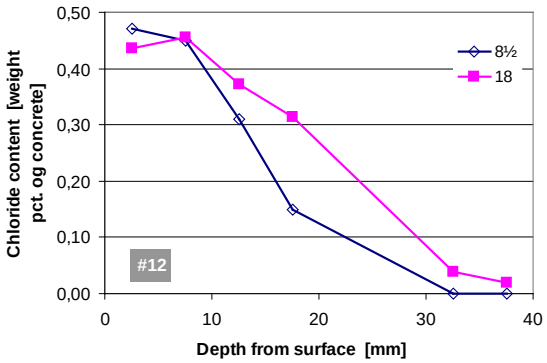

d) Chloride profile for concrete exposed to sea water in Hirtshals Harbour

Figure 15: Concrete type 12 after 18 years exposure

Figure 15 shows, that:

- The concrete surface is resistant to freeze/thaw and deicing salt.
- The paste matrix is homogeneous, and some cracks have appeared.
- The air-content is low and uneven distributed.
- Corrosion of reinforcement can be expected after >> 18 years.

a) Surface of concrete exposed to natural weathering

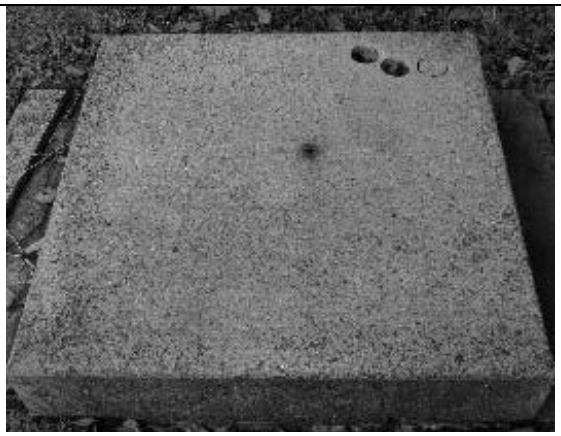

b) Surface of concrete exposed to natural weathering + deicing salts

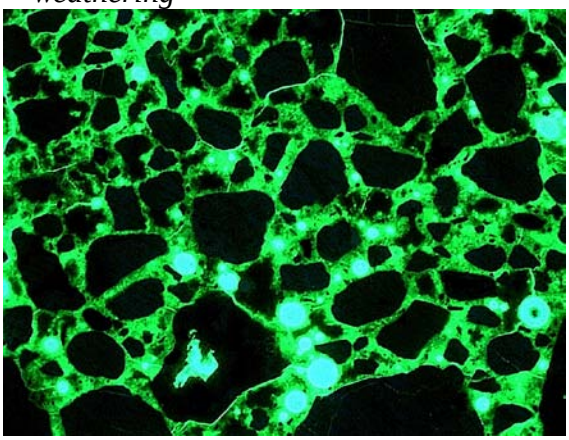

c) Microstructure of concrete exposed to sea water in Hirtshals Harbour

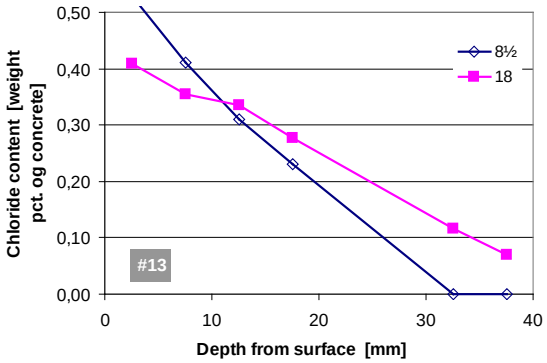

d) Chloride profile for concrete exposed to sea water in Hirtshals Harbour

Figure 16: Concrete type 13 after 18 years exposure

Figure 16 shows, that:

- The concrete surface is resistant to freeze/thaw and deicing salt.
- The paste matrix is homogeneous
- The air is uneven distributed.
- Corrosion of reinforcement can be expected after >> 18 years.

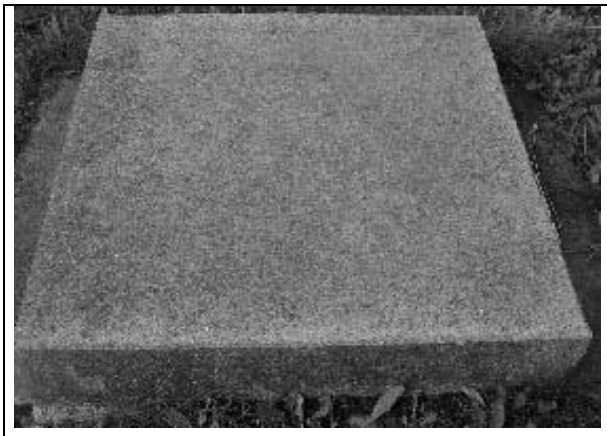

a) Surface of concrete exposed to natural weathering

b) Surface of concrete exposed to natural weathering + deicing salts

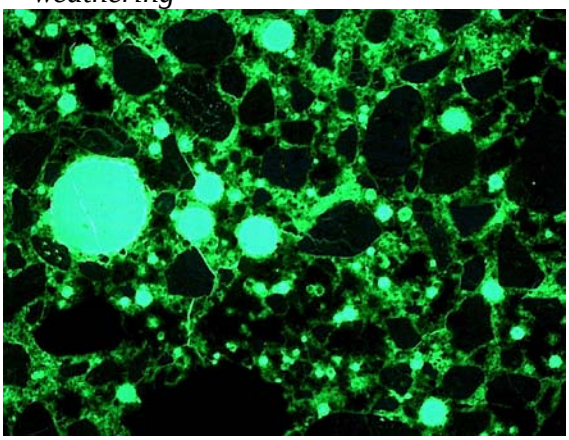

c) Microstructure of concrete exposed to sea water in Hirtshals Harbour

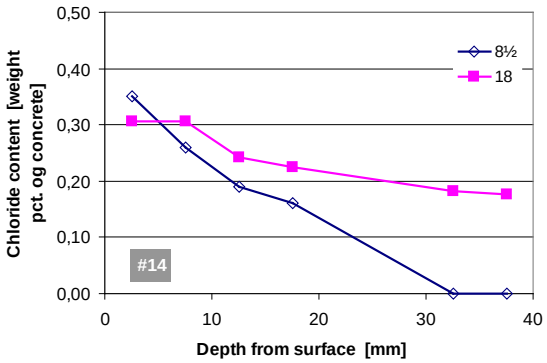

d) Chloride profile for concrete exposed to sea water in Hirtshals Harbour

Figure 17: Concrete type 14 after 18 years exposure

Figure 17 shows, that:

- The concrete surface is resistant to freeze/thaw and deicing salt.
- The paste matrix is homogeneous
- The air-content is fairly low.
- Corrosion of reinforcement can be expected before 18 years.
- The chloride profile has flattened, as was the case for concrete type 3.

a) Surface of concrete exposed to natural weathering

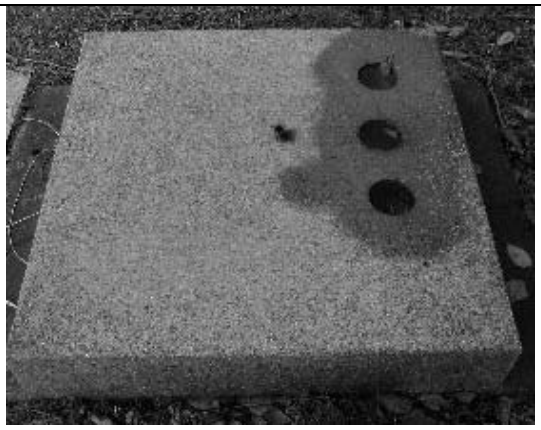

b) Surface of concrete exposed to natural weathering + deicing salts

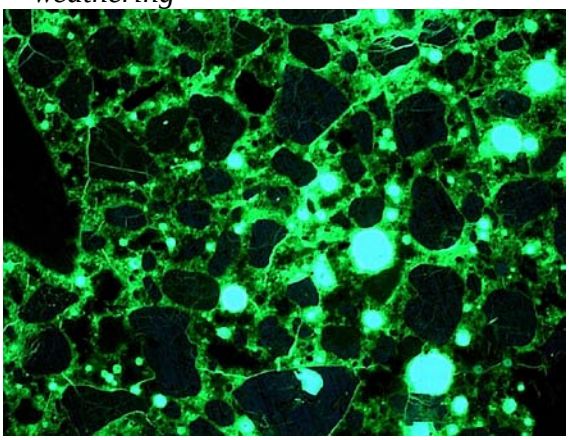

c) Microstructure of concrete exposed to sea water in Hirtshals Harbour

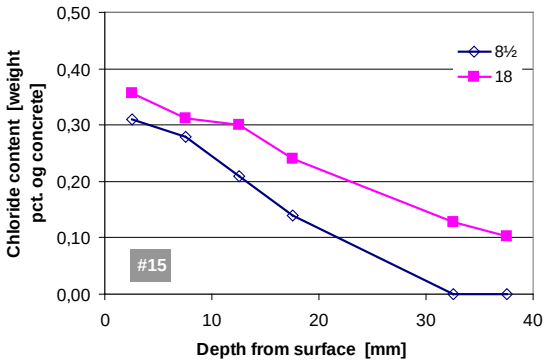

d) Chloride profile for concrete exposed to sea water in Hirtshals Harbour

Figure 18: Concrete type 15 after 18 years exposure

Figure 18 shows, that:

- The concrete surface is resistant to freeze/thaw and deicing salt.
- The paste matrix is homogeneous, and some cracks have appeared, both around the aggregate particles and in the paste.
- The air is not well distributed.
- Corrosion of reinforcement can be expected after > 18 years.
- A little amount of gel from ASR have been found in the aggregates in the outer layers of concrete in the tidal zone in Hirtshals Harbour /7/.

a) Surface of concrete exposed to natural weathering

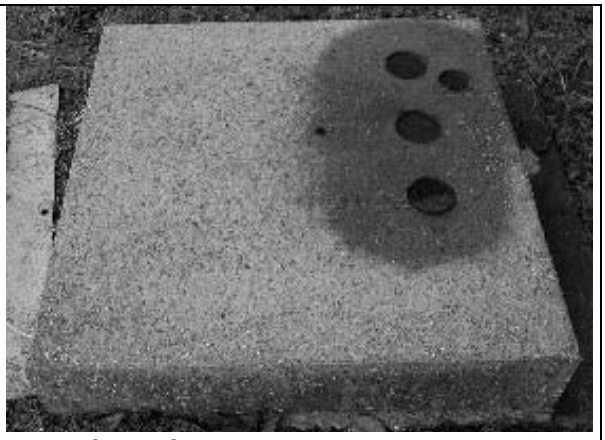

b) Surface of concrete exposed to natural weathering + deicing salts

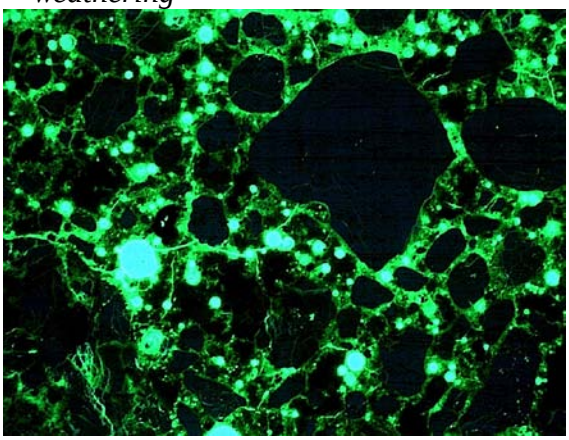

c) Microstructure of concrete exposed to sea water in Hirtshals Harbour

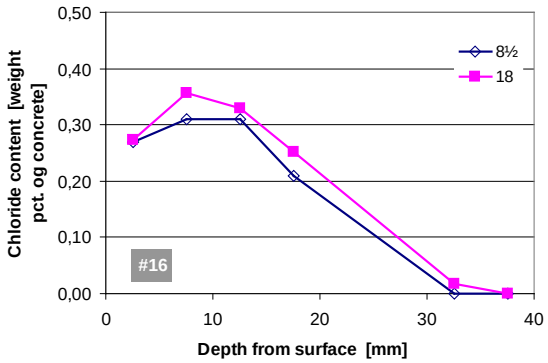

d) Chloride profile for concrete exposed to sea water in Hirtshals Harbour

Figure 19: Concrete type 16 after 18 years exposure

Figure 19 shows, that:

- The concrete surface is slightly vulnerable to freeze/thaw and deicing salt.
- The paste matrix is homogeneous, and some cracks have appeared.
- The air-content is fairly low.
- Corrosion of reinforcement can be expected after >>18 years.

6 DISCUSSION

6.1 Development of strength

Tables 6 to 10 present data for the strength development of the 16 different types of concrete. For the cylinders stored in 20 deg. C water (table 6), a slight decrease in compressive strength is observed for storage periods above 1 to 5 years for the weakest types of concrete. This is also reflected in the E-modulus in table 11 and 12. This phenomena might be caused by two mechanisms, both increasing the porosity of the concrete: i) A transformation of the ettringite and monocarbonates to products as C_3AH_6 or C_3AS_3 having higher density and therefor results in coarsening of the pore structure, ii) Wash-out of $Ca(OH)_2$ due to carbonation of the $Ca(OH)_2$

content in the storage basin. The phase transition have been detected earlier in 22 years old cement paste samples /9/, and xrd measurements on samples from Hirtshals shows, that the monosulphates and –carbonates have disappeared. This item will be further dealt with in /7/. A preliminary xrd-measurement on one of the cores from the Aalborg Portland test area tested at 18 years showed, that ettringite and monocarbonates still are present in concrete exposed to natural out-door climate.

6.2 Influence of microsilica on long term strength

From time to time it has been postulated, that the strength of microsilica containing concrete decreases with age. The data in tables 6 to 10 demonstrate that this is not the case. Table 9 in /10/ further support this.

6.3 Mineral additive and their influence on ASR

Unfortunately, the sand used for these concrete types did contain alkali reactive opaline quarts, as mentioned in section 3. However, ASR has only been found in concrete types 1, 3, 4, 11 and 15 after 18 years exposure in Hirtshals Harbour. On the flags on the inland exposure site, surface cracks presumably originating from ASR is seen on concrete types 1 (only the horizontal salted element), 4 (horizontal elements) and 11 (both horizontal and vertical elements).

6.4 Mineral additives and their influence on drying shrinkage

Table 13 and figure 3 shows that flyash and microsilica decreases the drying shrinkage. Autogeneous shrinkage has not been measured.

6.5 Chloride ingress

On the chloride profiles presented in figures 4 – 19, some different changes over time of the chloride profiles can be seen. In particular, the 18-year profiles for the three concrete with pure CEM I 42.5 – SR cement are very flat for depths above 20 mm. This is caused by the low chloride binding capacity of the cement, caused by the aluminate content. Addition of fly ash or microsilica reduces the chloride ingress, either because of an increased amount of aluminate or because of a more dense structure.

7 NEW ELEMENTS IN 2001

In the autumn of 2001 four of the elements in Hirtshals (#1, #2, #4 & #5) was removed from the harbour, and placed on the inland test area at Aalborg Portland. Four new concrete types replaced them.

The four new concrete types are based on two new cement types developed by Aalborg Portland during the last years. Both types are based on mineralized clinkers /8/. The two cements are CEM I 52.5 and CEM II A-L 52.5 respectively. The latter contains 14% limestone filler.

Table 17: Cement for the 2001 elements

	CEM I 52.5 N	CEM II / A-LL 52.5 R
C_3S, %	50	59
C_2S, %	24	14
C_3A, %	7	8
C_4AF, %	11	11
MgO, %	0.8	1.1
SO_3, %	3.2	2
LOI, %	2.1	
Eqv. Na_2O, %	0.6	0.6
Filler content, %	-	14
Blaine, m/kg	430	≈530[a)]
28 days strength[#], MPa	66	62

a): This value is the measured Blaine value. Due to the very different particle shapes between cement and fillers, this value can hardly be compared with the Blaine value for pure cements. However, the value indicates, that the fineness is much higher than the CEM I 52.5 cement.
[#]: CEN 197

Table 18: Concrete mix-design

		A	B	C	D
Cement-type		CEM I 52.5 N		CEM II / A-LL 52.5 R	
Cement	kg/m^3	340	280	340	280
Flyash	kg/m^3		35		35
Micro silica	kg/m^3		15		15
0/4 mm	kg/m^3	698	688	696	687
4/8 mm	kg/m^3	239	235	238	235
8/16 mm	kg/m^3	900	887	898	886
Conair 316	kg/m^3	0.14	0.26	0.15	0.29
Conplast 212	kg/m^3	1.30	1.34	1.34	1.34
Peramin F	kg/m^3	2.50	3.00	2.29	2.50
Water	kg/m^3	142	142	142	142
w/c–ratio [#)]	-	0.42	0.44	0.42	0.44
Slump	mm	90	80	150	150
Air content	%	5.8	5.4	5.8	7.2

[#)]: w/(c+2MS+0.4FA)

The 1½ m^3 concrete used for each type was mixed in a 3 m^3 paddle-pan mixer and transported to Aalborg Portland in a truckmixer to Aalborg Portland. Casting of all the elements and specimens were carried out indoors in the laboratory.

Compressive strength as well as measurements of drying shrinkage and freeze/thaw resistance according to the Scandinavian Slab Test is being performed. The results are presented in table 19 and figures 20 and 21 respectively. Air void characteristics, measured on hardened concrete, are given in table 20.

Table 19: Development of compressive strength, MPa. 20 °C watercured specimens

Concrete type	A	B	C	D
1 day	16.0	14.8	19.5	12.8
2 days	29.0	24.2	33.6	24.8
7 days	47.5	45.6	49.2	38.0
28 days	63.8	66.5	60.9	56.3
28 days [¤]	*74*	*77*	*71*	*65*
90 days	71.3	79.2	66.9	64.4

[¤]: Cube strengths calculated in accordance with the introductory remarks

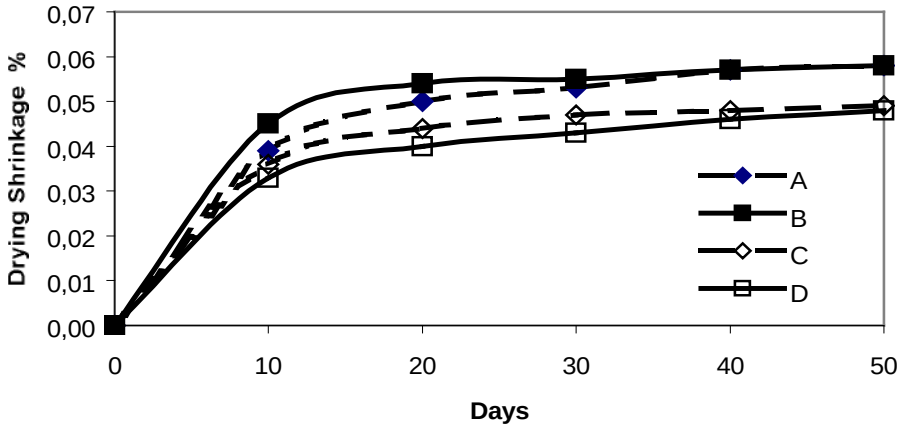

Figure 20: Drying shrinkage. 60% relative humidity and 20 deg. C

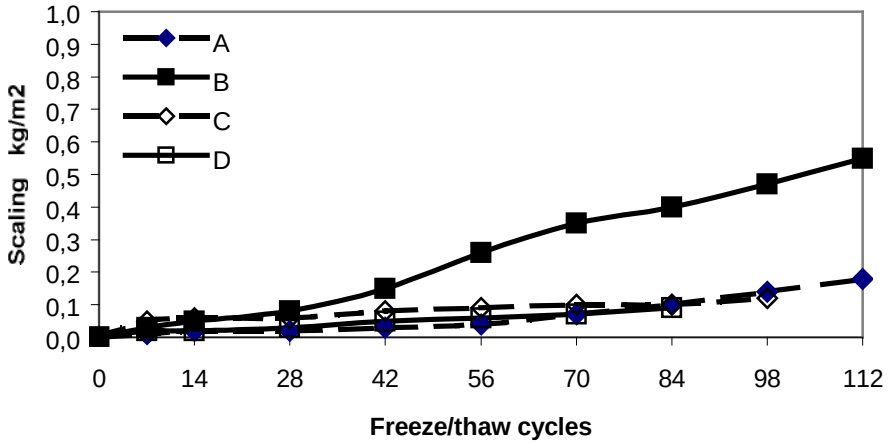

Figure 21: Freeze/thaw test with de-icing salt solution according to the Scandinavian slab test. According to the Swedish Standard SS137244, the durability for the four concrete types are judged as very good, acceptable, very good and very good respectively for #A, #B, #C & #D

Table 20: Air void characteristics for the four new concrete types (2001) in the durability project. The measurements have been carried out on specimens from the cubes used for freeze/thaw testing.

Concrete type	A	B	C	D
Total air, %	5.7	6.1	5.4	6.6
Specific surface, mm^{-1}	27.3	27.5	29.2	31.2
Spacing factor, mm	0.16	0.16	0.15	0.13
Air in binder-volume [b)]	18.6	19.2	17.7	20.5

[b)]: Binder volume = volume of cement + water + additives + air. For freeze/thaw durable concrete it is recommended, that the value is > 15%.

The scaling level for #B is unexpected high, and not in agreement with results from pre-testing. The air-void characteristics given in table 20 do not give indication of any deviance from the planned/expected air-void structure. Hence, the high scaling level cannot be explained by a low quality air-pore-structure. Special attention will be paid to this concrete during the coming years.

8 CONCLUSION

18 years of exposure of 16 different types of concrete has demonstrated that

- Use of cementitious materials as flyash and microsilica improves the long-term durability of concrete with regard to alkali silica reactions and chloride penetration.
- There is no sign of a negative strength development in concrete with microsilica.
- The low chloride binding capacity of cements with low aluminate content can be improved by addition of fly ash. Addition of microsilica reduces the chloride ingress, probably due to the finer pore structure and lower permeability.

It is believed that comparable tests can predict the performance of new types of cement and binders within a few years.

REFERENCES

1. Rasmussen, T.H., "Long-term Durability of Concrete". Nordic Concrete Research, Publication No. 4, 1985
2. Bager, D.H., "5-års resultater fra Aalborg Portlands langtidsforsøg", CtO's Informationsdag, 13. December 1989
3. Nepper-Christensen, P., Kristensen, B.W., Rasmussen, T.H., "Long-Term Durability of Special High Strength Concretes". Proceedings from the Third International on Durability of Concrete. Nice 1994. ACI Publication P-145
4. Dansk Ingeniørforenings Anvisning for Anvendelse af Flyveaske og Mikrosilika i Beton. Normstyrelsens publikationer NP-188-R, April 1987
5. Beton & Frost, Nordic Miniseminar, Køge 1984. Publication 22:85, the Danish Concrete Association 1985.
6. Juel, I.A., Herfort, D. "Principles of Phase Equilibria applied to Seawater and Sulfate Attack" ibid.
7. Juel, I.A., Ph.D. Thesis to be submitted in Spring 2002.
8. Rasmussen, S., Herfort, D., "Mineralised Clinker and Cement". Proceedings from the international seminar: Modern Concrete Materials: Binders, Additions and Admixtures, University of Dundee, Scotland, UK, September 1999
9. Bager, D.H., Hansen, T.B., "Influence of water-binding on the ice formation and freeze/thaw damage in cement paste and concrete", Nordic Concrete Research Proceeding from workshop Water in Cement Paste & Concrete – Hydration and Pore Structure, Skagen, Denmark October 1999. Nordic Concrete Federation 1999.
10. Bager, D.H., "Survey of some Danish HPC containing microsilica and flyash", ibid.
11. "Code of Practice for the structural use of concrete DS411.1999", Dansk Standard 1999
12. Lindvall, A., "Study of chloride penetration into concrete in marine environments – project description and preliminary results", ibid.

Application of the phase rule to Portland cement based systems

Duncan Herfort
M.Sc., Scientific Manager
Research and Development Centre, Aalborg Portland A/S
44 Rørdalsvej, P.O. Box 165, DK-9100 Aalborg
Email: dhe@aalborg-portland.dk

ABSTRACT

The principles for applying the phase rule to mineralogical systems are described. Examples are given of how it is applied to geological systems, and how it can be applied to the simple three component, $CaO\text{-}SiO_2\text{-}H_2O$, and five component, $CaO\text{-}SiO_2\text{-}Al_2O_3\text{-}SO_3\text{-}H_2O$, systems relevant to Portland cement. Examples are also given for how the phase rule can be used to predict the mineralogical changes resulting from carbonation and alkali-silica reaction.

Key words: phase rule, Portland cement, hydrate phases, equilibrium

1. INTRODUCTION

The phase rule, derived by J. William Gibbs in the 1870's and later explored in more detail by many others, is of fundamental importance to the understanding of phase equilibria, and is particularly useful in the construction of phase diagrams. The thermodynamic basis of the phase rule is described in most standard textbooks on mineralogy and physical chemistry. The usual form is

$$P + F = C + 2$$

where P is the number of phases, F is the number of degrees of freedom and C is the minimum number of components or chemical constituents necessary to describe the system. A phase is a chemically and physical homogeneous part of a system that is bound by and interfaced with adjacent phases. The definition of a degree of freedom should become apparent in the following discussion. For a more rigorous description of the phase rule the reader is referred to the standard textbooks.

2. APPLIED TO MINERALOGICAL SYSTEMS

Perhaps the most common application of the phase rule is in the use of phase diagrams used to study geological and artificial ceramic systems. Although it is commonly used by the cement chemist to describe the formation of Portland cement clinker at high temperature, it is rarely used to investigate hydrated cement systems.

2.1 Metamorphic petrology

A common application of the phase rule in metamorphic petrology is the so-called ACF representation within the 4-component system for contact metamorphosed intercalated layers of limestone and shale: ACFS, where A=Al_2O_3, C=CaO, F=FeO, and S=SiO_2 shown in figure 1. Compositions within the 4-component system for compositions where quartz occurs as an excess phase will plot onto the ACF sub-system where the phase assemblages shown are stable over a wide range of temperature and pressure. Where the composition plots at "1" the phase assemblage will consist of andalusite, cordierite and anorthite in addition to quartz. Since this assemblage consists of four phases and four components, the phase rule predicts two degrees of freedom which in this case are temperature and pressure.

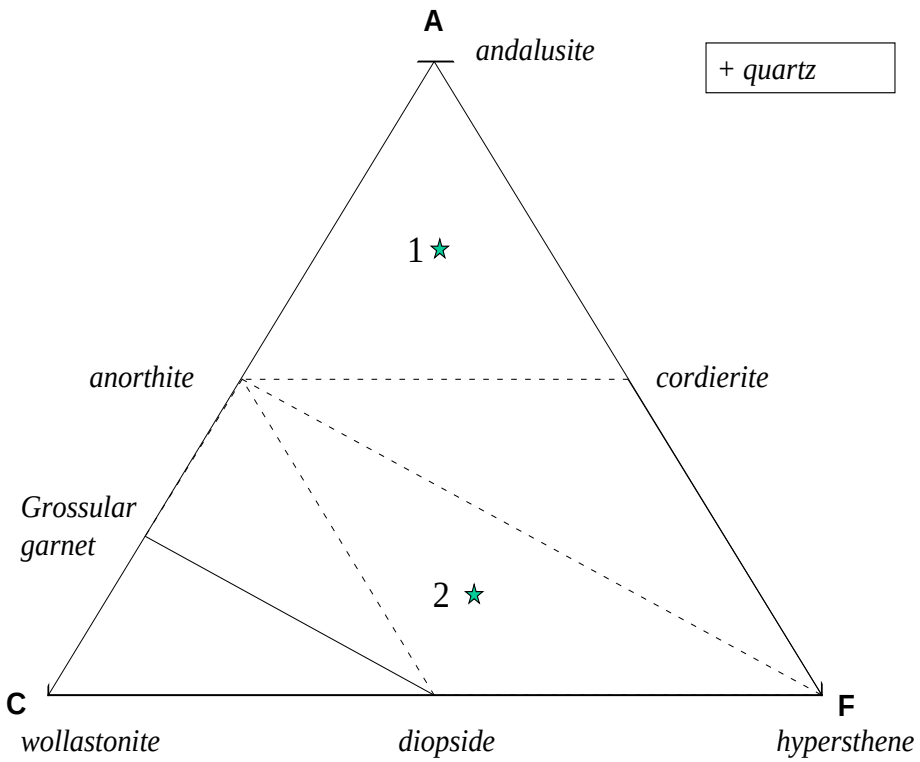

Figure 1. Example of AFC diagram (adapted from Mason, 1978)

2.2 The CaO-SiO_2-H_2O system

The same procedure can be applied to hydrated cement as shown in figure 2 for the CSH system corresponding to hydrated pure calcium silicate, e.g. mixtures of pure C_2S and C_3S. In order to simplify the discussion of this system the phase rule is condensed to P + F = C by maintaining

constant pressure and temperature. Composition “1” shown in figure 2 consists of just one phase, i.e. an aqueous solution. This corresponds to the situation where the solution is undersaturated in both CaO and SiO_2. According to the condensed phase rule this gives two degrees of freedom, which in this case corresponds to the number of directions in which the composition of the solution can change as a result of changes in the overall composition. This assemblage (here consisting of a single phase) is known as a divariant assemblage. The composition at “2” consists of three phases, i.e. C-S-H, CH and pore solution. This assemblage is known as an invariant assemblage since the phase rule gives zero degrees of freedom. Since there are no degrees of freedom the composition of the individual phases must remain constant for all total chemical compositions plotting within the triangle bound by these phases, with the compositions of the individual phases defined by the corners of the triangle. Changes in the chemical composition of invariant assemblages, therefore, only result in changes in the relative contents of the phases present. The composition at “3” consists of two phases, i.e. C-S-H and the pore solution. According to the phase rule, this leaves one degree of freedom, and the assemblage is known as a univariant assemblage. The degree of freedom allows changes in the Ca/Si ratio in both the C-S-H phase and the pore solution in response to changes in the overall composition. Only one degree of freedom exists because the Ca/Si ratios in both phases are mutually dependent.

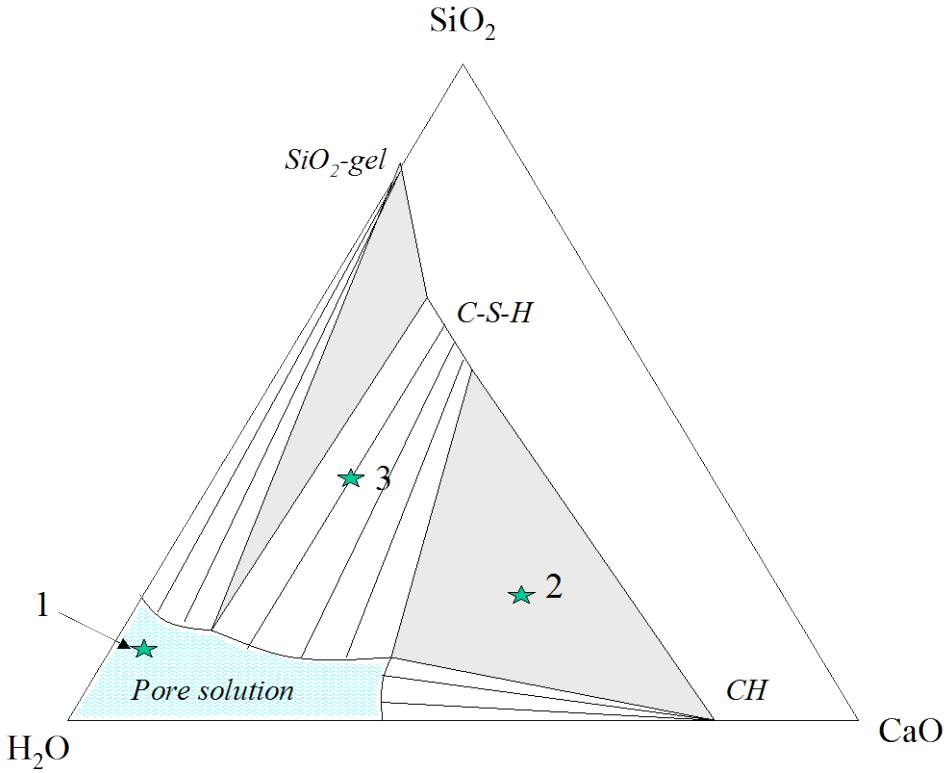

Figure 2. CSH diagram (adapted from Taylor, 1997)

2.3 The $CaO-SiO_2-Al_2O_3-SO_3-H_2O$-system

The simplest Portland cement system is the $CaO-SiO_2-Al_2O_3-SO_3-H_2O$, five component system, corresponding to white Portland cement with a negligible iron and alkali content. The introduction of two additional components should, according to the phase rule, result in the addition of two phases and/or degrees of freedom. For normal Portland cement compositions two additional phases result giving an invariant assemblage consisting of C-S-H, CH, ettringite, monosulfate and the pore solution. Over sulfated cements would result in an invariant assemblage consisting of C-S-H, CH, ettringite, gypsum and pore solution pore solution, whilst under-sulfated cements result in C-S-H, CH, hydroxy-AFm, monosulfate and the pore solution. Whilst the composition of the individual phases remains constant within each assemblage, major changes to the pore solution composition occur between assemblages as shown in figure 3.

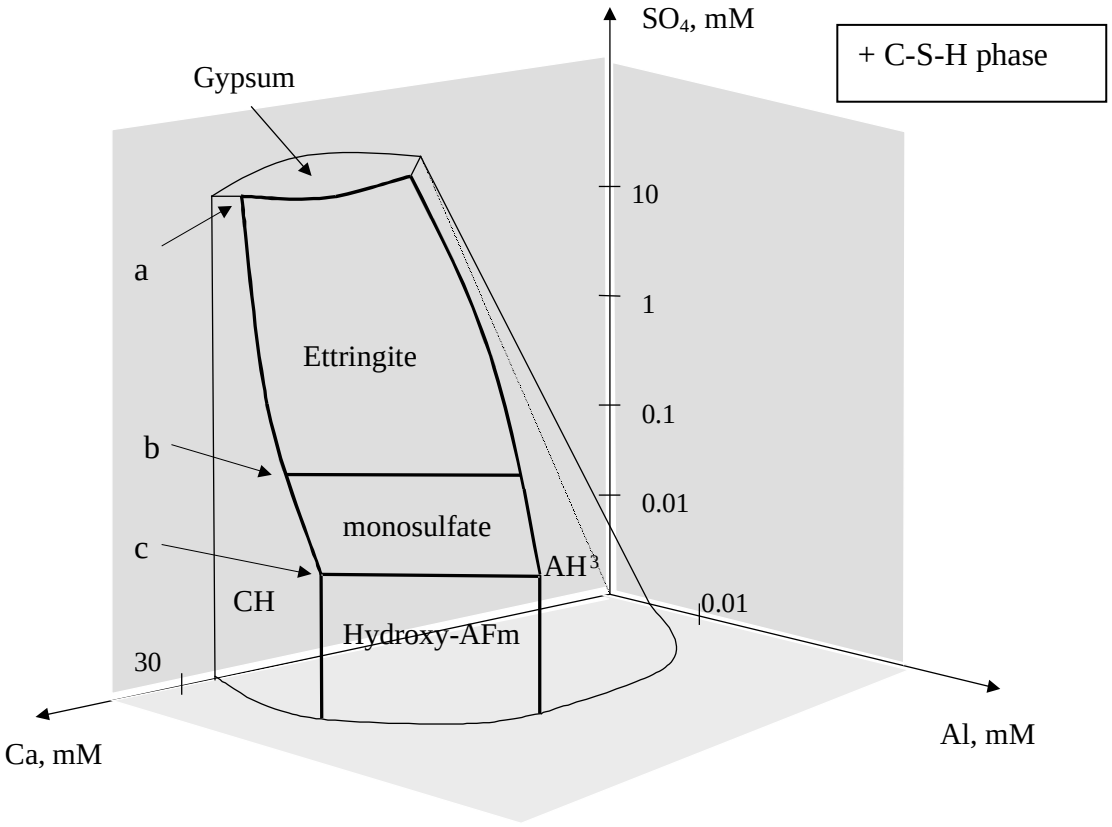

Figure 3. Phase diagram for the $CaO-Al_2O_3-SO_3-H_2O$ sub-system (adapted from Damidot & Glasser, 1993)

This can be seen at the invariant points a, b and c corresponding to the pore solution compositions at equilibrium with the three assemblages that these points define (*viz.* gypsum+ettringite+portlandite, ettringite+monosulfate+portlandite, and monosulfate+hydoxy-Afm+portlandite). The pore solution in concrete produced from over-sulfated cement in which gypsum remains as a stable phase contains approximately 25 mmol/l SO_4 (invariant point a), whilst the pore solution in concrete containing cement with a normal sulfate content contains approximately 0.1 mmol/l SO_4 (invariant point b). Under-sulfated cements, or cements containing high contents of fly ash or blast furnace slag, will result in a pore solution containing approximately 0.01 mmol/l SO_4 consistent with the absence of ettringite (invariant point c).

3. DISCUSSION

An interesting feature of the univariant assemblage described in section 2.2 for the CSH system is the absence of portlandite (fig.2). This is analogous to the situation in hydrated Portland cement in which portlandite is exhausted at high levels of replacement by silica rich pozzolans, after which, further addition of pozzolans results in a reduction in the Ca/Si ratio in the C-S-H phase. This is of course not possible in the presence of portlandite in the invariant assemblage, since this rules out changes in the composition of any of the phases present. Portlandite can also become exhausted by leaching of Ca (which is much more soluble than the other components in Portland cement except for the alkalis), severe magnesium sulfate attack or carbonation. Decalcification of the C-S-H phase is the result in all cases and can continue until silica gel is the final result as occurs in fully carbonated concrete. The degree of freedom which allows decalcification to occur, of course also permits changes in the incorporation of other components, or distribution of components between coexisting phase. Alkalis are perhaps the most important components in this regard where increased concentrations of alkalis in the C-S-H phase can normally only occur in the absence of portlandite. The increased concentration of alkalis in the C-S-H phase leads to lower concentrations in the pore solution and lower pH. Lower pH's are observed for all of mechanisms which lead to decalcification of the C-S-H phase, including carbonation and reaction with high contents of pozzolans. The increased uptake of alkalis in the C-S-H phase is perhaps the best explanation for the reduced risk of alkali-silica reaction in pozzolan rich systems. Similarly, the reduction in pH in carbonated concrete, which leads to the greater risk of corrosion of steel re-enforcement, is also directly related to de-calcification of the C-S-H phase.

4. CONCLUDING REMARKS

The phase rule, and graphic representations of phase assemblages based on the phase rule, can be applied to all multi-component systems for Portland cement, including the additional components involved in chemical attack from sulfate and saline rich environments. Detailed discussion of these applications are given in Juel & Herfort, 2001 and Nielsen & Herfort, 2001, published in these proceedings.

REFERENCES

1. Mason, R., "Petrology of the metamorphic Rocks", Pub. George Allen & Unwin Ltd., 1978, ISBN: 0-04-552013-5
2. Taylor, H.F.W., "Cement Chemistry", Pub. Thomas Telford Services Ltd., 1997, ISBN: 0 7277 2592 0
3. Damidot, D. & Glasser, F.P., "Thermodynamic Investigation of the $CaO-Al_2O_3-CaSO_4-H_2O$ System at 25ºC and the Influence of Na_2O", Cement and Concrete Research, Vol. 23, pp. 221-238, 1993
4. Juel, I.A. & Herfort, D., "Principles of Phase Equlibria applied to Seawater and Sulfate Attack.", published in these proceedings.
5. Nielsen, E.P. & Herfort, D**.,** "The durability of white Portland cement to chloride and sea water attack.", published in these proceedings.

Principles of Phase Equilibria applied to Seawater and Sulfate Attack.

Iver Juel
M.Sc., Industrial Ph.D. student.
Research and Development Centre, Aalborg Portland A/S 44
Rørdalsvej, P.O. Box 165, DK-9100 Aalborg
Email: iaj@aalborg-portland.dk

Duncan Herfort
M.Sc., Scientific Manager
Research and Development Centre, Aalborg Portland A/S
44 Rørdalsvej, P.O. Box 165, DK-9100 Aalborg
Email: dhe@aalborg-portland.dk

ABSTRACT

The mineralogy of concrete altered by chemical attack is described using a model based on the phase rule. The phase rule constraint is applied to the multi-component systems involved in chemical attack on concrete, ranging from the 6 component system corresponding to the simplest type of sulfate attack on hydrated Portland cement, to systems containing 10 or more components resulting from sea water attack. The model predicts that concrete altered by chemical attack is governed by the existence of stable or metastable equilibrium within localised zones, even though a state of equilibrium does not exist across the entire system. The model was tested experimentally on laboratory samples, and by petrographic investigation of concrete slabs of various compositions exposed to seawater for 20 years. Results from electron microprobe analysis on the concrete slabs are presented here.

Key words: Sulfate and seawater attack, phase equilibria, Friedel's salt, solid solution, EPMA.

1. INTRODUCTION

Thermodynamic modeling of the equilibrium phase compositions of hydrated Portland cement and hydrated Portland cement systems subjected to external chemical attack, such as from sulfate rich ground water or sea water, is largely restricted to studies of more simple systems containing a reduced number of components. Most of this work is relevant to either sulfate attack [e.g. 1,2,3,4], or the binding of chlorides [e.g. 5, 6]. The phase assemblages in these studies are generally consistent with the phase rule in which, at constant temperature and pressure, the number of phases is equal to the sum of the number of degrees of freedom and the number of components used to describe the system. For all of these simple sub-systems which are assumed to be invariant, the number of phases is by definition equal to the number of components.

Whilst compatibility with the phase rule is implicit in some of the more practical approaches at predicting the equilibrium assemblages of hydrated Portland cement from the total chemistry of the system, such as in [7], most studies of this type do not apply the same rigorous control as described above for the thermodynamic modelling, and any agreement with the phase rule appears to be more by accident than design. The purpose of calculating the phase assemblages in many studies has been to calculate the total volume of hydrate phases that in turn can be used to calculate the capillary porosity. The most widely recognised method for this is the Powers method [8], which assigns a fixed density to the entire hydrate phase assemblage, regardless of cement composition. The Powers method has since been refined by a number of workers as in [9] where the porosity is calculated from the five solid phases which, along with the pore solution, make up the 6 phases in the invariant phase assemblage which forms on hydration of common, essentially 6-component Portland cement.

In the work described in this paper, a model is described where the phase rule constraint is applied to the multi-component systems consisting of CaO, SiO_2, Al_2O_3, Fe_2O_3, MgO, $CaSO_4$, $CaCl_2$ and H_2O.

The model is tested on concrete slabs exposed to seawater for 18 years in addition to laboratory samples stored under more controlled conditions. The tests consist of detailed mineralogical and petrographic examination of the samples, including optical microscopy, XRD, EPMA (Electron Probe Microanalysis) and chemical analysis of the pore solutions. Only the results from the EPMA on selected concrete slabs are presented in this paper. The results presented here are largely reproduced from an earlier publication [10].

2. MODEL DESCRIPTION

The model is based on the phase rule, which states that the number of phases plus degrees of freedom equals the number of components plus two. Assuming constant temperature and pressure, the phase rule is condensed so that the number of phases plus the degrees of freedom equals the number of components. An invariant mineral assemblage, 5n th5s case, would have the same number of phases and components.

The phases included in the model in the examples given are: C-S-H, CH, FH_3, brucite, monosulfate, ettringite, gypsum, Friedel's salt and Mg-silicagel. In the calculations we assume that the cement is fully hydrated. Water is assumed to occur in excess and corresponds to the pore solution, which although part of the phase assemblage, is not shown in the diagrams which only include the solid phases. The phase compositions are assumed to be constant. In the presence of portlandite, the C-S-H phase was fixed at $1.7CaO{\cdot}1.0SiO_2{\cdot}0.05Al_2O_3{\cdot}4H_2O$, whilst the other phases were assigned standard stoichiometric compositions.

2.1 The CaO-SiO_2-Al_2O_3-Fe_2O_3-MgO-$CaSO_4$-H_2O system

The phase assemblage of a hydrated ordinary Portland cement is shown in figure 1 as a function of the $MgSO_4$ content. At low contents of $MgSO_4$ the phase assemblage consists of C-S-H, CH, FH_3, brucite, monosulfate and ettringite. At about 4 weight % $MgSO_4$ all the monosulfate has been converted into ettringite and brucite. In accordance with the phase rule a new phase must now appear (or a degree of freedom), which in this case is gypsum. As more $MgSO_4$ is added to

the system more gypsum and brucite are formed at the expense of portlandite. At about 29 weight % $MgSO_4$ all the portlandite has reacted to form gypsum. At this point, either an extra phase will start to form, or a degree of freedom is introduced. In figure 2 Mg-silicagel is assumed to form, although decalcification of the C-S-H phase may be an equally plausible scenario.

Provided there are no degrees of freedom which allow the concentration of SO_4^{2-} or other components in the pore solution to change within a given assemblage, this can only happen when there is a shift from one assemblage to another.

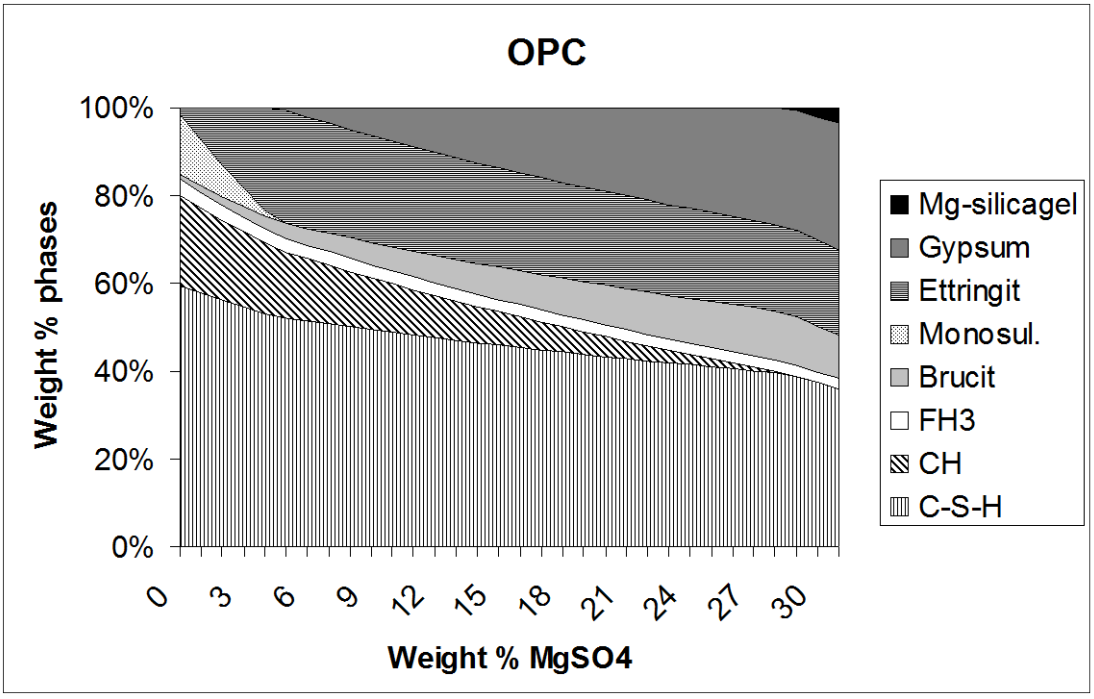

Figure 1. The phase assemblage of a hydrated ordinary Portland cement shown as a function of the $MgSO_4$ content.

2.2 The CaO-SiO_2-Al_2O_3-Fe_2O_3-$CaSO_4$-$CaCl_2$-H_2O system

The phase assemblages of hydrated ordinary Portland cement are shown in figure 2 as a function of the $CaCl_2$ content. At low contents of $CaCl_2$ the phase assemblage consists of C-S-H, CH, FH_3, monosulfate, ettringite and a minor amount of Friedel's salt. As the amount of $CaCl_2$ increases monosulfate is converted into ettringite and Friedel's salt. At about 1.5 weight % $CaCl_2$ monosulfate disappears and gypsum appears instead. After this Friedal's salt continues to form as ettringite is depleted. At about 2.5 weight % $CaCl_2$ ettringite is used up and no more aluminate is available for binding further additions of $CaCl_2$. At this point the concentration of $CaCl_2$ in the pore solution will increase as a degree of freedom is introduced to the system. This extra degree of freedom is shown as "$CaCl_2$,aq" in figure 2.

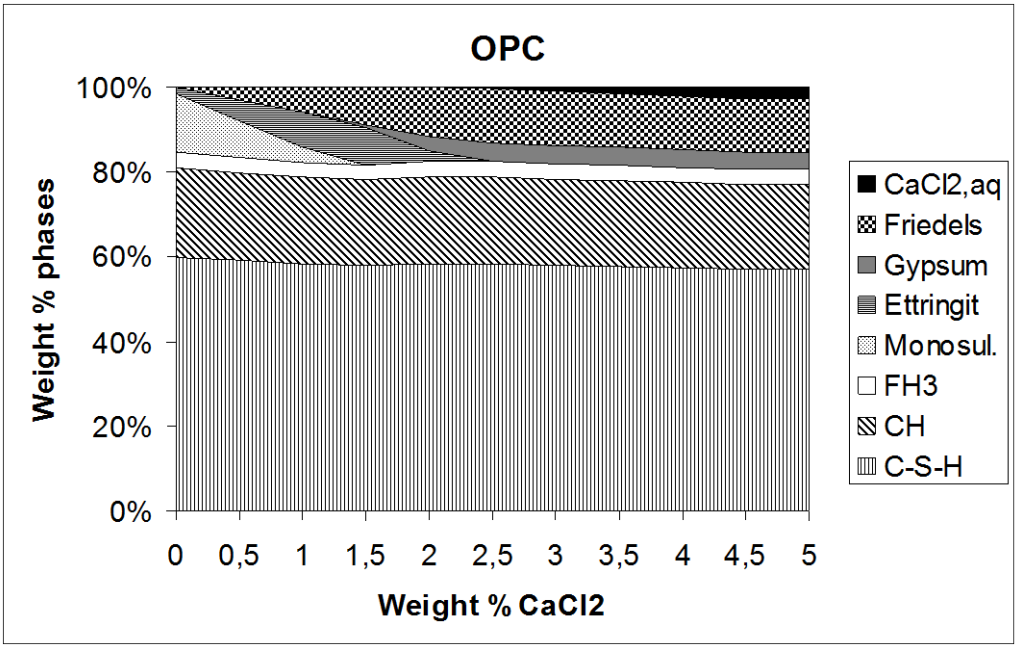

Figure 2. The phase assemblage of a hydrated ordinary Portland cement shown as a function of the $CaCl_2$ content.

2.3 The CaO-SiO_2-Al_2O_3-Fe_2O_3-MgO-$CaSO_4$-$CaCl_2$-H_2O system

In order to describe the mineralogy of seawater attack on concrete more adequately it is necessary to include both magnesium sulfate and chlorides in the system (not to mention the alkalis which for the purpose of this paper are excluded). In this 8 component system the invariant phase assemblage contains 8 phases. In the following discussion we will assume C-S-H, CH, MH, FH_3 and the pore solution to be stable in all assemblages (which is the case except at very high $MgSO_4$ contents) and only concentrate on the remaining 3-component sub-system essentially consisting of different combinations of AFt and AFm phases, e.g. ettringite, monosulfate and Friedel's salt, etc. To facilitate this, the 3 component sub-system, C_3A-$CaSO_4$-$CaCl_2$, is used. In figure 3 the composition of a typical CEM I Portland cement projected onto this sub-system is seen to plot on the tie line connecting monosulfate and ettringite. If monosulfate is considered to be unstable phase, as suggested in [2, 3 ,4 ,5], the stable phase assemblage would contain hydrogarnet or the hydroxy-AFm phase instead. For the purpose of this paper, however, monosulfate is assumed to persist as a metastable phase and to participate in the equilibrium phase assemblages within the system. In the case of seawater attack the composition of the system will follow the path indicated by the arrow. Monosulfate is initially converted into ettringite and Friedel's salt. Since there are no degrees of freedom, the chloride concentration must remain constant, probably at a few mmol/l, as suggested in [5]. Monosulfate disappears at the tieline connecting ettringite and Friedal's and gypsum forms instead. As the content of $CaSO_4$ and $CaCl_2$ increases in the system ettringite is converted into Friedel's salt and gypsum until ettringite disappears completely at the tieline between gypsum and Friedel's salt. Once again the chloride concentration will remain constant at a few mmol/l within the stability field for ettringite+gypsum+Friedal's salt, albeit at a higher concentration than the situation where monosulfate occurred as a stable phase. Any further addition of $CaSO_4$ and $CaCl_2$ to the system will lead to the formation of gypsum and an increase in the chloride concentration in the pore solution which is now permitted by the introduction of a degree of freedom.

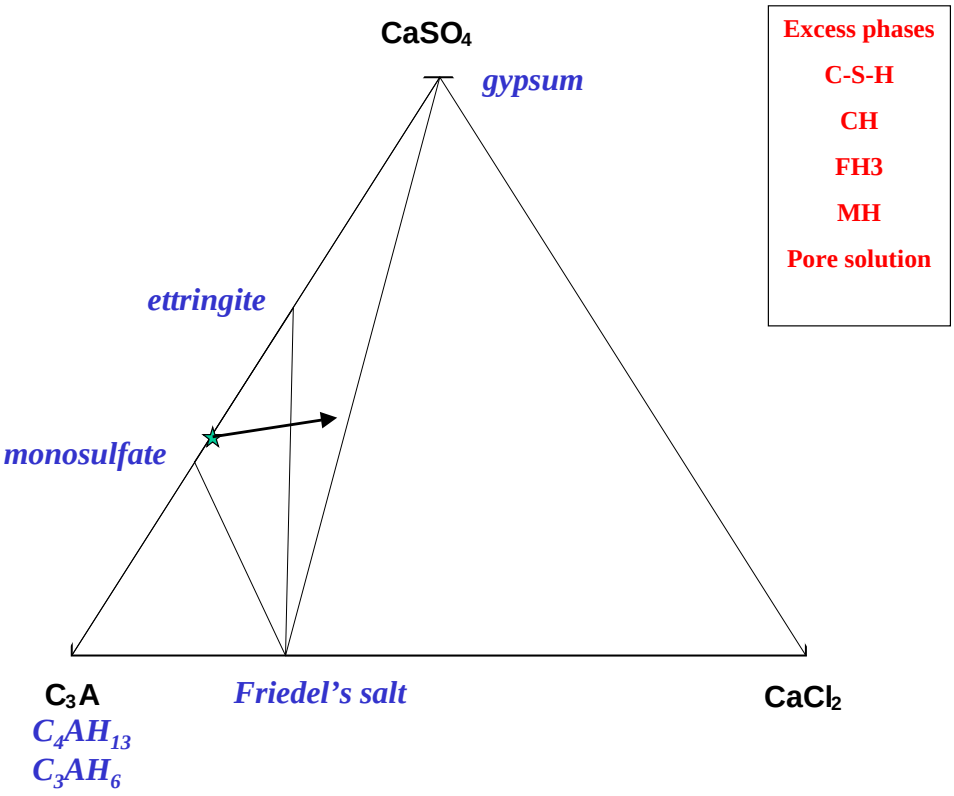

Figure 3. The 3 component sub-system C_3A-$CaSO_4$-$CaCl_2$. See text for explanation.

3. EXPERIMENTAL

3.1 Materials

The concrete slabs were produced in 1983 from CEM I Portland cements at different water cement ratios and with different levels of replacement by fly ash and silica fume . The concrete slabs, which measure 2x1x0.2m, have been partially submerged in the tidal zone on the North Sea coast of Denmark, with the upper regions subjected to cycles of wetting and drying, in addition to freeze/thaw. Cores were drilled from the slabs perpendicular to the surface. Two polished thin sections measuring 30x50 mm were then taken, which positioned end to end cover the entire distance of 100 mm from the surface to the centre of the slabs. The thin sections were examined by optical microscopy prior to X-ray microanalysis.

3.2 EPMA

EPMA was performed using a TRACOR NORTHERN automatic JEOL JCXA733/ superprobe with a take off angle at 40°, current intensity 2 nA and the acceleration voltage 15 kV. The electron beam was focused to a spot size diameter of 1-2 μm. Ca, Si, Al, Fe, Na, K and Mg were analysed by EDS, whilst S and Cl were analysed by WDS. Natural minerals were used as calibration standards. Individual sets of analyses were performed across narrow zones of cement matrix, approximately 5 mm wide, and parallel to the surface. Within each zone 150-200 spot

analyses were performed, evenly distributed across regions of both inner and outer product, and avoiding air voids, unreacted fly ash and aggregate.

4. RESULTS

4.1 CEM I PC

Selected EPMA results are shown in figs. 4 to 6. The same data is used for all three figures and are the result of analyses performed just ahead of the carbonation front, approximately 5 to 10 mm from the concrete surface. The average chloride content in this region was found to be 1.41 wt% of the solid phases. The Si/Ca versus Al/Ca plots in figure 4 are consistent with a mixture of C-S-H, CH and AFm phases. Ettringite was only observed in the original air voids (EPMA results of the air voids are not included in figs. 4 to 6). Ettringite is, of course, still regarded as forming part of the same equilibrium phase assemblage as the other phases found in the paste.

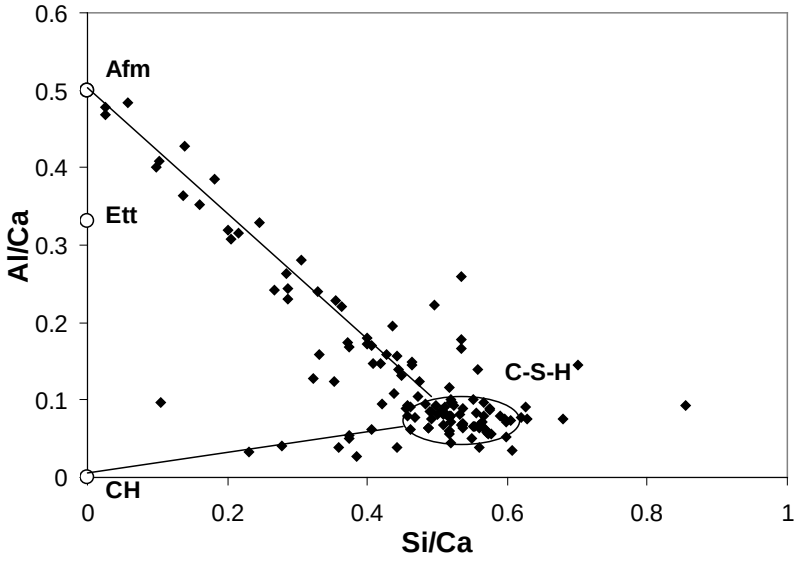

Figure 4. EPMA results showing Al/Ca v. Si/Ca plots. Water/powder ratio of 0.54.

Al/Ca versus S/Ca ratios are plotted in figure 5. These results are consistent with a mixture of C-S-H, monosulfate and some other non-sulfate bearing AFm phase. The monosulfate appears to be intimately mixed with the C-S-H phase at a scale below the resolution of the method, (approximately 2 μm). It is assumed that monosulfate and the other non-sulfate bearing AFm phase occurs as a physical mixture, since solid solution at equilibrium would not occur over a wide range of Al/Ca ratios.

The plots in figure 6 show that the AFm phase consists of a mixture of Friedel's salt and another AFm phase, presumably the hydroxy-AFm phase, $C_3A.Ca(OH)_2.12H_2O$, or monocarbonate, $C_3A.CaCO_3.12H_2O$. The ratio of Friedel's salt to the other AFm phase appears to be constant over the entire range of Al/Ca ratios and this mixture is therefore assumed to be a solid solution. The normative contents of AFm phases (expressed as wt% of the solid phases) are calculated from the average composition of the paste determined by EPMA. Calculated as a mixture of

Friedel's salt and hydroxy-AFm, the normative content of the AFm phases was found to 11.2% monosulfate and 15.3% AFm solid solution, with the solid solution consisting of 0.4 w/w Friedel's salt and 0.55 w/w hydroxy-AFm phase.

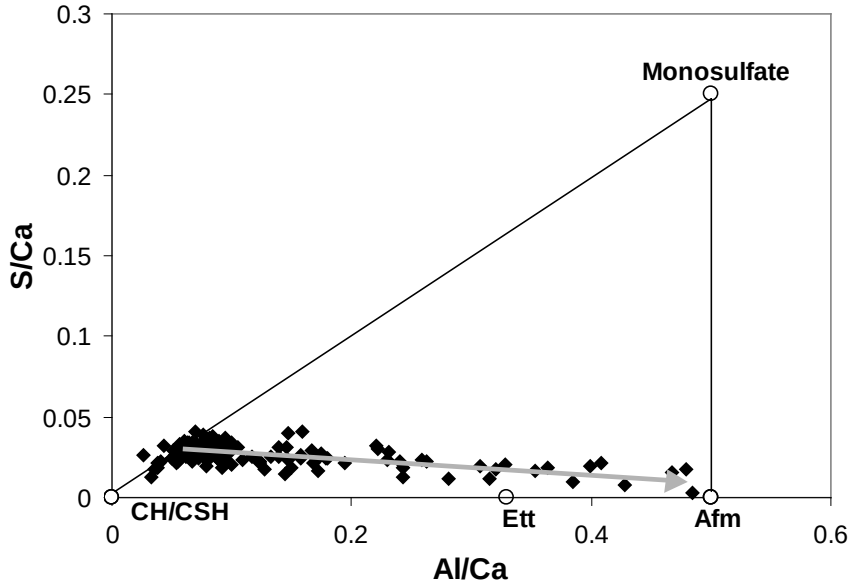

Figure 5. EPMA results showing S/Ca v. Al/Ca plots from same data used in fig.4.

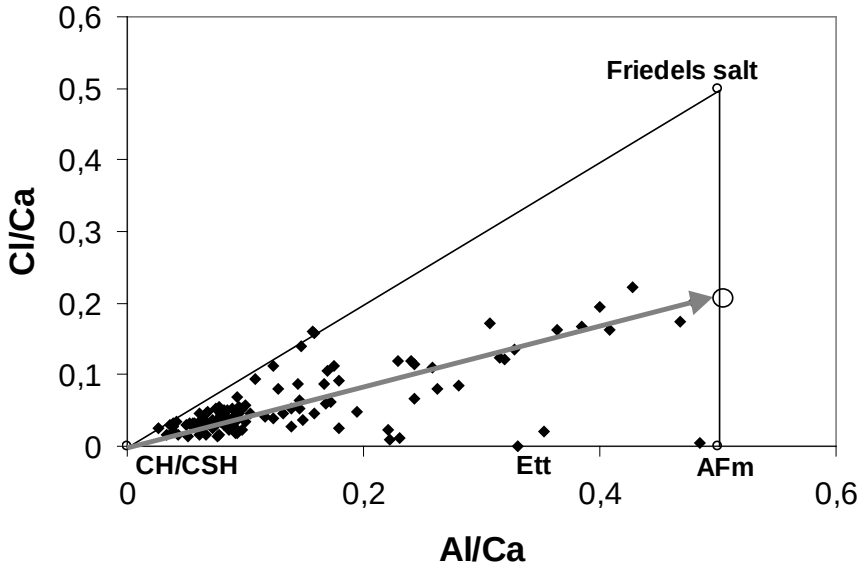

Figure 6. EPMA results showing Al/Ca v. Cl/Ca plots from same data used in figs 4 and 5.

4.2. CEM II/A-V Portland fly ash cement.

The results shown in fig. 7 are from a zone, 90 to 95 mm from the concrete surface. The average chloride content in this region is only 0.36 wt% of the solid phases as determined by EPMA. The S/Ca versus Al/Ca plots are consistent with a mixture of C-S-H, CH, monosulfate and a non-sulfate bearing AFm phase.

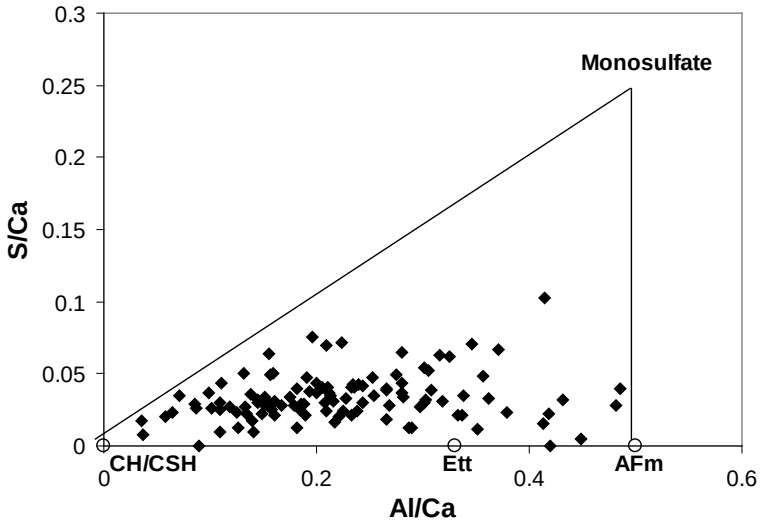

Figure 7. EPMA results showing S/Ca v. Al/Ca plots. Water powder ratio of 0.54

Cl/Ca versus Al/Ca ratios are plotted in figure 8. As for the Portland cement without fly ash the analysis shows that the non-sulfate bearing AFm phase consists of a solid solution of Friedel's salt and another AFm phase. The weight fraction of Friedel's salt in this solid solution phase is calculated to be approximately 0.07 w/w.

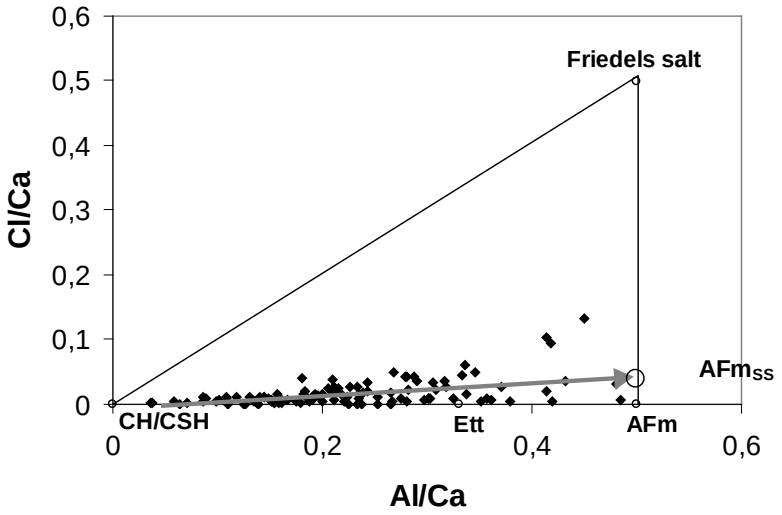

Figure 8. EPMA results showing Al/Ca v. Cl/Ca plots.

5. DISCUSSION

EPMA analyses have indicated an assemblage consisting of ettringite, monosulfate, and a solid solution phase consisting of a mixture of Friedel's salt and another non-chloride or sulfate bearing AFm phase. The latter was initially assumed to be the hydroxy-Afm phase in good agreement with [5], especially since close scrutiny of that paper suggests a region of immiscibilty at Friedel's salt weight ratios above 0.6 consistent with our results.

However, the presence of three AFm phases in addition to ettringite violates the phase rule by exceeding the maximum number of phases. The simplest way of resolving this is to introduce CO_2 as an additional component and assume the unknown end-member phase to be monocarbonate rather than the hydroxy-Afm phase. This is in agreement with pore solution data for equilibrium assemblages including monocarbonate [e.g. 3], in which the concentration of CO_3^{2-} is generally an order of magnitude less than in seawater.

6. CONCLUSIONS

EPMA analysis of concrete containing CEM I Portland cement and CEM II/A-V Portland Cement, indicates extensive solid solution between Friedel's salt and monocarbonate. This solid solution phase appears in turn to form only limited solid solution with the monosulfate phase. The monosulfate phase itself appears to intimately mixed with the C-S-H and ettringite is almost exclusively found in the original air. Pure Friedel's salt has not been identified in any of the concretes studied, even in regions close to the surface after 18 years of exposure to sea water.

REFERENCES

1. Atkins, M., Macphee, D., Kindness, A. and Glasser, F.P. "Solubility Properties of Ternary and Quaternary Compounds in the CaO- Al_2O_3-SO_3-H_2O system", *Cement and Concrete Research* Vol.21, 1991, pp. 991-998.
2. Damidot, D. and Glasser, F.P. "Thermodynamic ivestigation of the CaO-Al_2O_3-$CaSO_4$-H_2O system at 50ºC and 85ºC", *Cement and Concrete Research* Vol.22, 1992, pp. 1179-1191.
3. Damidot, D. and Glasser, F.P., "Thermodynamic investigation of the CaO-Al_2O_3-$CaSO_4$-H_2O system at 25ºC and the influence of Na_2O", *Cement and Concrete Research* Vol.23, 1993, pp. 221-237.
4. Damidot, D. and Glasser, F.P. "Thermodynamic Investigation of the CaO-Al_2O_3-$CaSO_4$-$CaCO_3$-H_2O closed system at 25ºC and the influence of Na_2O". *Cement and Concrete Research* Vol.27, 1995, pp. 129-134.
5. Damidot, D., Birnin-Yauri, U.A. and Glasser, F.P. "Thermodynamic Investigation of the CaO-Al_2O_3-$CaCl_2$-H_2O closed system at 25ºC and the influence of Na_2O", *il cemento* 4. 3, 1994, pp. 243-254.
6. Birnin-Yauri, U.A. and Glasser, F.P., "Friedel's salt, $Ca_2Al(OH)_6(Cl,OH).2H_2O$: its solid solution and their role in chloride binding", *Cement and Concrete Research* Vol.28, 1998, pp. 1713-1723.
7. Taylor, H.F.W., Cement Chemistry, 2nd edition. Pub. Thomas Telford, 1997. (ISBN: 0 7277 2592 0), p.209.

8. Powers, T.C., “Physical Properties of Cement Paste”, Chemistry of Cement – *Proceedings,* 4th International Symposium on the Chemistry of Cement. (1960) vol. II, Paper V-1, pp. 577-613.
9. Jennings, H.M. and Tennis. P.D., “Model for Developing Microstructure in Portland Cement Pates”, *Journal of the American Ceramic Society,* 77 (12), 1994, pp. 3161-3172.
10. Herfort, D. and Juel, I., “The mineralogy of sulfate and sea water attack on concrete interpreted from EPMA analysis”, *Proceedings,* 23rd International conference on cement microscopy, Albuquerque, 2001, pp. 213-225.
11. Lea, F.M. “Chemistry of Cement and Concrete”, Hewlett,P.C.eds, 4th edition, publ. Arnold, ISBN 0-340-56589-6. 1998. Page 309.
12. Tang, L. and Nilsson, L.-O. ”Chloride Binding Capacity and Binding Isotherms of OPC Pastes and Mortars”, *Cement and Concrete Research* Vol.23, 1993, pp. 247-253.
13. Delagrave, A., Marchand, J., Ollivier, J.-P. Julien, S. and Hazrati, K., ”Chloride Binding Capacity of Various hydrated Cement Paste Systems”, *Advanced Cement Based Materials*, Vol 6, 1997, pp. 28-35.
14. Lambert, P., Page, C.L. and Short, N.R., ”Pore Solution Chemistry of the Hydrated System Tricalcium Silicate/Sodium Chloride/Water”, *Cement and Concrete Research* Vol. 15, 1985, pp. 675-680.
15. Theissing, E.M., Mebius-Van De Laar, T. and De Wind, G., ”The Combining of Sodium Chloride and Calcium Chloride by the Hardened Portland Cement Compounds C_3S, C_2S, C_3A and C_4AF”, *Proceedings,* 8th International Symposium on Chemistry of Cement, Rio de Janeiro, 1986, pp. 823-828.
16. Justnes, H., ”A Review of Chloride Binding in Cementitious Systems” *Nordic Concrete Research,* Vol. 21, 1998, pp. 48-63.

Studies on the effect of secondary cementitious materials on chloride ingress

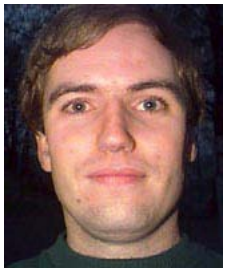

Anders Lindvall
Ph.D.-student
Department of Building Materials
Chalmers University of Technology
SE-412 96 Göteborg
E-mail: lindvall@bm.chalmers.se

Lars-Olof Nilsson
Ph.D., Professor
Department of Building Materials
Chalmers University of Technology
SE-412 96 Göteborg
E-mail: nilsson@bm.chalmers.se

ABSTRACT

Concrete specimens made from different concrete mixes have been exposed in marine and road environments. The concrete mixes included different w/b, binders (Portland Cement, Fly ash and Silica Fume) and admixtures. The environments around the concrete specimens have been documented by collecting data on salinity and water-temperature (marine exposure) and on spread of de-icing salt and meteorological data (road exposure). Chloride penetration profiles have been determined by thorough profile grinding and analysis of calcium and chloride content. Additionally the chloride diffusivities for some of the concrete mixes have been determined. The effect of concrete composition and age on the chloride ingress are presented and discussed.

Key words: Concrete, Portland cement, Fly ash, Silica fume, Chloride ingress, Marine exposure, Road exposure, Chloride diffusivity.

1. INTRODUCTION

1.1 General

In two Nordic research projects different concrete mixes have been exposed in marine and road environments. The concrete compositions included different w/b (ranging from 0.25 to 0.75), a number of Nordic cements (including Danish SRPC[1], Swedish OPC[2] and Swedish SRPC[3]),

[1] CEM I 42.5 SR/LA (Danish Sulfate Resistant Portland Cement).
[2] CEM I 42.5 (Swedish Ordinary Portland Cement).
[3] CEM I 42.5 BV/SR/LA (Swedish Sulfate Resistant Portland Cement).

secondary cementitious materials (silica fume – SF, fly ash – PFA and slag – GGBS) and several additives and admixtures (lime filler, air entraining agents etc.).

The specimens in both the marine and road exposure have been periodically sampled for chloride penetration profiles. The chloride penetration profiles have been used for development and quantification of prediction models. Additionally some of the concrete mixes have been analysed with the CTH rapid test for determining chloride diffusivity, NT BUILD 492 [12], to achieve D_{CTH}.

1.2 Marine exposure

The marine exposure has been a part of a Swedish national research project called "BMB" – Durability of Marine Concrete Structures [1]. As a part of this project some 40 concrete slabs with different concrete compositions have been exposed to saline seawater. The exposure has been made at the Träslövsläge field station some 90 km south of Göteborg. The specimens have been hanging vertically on a pontoon, partly submerged in seawater, to simulate a submerged, a splash and an atmospheric zone. Until now chloride penetration profiles from up to five years exposure at the marine exposure station are available [2-4]. Apart from chloride ingress the concrete blocks are also used to study frost and salt attack, moisture ingress and reinforcement corrosion. However the results from these investigations are not presented in this paper.

1.3 Road exposure

The road exposure has been a part of Nordic research project called "BTB" – Durability of Road Concrete Structures [5]. As a part of this project a large number of concrete blocks with different concrete compositions are exposed close to a road where de-icing salts are spread. The exposure is made at a field station along highway Rv40 west of Borås, some 50 km from Göteborg. The concrete blocks have been placed along the highway to simulate the exposure of de-icing salts on side-beams. Until now chloride penetration profiles from up to two years exposure at the road exposure station are available, [5-6]. Apart from chloride ingress the concrete blocks are also used to study frost and salt attack, moisture ingress and reinforcement corrosion. However the results from these investigations are not presented in this paper.

2. FIELD STATIONS AND EXPOSURE CONDITIONS

2.1 Marine exposure

At the marine field station concrete slabs, measuring 1000x700x100 mm, have been mounted on floating pontoons in the harbour of Träslövsläge. The pontoons are placed in shelter behind the jetty, which means that they are not exposed to larger waves, see figure 1.

Figure 1 – The field station in the harbour of Träslövsläge. Concrete slabs are hanging from both sides of the floating pontoons.

Three zones can be identified on the concrete slabs hanging on the pontoons: submerged, splash and atmospheric zones, see figure 2. The numbers indicate where the cores analysed for chloride ingress have been taken (1-3 – atmospheric zone, 4-6 – splash zone and 7-10 – submerged zone). Since the slabs are 1000 mm high this means that the extension of the atmospheric and splash zones are each 300 mm and the submerged zone is 400 mm.

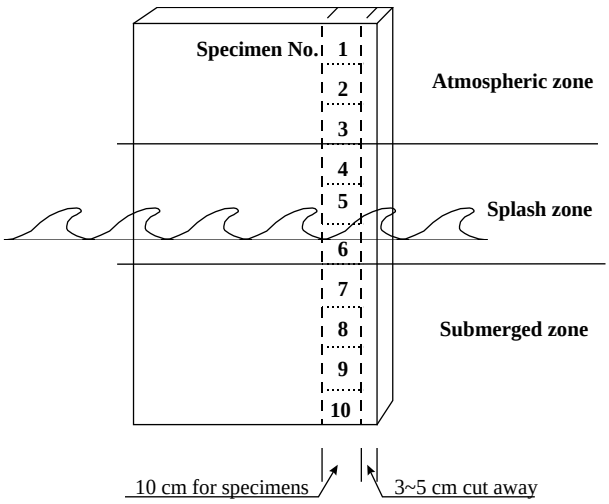

Figure 2 – The concrete slabs exposed at the Träslövsläge field station. Division into submerged, splash and atmospheric zones. [3].

By hanging the concrete slabs on floating pontoons they will always have roughly the same position to the water-surface. This means also that the wave-actions on the concrete slabs are limited, since the pontoons both follow the water-movements and are protected behind the jetty, which means that the waves will very seldom reach high heights. Thus the splash zone, i.e. location 4-6 on the concrete slabs, becomes very limited and is hard to examine by taking cores with a diameter of 100 mm. In this paper we therefore have chosen to exclude the results from the splash zone.

The environmental conditions have been documented in terms of variations in water temperature and salinity over the year. The salinity shows small variations over the year with a mean value of about 9-10 g Cl per litre [7]. The variations in water temperature are shown in figure 3.

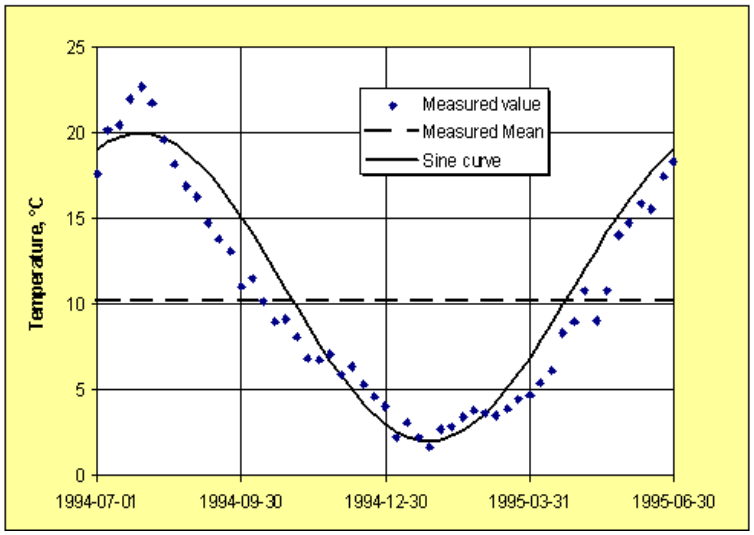

Figure 3 – The yearly variations 1994/95 in water temperature at the field station in Träslövsläge. [3].

2.2 Road exposure

The concrete blocks exposed on the field station at Rv40, measuring 300x300 mm in cross-section and 400 mm ("cubes") or 1200 mm long ("beams"), are placed close to the barrier along the road, see figure 4.

Figure 4 – The Rv40 field station. Concrete blocks placed along the highway Rv40.

The blocks are slightly tilted away from the road to simulate the upper surface of a side-beam on a bridge, see figure 5. To minimize capillary suction from beneath the concrete blocks are placed on gravel. However, some capillary suction may still occur.

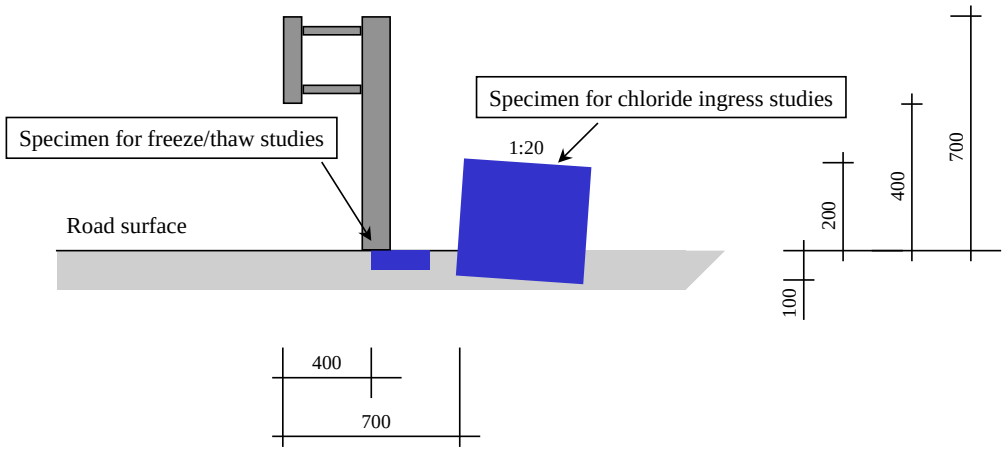

Figure 5 – The concrete blocks placed along Rv40, close to the barrier.

The environmental conditions at the field station have been thoroughly documented, by data from a meteorological station at the site together with data about the road environment. In figure 6 the registered air temperatures and humidities during the winters of 1996/97 and 1997/98 are presented. In table 1 data on the spread of de-icing salt for the same period are given.

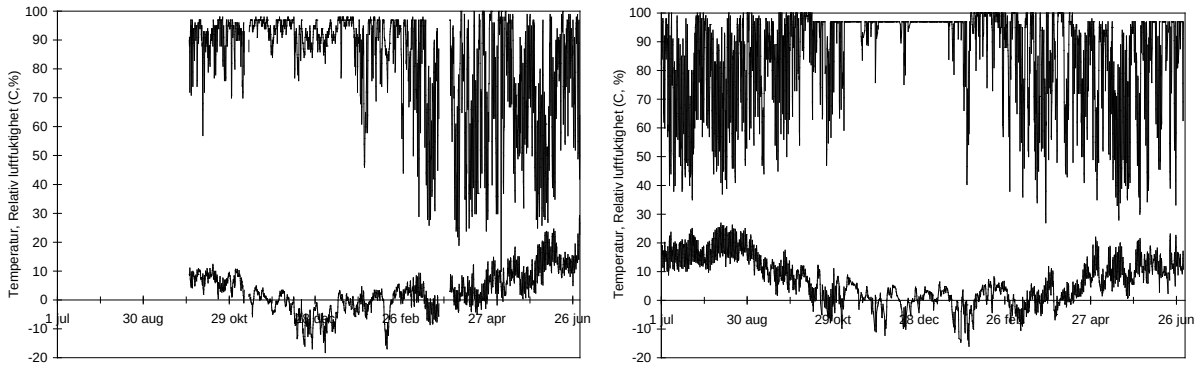

Figure 6 – Variations in the air temperatures and humidities, RH, during the winters 1996/97 and 1997/98 at the field station along Rv40. Left picture 1996/97; right picture 1997/98.

The air temperature varies between some –15°C and +25°C, with fairly low monthly variations, and the air humidity varies between 20%RH and 100%RH, with large monthly variations.

Table 1 – Spread of de-icing salt on Rv40 during the winters 1996/97 and 1997/98 on Rv40.

Year	Month	Occasions	Year	Month	Occasions
			1997	October	13
1996	November	22	1997	November	29
1996	December	34	1997	December	30
1997	January	35	1998	January	28
1997	February	23	1998	February	18
1997	March	8	1998	March	23
1997	April	4	1998	April	16
1996/97	Total	126	1997/98	Total	157

Each time de-icing salts are spread on the road, approximately 10 g/m^2 are spread. This means that during the winter 1996/97 some 12.6 ton/km and during the winter of 1997/98 some 15.7 ton/km of de-icing salts have been spread!

3. CONCRETE COMPOSITIONS

In the following section information is given about the different concrete mixes and which concrete mixes that have been exposed in both the marine and road environments. It should be noticed that no efficiency-factors have been used when w/b has been determined for the different concrete mixes.

3.1 Marine exposure

The mix proportions for the concrete specimens exposed at the marine exposure station in Träslövsläge are summarised in table 2.

Table 2 – The mix proportions for the concrete specimens exposed at the marine exposure station in Träslövsläge. [2].

Mix No.	Binder type	Binder kg/m^3	Aggregate kg/m^3	w/b	Air content %
1-40(Ö)	100% Swedish SRPC	420	1692	0.40	6.0
1-50		370	1689	0.50	6.4
2-40	100 % Swedish OPC	420	1692	0.40	6.2
2-50		390	1646	0.50	5.8
3-35	95% Swedish SRPC + 5% SF	450	1687	0.35	5.8
3-40		420	1685	0.40	6.1
3-50		370	1683	0.50	6.0
3-75		240	1809	0.75	5.9
4-40	90% Swedish SRPC + 10% SF	420	1677	0.40	6.6
9-40	95% Danish SRPC + 5% SF	420	1685	0.40	6.5
10-40	78.5% Danish SRPC + 17% PFA + 4.5% SF	420	1680	0.40	6.5
11-35	85% Danish SRPC + 10% PFA + 5% SF	450	1682	0.35	5.7
12-35	85% Swedish SRPC + 10% PFA + 5% SF	450	1682	0.35	6.4
H1	95% Swedish SRPC + 5% SF	500	1823	0.30	0.8
H2	90% Swedish SRPC + 10% SF	500	1814	0.30	1.1
H3	100% Swedish SRPC	492	1845	0.30	3.6
H4	95% Swedish SRPC + 5% SF	420	1685	0.40	5.9
H5	95% Swedish SRPC + 5% SF	551.2	1812	0.25	1.3
H6	95% Swedish SRPC + 5% PFA	517.9	1800	0.30	2.8
H7	95% Swedish SRPC + 5% SF	500	1823	0.30	1.3
H8	80% Swedish SRPC + 20% PFA	616.3	1629	0.30	3.0
H9	100% Swedish SRPC	500	1832	0.30	2.9

Swedish SRPC – CEM I 42.5 BV/SR/LA (Swedish Sulphate Resistant Portland Cement).
Swedish OPC – CEM I 42.5 (Swedish Ordinary Portland Cement).
Danish SRPC – CEM I 42.5 SR/LA (Danish Sulphate Resistant Portland Cement).
SF – Silica fume.
PFA – Pulverized Fuel Ash

3.2 Road exposure

The mix proportions for some of the concrete compositions exposed at the road exposure station at Rv40 are summarised in table 3. In table 3 information is added about which concrete mixes that are exposed both in marine and road environments (last column).

Table 3 – The mix proportions for the concrete used in the road exposure at Rv40. [5]).

Mix No.	Binder type	Binder kg/m^3	Aggregate kg/m^3	w/b	Air content %	Correspond. mix in marine exposure
201	100% Swedish SRPC	420	1738	0.40	4.5%	1-40
202	(CEM I 42.5 BV/SR/LA)	380	1712	0.50	4.5%	1-50
236		260	1799	0.75	4.5%	-
203		500	1812	0.30	NA	H3
204		450	1834	0.35	NA	7-35
205		380	1805	0.50	NA	-
215	100 % Swedish OPC	420	1726	0.40	4.5%	2-40
216	(CEM I 42.5)	390	1681	0.50	4.5%	2-50
217		520	1739	0.30	NA	-
218		410	1716	0.50	NA	-
206	95% Swedish SRPC + 5% SF	420	1720	0.40	4.5%	3-40
207	(CEM I 42.5 BV/SR/LA + 5%SF)	380	1697	0.50	4.5%	3-50
208		500	1792	0.30	NA	H1
209		450	1801	0.35	NA	6-35
210		380	1776	0.50	NA	-
225	90% Swedish SRPC + 10% SF	420	1703	0.40	4.5%	-
226	(CEM I 42.5 BV/SR/LA + 10%SF)	500	1770	0.30	NA	H2
227		450	1796	0.35	NA	-

SRPC- Sulphate Resistant Portland Cement.
OPC – Ordinary Portland Cement.
SF – Silica Fume.
PFA – Pulverized Fuel Ash.
NA – Natural air (approximately 2%)

4. DETERMINATION OF CHLORIDE INGRESS

4.1 Sampling

To determine the chloride content in the concrete cores have been taken from selected positions on the concrete specimens. The concrete slabs in the marine exposure have been divided into a submerged, a splash and an atmospheric zone. Cores have been taken from each of these three zones. As mentioned earlier, we have chosen to only use the cores taken from the submerged and atmospheric zones. The blocks from the road exposure have been examined on the horizontal and vertical surfaces facing towards the traffic on the road. The cores have been drilled in the exposure direction for each specimen.

Powder samples have been taken from the cores by means of profile grinding. The profile grinding has been done on a modified turning lathe, equipped with a saw-blade, at certain depth intervals, with an accuracy of ±0.5 mm. After the grinding, the powder samples have been dried in 105°C and then stored in desiccators before chloride analysis.

4.2 Chloride and calcium analysis

The chloride content has been determined by dissolving the powder in acid and soda and analyse it for chloride and calcium with potentiometric titration. The procedure to determine the chloride content principally agrees with AASHTO T260 [8], except that the sample size is about 1 g to facilitate a parallel calcium analysis. The procedure to determine the chloride and calcium is further described in [3] or [9].

Since the calcium content in the aggregate is negligible for the examined concrete mixes, the binder content can be estimated from the calcium content in the powder sample. Chloride penetration profiles have been established as the quotient between the chloride and calcium content as a function of the depth. With this procedure possible effects from variations in the aggregate content in the concrete can be minimised.

4.3 Curve-fitting of chloride penetration profiles

The measured chloride penetration profiles have been used for curve-fitting to the error-function solution of Fick's second law. The curve-fitting has been done in such way that the inner part of each profile is fitted where the coefficient of correlation, R, is larger than 0.95. The corresponding regression parameters, an apparent diffusion coefficient, D_{F2}, and an apparent surface chloride concentration, C_{sa} have been collected.

5. CHLORIDE DIFFUSIVITY WITH THE CTH-METHOD

The chloride diffusivity, D_{CTH}, has been determined on cores with NT BUILD 492 [12]. D_{CTH} has been determined on cores, diameter 100 mm, by applying a current over the core forcing chloride-ions from a solution of sodium chloride to penetrate into the concrete. Finally the penetration depth is determined and D_{CTH} is evaluated. The method is further described in [10] and [12].

6. RESULTS

6.1 Chloride penetration profiles

The measured chloride penetration profiles after five years exposure at the Träslövsläge field station and two years exposure at the Rv40 field station are published in [2] and [5] respectively. In figure 7 an example of the chloride penetration profiles from Rv40 after two years exposure is presented.

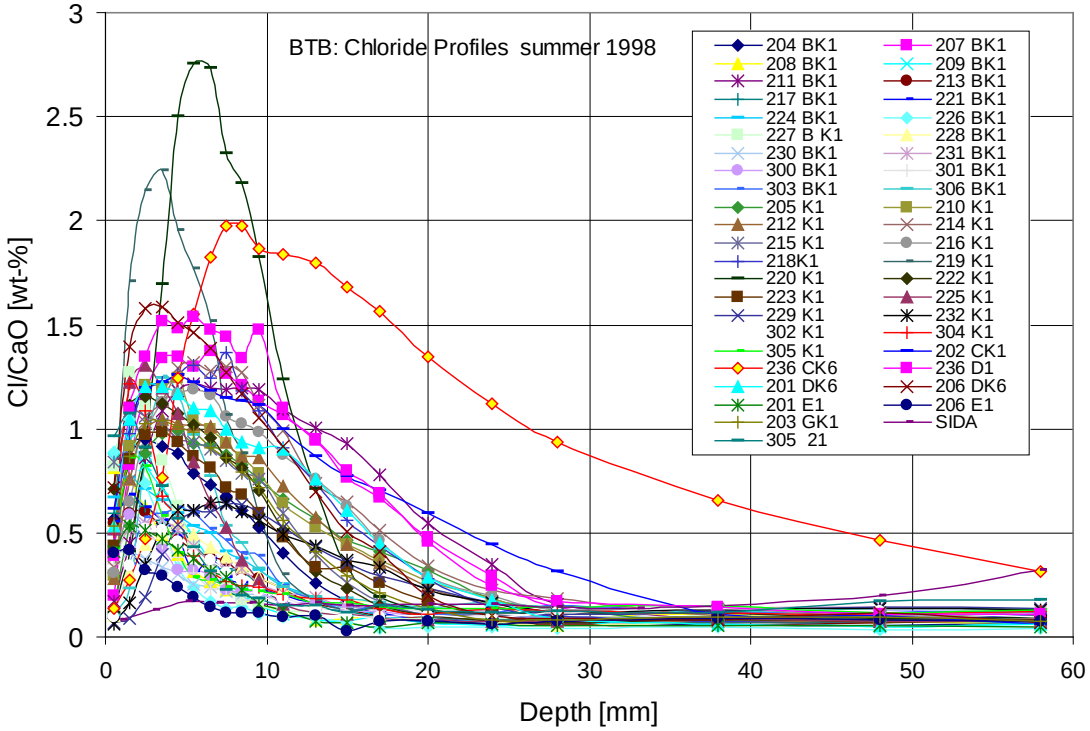

Figure 7 – Chloride penetration profiles after two years exposure at the Rv40 field station. Based on data from [6].

6.2 Curve-fitting for D_{F2} and C_{sa} and chloride diffusivity - D_{CTH}

The chloride penetration profiles after five years of exposure from the Träslövsläge field station and the chloride penetration profiles after two years of exposure from the Rv40 field station have been used for curve-fitting to the error-function solution of Fick's second law. The curve-fitting has resulted in an apparent chloride diffusion coefficient, D_{F2}, and an apparent surface chloride concentration, C_{sa}. It should be noticed that, in our opinion, these parameters not at all are the true chloride diffusion coefficient and surface chloride concentration, but simply represent the regression parameters of each chloride penetration profile. Additionally D_{F2} from the concretes in the road exposure depends on how the exposure time is defined. At least for short exposure periods D_{F2} will be very different if calculated from the start of the exposure or from the start of the exposure for de-icing salt. These times can be significantly different, e.g. if the exposure starts in spring after the season for spreading of de-icing salts this means that the concrete will be exposed for up to 6 months before the first exposure for chlorides from de-icing salts (in the autumn).

In table 4 data on the evaluated parameters D_{F2} and C_{sa} from the marine submerged and atmospheric zones after five years exposure and two years exposure in the road environment are presented. Furthermore data on D_{CTH} determined in the laboratory, on unexposed concrete at an age of six months, are presented in table 4.

Table 4 – Chloride diffusivity, D_{CTH}, for unexposed concrete with an age of six months and curve-fitted parameters D_{F2} and C_{sa} for the marine submerged and atmospheric zones (after five years exposure) and the road environment (after two years exposure). Based on data from [2] and [6].

Mix	Binder type	w/b		Marine sub-merged, 5 years		Marine atmo-spheric, 5 years		Road, 2 years	
No.			D_{CTH} *	D_{F2} +	C_{sa} -	D_{F2} +	C_{sa} -	D_{F2} +	C_{sa} -
201 1-40	Swedish SRPC	0.40	12.2	1.33	5.31	1.08	1.44	1.6	2.4
202 1-50	Swedish SRPC	0.50	19.9	2.31	5.48	1.78	1.64	4.0	1.7
203 H3	Swedish SRPC	0.30	2.5	1.49	3.80	0.49	3.40	0.79	2.3
204 7-35	Swedish SRPC	0.35	4.3	-	-	-	-	0.55	2.4
206 3-40	Swedish SRPC + 5% SF	0.40	4.4	1.26	4.91	0.49	2.04	1.2	2.6
207 3-50	Swedish SRPC + 5% SF	0.50	13.4	1.09	5.17	1.29	2.49	2.1	2.4
208 H1	Swedish SRPC + 5% SF	0.30	0.6	0.50	4.74	0.15	1.60	0.28	0.9
209 6-35	Swedish SRPC + 5% SF	0.35	1.6	-	-	-	-	0.35	1.2
215 2-40	Swedish OPC	0.40	7.1	1.93	4.25	0.75	2.57	0.63	3.1
216 2-50	Swedish OPC	0.50	18.2	-	-	-	-	1.6	2.1
226 H2	Swedish SRPC + 10% SF	0.30	0.3	0.14	4.87	0.08	2.02	0.30	1.5
3-35 3-75	Swedish SRPC + 5% SF Swedish SRPC + 5% SF	0.35 0.75	2.9 33.9	- -	- -	- -	- -	-	-
4-40	Swedish SRPC + 10% SF	0.40	3.2	-	-	-	-	-	-
9-40	Danish SRPC + 5% SF	0.40	5.3	-	-	-	-	-	-
10-40	Danish SRPC + 17% PFA + 4.5% SF	0.40	0.6	0.78	7.38	0.26	3.14	-	-
11-35	Danish SRPC + 10% PFA + 5% SF	0.35	0.8	-	-	-	-	-	-
12-35	Swedish SRPC + 10% PFA + 5% SF	0.35	1.0	0.76	5.18	0.20	1.65	-	-
H4	Swedish SRPC + 5% SF	0.40	2.7	0.76	4.93	0.45	1.90	-	-
H5	Swedish SRPC + 10% SF	0.25	0.9	0.21	4.38	0.16	1.96	-	-
H6	Swedish SRPC + 5% PFA	0.30	4.4	-	-	-	-	-	-
H7	Swedish SRPC + 5% SF	0.30	0.6	-	-	-	-	-	-
H8	Swedish SRPC + 20% PFA	0.30	1.5	0.51	5.28	0.26	3.58	-	-
H9	Swedish SRPC	0.30	2.7	-	-	-	-	-	-
205 236	Swedish SRPC	0.50 0.75	- -	- -	- -	- -	- -	2.1 9.6	1.4 2.6
217 218	Swedish OPC	0.30 0.50	- -	- -	- -	- -	- -	0.60 1.4	0.8 2.5
210	Swedish SRPC + 5% SF	0.50	-	-	-	-	-	1.6	1.6
225 227	Swedish SRPC + 10% SF	0.40 0.35	- -	- -	- -	- -	- -	0.30 0.21	2.5 1.8

* : D_{CTH} – x 10^{-12} m^2/s. 0.5 years unexposed to chlorides.

\+ : D_{F2} – x 10^{-12} m^2/s.

\- : C_{sa} – mass-% of binder.

- : No data available

In table 5 D_{F2} and C_{sa} for some other exposure times for selected concrete compositions from the marine submerged and atmospheric zones are presented. The following exposure times are included: 0.6-0.8 years, 1-1.3 years and 2-2.4 years.

Table 5 – Curve-fitted parameters D_{F2} and C_{sa} for the marine submerged and atmospheric zones. Based on data from [2].

Index	Composition	w/b	D_{F2}[+] Age			C_{sa}[-] Age		
	Submerged zone		0.6-0.8	1-1.3	2-2.4	0.6-0.8	1-1.3	2-2.4
1-40	Swedish SRPC	0.40	4.36	3.20	3.27	2.83	3.28	3.33
1-50	Swedish SRPC	0.50	5.59	7.13	3.27	2.54	4.11	3.79
3-40	Swedish SRPC + 5% SF	0.40	3.78	1.68	-	3.37	3.93	-
3-50	Swedish SRPC + 5% SF	0.50	5.59	3.60	2.82	2.53	4.88	3.73
12-35	Swedish SRPC + 10% PFA + 5% SF	0.35	1.86	-	0.80	1.86	-	3.45
H8	Swedish SRPC + 20% PFA	0.30	-	1.52	-	-	3.01	-
	Atmospheric zone							
1-40	Swedish SRPC	0.40	3.00	-	0.81	1.30	-	1.22
1-50	Swedish SRPC	0.50	3.51	-	2.49	0.98	-	1.56
3-40	Swedish SRPC + 5% SF	0.40	1.51	-	-	1.02	-	-
3-50	Swedish SRPC + 5% SF	0.50	2.63	-	2.02	1.26	-	1.63
12-35	Swedish SRPC + 10% PFA + 5% SF	0.35	1.23	-	0.63	1.39	-	0.76
H8	Swedish SRPC + 20% PFA	0.30	-	0.51	-	-	0.51	-

[+] : D_{F2} – x 10^{-12} m^2/s.
[-] : C_{sa} – mass-% of binder.
- : No data available

7. DISCUSSION AND ANALYSIS

7.1 Comparison marine/road environments

The influence from the exposure environment on the chloride penetration has been studied. In figure 8 chloride penetration profiles for two concrete mixes exposed in both in marine and road environments are presented. The profiles with indexes 202 (100% Swedish SRPC) and 207 (95% Swedish SRPC + 5% SF) are from the road exposure and the profiles with indexes 1-50 (100% Swedish SRPC) and 3-50 (95% Swedish SRPC + 5% SF) come from the marine exposure. The indexes A and S indicate if the profiles come from the marine atmospheric or submerged zones respectively. The continuous lines indicate that the profile comes from a concrete made from 100 % Swedish SRPC and the broken lines indicate that the profile comes from a concrete made from 95 % Swedish SRPC + 5% SF.

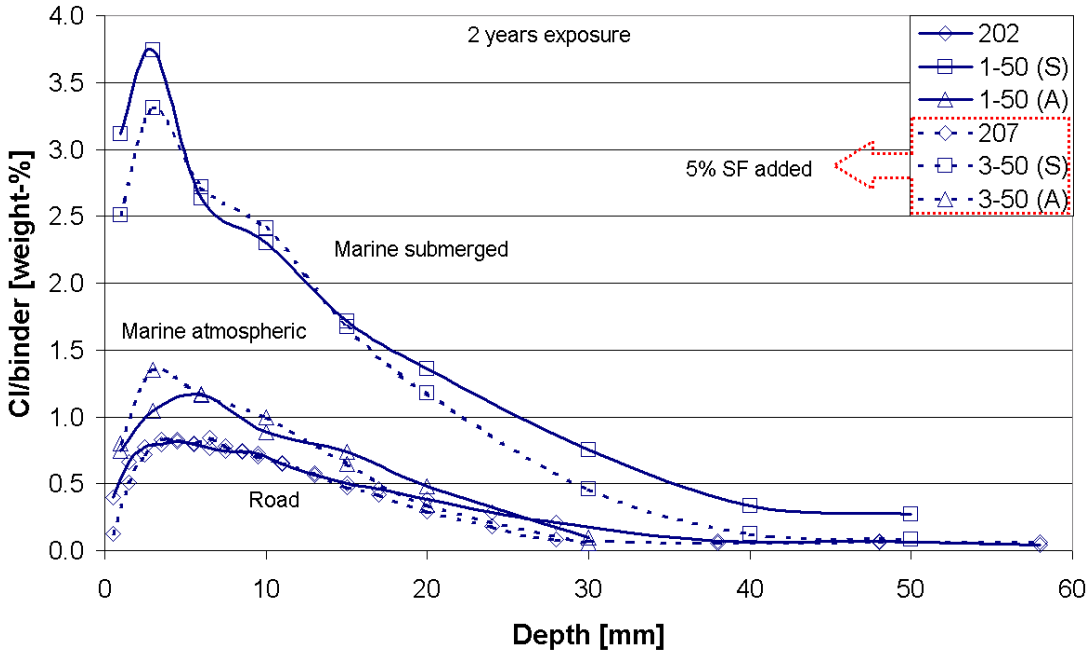

Figure 8 – Chloride penetration profiles after two years exposure at the Träslövsläge and Rv 40 field stations. Based on data from [2] and [3].

The concrete without SF has a slightly higher chloride penetration compared to the concrete with an addition of 5% SF. The chloride penetrations in the road environment correspond fairly well with the chloride penetration in the marine atmospheric zone. However, the exposure time for chlorides in the road environment is only approximately half of the exposure time in the marine exposure, since de-icing salts are only spread some six months during a year.

7.2 Influence from type of binder on D_{F2} and C_{sa}

In general the apparent diffusion coefficient, D_{F2}, decreases with increasing exposure time, while the apparent surface chloride concentration, C_{sa}, increases with increasing exposure time. This behaviour can be seen in figure 9a, 9b and 9c where D_{F2} and C_{sa} for some of the concretes exposed at the Träslövsläge field station are plotted against the exposure time. Two concrete compositions with Swedish SRPC and Swedish SRPC+5%SF respectively (w/b=0.40 and 0.50), one concrete with Swedish SRPC+20%PFA (w/b=0.30) and one concrete with Swedish SRPC+10%PFA+5%SF (w/b=0.35). To make the decrease of D_{F2} in time clearer the data are plotted in a log-log scale. It should be pointed out that the zone with largest chloride penetration does not necessarily has to be the severest zone for reinforcement corrosion, since this process also involves the availability of oxygen and galvanic contact.

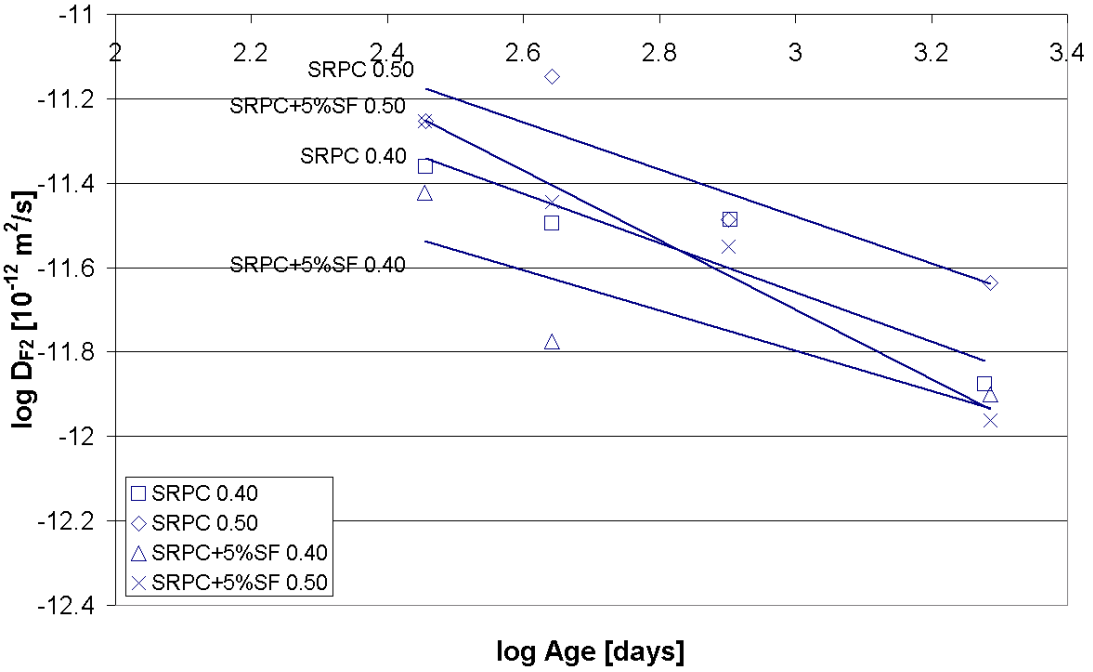

Figure 9a – The decrease in time D_{F2} from the marine submerged zone. Concretes made from Swedish SRPC and Swedish SRPC + 5% SF (w/b=0.40 and 0.50). Based on data from [2].

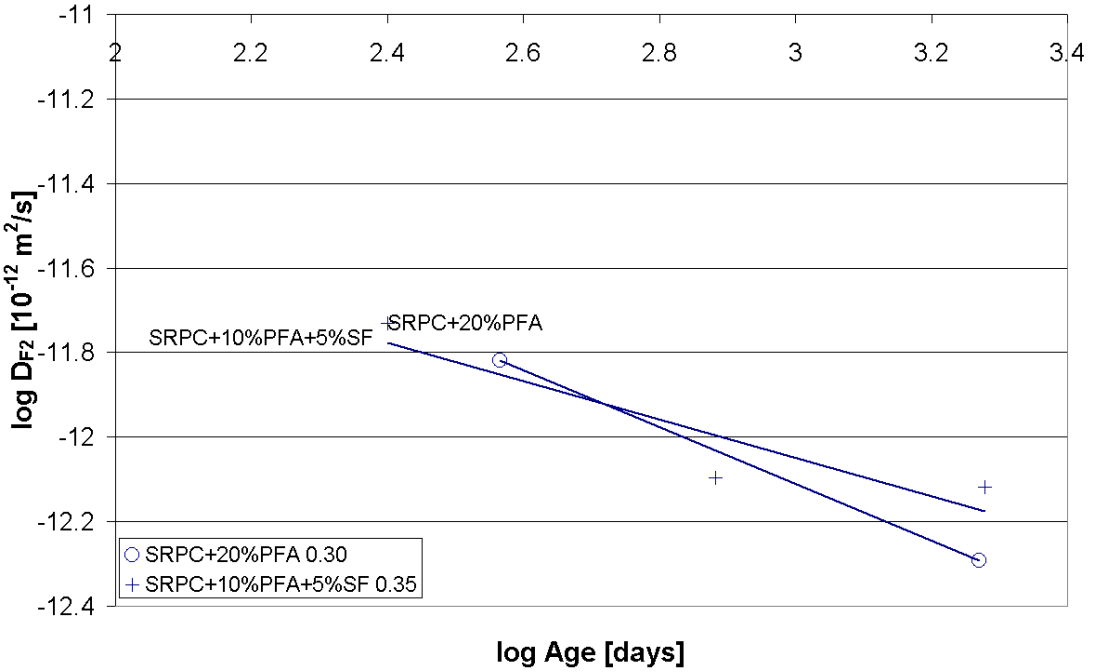

Figure 9b – The decrease in time D_{F2} from the marine submerged zone. Concretes made from Swedish SRPC + 20%PFA (w/b=0.30) and Swedish SRPC + 10%PFA + 5%SF (w/b=0.35). Based on data from [2].

In prediction models for chloride ingress into concrete, the decrease in D_{F2} with time is usually described with an age-factor. The age-factor evaluated with the DuraCrete-model for chloride ingress, described in [11], ranges from 0.45 for Swedish SRPC+10%PFA+5%SF to 0.82 for Swedish SRPC 0.40. However, these data are based only on measurements from up to four

different times, which makes it hard to see any significant differences in behaviour between the concrete mixes.

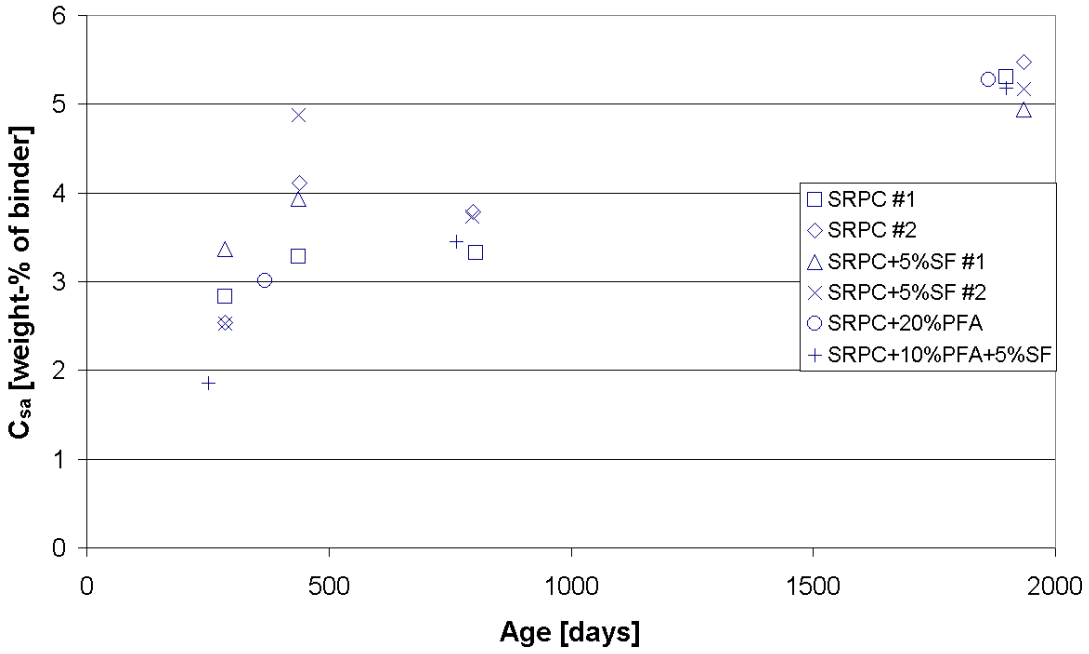

Figure 9c – The development in time for C_{sa} from the marine submerged zone. Based on data from [2].

C_{sa} show an increase for all the examined concrete mixes with increasing exposure time. There seems not to be any significant differences in increase of C_{sa} between the types of different binders. There are indications of an increase of chlorides in the surface zone of the concrete. However, this effect may also be a result of an increasing depth of the outer convection zone, c.f. [6].

7.3 Influence from type of binder and exposure environment

The magnitude of both D_{F2} and C_{sa} follows the order {submerged zone > atmospheric zone in the marine exposure}. In figure 10a, 10b and 10c the time-dependencies of D_{F2} and C_{sa} respectively for the marine atmospheric and submerged zones are presented. To make the decrease in D_{F2} clearer the data are plotted in a log-log scale. The solid lines give the trend for the submerged zone, denoted with “S”, and the broken lines give the trend for the atmospheric zone, denoted with “A”.

However, it should be pointed out that the zone with largest chloride penetration does not necessarily has to be the severest zone for reinforcement corrosion, since this process also involves the availability of oxygen and galvanic contact.

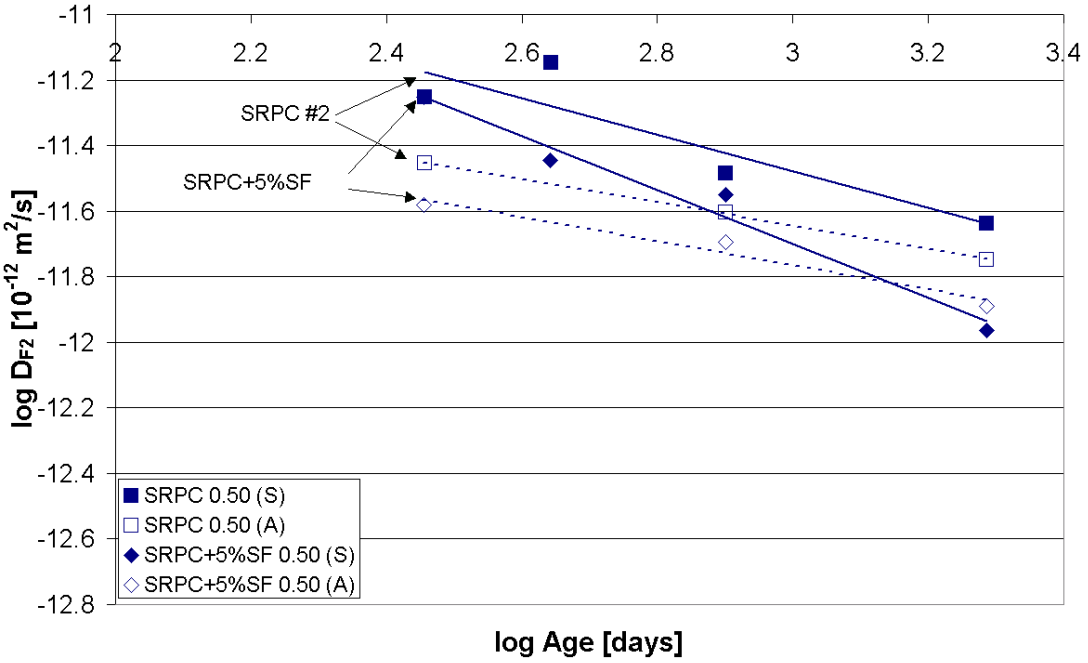

Figure 10a – The development in time for D_{F2} from the marine atmospheric and submerged zones. The solid lines give the trend for the submerged zone and the broken lines give the trend for the atmospheric zone. Concretes made with Swedish SRPC and Swedish SRPC + 5% SF (w/b=0.50). Based on data from [2].

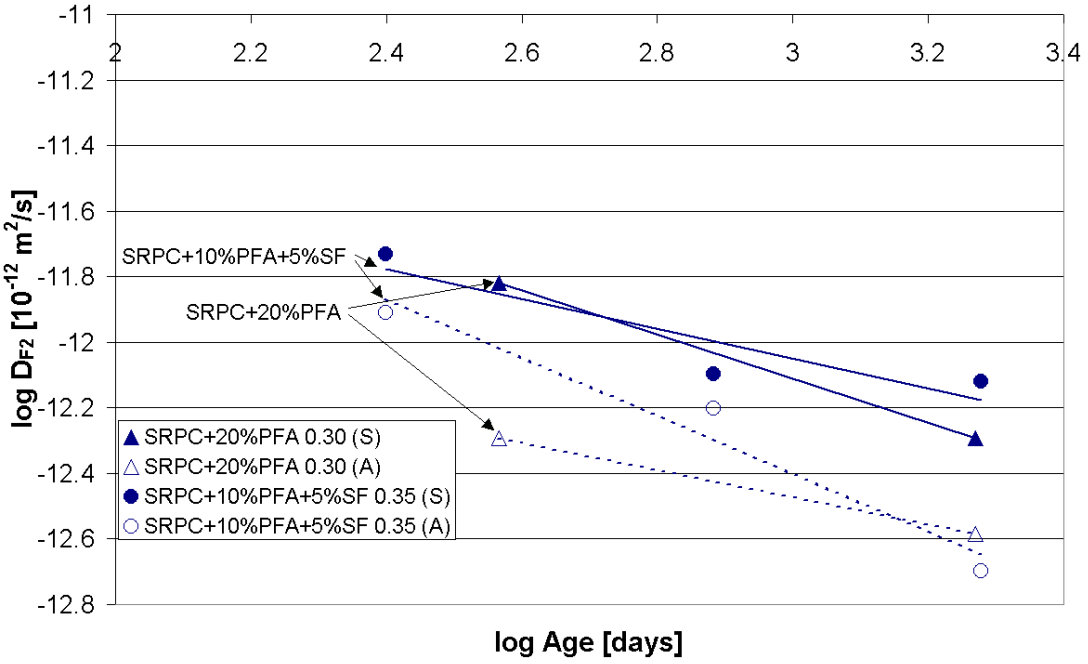

Figure 10b – The development in time for D_{F2} from the marine atmospheric and submerged zones. The solid lines give the trend for the submerged zone and the broken lines give the trend for the atmospheric zone. Concretes made with Swedish SRPC + 20%PFA (w/b=0.30) and Swedish SRPC + 10%PFA + 5%SF (w/b=0.35). Based on data from [2].

D_{F2} seems to be larger in concrete mixes with only SRPC and show a decrease with increasing amount of admixtures. The lowest values of D_{F2} are found for a concrete with made from

Swedish SRPC + 20% PFA (w/b=0.30). The differences in the decrease of D_{F2} in time between the different concrete mixes or the exposure environment are fairly small. D_{F2} is, as expected, larger for all concrete compositions in the submerged zone compared to the atmospheric zone.

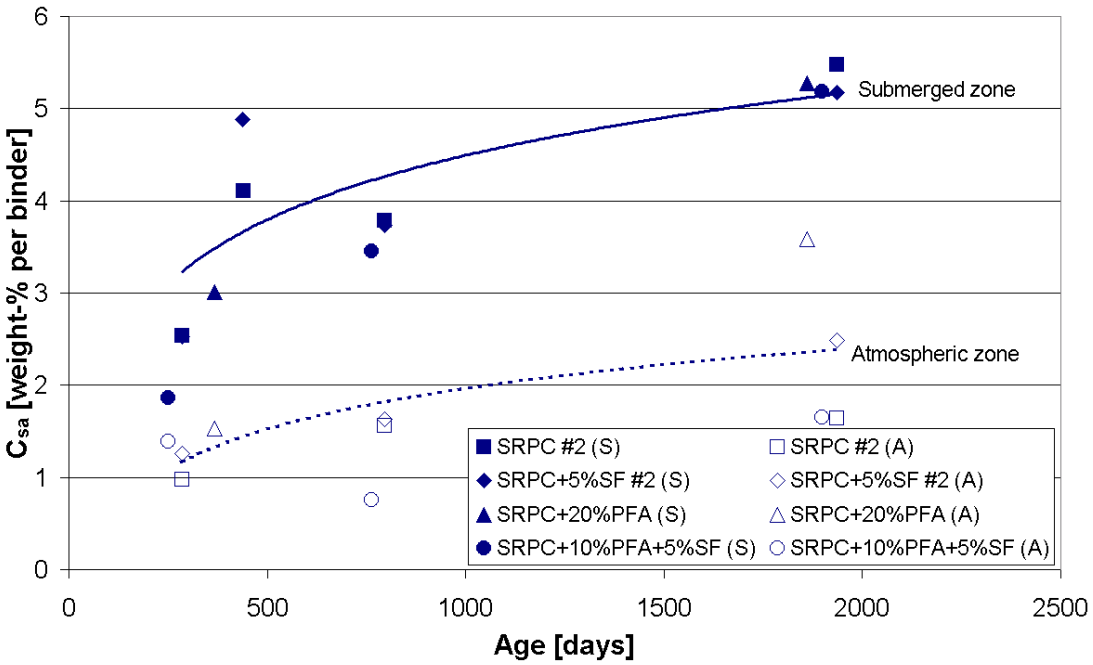

Figure 10c – The development in time for C_{sa} from the marine atmospheric and submerged zones. The solid line gives the trend for the submerged zone and the broken line gives the trend for the atmospheric zone. Based on data from [2].

There is a significant difference in C_{sa} between the submerged and atmospheric zones for all exposure times. However, the increase of C_{sa} with increasing exposure time is approximately the same in both the submerged and atmospheric zones. Furthermore there seems not to be any significant differences in C_{sa} between different binders, especially not in the submerged zone. This differences between different binders become smaller with increasing exposure times.

The effects of different additives on D_{F2} have been studied. In figure 11a and 11b D_{F2} from the marine submerged zone and the road environment are plotted against w/b. In the marine environment D_{F2} has been evaluated after approximately five years exposure and in the road environment D_{F2} has been evaluated after approximately two years exposure.

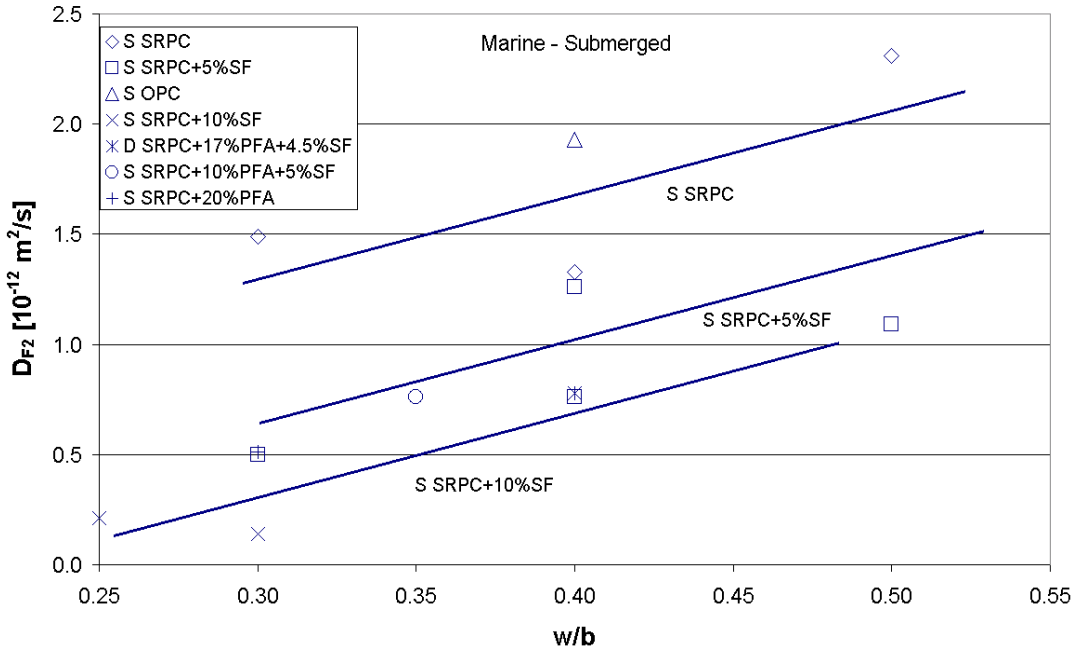

Figure 11a – D_{F2} evaluated after five years exposure in the marine submerged zone as a function of w/b. Based on data from [2].

Compared with a concrete made from only SRPC D_{F2} for a concrete with 5% SF is some 50% lower and for a concrete with 10% SF some 65% lower. The use of only PFA or a combination of SF and PFA seems to have a similar effect. A similar effect from the use of SF can also be seen if D_{F2} for the atmospheric zone is plotted against w/b.

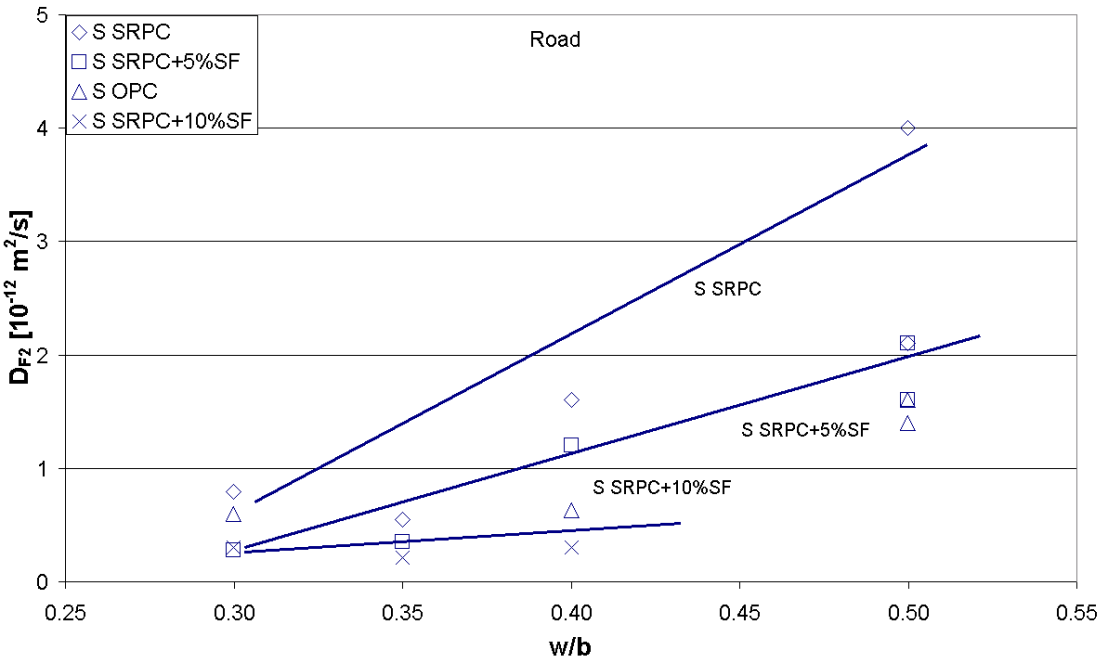

Figure 11b – D_{F2} evaluated after two years exposure in the road exposure as a function of w/b. Based on data from [5].

The concrete exposed in the road exposure show the same behaviour as the concrete exposed in marine exposure, where D_{F2} shows a decrease with increasing addition of SF. However, the effect is more marked for higher w/b, where the decrease in D_{F2} is negligible for w/b=0.30 and significant for w/b=0.40 and higher.

The shapes of the increase in D_{F2} with increasing w/b and amounts of SF are different in the marine and road environments. For low w/b the difference in D_{F2} for concretes made with different amounts of SF is almost negligible in the road environment while there are large variations in the marine environment. For higher w/b there are significant differences in D_{F2} depending on the amount of SF in both environment. Thus it seems to be favourable to have an addition of SF in concretes with low w/b in the marine environment but not in the road environment.

7.4 Influence from type of binder on chloride diffusivity

Each concrete composition exposed at the Träslövsläge field station has also been tested with the CTH rapid test for determining chloride diffusivity, NT BUILD 492 [12]. In figure 12a and 12b the measured chloride diffusivities, D_{CTH}, are presented.

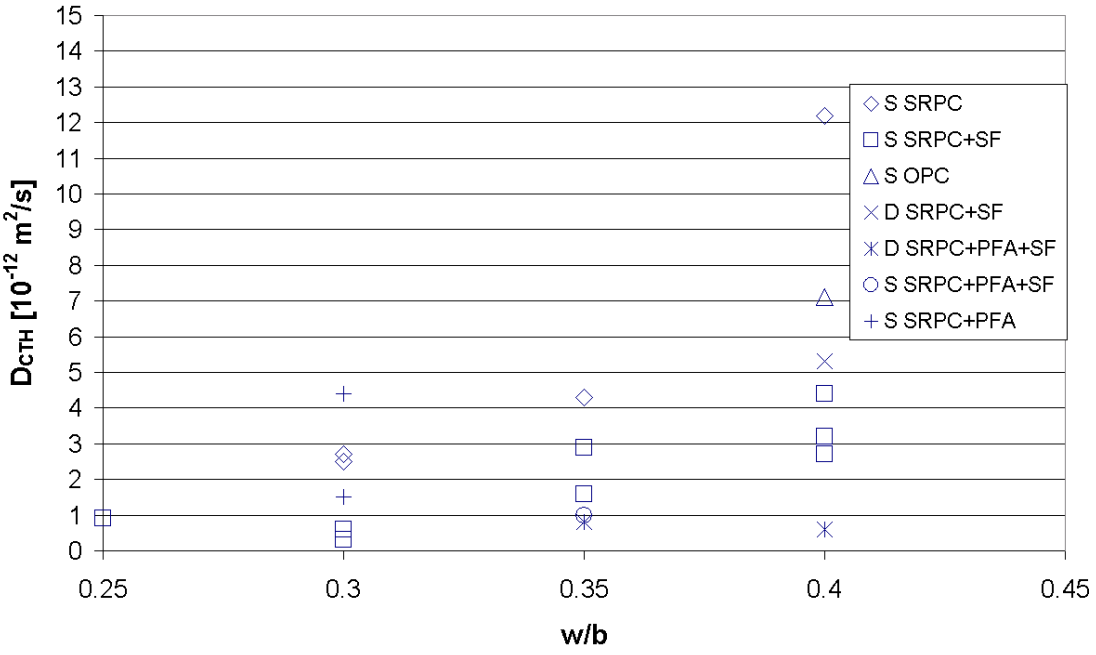

Figure 12a – Chloride diffusivities, D_{CTH}, determined with NT Build 492 [12]. Data from [4].

Additions of SF, PFA and a combination of PFA and SF have a significant effect on the D_{CTH}, where D_{CTH} decreases with increasing amounts of PFA and SF. The lowest values of D_{CTH} are found for concretes made either from Swedish or Danish SRPC together with PFA and SF (concrete mixes 10-40, 11-35 and 12-35). Compared with a concrete made with only SRPC D_{CTH} can be reduced with over 90% if a combination of SF and PFA are used. It can be also seen that a concrete made from SRPC with an addition of either SF or PFA has significantly lower D_{CTH} compared to a concrete made from only OPC or SRPC.

In figure 12b D_{CTH} for some concrete compositions with Swedish SRPC and additions of 5% and 10% SF are presented. It is also indicated if an air-entraining agent (AEA) has been added to the concrete mix.

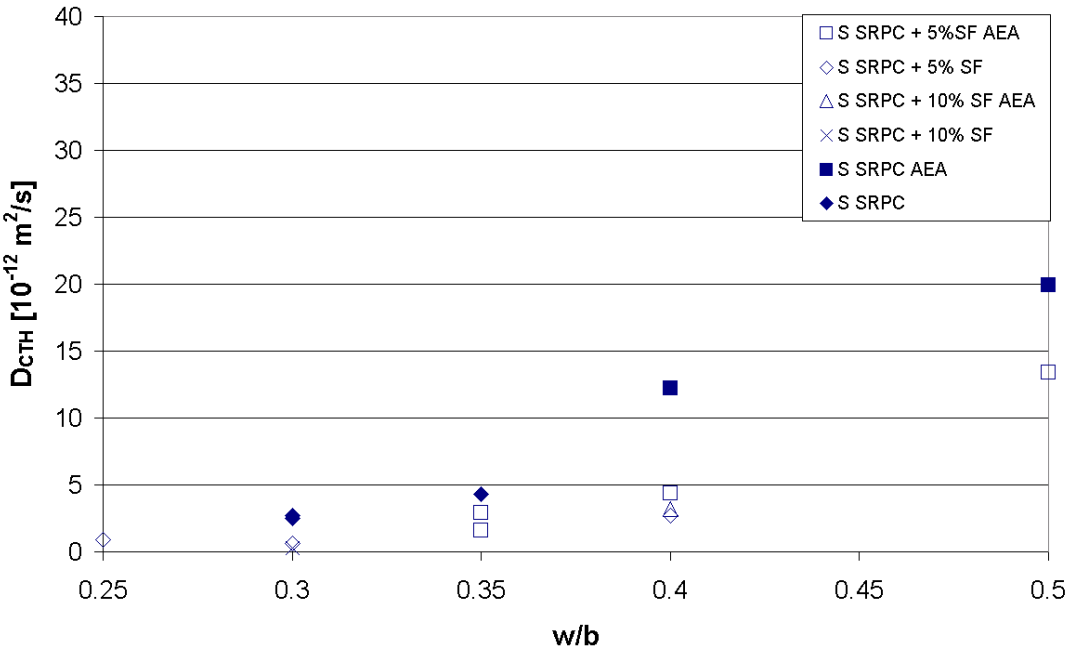

Figure 12b – Chloride diffusivities, D_{CTH}, determined with NT Build 492 [12]. Selection of Swedish SRPC concrete and Swedish SRPC + SF concrete. Data from [4].

An addition of 5% SF reduces D_{CTH} with some 50% compared to a concrete made from only SRPC. A concrete with an addition of 10% SF has some 25% lower D_{CTH} compared to a concrete with an addition of 5% SF. There seems not to be any significant effect from an addition of AEA on D_{CTH}.

8. CONCLUSIONS

The environmental conditions have a large influence on the chloride penetration. The chloride penetration in the marine atmospheric zone and the road environment correlate fairly well, while the chloride penetration in the marine submerged zone is significantly larger.

The apparent diffusion coefficient, D_{F2}, decreases with an addition of silica fume (SF), both for exposure in marine and road environments. Furthermore D_{F2} shows a decrease with increasing amount of SF. With an addition of 5% SF D_{F2} is some 50% lower and with 10% SF some 65% lower compared to a concrete with only Portland cement (CEM I). The same behaviour is achieved if pulverized fly ash (PFA) or a combination of PFA and SF has been used.

A concrete composition with a combination of Danish SRPC (CEM I 42.5 SR/LA), PFA and SF becomes extremely dense. Compared with a concrete made of only SRPC the chloride diffusivity, D_{CTH}, can be reduced with over 90%. A concrete with an addition of 5% SF reduces the chloride diffusivity, D_{CTH}, with some 50% compared to a concrete made from only SRPC. An addition of 10% SF give an additional reduction of D_{CTH} with some 25% compared to an addition of 5% SF.

REFERENCES

1. Sandberg, P., "Systematic collection of field data for service life prediction of concrete structures", in *Durability of Concrete in Saline Environment*, Cement AB, Stockholm, 1996, pp. 7-22.
2. Andersen, A., Hjelm, S., Janz, M., Johannesson, B., Pettersson, K., Sandberg, P., Sørensen, H., Tang, L. & Woltze, K., "Total chloride profiles in uncracked concrete exposed at Träslövsläge marine field station – Raw data from 1992 to 1997", Report TVBM-7126, Division of Building Materials, Lund Institute of Technology, Lund, 1998.
3. Luping, T. & Andersen, A. "Chloride ingress data from five years field exposure in a Swedish marine environment", *Proceedings*, 2nd International RILEM Workshop on Testing and Modelling the Chloride Ingress into Concrete, Paris, September 2000, 2000, pp. 105-119.
4. Tang, L., "Chloride penetration profiles and diffusivity in concrete under different exposure conditions", Publication P-97:3, Department of Building Materials, Chalmers University of Technology, Göteborg, 1997, 53 pp.
5. Utgenannt, P., "Field Exposure Site at Highway Rv40. List of specimens and tests up till autumn 1998" (in Swedish), BTB report 12, SP Building Technology, Borås, 1998.
6. Nilsson, L.-O., Andersen, A., Luping, T. & Utgenannt, P. "Chloride ingress data from field exposure in a Swedish road enviroment", *Proceedings*, 2nd International RILEM Workshop on Testing and Modelling the Chloride Ingress into Concrete, Paris, September 2000, 2000, pp. 69-83.
7. Lindvall, A., "Studies on chloride penetration into concrete in marine environments – project description and preliminary results", To be published in proceedings from NCR Miniseminar on "Durability of exposed concrete containing secondary cementitious materials" held in Hirtshals 21-23 November 2001.
8. AASHTO, "Standard Method of Sampling and Testing for Total Chloride Ion in Concrete and Concrete Raw Materials", American Association of State Highway and Transportation Officials, Designation: T 260-84, Washington, 1984.
9. Andersen, A. "HETEK, Investigation of chloride penetration into bridge columns exposed to de-icing salt". The Danish Road Directorate, Report No. 82, København, 1996. 37 pp.
10. Tang, L., "Chloride Transport in Concrete – Measurement and Prediction". Publication P-96:6, Department of Building Materials, Chalmers University of Technology, Göteborg, 1996. 88 pp.
11. DuraCrete, "Statistical quantification of the variables in the Limit State Functions", Document BE95-1347/R9, The European Union – Brite EuRam III, Contract BRPR-CT95-0132, Project BE95-1347, CUR, Gouda, 2000. 130 pp.
12. NT Build 492, Chloride diffusivity in hardened concrete, NORDTEST, 1999.

Chloride Profiles in Concrete Specimens Exposed to a High-way Environment for Five Years

Dimitrios Boubitsas
M.Sc.Civ.Eng. Doctoral Student
SP Swedish National Testing and Research Institute
Lund Institute of Technology
P.O. Box 118.SE-221 00 Lund
E-mail: dimitrios.boubitsas@byggtek.lth.se

ABSTRACT

In 1996 a field exposure site was established in the south-western part of Sweden. Specimens of different concrete qualities have been exposed to an aggressive environment. For some of the specimens the chloride profile was determined. The results from these chloride profile determinations are reported in this paper. The method used for determinations of the chloride profiles was the RCT-method. According to the results in this investigation the use of industrial by-products as blast-furnace slag and silica fume as binder in concrete seems to reduce the chloride penetration, at least for water/binder ratios of 0.40 and lower.

Key words: concrete, blast-furnace slag, silica fume, field exposure, chloride profiles

1. INTRODUCTION

In 1996 a field exposure site was established at the high-way R40 between Borås and Gothenburg in the south-western part of Sweden, Figure 1. Since then a great number of specimens of different concrete qualities have been exposed to a harsh winter climate during five years with moisture, frost and de-icing salts. Climatic data for the exposure site is presented in /1/.

All the specimens used for test of the frost resistance under field conditions were brought to the laboratory in May 2001 after five years of exposure. On some of the specimens the chloride profile was determined as a complement to the analysis of the frost damages. The results from these chloride profile determinations are reported in this paper.

2. CONCRETE QUALITIES TESTED

The concrete qualities tested are presented in Table 1. For all the qualities the maximum aggregate size was 16 mm. The fresh air content was about 4.5 % for all the mixtures and the air-entraining agent used was Cementa L16. After casting the specimens were stored in the moulds for one day, then in water for 6 days and finally in air (65±5 % RH and +20±2 °C) for 21 days. Then the specimens were placed on the field site in the autumn 1996 when they were about 30 days old.

Figure 1 – The field exposure site at the high-way R40 between Borås and Gothenburg

Table 1 – Composition of the concrete qualities used for analysing the chloride profiles

Concrete quality	Cement Quality	Cement (kg)	Water/binder ratio	Equivalent w/c- ratio	Air content (%)	Slump (mm)	Carb. depth (mm)***)
CEM I	Degerh anl*)	500	0.30		3.8	240	<1
CEM I	”	450	0.35		5.9	190	<1
CEM I	”	420	0.40		3.1	125	<1
CEM I	”	370	0.50		2.8	90	<1
CEM I	”	260	0.75		8.7	100	4-5
	Degerh anl	475	0.30	0.29	3.1	100	<1
CEM I	”	427.5	0.35	0.33	2.1	90	<1
+ 5%****)	”	399	0.40	0.38	3.1	105	<1
Silica fume	”	361	0.50	0.48	5.6	70	<1
	”	237.5	0.75	0.72	4.0	70	1-2
CEM I	Degerh anl	350	0.30	0.34	4.3	230	<1
+ 30%****)	”	315	0.35	0.40	3.2	130	<1
Blast	”	294	0.40	0.45	2.2	110	<1
furnace	”	256	0.50	0.57	4.0	80	<1
slag	”	175	0.75	0.85	6.8	100	7
CEM III	CEM III**)	520	0.30		3.6	200	<1
CEM III	”	460	0.35		3.3	200	<1
CEM III	”	420	0.40		3.1	120	<1
CEM III	”	380	0.50		4.1	70	3-5
CEM III	”	255	0.75		8.3	90	8-10

*) CEM I, sulphur resistant, low alkali, low C_3A

**) CEM III with 70% blast furnace slag by weight

***) Carbonation depth measured after five years of exposure by using the so called phenofatalein method

****) Percentage of the amount of binder

3. DETERMINATION OF THE CHLORIDE PROFILE

The specimens on the exposure site had the dimensions 150x150x75 mm and were sawn from 150 mm cubes. During the exposure the sawn surface was turned upwards for each of the specimens.

One cylinder with the diameter 50 mm was drilled from each specimen. Four millimeter thin slices were sawn from the cylinder with the centers of the slices located 2, 7.5, 13, 18.5, 24, 29.5 and 35 millimeters from the sawn surface of the specimen.

The slices were dried at +105 °C and then they were crushed and ground to a fine powder. The powder was then analysed according to the so called RCT-method /2/ which is based on measurements by using an electrode sensitive to chloride ions.

4. RESULTS

The chloride profiles for the four different binder types are presented in Figures 2-5.

In Figure 2 the chloride profiles are shown for concrete with CEM I as the only binder. The chloride content in the slice closest to the surface, with the center two millimeters from the surface, is decreasing with increasing value of the water/binder ratio. Sometimes this is explained by the fact that uncarbonated concrete has a higher binder capacity than carbonated and that the total chloride content therefore becomes higher. This explanation, however, does not seem so probable when the profiles are compared with the values of the carbonation depths as presented in Table 1. The carbonation depths are less than 1 mm for the four concrete qualities with the lowest water/binder ratios but the chloride profiles seem to be affected to a depth far beyond that. The chloride contents do not appears in a “correct” order (higher chloride content for higher water/binder ratios) until the depth is about 12 millimeters.

For the concrete quality with a water/binder ratio of 0.75, the peak of the chloride profile occurs at the depth of about 12 mm while the carbonation depth is only 4-5 millimetres.

It is not possible, by using the results from this investigation, to explain the shape of the chloride profiles close to the surface. One explanation, however, may be that chlorides are washed out by rainwater from the concrete layer close to the surface. This effect ought to be most pronounced for the most permeable concrete qualities, i.e. those with the highest water/binder ratios. This agrees with the results in this investigation.

The trends are exactly the same for the concrete qualities with the contents of 5 % silica fume. The penetration depths, however, are lower when compared with concrete qualities without silica fume, especially for water/binder ratios of 0.40 and lower. This is also illustrated in Figures 6 and 7.

The chloride profiles for the concrete containing 30% blast-furnace slag are very similar to those corresponding to concrete containing 5% silica fume. The chloride contents are, however, lower for concrete with CEM III as binder and the profiles seem to be less influenced by the water/binder ratio, at least where water/binder ratios of 0.50 and lower are concerned.

5. CONCLUSIONS

According to the results in this investigation the use of industrial by-products as blast-furnace slag and silica fume as binder in concrete influences the chloride penetration in concrete. The use of slag and silica fume seems to reduce the chloride penetration, at least for water/binder ratios of 0.40 and lower. One must, however, be aware of the fact that this does not automatically mean that the risk for chloride induced reinforcement corrosion is reduced. This risk is also influenced by, for example, the chloride threshold value, the oxygene permeability, the existence of other ions in the pore solution, etc. These parameters are not dealt with in this investigation.

REFERENCES

1. Utgenannt, P., ” Climatic Conditions at the field exposure site at high-way R40,” BTB-Report, October 1996. (In Swedish).
2. SP Swedish National Testing and Research Institute, “ SP-Method 0433 Rapid Chloride Test,” (In Swedish).

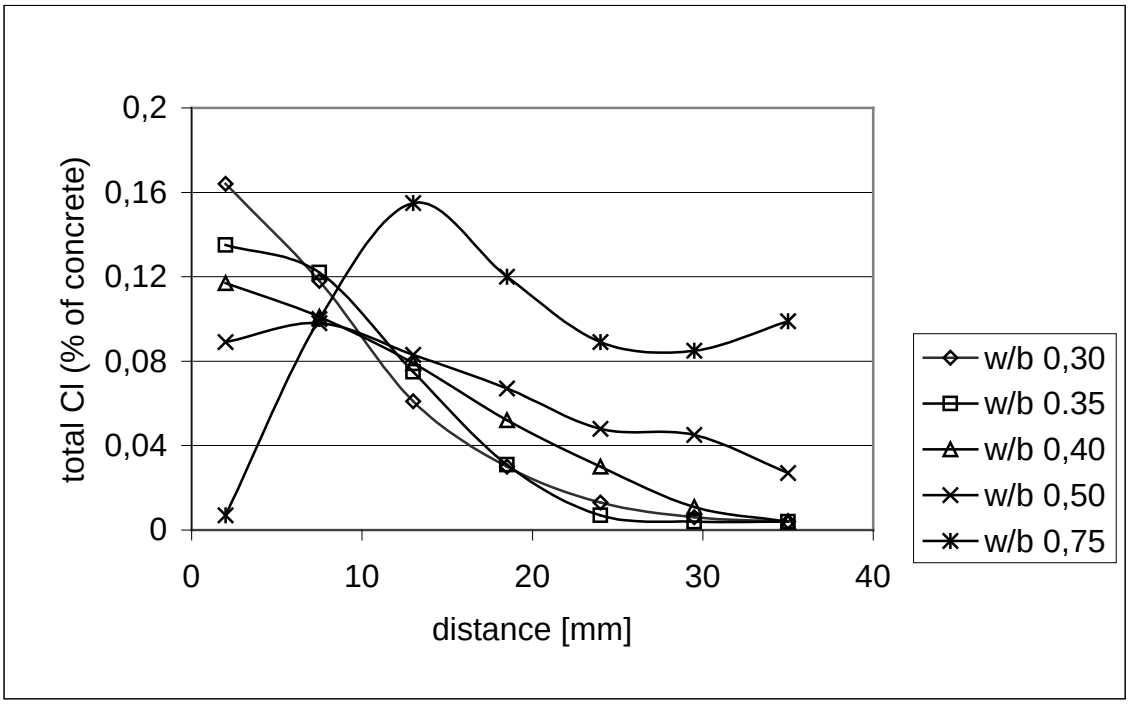

Figure 2 - Chloride content as function of the distance from the surface for different water/binder ratios. Concrete with CEM I as binder

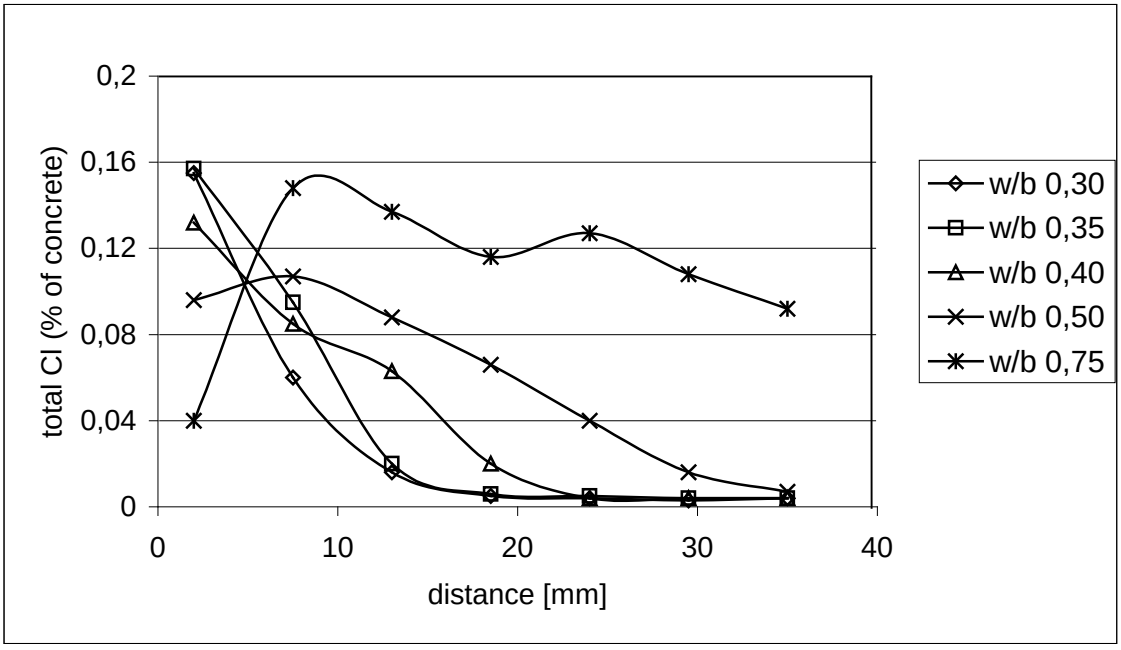

Figure 3 - Chloride content as function of the distance from the surface for different water/binder ratios. Concrete with CEM I and 5% silica as binder.

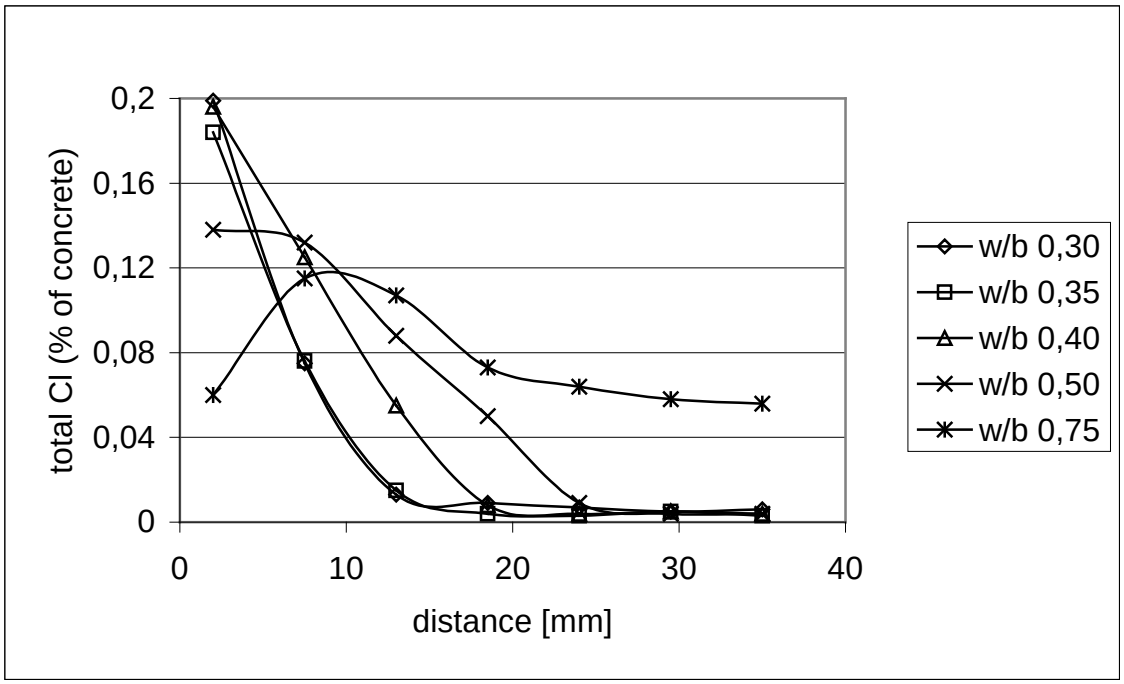

Figure 4- Chloride content as function of the distance from the surface for different water/binder ratios. Concrete with CEM I and 30% blast-furnace slag as binder.

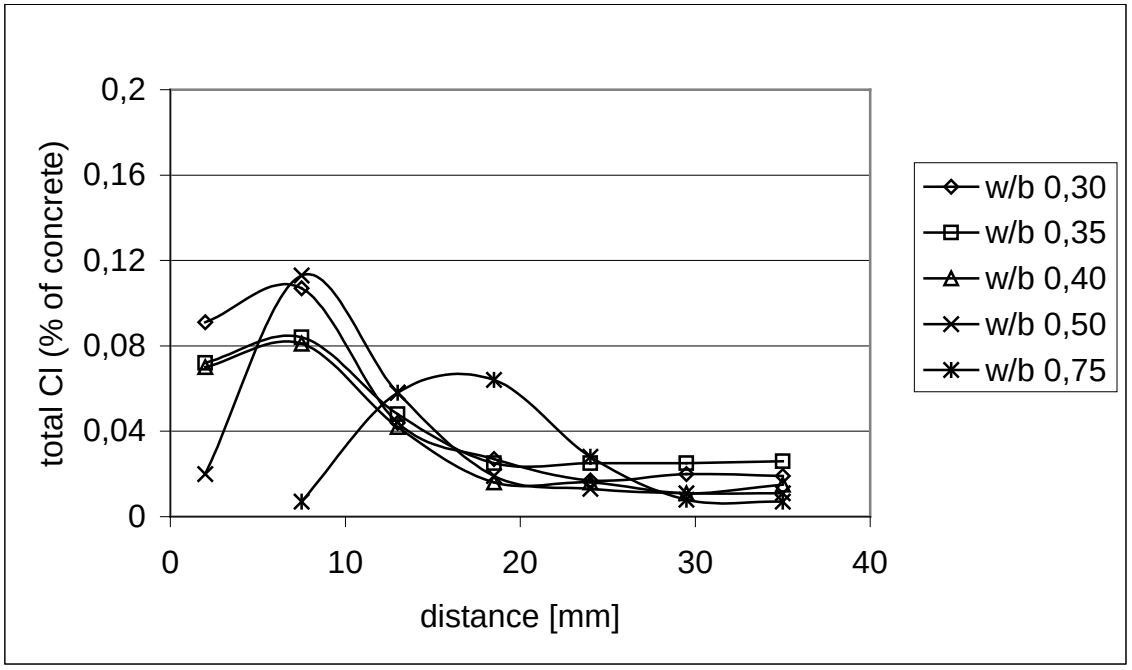

Figure 5- Chloride content as function of the distance from the surface for different water/binder ratios. Concrete with CEM III as binder.

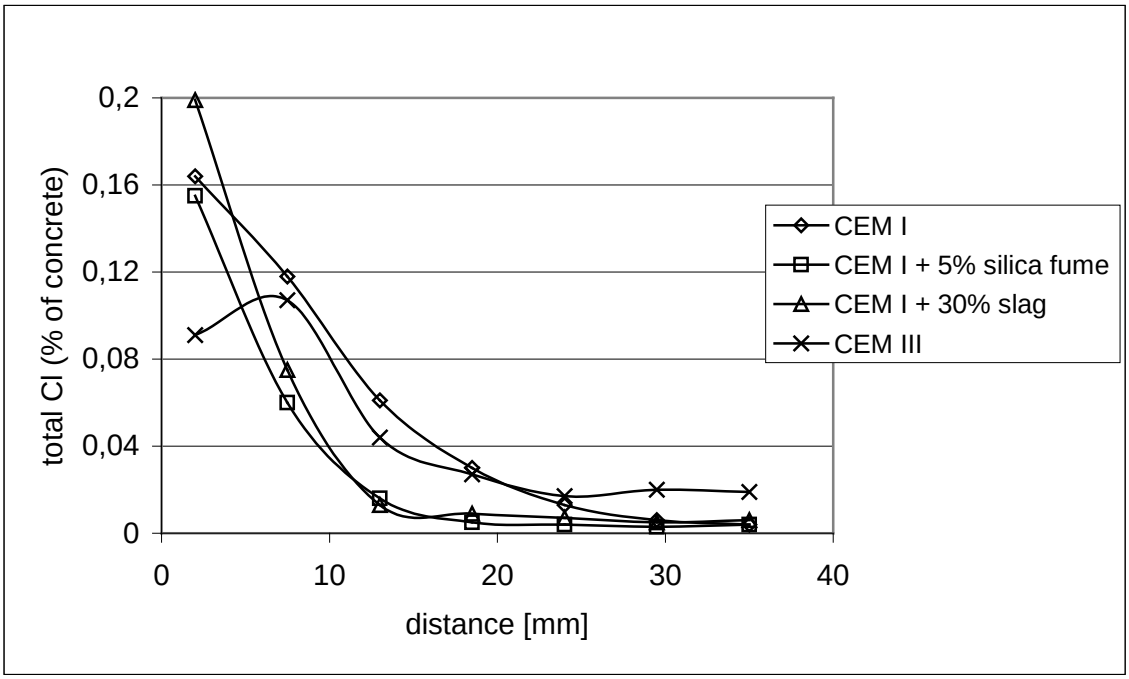

Figure 6 – Chloride profiles for concrete qualities with different types of binder. Concrete qualities with a water/binder ratio of 0.30.

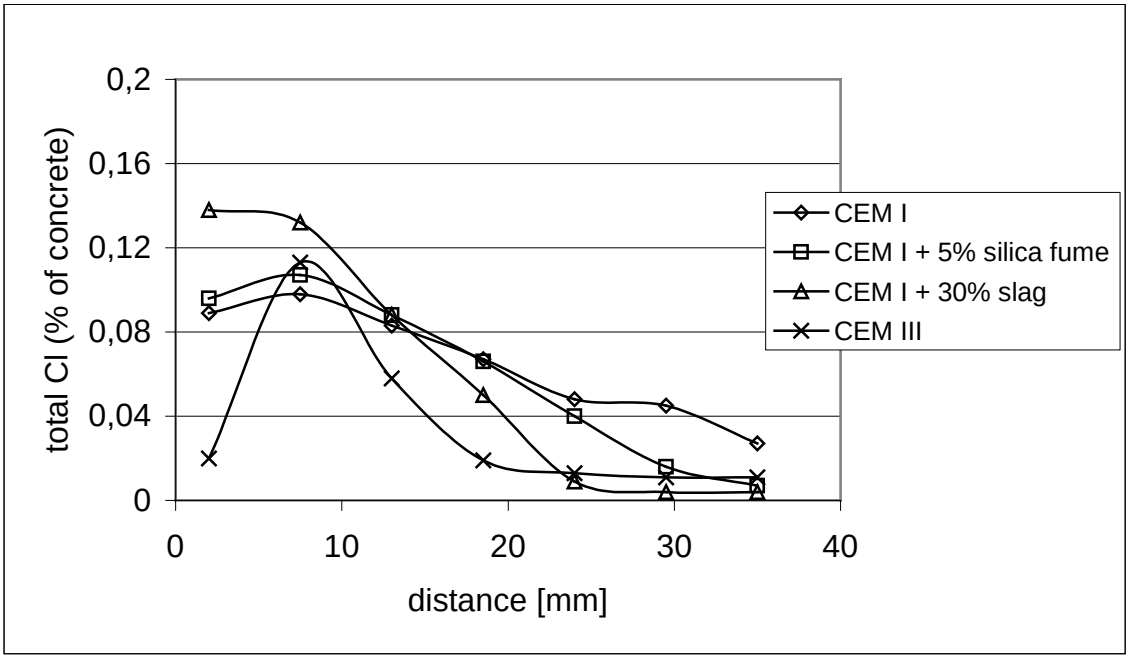

Figure 7 – Chloride profiles for concrete qualities withdifferent types of binder. Concrete qualities with a water/binder ratio of 0.50.

Chloride Migration Coefficient of Self-Compacting Concrete

Bertil Persson
Senior Lecturer, PhD Eng.
Dept. of Building Materials
Lund Institute of Technology
P. O. Box 118
SE-221 00 LUND
SWEDEN
E-mail: bertil.persson@byggtek.lth.se

ABSTRACT

In this article laboratory and analytical studies of the chloride migration coefficient are performed. The result of studies on chloride ingress of Self-Compacting Concrete are compared with the corresponding properties of normal concrete with the same water-cement ratio and air content. Both 28 and 90 days' age applied at the start of the testing. Six Self-Compacting Concrete were studied and 2 normal concrete, all with water-cement ratio = 0.39. The effect of normal and reversed order of mixing (filler last), increased amount of filler, type of filler, limestone powder, increased air content and large hydrostatic concrete pressure were investigated.

Keywords: Chloride Migration, Fly Ash, Limestone Filler, SCC, Self-compacting Concrete, Silica Fume.

1. INTRODUCTION, LIMITATIONS AND OBJECTIVE

1.1 Introduction

Concrete that does not require any energy for compacting in order to cover the reinforcement or fill out the mould has attracted a great deal of interest during the last years. Swedish experience now exists from 19 full-scale bridges and other full-scale projects with Self-Compacting Concrete, SCC [1], Appendix 1. The technique has also been introduced for dwelling houses and office buildings [2]. Recently SCC has been introduced for production of poles, piles and pillars [3]. Regarding concrete under severe circumstances for construction of bridges, dams, tunnel and so forth, the requirements of durability are superior. Therefore a higher level of documentation is required for concrete under severe conditions than for concrete that is used for dwelling houses or office buildings. The primary durability properties are salt frost scaling, internal frost resistance, sulphate resistance and chloride ingress for concrete under severe situations.

1.2 Limitations

Start of the testing of the chloride migration coefficient, *D*, took place both at 28 and 90 days' age. Eight concretes were studied, 2 normal concrete, NC, and 6 SCCs all with water-cement ratio, *w/c* = 0.39 (*c* was defined as Portland cement). The concrete was sealed from casting until testing. All the specimens were core-drilled from a larger specimen of concrete. In this way the effects of bleeding, carbonation, concrete skin, crazing, segregation and so forth were avoided. The following parameters were studied:

1. Normal and reversed order of mixing (filler first or last).
2. Different filler amount (low or high).
3. Limestone powder of geologicalyl old or young type (≈ 200 or 20 million years old).
4. Different air content (normal or increased air-entrainment).
5. Hydrostatic pressure on the fresh concrete mass.
6. Ambient environment like fresh water, sea water, salt water, sulphate water, frost cycles or 5°C.

1.3 Objectives

In this project the objectives were to investigate the chloride migration coefficient, *D,* defined by Tang [4], salt frost scaling, internal frost resistance and sulphate resistance of SCC that contains increased amount of filler, different types of casting and air content and to compare the result of salt frost scaling, internal frost resistance, sulphate resistance and chloride ingress of SCC with the corresponding properties of normal concrete, NC, with the same *w/c*.

2. PREVIOUS RESEARCH

2.1 Effect of *w/c* on the chloride migration coefficient

Figure 2.1 shows the chloride migration coefficient, *D,* of SCC with quartzite filler and of NC. All concrete mixes contained Slite Standard Portland cement except for concrete with w/c = 0.27, in which the low-alkali Portland cement Degerhamn was used, Appendix 1. The mix compositions of the concrete of series 1 is given in Appendix 2.1. The measurement was performed with a Rapid Test Method developed by Tang at Chalmers Technical University [4,5]. The results of the measurement are shown in Figure 2.1 and Appendix 2.2. For SCC with w/c = 39%, the chloride migration coefficient, $D = 14 \cdot 10^{-12}$ m^2/s was obtained. The following expression for the chloride migration coefficient, *D*, at 3 years' age was obtained (10^{-12} m^2/s, w/c in%), c:

$$D = (0.97 \cdot w/c - 25) \cdot 10^{-12} \text{ m}^2/\text{s} \quad \{0.27 < w/c < 0.80;\ R^2 = 0.96\} \quad (2.1)$$

2.2 Effect of additives on the chloride migration coefficient

The chloride migration coefficient, *D,* was studied for 3 Portland cement concretes and one silica fume concrete Figure 2.2 [5]. The mix proportions are found in Appendix 2.3. The chloride migration coefficient, D was largely decreased in concrete with silica fume compared with a pure Portland cement based concrete with the same water-binder ratio, *w/b* [6]. Two different concrete mixes based on the different cements and pozzolans having the same active porosity can have very different shape of the pore system, therefore resulting in different tortuosity factors [6]. The relation between the binding capacity of chlorides and the cement content follows the same pattern as the relation between the tortuosity factor and porosity, i.e. for the same type of cement and Pozzolan based concrete with different *w/b*s the binding capacity decreases with the cement content [6].

The electrical conductivity was studied on concrete discs of NCs for the Great Belt Link, [7-9]. The mix proportions of the experiment are given in Appendix 2.4. Especially in silica fume concrete the conductivity of NCs was reduced substantially [8]. The effect of fly ash on the electrical conductivity in Portland cement concrete was unclear [8], Figure 2.2.

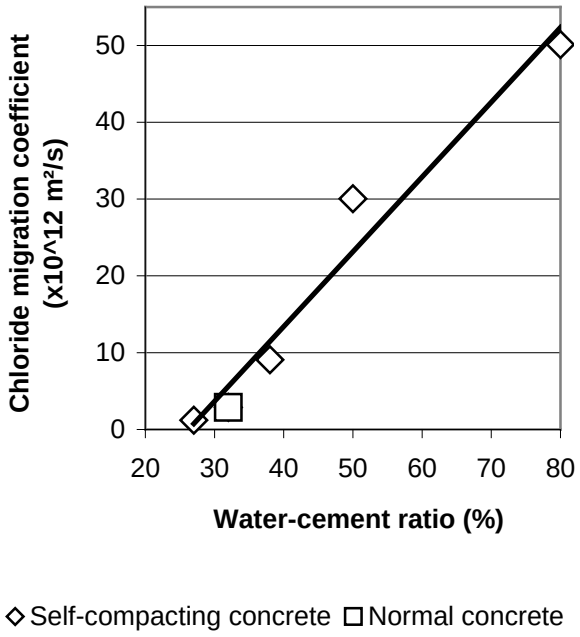

Figure 2.1 – The chloride migration coefficient, D versus w/c.

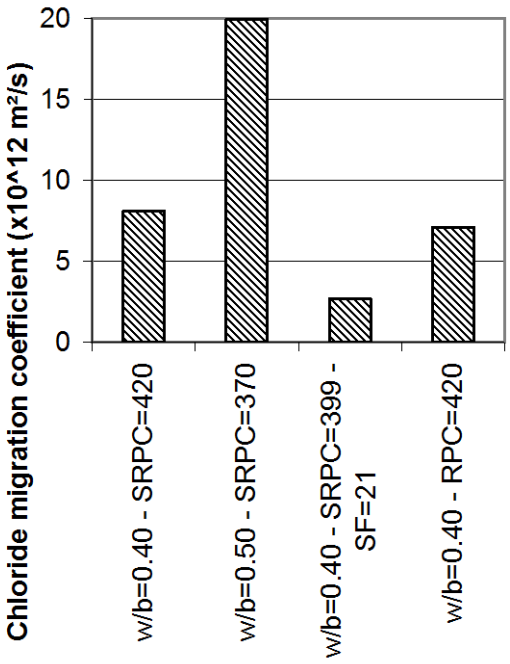

Figure 2.2. – The chloride migration coefficient, D for NCs with different cement types and 5% silica fume, w/b=0.4-0.5 [5].

In another project 4 types of SCCs and one NC for marine environment were studied, Figure 2.4 [10]. The mix proportions of the concrete of series 2 in the experiment are given in Appendix 2.5. A large decrease of the chloride migration coefficient, *D*, was observed when using slag cement or silica fume concrete. Also in this case the effect on the chloride migration coefficient, *D*, of fly ash in Portland cement concrete was found to be unclear [10]. When using as much as 68% slag of the slag cement, the chloride binding ability of the concrete increased and therefore a low chloride migration coefficient, *D*, was found, Figure 2.4 [10].

2.3 Effect of self-desiccation on the chloride migration coefficient, D

Buenfeld [11] called the attention to the detail that chlorides could not be transported in air. During self-desiccation in concrete with low *w/c*, chlorides may be transported from the surface of the concrete to the depth of liquid water front but no further since the pores at self-desiccation are partly disconnected by air filled voids. For concrete presently being used under severe environments, i.e. with low $w/c \leq 0.40$, this depth of water ingress varies from 2 cm up to 5 cm even after 7 years of exposure Figure 2.5 [12-14]. During 7 years the value of the chloride migration coefficient, *D*, decreases substantially as compared to the initial value at young age. Hydration products will occupy all space in the concrete since the volume is limited for those to increase at low *w/c* [15]. The shortage of space in concrete with low *w/c* will actually stop both hydration and chloride ingress hand in hand with the effect of self-desiccation in the cover layer of the reinforcement. The cover layer of reinforcement exceeds 5 cm in severe conditions, Figure 2.6 [16]. The following equations apply to self-desiccation [17]:

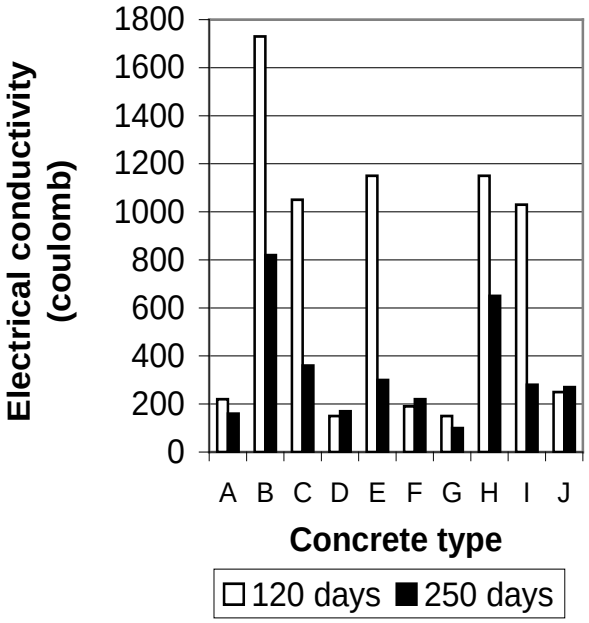

Figure 2.3 - Electrical conductivity for concrete discs of NCs for the Great Belt Link [7-9]. Notations: A-E = SRPC (sulphate resistant cement); F-J = RPC (rapid cement); A = PFA (fly ash) + SF (silica fume); C, E = PFA; D = SF; G = PFA (fly ash) + SF (silica fume); I = PFA; J = SF [7-9].

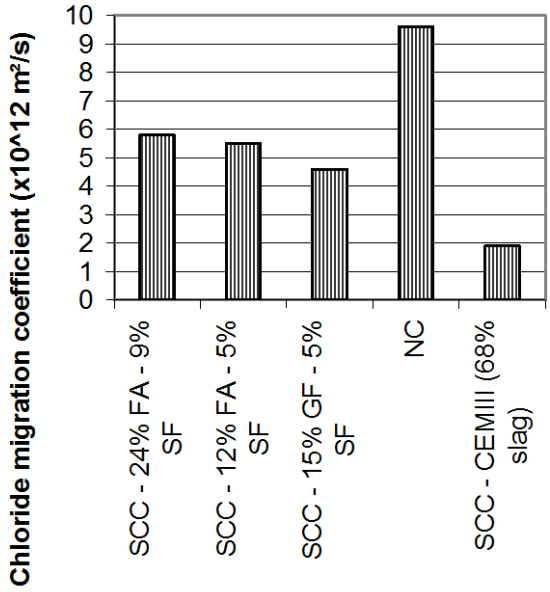

Figure 2.4 – The chloride migration coefficient, D, for SCC with additives [10]. FA = fly ash; SF = silica fume.

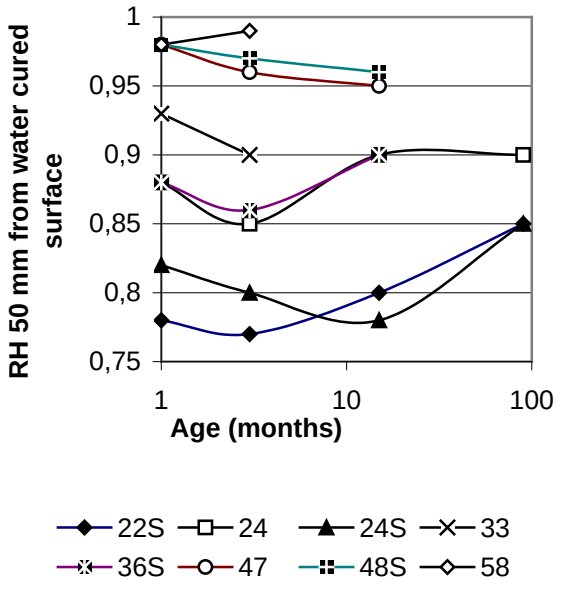

Figure 2.5 –RH at the depth of 50 mm from the free water vs age [17]. R = reference; S = 10% silica fume; 20 = w/c (%).

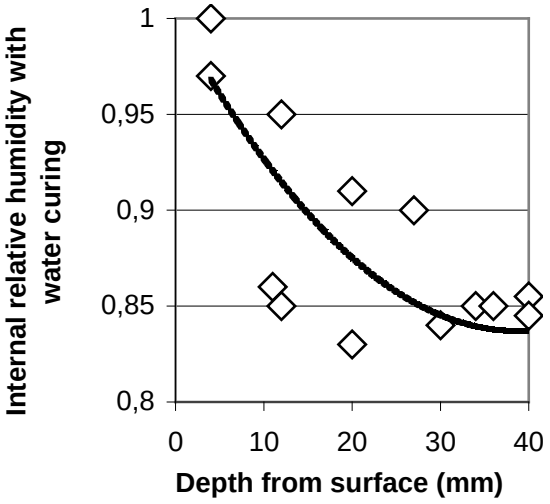

Figure 2.6 – RH measured after 2 years vs depth from water cured surface (w/b=0.4, 5% SF) [16].

$RH(t,w/c)_s = 1.13\cdot[1-0.065\cdot ln(t)]\cdot\cdot(w/c)^{0.24\cdot[1-0.1\cdot ln(t)]}$ $\{0.22<w/c<0.58; R^2=0.76\}$ (2.2)

$RH(t,w/c) = 1.09\cdot(w/c)^{0.17\cdot(1+0.0451\cdot t)}$ $\{0.22<w/c<0.58; R^2=0.54\}$ (2.3)

t denotes the age (1<t <15 months)
s denotes 10% silica fume
c denotes cement content (kg/m^3)
w denotes water content (kg/m^3)

$RH(wbr_{eff}, t) = 0.38\cdot[w/(c+2\cdot s)+2.4 -0.1\cdot lnt]+\Delta RH_{sl}$ $\{R^2= 0.83\}$ (2.4)

t denotes the age ($1<t<1000$ days)
wbr_{eff} denotes water to equivalent cement ratio ($0.22<w/(c+2\cdot s)<0.38$)
ΔRH_{sl} = - 0.035 for 5-10% silica fume slurry at age, $t \leq 28$ days

Calculations with equations (2.2) – (2.4) are shown in Figure 2.7-8. Reinforcement corrosion owing to chloride ingress will normally be hindered by use of High Performance Concrete, HPC, with sufficiently low $w/b \leq 0.40$, a adequate concrete cover provided that the surface is free from cracks [18]. Formulas in general used for estimating the chloride ingress were introduced some 30 years ago for water-saturated structural concrete in use at that time, i.e. with $w/c > 0.40$. These formulas do not account for self-desiccation since concrete with sufficiently low w/c was not in use at the time [19]. A great step in the understanding of the chloride migration coefficient, D, in NC with $w/c > 0.40$ was taken when the binding capacity related to the cement content was clarified [20]. Rapid tools for examining concrete were a great advantage when optimising concrete in use under severe conditions in sea [21]. Different models for estimating chloride ingress were put forward but still the relation to self-desiccation was not considered nor understood [22,23].

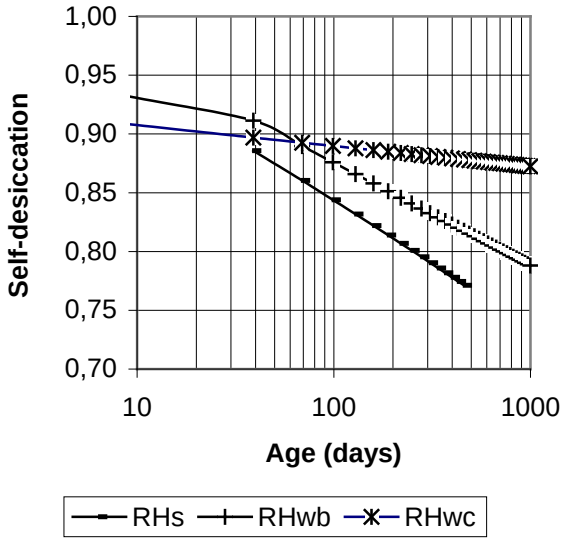

Figure 2.7 – Self-desiccation with c = 400 kg/m³(; s = 40 kg/m³) and w = 175 kg/m³.

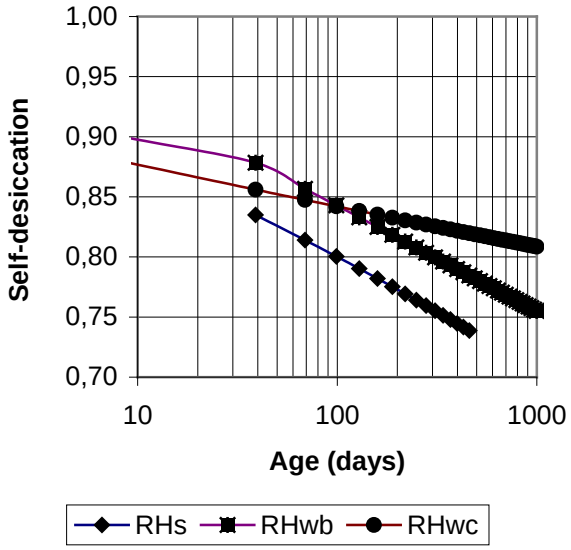

Figure 2.8 – Self-desiccation with c = 450 kg/m³(; s = 45 kg/m³) and w = 150 kg/m³.

3. MATERIALS, MANUFACTURE AND METHODS

3.1 Material

Crushed gneiss (E-modulus 61 GPa and strength 230 MPa), natural sand, limestone filler Köping 500 or Ignaberga 200 and Degerhamn cement were used in the mix compositions, Appendices 1 and 3.1. Melamine-based superplasticiser was used for NC (branch Flyt 97M), polycarboxyl ether for SCC (branch Glenium 51) and air-entertainment agent based on fir oil and fatty acids (branch Microair).

3.2 Manufacture of specimen

Manufacturing and curing of the large specimen of concrete (until the test specimen were core drilled) were performed in the following way:

1. New mixing order (N) with material except for filler mixed for ½ min. with water and air-entertainment.
2. Then half the amount of superplasticiser mixed for ½ min [25].
3. Finally the remaining superplasticiser with filler mixed for 2 min. [25].
4. Ordinary mixing order (O) with all dry material at the start mixed for ½ min. with water and air-entertainment.
5. Then all the material with the superplasticiser mixed for 2½ min.
6. Casting of large specimen in steel mould with 0.23 m in diameter and 0.3 m or 6 m in height filled with concrete.
7. NC vibrated 10 + 10 + 10 s (SCC was not vibrated).
8. Sealed curing at 20 °C until the specimens were core-drilled from the large specimen.

From the pour the following specimens were cored at 28 and 90 days' age:

1. For determination of the chloride migration coefficient, D: 3 discs 100 mm in diameter and 50 mm in height [4].
2. When testing the effect of hydrostatic pressure the specimen was cored 0.5 m from the bottom of the 6 m long specimen
3. Between drilling and testing the cylinders were stored in water saturated by limestone powder.
4. Sealed curing or air curing at an ambient relative humidity, RH = 60% until testing of strength, creep and shrinkage.

Specimen for mechanical tests were done in the following way:

1. Ordinary mixing order (O) with dry material at the start mixed for ½ min. with water and air-entertainment.
2. Then all the material with the superplasticiser mixed for 2½ min.
3. Casting of cubes 100 mm in steel mould with concrete.
4. NC vibrated 10 + 10 + 10 s (SCC was not vibrated)

3.3 Methods

Between drilling and rapid testing the specimens were stored in water saturated with limestone powder. The determination of the chloride migration coefficient, *D*, was performed in an apparatus developed by Tang, Appendix 3.2 [4]. After sawing, brushing and washing away any burrs from the surface of the specimen, excess of water was wiped off the surface of the

specimen. When the specimens were surface-dry, they were placed in a vacuum container to a pressure in the range of 1-5 kPa within a few minutes, Figure 3.1 [4]. The vacuum was maintained for 3 h, and then, with the vacuum pump still running, the container was filled with water saturated with $Ca(OH)_2$ in order to immerse the specimen. The vacuum was maintained another h before air was allowed to enter the container. The specimen was then kept in the solution for 18 h. The catholyte solution was 10% NaCl (100 g NaCl in 900 g water, about 2 N) and the anolyte solution 0.3M NaOH in distilled water (about 12 g NaOH in 1 l water). The testing procedure was performed in the following way:

1. The catholyte solution, 10% NaCl was filled in the 12-l container, Figure 3.2.
2. A rubber sleeve was assembled to the specimen, Appendix 3.2.
3. The specimen were placed on the plastic support in the catholyte reservoir (10% NaCl).
4. The sleeve was filled with 300 ml anolyte (0.3 M NaOH), Figure 3.3.
5. A anode was immersed into the anolyte solution, Appendix 3.2.
6. The cathode was linked to the negative pole and the anode to the positive of the power supply.
7. The initial current through the specimen was measured with a power supply at 30 V.
8. Voltage was adjusted [4]
9. The temperature in anolyte solution was recorded by thermocouple.
10. The test duration was chosen according to [4], normally 24 h.
11. The final current and temperature recorded before the test was terminated.

The chloride penetration depth was determined in the following way:

1. The specimen was disassemble in the opposite way of assembling, Figure 3.3
2. The specimen was split into two pieces, Figure 3.4
3. Point-one M silver nitrate solution was sprayed to the freshly split specimen, Figure 3.5-6
4. When the white silver chloride precipitation was clearly visible on the surface of the specimen it was measured with an accuracy of 0.1 mm from the centre to both edges at intervals of 10 mm to obtain seven depths, Figure 3.6.

Figure 3.1 - The surface-dry specimens were placed in a vacuum container to a pressure in the range of 1-5 kPa within a few minutes.

Figure 3.2 - The catholyte solution, 10% NaCl filled in the 12-l container.

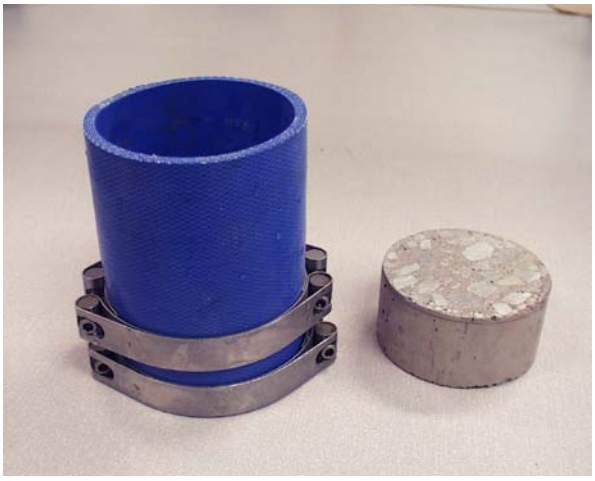

Figure 3.3 - Specimen with rubber sleeve [4].

Figure 3.4 - The split specimen [4].

Figure 3.5 - Point-one M silver nitrate solution sprayed to the specimen [4].

Figure 3.6 – Test specimen after preparation for chloride penetration measurement [4].

4. RESULTS

4.1 Mechanical properties

The choice of mix composition may be linked to the derived strength and is influenced by the grading curve of all solid particles in the fresh mix composition (silica fume, cement filler, sand, gravel and stone fraction). Figure 4.1 shows the grading curve of the mix composition in the present tests, Appendix 3.1. The strength development of the tests is shown in Figure 4.2. The following points were found for the influence of particle grading on the strength and for the grading of the particles:

1. Gap grading was not feasible.
2. Filler had a large effect on strength
3. The particle distribution could be improved by a fitting of the type and amount of filler.

$p_m = 0.102 \cdot ln(d) + 0.583$ $\{R^2 = 0,96\}$ (4.1)

ln(d) denotes natural logarithm of sieve dimension (*0.002<d<10* mm)
p_m denotes the material passing through (by weight)

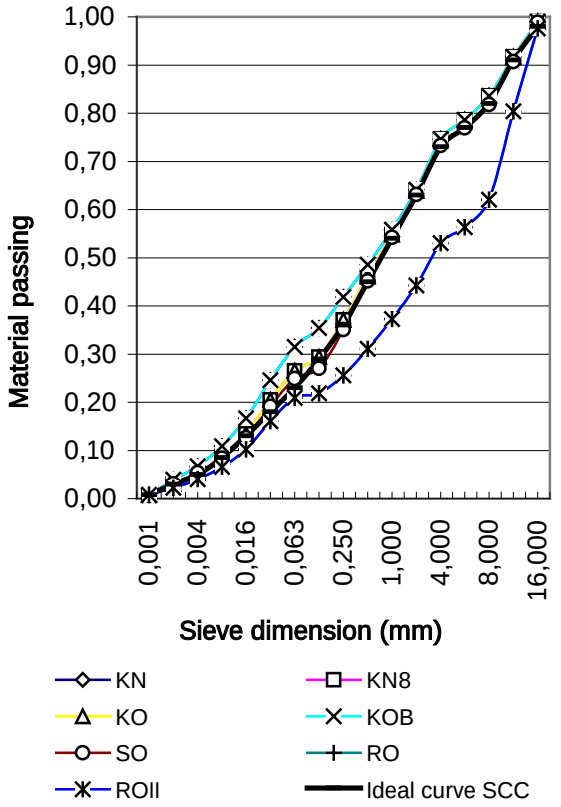

Figure 4.1 –Grading curves of all solid particles in the fresh mix. Notations: B = increased amount of filler; K = Köping 500 limestone filler; N = new way of mixing (filler last); O = ordinary way of mixing.

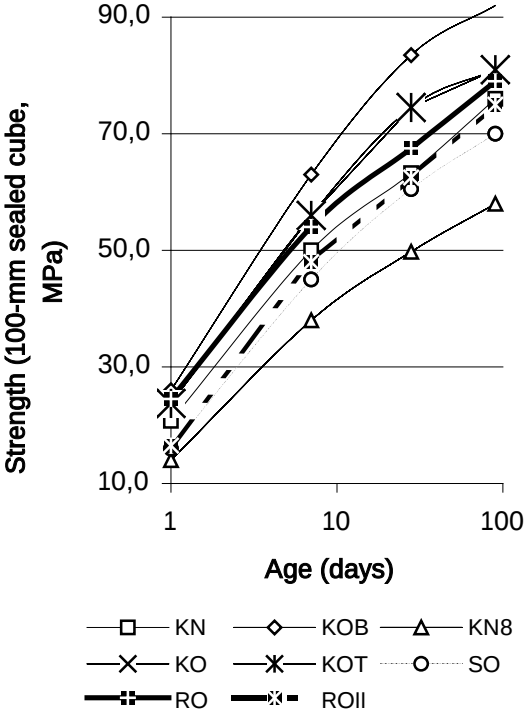

Figure 4.2 - Strength development of concrete in the tests. R = reference; S = Ignaberga 200 limestone filler; T = 5.5 m hydrostatic pouring pressure instead of 0.5 m; II = second reference.

Besides it was found that the following empirical relationships existed between strength and filler content taking into account also the type of filler and the effect of air-entrainment:

$f_{cc} = k_N \cdot k_S \cdot k_8 \cdot [(14.6 \cdot p + 12.3) \cdot \ln(t) + 51 \cdot p + 23]$ {$R^2 = 0.70$}
(4.2)

f_{cc} denotes compressive strength (100-mm cube, MPa)
k_N = *0.89* applies for new order of mixing (filler at last); k_N = *1* otherwise
k_S = *0.82* applies for Ignaberga 200 limestone filler in these tests; k_S = *1* otherwise
k_8 = 0.74 applies for 8% air content; k_8 = *1* for 6% air content.
ln(t) denotes the natural logarithm of concrete age (*1* < *t* < *100* days)
p denotes content of limestone powder (*0.03* < *p* < *0.15* by vol.)

Figure 4.3 shows the strength estimated with equation (4.2) versus the measured one. The agreement was good between strength estimated with equation (4.2) and the measured one.

4.2 Chloride migration coefficient, D

The following equation was used to calculate the chloride migration coefficient, D [4]:

$D = 0.0239 \cdot (273+T) \cdot L \cdot / [(U-2) \cdot t] \cdot \{x_d - 0.0238 \cdot [(273+T) \cdot L \cdot x_d)/(U-2)]^{½}\}$
(4.3)

t denotes the test duration (h)
x_d denotes the average chloride penetration depth (mm)
D denotes the non-steady-state migration coefficient, x10 $^{-12}$ m²/s
L denotes the thickness of the specimen (mm)
T denotes the average initial and final temperatures in the anolyte solution (°C)

Significant differences were obtained between the chloride migration coefficient, *D*, of SCC and that of NC, Figure 4.4 and Appendix 4. As an average was a 60% increase of the chloride migration coefficient, *D*, observed in SCC compared with that of NC. The reasons for the enlargement of the chloride migration coefficient, *D*, in SCC compared with *D* in NC are not clarified. The effect of filler on strength makes it possible to use less cement in SCC than in NC. On the other hand less cement in concrete lowers the porosity, which works in the other direction. More cement in the concrete increased the ability of the concrete to bind chlorides [6]. Figure 4.5 shows that less cement content in SCC than in NC increased *D*. The studies described here and also those described in Chapters 2.1-2 for concrete without mineral additives were used to obtain the following empirical equations for *D*, Figures 4.6-8 [5,10]:

$$D=\{[(0.0055\cdot ln(t)-0.2122)\cdot c-3.5\cdot ln(t)+104]\cdot(4\cdot w/b-1.2)/0.4\}\cdot(10^{-12}) \quad \{R^2=0.88\} \quad (4.4)$$

c denotes the cement content ($375 < c < 450$ kg/m³)
D denotes the chloride migration coefficient (x10^{-12} m^2/s)
$ln(t)$ denotes the natural logarithm of concrete age ($1 < t < 36$ months)
w/b denotes the water-binder ratio, 1:1 ($0.35 < w/b < 0.50$)

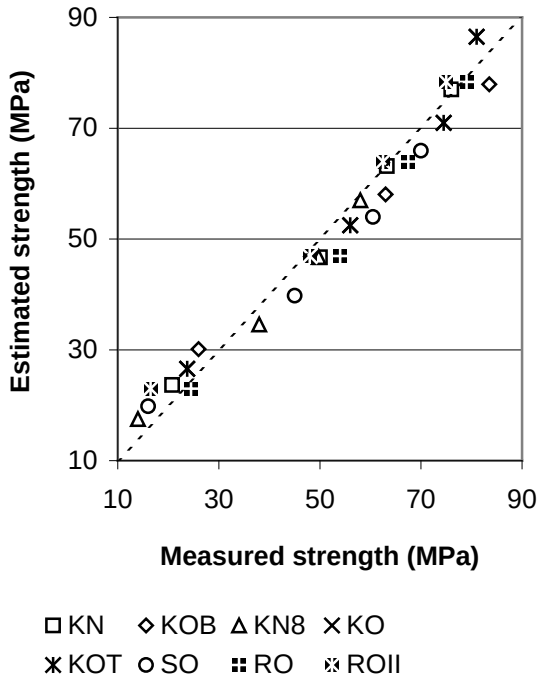

Figure 4.3 – Strength estimated by equation (4.2) vs measured strength. Notations: B = increased amount of filler; K = Köping 500 limestone filler; N = new way of mixing (filler at last); O = ordinary way of mixing.

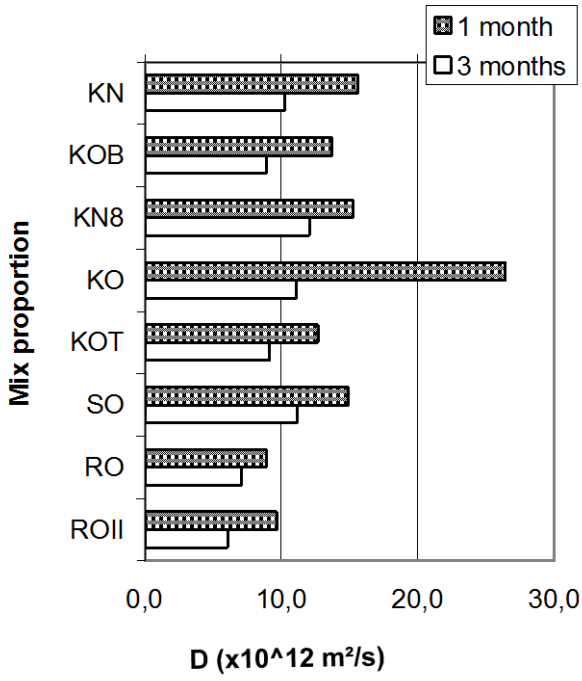

Figure 4.4 – Chloride migration coefficient, D, for concrete in series 3, Appendix 4. . Notations (cont.): R = reference; S = Ignaberga 200 limestone filler; T = 5.5 m hydrostatic pouring pressure instead of 0.23 m; II = second.

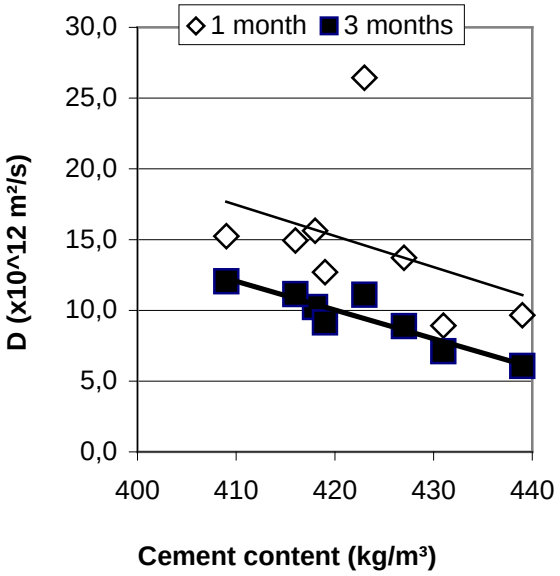

Figure 4.5 – The chloride migration coefficient, D, versus cement content, Appendix 4. Starting age is given.

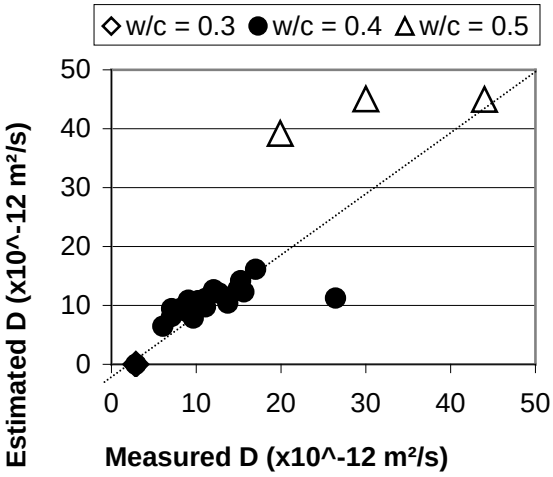

Figure 4.6 – Comparison with values of the chloride migration coefficient, D, estimated with equation (4.5) and measured values of the chloride migration coefficient, D [5,10].

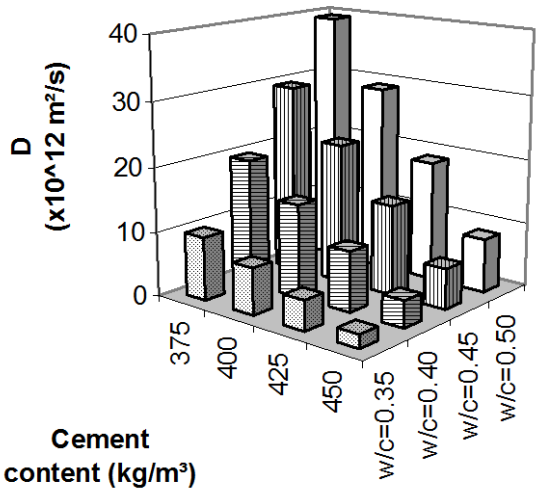

Figure 4.7 – Values of the chloride migration coefficient, D, at 3 months' age estimated with equation (4.5) at different cement content and w/c.

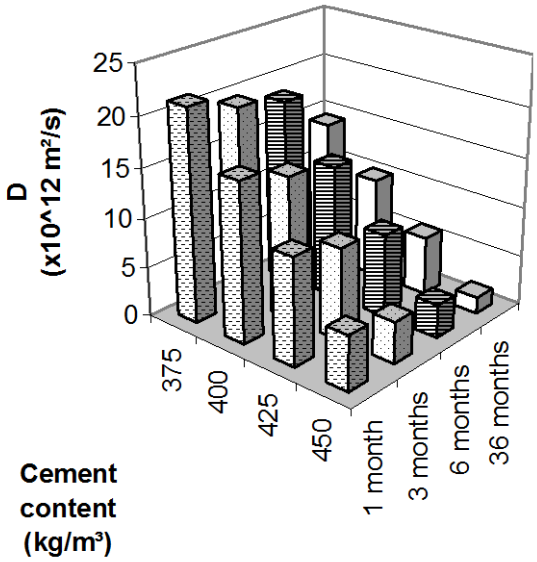

Figure 4.8 - Values of the chloride migration coefficient, D, at w/c = 0,4 estimated with equation (4.5)

5. DISCUSSION

5.1 Effect of method of compaction and method of mixing

The coefficient of variation between the repeated tests of chloride migration coefficient, *D* (standard deviation to average the chloride migration coefficient, *D*, ratio) was calculated in order

of the estimated accuracy. On average the tests of SCC showed smaller coefficient of variation than in the tests of NCs did, probably due to the fact that vibration was avoided in SCCs. The transition zone remained unaffected in SCC but was affected in NC due to different movements of cement paste and aggregate in NC in turn due to vibrations. *D,* of SCC with limestone powder was larger than that of NC with large significance. The effect of mixing order and type of concrete on the chloride migration coefficient, *D,* for concretes in series 3 was calculated. It was shown that the mixing order did not affect the chloride migration coefficient, *D,* and that the chloride migration coefficient, *D,* was about 60% lower for NC than for SCC with limestone powder.

5.2 Effect of age and aggregate content

The effect of age at testing and way of compaction on the chloride migration coefficient, *D,* for concretes in series 3 was calculated. Again it was shown that the chloride migration coefficient, *D,* was 60% lower for NC than for SCC with limestone filler, independent of age at testing. On average the chloride migration coefficient, *D,* was 60% lower at 90 days' age at testing than at 28 days' age at testing. Figure 5.1 shows that the chloride migration coefficient, *D,* was lower at higher aggregate content, which seems logical. It is not possible for chloride to pass aggregate.

5.3 Effect of filler and cementitious materials

Figure 5.2 shows that the chloride migration coefficient, *D,* decreased in concrete at higher cement-powder ratio, *c/p,* i.e. concrete with pure cement binder (*c/p* = 1) had a lower *D* than concrete with limestone powder had. Probably concrete with pure cement without limestone filler binds more chloride than concrete based on cement with limestone powder does.

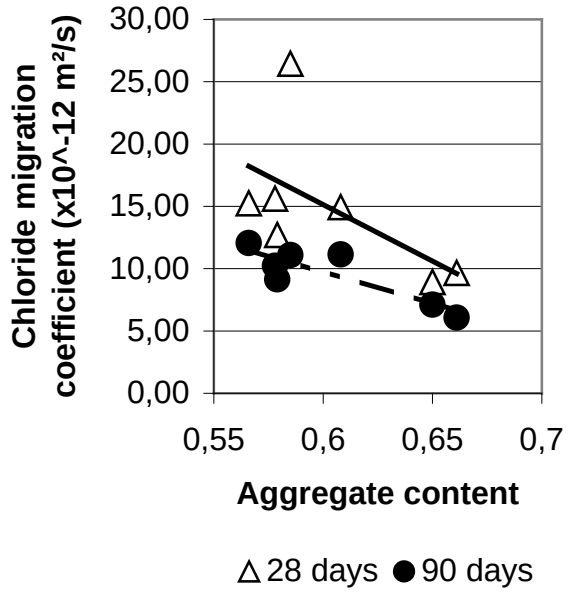

Figure 5.1 - Chloride migration coefficient, D, versus aggregate content. Testing age.

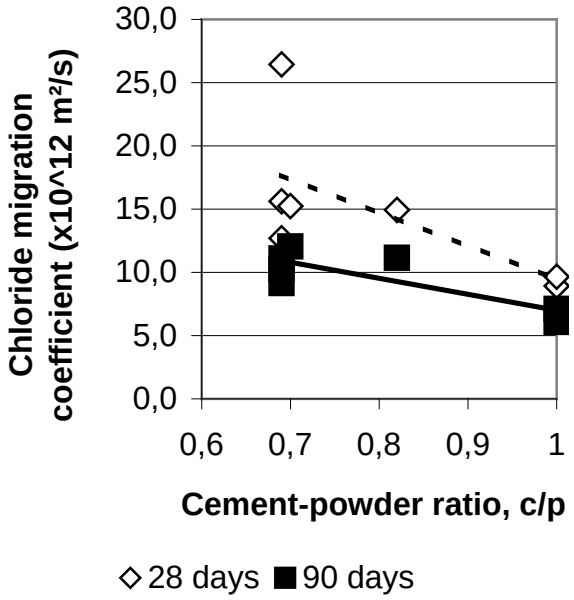

Figure 5.2 - D decreased in concrete at higher cement-powder ratio, c/p.

From the results and from the references [5,10] it was obvious that Pozzolan like silica fume and slag had an effect on the value of the chloride migration coefficient, *D*. From the results obtained by Tang and Nilsson [5] and further by Boubitsas and Paulou [10] it was possible to estimate the effect of Pozzolan on the chloride migration coefficient, *D,* assuming that the concrete performed in accordance with equation (4.5) above. The effect of 1 kg of the different additives was

adjusted to the effect of 1 kg cement content on the chloride migration coefficient, *D*, in equation (4.5) for the measured results to coincide with the estimations. The ratio of the effect of 1 kg of the additive to 1 kg of cement on the chloride migration coefficient, *D*, is here called the efficiency factor. The recalculation of the amount of cement into an equivalent amount achieved this. From previous research it was known that silica fume had a substantial effect on strength, self-desiccation and hydration [17]. For strength large efficiency factors were obtained at early ages but declining to less than 0 after about 90 months [24-27]. For hydration the opposite results were found. The present results were only obtained at 1 and 6 months' age, i.e. the efficiency factor (effect of 1 kg additive to the effect of 1 kg cement on the chloride migration coefficient, *D*) may very well be time dependent. The following equation was obtained for the Pozzolan interaction between Portland cement, silica fume, fly ash and slag as regards the chloride migration coefficient, D [4,5,10,28]:

$$c_{eq.} = c + 0{,}21 \cdot fl + 1{,}6 \cdot sf + 1{,}03 \cdot sl \qquad \{R^2 = 0{,}81\} \qquad (5.1)$$

$c_{eq.}$ denotes the equivalent amount of cement to be used in equation (4.5)
c denotes amount of Portland cement
fl denotes the amount of fly ash
sf denotes the amount of silica fume
sl denotes the amount of slag

5.4 Effect of porosity and self-desiccation

Porosity was calculated in order to detect its effect on the chloride migration coefficient, *D* [29]. Figure 5.3 shows little influence of the calculated porosity on the chloride migration coefficient, *D*. Even though the calculated porosity was somewhat larger for NC than for NC, the chloride migration coefficient, *D*, of NC was smaller probably due to the chloride binding ability of the cement gel [6].

As shown above chlorides cannot be transported in the air or in voids of vacuum that were obtained due to self-desiccation. However, it is not feasible to measured *RH* in concrete during chloride transport since water is required for this transport to take place. Therefore the chloride migration coefficient, *D*, from these tests and from other tests [5,10] were related to RH with self-desiccation, equation (2.4). Factors of the efficiency factor (effect of 1 kg additive to the effect of 1 kg cement on the chloride migration coefficient, *D*, shown in equation (5.1) were used in order to estimate *RH*. The dependence of the cement content on the chloride migration coefficient, *D*, was dominating besides the effect of *RH*, Figure 5.4. The following formula was calculated in order to describe the effect of self-desiccation on the chloride migration coefficient, *D*, taking into account the cement content ($x10^{12}$ m²/s):

$$D = 3000 \cdot e^{-0{,}0118 \cdot c} \cdot (RH)^{0{,}04 \cdot c - 9{,}1} \qquad (5.2)$$

c denotes cement content (kg/m³)
RH denotes the internal relative humidity with self-desiccation, equation (2.4)

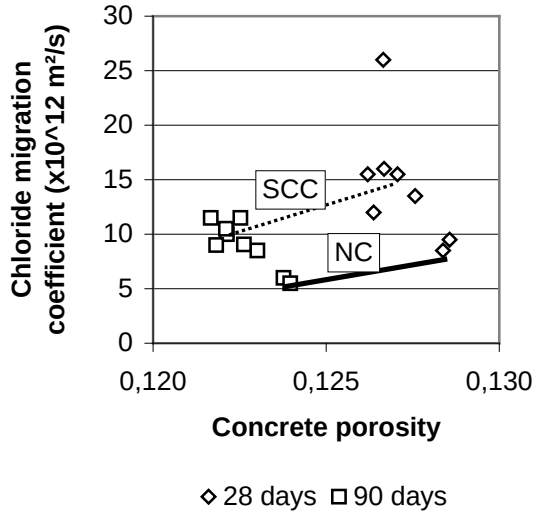

Figure 5.3 – Chloride migration coefficient versus calculated porosity.

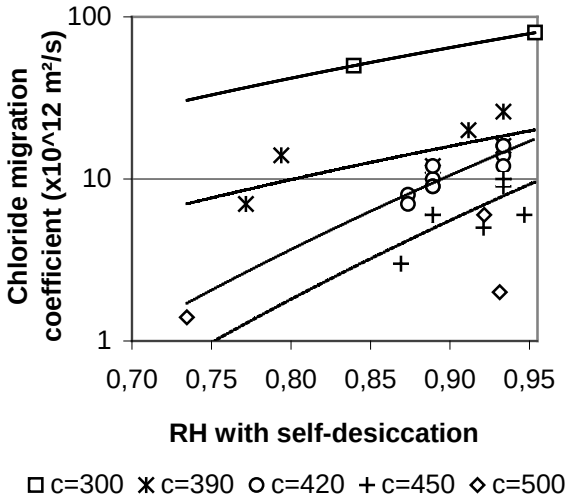

Figure 5.4 –chloride migration coefficient, D, measured acc. to [5,10] and self-desiccation calculated acc. to equation (2.4).

5. CONCLUSIONS

The following conclusion were drawn [30]:

1. The chloride migration coefficient, D, was 60% larger in limestone filler SCC than in NC.
2. D of SCC with 5% silica fume and 12% fly ash was 60% of that in NC.
3. At 90 days" age of testing D was about 60% of that at 28 days" age of testing
4. The efficiency factor of silica fume compared to Portland cement for D seems to be 1.6.
5. The efficiency factor of blast furnace slag compared to cement for D seems to be 1.
6. The efficiency factor of fly ash compared to Portland cement for D seems to be 0.2.
7. Self-desiccation played a roll as to explain the low value of D in concrete with low w/c.

ACKNOWLEDGEMENT

Financial support from the Development Fund of the Swedish Construction Industry is acknowledged. Thanks are also due to Professor Göran Fagerlund for his critical reviews.

REFERENCES

1. Nilsson, M., Petersson, Ö., "The First Bridge made of SCC." *Väg- och Vattenbyggaren* 2/98, 1998, pp. 28-31.
2. Söderlind, L., "Full-scale Tests of SCC for Dwelling Houses." RILEM symposium on Self Compacting Concrete. Stockholm. Ed.: Skarendahl and Petersson, 1999, pp. 723-728.
3. Persson, B., "Mix Proportions and Strength of SCC for Production of High Strength Poles, Piles and Pillars." Contribution to 1. Münchener Baustoffseminar Selbstverdichtender Beton 9 Oktober 2001. Ed.: Peter Schiessl, 2001, pp. 31-39
4. CTH Rapid Test for Determination of the Chloride Migration Coefficient, *D*, in Concrete. NT BUILD 492, 2000.
5. Tang, L., Nilsson, L.-O. "Modelling of chloride penetration into concrete – Tracing five years" field exposure." *Concrete Science Engineering*. Vol. 2, 2000, pp. 170-175.

6. Johannesson, B., “Transport and Sorption Phenomena in Concrete and Other Porous Media.” TVBM-1019. LTH Byggnadsmaterial. Lund, 2000, 491 pp.
7. AASHTO T 271-831. Rapid Determination of Chloride Permeability of Concrete.
8. Geiker, M., Thaulow, N., Andersen, P. J., “Assessment of Rapid Test of Concrete Permeability Test of Concrete with and without Mineral Admixtures”. Durability of Concrete and Components. Brighton. Chapman & Hall ,1990, pp. 52-61.
9. Persson, B., “A Background for the Choice of Mix Design of the Concrete for the Great Belt Link.” Report U91.02 Div. Building Materials, 1991, 102 pp.
10. Boubitsas, D., Paulou, K., “Self Compacting Concrete for Marine Environment.” TVBM-5048. Lund Institute of Technology. Lund University. Lund, 2000, 55 pp.
11. Buenfeld, N. Personal information. Imperial College. London, 2001.
12. Persson, B., “Moisture in Concrete Subjected to Different Kinds of Curing.” *Materials and Structures* 30, 1997, pp. 533-544.
13. Persson, B., “Self-desiccation and Its Importance in Concrete Technology.” *Nordic Concrete Research*. Vol. 20, 1998, pp. 120-129.
14. Persson, B., “Shrinkage of High Performance Concrete.” *Proceedings of an International RILEM Conference on early Age Cracking in Concrete.* Haifa. 2001. Ed. by A Bentur, 2001, pp. 301-311.
15. Powers, T.G., Brownyard, T.L., “Studies of the Physical Properties of Hardened Portland Cement Paste.” PCA 22, 1948, 473-488, pp. 845-864.
16. Nilsson, L.-O., Hedenblad, G., Norling-Mjörnell, K., ”Suction after long time, Concrete Handbook,” HPC, Svensk Byggtjänst, Stockholm, 2000, pp. 209-226.
17. Persson, B., “Seven-year Study of the Effect of Silica Fume.” *ABCM* 7, 1998, pp. 139-155
18. Castel, R, Francois, G., Arliguie, A., “Clarification of Corrosion of Reinforcement in Concrete Structures Exposed to Chloride Environment.” Nordic Seminar. Gothenbourg, 2001, 10 pp.
19. Collepardi, M., et al. ”The Kinetics of Chloride Ions Penetration in Concrete.” *Il Cemento*. 67, 1970, pp. 157-164.
20. Tuutti, K., “Corrosion of Steel in Concrete.” Report 4:82. CBI. Stockholm, 1982.
21. Tang, L., Nilsson, L.-O., “Rapid Determination of Chloride Diffusivity of Concrete by Applying an Electric Field.” *ACI Material Journal* 49/1, 1992, pp. 49-53.
22. Maage, M., Helland, S., Carlsen, J. E., “Chloride Penetration in HPC Exposed to Marine Environment.” RILEM Workshop on Durability. Ed.: H. Sommer, 1994, pp. 194-207.
23. Poulsen, E., “Prediction Models.” STAR 53. Danish Road Direct. Ed. L.-O. Nilsson, 1996.
24. Persson, B., “Long-term Shrinkage of High Performance Concrete.” *10th Congress on the Chemistry of Cement*. 2ii073. Gothenburg, 1997, Ed.: Justnes, H., 9 pp.
25. Ö. Pettersson., “Dispersion and Frost Resistance”. Investigation of Four Types of Limestone Filler for SCC. 2000-27, Cement and Concrete Research Institute. Stockholm, 2000, 14 pp.
26. Persson, B., “Long-term Effect of Silica Fume on the Principal Properties of Low-Temperature-Cured Ceramic.” Cement and Concrete Research 27, 1997, pp. 1667-1680
27. Persson, B., “Pozzolanic Interaction between Portland Cement and Silica Fume in Concrete.” *Sixth CANMET/ACI Int. Conference*. Bangkok. 1998, 631-660.
28. Persson, B., “Chloride Diffusion Coefficient and Salt Frost Scaling of Self-Compacting Concrete and of Normal Concrete.” Nordic Seminar. Gothenburg. Ed. by Nilsson, L.-O., 2001, 13 pp.
29. Neville, A.M., Brooks, J. J., Concrete Technology. Longman Singapore Publ. 1987, 101.

30. Persson, B. “Assessments of the Chloride Migration Coefficient, Internal Frost Resistance, Salt Frost Scaling and Sulphate Resistance of SCC.” TVBM-3100. Lund University. 2001, 86 pp.
31. Berglund, T., “Factors for Recalculation of Compressive Strength of High-Performance Concrete.” Report TVBM-5023. Lund University. 1992, 48 pp.

Appendix 1 - Chemical composition and physical properties of cements (%).

Components	Slite Std, N	Degerhamn, SL
CaO	62	65
SiO_2	20	21.6
Al_2O_3	4.4	3.5
Fe_2O_3	2.3	4.4
K_2O	1.4	0.58
Na_2O	0.2	0.05
MgO	3.5	0.78
SO_3	3.7	2.07
Ignition losses	2.4	0.47
CO_2	1.9	0.14
Clinker minerals: C_2S	14	21
C_3S	57	57
C_3A	8	1.7
C_4AF	7	13
Water demand	28%	25%
Initial setting time	154 min.	145 min.
Density	3122 kg/m^3	3214 kg/m^3
Specific surface	364 m^2/kg	305 m^2/kg

N = cement CEM I 52.5 R; SL = slowly hardening cement, CEM I 42,5 BV/SR/LA

Appendix 2.1 –Mix composition (kg/m³); strength of concrete (series 1, MPa).

Mix	Cement, c	Type	Silica fume	w/(c+s)	w/(c+2s)	Sand filler	Air (%)	Strength
SCC27	500	SL	50	0.24	0.22	50	1.3	141
NC32	389	N		0.32	0.32	106	12	55
SCC38	400	N		0.38	0.38	145	1.4	86
SCC50	340	N		0.50	0.50	165	3.5	61
SCC80	260	N		0.80	0.80	185	1.9	27

Notations: s = silica fume; N = cement CEM I 52.5 R; NC = normal compacting concrete; SCC = self-compacting concrete; SL = slowly hardening cement, CEM I 42,5 BV/SR/LA

Appendix 2.2 – Chloride migration coefficient, *D*, for normal (NC) and self-compacting (SCC) concrete series 1 (x10^{12} m^2/s)

Concrete	Specimen 1						Specimen 2						Specimen 3						Average
Measured value	U	T	L	x_d	t	D	U	T	L	x_d	t	D	U	T	L	x_d	t	D	$D_{avrerage.}$
SCC27	60	21.8	50	21.6	96	1.26	60	21.8	50	12	96	0.68	60	21.8	50	29.6	96	1.74	1.22
NC32	50	23.3	50	10.6	24	2.84	50	23.3	50	11.3	24	3.04	50	23.3	50	10.3	24	2.75	2.88
SCC38	30	21.6	50	20.2	24	9.30	30	21.6	50	20.6	24	9.49	30	21.6	50	18.44	24	8.43	9.07
SCC50	20	21.7	50	40.9	24	29.79	20	21.7	50	40.5	24	29.48	20	21.7	50	42.25	24	30.83	30.04
SCC80	15	22.1	50	50	24	50.11	15	22.1	50	50	24	50.11	15	22.1	50	50	24	50.11	50.11

Notations [4]: t denotes the test duration (h)
x_d denotes the average chloride penetration depth (mm)
D denotes the non-steady-state migration coefficient, x10^{-12} m^2/s
L denotes the thickness of the specimen (mm)
T denotes the average initial and final temperatures in the anolyte solution (°C)

.

Appendix 2.3 - Mix composition and chloride migration coefficient, *D*, of NCs [5].

Material/mix- *w/b* (%)	1-40	1-50	H40	2-40
Cement Degerhamn. CEM I 42.5 BV/SR/LA	420	370	399	420 (Slite Std)
Silica fume			21	
Water	168	185	168	168
w/(c+s)	0.40	0.50	0.40	0.40
w/(c+2·s)	0.40	0.50	0.38	0.40
Air content (% vol.)	6	6.4	5.9	6.2
Aggregate	1692	1684	1685	1675
D (10^{-12} m^2/s)	8.1	19.9	2.7	7.1

Appendix 2.4 - Mix composition NC mixes tested for use at Great Belt Link [8].

Material/mix	A	B	C	D	E	F	G	H	I	J
SRPC (sulphate resistant)	310	405	370	345	370	345				
RPC (rapid cement)							310	405	370	345
PFA (fly ash)	70		70		70		70		70	
SF (silica fume)	30			30		30	30			30
w/(c+0.4·FA+2·s)	0.34	0.33	0.32	0.33	0.31	0.32	0.36	0.34	0.33	0.35
Current pass. (coulomb)	220	1730	1050	150	1150	190	150	1150	1030	250

Appendix 2.5 - Mix composition and chloride migration coefficient of SCCs series 2 [10].

Material/mix composition	D	F	G	RO II	T
Crushed aggregate Bålsta 8-16	496	494	580	876	495
Natural sand Bålsta 0-8	699	728	800	727	714
Natural sand SÄRÖ 0-2	505	465	220	149	521
Fly ash	89	55			
Glas filler			60		
Cement Aalborg (CEM I 42.5 SR)	375				
Cement Degerhamn (CEM I 42.5 BV/SR/LA)		440	420	438	
Slag cement (CEM III/B, 68% slag)					470
Silica fume Elkem (granulate)	35	18	21		
Air-entrainment (wet, g, 10% dry)	0.498	0.501	0.500	482	0.498
Superplasticiser (wet, 35% dry)	5.25		4.24	5.92	3.52
Water	191	172	162	171	183
w/(c+0.4·FA+2·s+0.6·slag)	0.40	0.35	0.35	0.39	0.53
Slump (flow) (mm)	690	725	720	150	737
Flow time until diameter 500 mm (s)	7	8	8		6.5
Density	2247	2300	2306	2368	2281
Aggregate content (>0.125, % vol.)	0.64	0.64	0.60	0.66	0.65
Air content (%)	6.4	6.2	6.3	6.1	5.7
28-day cube strength (100 mm, MPa)	61	70	64	63	79
28-day 150-mm cylinder strength (MPa) [31]	56	64	59	58	72
D (x10^{12} m²/s)	5.8	5.5	4.6	9.6	1.9
Salt frost scaling 112 cycles (kg/m²)	0.461	0.174	0.182	0.387	0.509

D = Danish fly ash mix composition; F = optimum fly ash mix composition; G = glass filler mix composition; RO II = reference mix composition; T = German slag mix composition.

Appendix 3.1. Mix composition and properties of NC and SCC in series 3.

Material/mix composition	KN	KOB	KN8	KO	KOT	SO	RO	ROII
Crushed aggregate Bålsta 8-16	363	371	355	367	363	402	862	876
Natural sand Bålsta 0-8	853	872	836	864	855	786	715	727
Natural sand SÄRÖ 0-2	316	135	309	320	316	422	146	149
Limestone filler Köping 500	183	375	180	186	184	94	0	
Cement Degerhamn (CEM I 42,5 BV/SR/LA)	418	427	409	423	419	416	431	438
Microair (wet, g, 10% dry)	585	213	1203	106	117	125	474	482
Superplasticiser(wet, 35% dry)	2,97	4,13	3,2	3,39	3,69	2,99	7,32	5,92
Water	163	167	160	165	163	162	168	171
w/c	0,39	0,39	0,39	0,39	0,39	0,39	0,39	0,39
Air content (%)	5,6	4,9	8	5,5	6,3	5,6	5,8	6,1
28-day 100-mm cube strength (MPa)	63	84	50	75	75	61	68	63
28-day 150-mm cyilnder strength (MPa)	58	76	46	68	62	56	62	58
Slump flow (mm)	720	780	735	620	640	710	110	150
Flow time until 500 mm (s)	5	7	8	10	8	5	-	-
Density	2297	2348	2250	2323	2300	2285	2325	2368
Aggregate with filler (% vol.)	0,643	0,654	0,630	0,652	0,645	0,641	0,650	0,661

Notations: B = increased amount of filler; K = Köping 500 limestone filler; N = new way of mixing (filler at last); O = ordinary way of mixing (filler first); R = reference; S = Ignaberga 200 limestone filler; T = 5.5 m hydrostatic pouring pressure instead of 0.23 m; II = second; 8 = 8 % air content.

Appendix 3.2 - The determination of the chloride migration coefficient, *D*, in an apparatus developed by Tang [4].

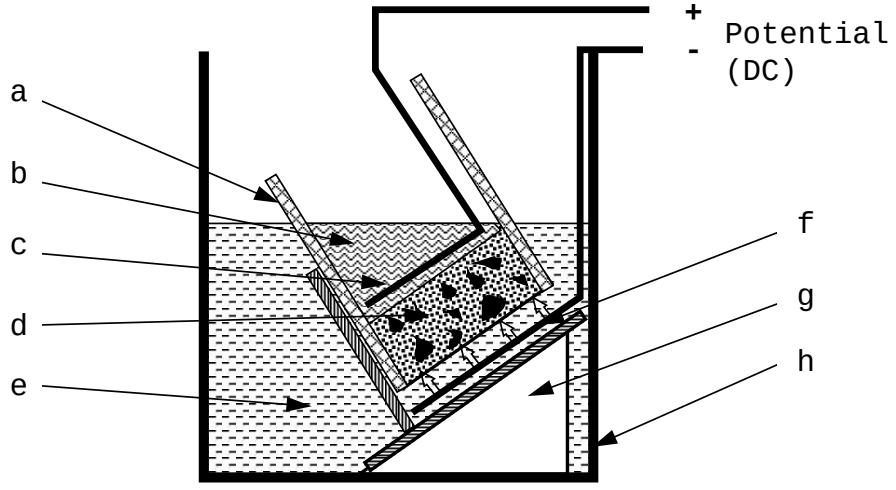

a. Rubber sleeve
b. Anolyte
c. Anode
d. Specimen
e. Catholyte
f. Cathode
g. Plastic support
h. Plastic box

Appendix 4 – Chloride migration coefficient, *D*, for concretes in series 3 (x10 ^{12} m2/s)

Mix proportion	Sample 1						Sample 2						Sample 3						Average
Value	U	T	L	x_d	t	D	U	T	L	x_d	t	D	U	T	L	x_d	t	D	$D_{av.}$
KN 28	25	22,15	50	25,6	24	14,41	25	22,2	50,0	29	24	16,46	25	22,15	50	28,25	24	16,00	15,62
KN 90	30	22,2	50	20,1	24	9,27	30	22,2	50,0	24,1	24	11,24	30	22,2	50	22	24	10,20	10,24
KOB 28	25	21,5	50	24,14	24	13,50	25	21,5	50,0	24,86	24	13,94	25	21,5	50	23,57	24	13,16	13,72
KOB 90	30	21,7	50	20	24	9,20	30	21,8	50,0	18,7	24	8,6	30	21,7	50	19,3	24	8,86	8,88
KN8 28	25	22,3	50	25,1	24	14,11	25	22,3	50,0	26,9	24	15,20	25	22,3	50	28,9	24	16,40	15,24
KN8 90	30	22,7	49	27,9	24	12,90	25	22,7	49,0	20,3	24	11,05	25	22,7	49	22,3	24	12,22	11,98
KO 28	20	23	51	31,9	24	23,39	20	23,0	51,0	32,3	24	23,70							23,55
KO 90	25	21,75	50	19,9	24	10,98	25	21,8	50,0	20,3	24	11,22							11,10
KOT 28	25	23,3	50	22	24	12,29	25	23,3	50,0	23,7	24	13,32	25	23,3	50	22,3	24	12,47	12,70
KOT 90	30	23,2	50	20,9	24	9,69	30	23,2	50,0	18,4	24	8,46	25	23,2	50	17	24	9,30	9,07
SO 28	25	21,8	50	27,2	25	14,74	25	21,8	50,0	26,3	25	14,22	25	21,8	50	29,1	25	15,84	14,48
SO 90	25	21	52,5	18,9	24	10,84	25	21,0	52,5	21	24	12,15	25	21	52,5	18,3	24	10,47	11,49
RO 28	30	21,5	50	20	24	9,20	30	21,5	50,0	18,9	24	8,66							8,93
RO 90	30	20,8	50	18,5	24	8,44	30	20,8	50,0	14	24	6,25	30	20,8	50	14,8	24	6,64	7,11
ROII 28	25	21,2	51	18,1	24	10,08	25	21,2	51,0	16,2	24	8,93	25	21,2	51	17,9	24	9,96	9,66
ROII 90	30	21,5	52	12,1	24	5,54	30	21,5	52,0	14,7	24	6,84	30	21,5	52	12,7	24	5,84	6,07

Notations: see above; 90 = 90 days" starting age.

Life-time prediction of high performance concrete with respect to durability (CONLIFE)

Susanne Palecki
Scientific co-worker
Institute of Building Physics and Material Science, University of Essen, Universitätsstr. 15, 45141 Essen, Germany
E-mail:susanne.palecki@uni-essen.de

Max J. Setzer
Prof. Dr., Head of Institute, Project Co-ordinator
Institute of Building Physics and Material Science, University of Essen, Universitätsstr. 15, 45141 Essen, Germany
E-mail:mj.setzer@uni-essen.de

ABSTRACT

In the last years the use of High-performance concrete (HPC) has grown rapidly, even without the necessary know-how about the long-term behaviour. With regard to the lacking of life-time data of HPC, in this European project a research program has been worked out, studying systematically the durability of different concrete design concepts, exposed to various climatic conditions in Europe. Due to the correlation between laboratory and field tests as well as the study of in-service structures, a widespread analysis of deterioration mechanisms is possible, which should finally help to develop physical and chemical failure models. In the end, the understanding of these mechanisms enables to predict the service-life of HPC constructions.

Key words: high-performance concrete, life cycle, frost resistance, EU-Project

Project Partners: Universität Weimar (DE)
Dyckerhoff Zement GmbH (DE)
Italcementi S.p.A (IT)
Norwegian Building Research Institute (NO)
Helsinki University of Technology (FIN)
Icelandic Building Research Institute (IS)
MC Bauchemie GmbH (DE)
Swedish National Research Institute (SE)
Technical Research Centre of Finland (FIN)

1. INTRODUCTION

Within the manufacturing of high-performance concrete (HPC) technical risks arise. In HPC industrial by-products and admixtures are combined with an ultra strength concrete. Such an expansion of the limits of a structural material like concrete makes life-time prediction rather impossible. In the past the investigations about HPC have been too much concentrated on increasing the strength and not enough on environmental aspects. For the concrete design of a new construction, it is essential to define the environmental conditions, which the structure will be exposed to. Then the optimised composition for a long life span can be selected.

The main output of this EU project - the development of deterioration models for life-time prediction of various types of HPC under practical conditions - requires the fundamental study of the involved materials. The physical and chemical analysis of the reactivity and workability of alternative binder and admixtures for HPC and sampled cores of the field will help to find out the different ways to design durable concrete structures **(Task 1&2).** The durability testing in the laboratory as well as in the field under different European climatic conditions will show the behaviour of various HPC specimens with industrial by-products and modern admixtures **(Task 3).** The result is the development of recommendations, which include rules for the production of durable and environmentally friendly HPC, the classification of design concepts to the exposure classes and following life-time evaluation **(Task 4).**

2. BACKGROUND & OBJECTIVES

2.1 Background of the project

Each material has a fixed life span because they are exposed to chemical, physical or mechanical changes, which reduce their performance criteria. The life-time of a material can be divided into three term's durability, performance over time and service life. All these terms express a human perception of the quality of a material in the environment. Performance over time is a function of the specific properties and their variation over the time. With this function the prediction of the service-life can be solved /5/.
Basically, service-life data can be received from both experiences of former application as well as testing. Up to now, data of actual service-lives of constructions are poorly documented. Service-life data of HPC constructions from all over Europe are very limited. Therefore, for a material like HPC data must be generated from testing and studies on former construction must be done soon.
To obtain life-time data, it is state-of-the-art to involve laboratory exposure, field exposure and the assessment of actual in-service performance. This way of testing includes the measurement of the rate at which specific changes of the properties of the material occur in dependence on the time.

The service-life of a construction depends on the climatic conditions, which include geographical location. The number of different exposure sites and the amount of possible combinations are quite large. On one hand, it is experimentally difficult to combine several degradation mechanisms. The fact is on the other hand that primary factors causing degradation mechanisms are usually few in number.

Under this scope, the project will identify these essential deterioration factors, in order to enable the projection to all degradation mechanisms, which would occur in service.

The committee consists of partners from the construction industry as well as from research institutes from totally seven European countries (including sub-contractors), which represents four different climatic regions. Most of the partners have already long-term experiences in the field of the analysis of concrete deterioration mechanisms and are also members of the RILEM TC IDC 176 "*Internal Damage of concrete due to frost attack*". Therefore, the work program has been designed in accordance with the work of this RILEM group.
The total budget of the CONLIFE project amounts to 2.000.000 €. The EU commission supports the project with 1.310.000 €.
The CONLIFE project has been clustered with another European project with the title "Design and function of novel polymeric admixtures for more durable high-performance concrete" (SUPERPLAST).

2.2. Objectives

The objective of this project is, as already mentioned, the development of degradation models of HPC exposed to various environmental conditions in order to predict the life-time of HPC constructions. Therefore, the project represents four different climatic regions, essential for basic deterioration mechanisms. Finally a classification of the mixtures under various exposure sites in the field can be done.

For the receipt of life-time data, field studies as well as the continuos analysis of in-service structures have a great impact on the final result. The primary problem of field exposure tests is the duration of testing, because it can take a long time until property changes as well as deterioration mechanisms can be detected. Hence, it is quite difficult as well to specify between the separate degradation mechanisms and to isolate the different effects. As written in the final report of the technical RILEM committee /4/, CIB W80/Rilem 71-PSL *"Prediction of service life of building materials and components"*: "If delays in the use of potentially satisfactory new materials or traditional materials in new environments are to be minimised, service-life must be predicted from short-term test data".

Therefore, this project involves accelerated test procedures, which have been proved by former European projects ("*Standard methods for testing the resistance of concrete to freezing and thawing*"(MAT 1-CT 94-0055), *"Probabilistic Performance Based Durability Design of Concrete Structures"*(BE95-1347)), and combines these investigations with practical studies on actual constructions and new test stands in the field.

3. PROGRESS & ACHIEVEMENTS

3.1. Task 1 - Development of a European Database and Outdoor studies

Within the first period of the project a database with information about former experiments will be developed. Herein all partners will fill in results from their experiences of former investigations. This means details about tested materials as well as test results. The database will be completed by including the results of this project at the end of its running time.

Secondly, all partners will select samples from real HPC structures from the field, which will be investigated within the framework of WP2, in order to understand the damage behaviour in practise.

3.2. Task 2 – Material Analysis

All involved materials will be analysed and tested within this stage of the project. This includes the determination of the chemical and physical properties of all incorporated constituents, in order to study the effects of additives and admixtures on the different parameters of the total system e.g. air void characteristic, workability, chemical reactivity, etc.
In the following table a short overview of the involved materials is given.

Table 1 - Overview of materials.

Materials		source
cement	CEM I 52.5 R	Aalborg, Denmark
	CEM I 42.5 R	Dyckerhoff, Germany
	CEM I 52.5 R	Italcementi, Italy
Aggregates – basalt, Rhine sand		Germany
Silica slurry		Norway
Superplasticizer & Air entraining agent		MC Bauchemie, Germany
Blast furnace slag		Dyckerhoff, Germany
Fly ash		Aalborg, Denmark

As can be seen from the table above, 3 different cements, which are typical for the appropriate region, will be used within the test program. In order to compare the different mixtures from the various regions, only one type of aggregates is involved. The consortium has decided to include basalt and Rhine sand from Germany, which have a high compressive strength and frost resistance. The superplasticizer is a polycarboxylate-ether product.

Beyond this, also compatibility tests of the different constituents in combination will be performed within this work package. The adjustment of superplasticizer dosage with regard to a defined slump will be done by trial mixtures. Furthermore, the flow ability of the various mixtures will be determined by rheological tests. At the end of this task, the boundary conditions of all mixtures will be defined.

3.3. Task 3 - Durability Testing

As the consortium represents several climatic regions, as listed below, the different exposure classes according to EN 206 can be simulated in practise, so that each HPC mixture will be exposed to relevant climatic conditions of Europe.

- Moderate climate (Germany)
- Mild and harsh climatic conditions (Northern Italy)
- Harsh and severe climate (Denmark, Norway, Sweden, Iceland)
- Extreme severe climate (Northern Norway, Finland)

Beyond this, also national differences between the separate materials have been taken into account, so that a wide range of constituents, typical for the appropriate region is incorporated in the project, which could be seen within table 1.

Within the mixture plan, the following variation of the composition will be implemented. Here, both mixtures at the borderline to normal strength concrete (w/c = 0,42) as well as high-performance concrete with very low w/c ratios will be tested.

- Variation of water/binder ratio (0,3 – 0,42)
- Addition of silica, fly ash and blast furnace slag in various concentrations
- Adjustment of superplasticizer dosage due to defined consistency
- Addition of air entrained agent

The overview of the mixtures with the German cement is exemplary presented in Table 2.

Table 2- Mix plan

			cement A - Germany																				
		variation of	basic mixtures	and w-c ratio		Blast furnace slag	w/c 0.3	Blast furnace slag	w/c 0.42	silica fume	w/c 0.3	silica fume	w/c 0.42	fly ash	w/c 0.3		fly ash	w/c 0.42		References	for basic mixtures	with airentrainment	No silica fume	
		Mixture	A1	A2	A3	A4	A5	A6	A7	A8	A9	A10	A11	A12	A13	A14	A15	A16	A17	A18x	A19x	A20x	A21	A22
variables	description of variables	material code	1	2	3	4	5	6	7	8	9	10	11	12	13	14	15	16	17	18	19	20	21	22
Cement	A	1000000																						
	B	2000000																						
	C	3000000																						
w/c ratio	0,3	0100000																						
	0,35	0200000																						
	0,42	0300000																						
Blast furnace slag	7% special bfs	0010000																						
	30% typical bfs	0030000																						
silica fume	3%	0001000																						
	7%	0002000																						
	10%	0003000																						
fly ash	10%	0000100																						
	20%	0000200																						
	40%	0000300																						
superplasticizer	A (1-3%)	0000010																						
air entrained agent	4,5-5,5% voids	0000001																						
		mixture code	1102010	1202010	1302000	1100010	1102010	1300010	1302010	1100010	1103010	1300010	1303010	1102110	1102210	1102310	1302110	1302210	1302310	1102011	1202011	1302011	1000010	1000000
		Testmixtures	x		x		x				x				x							x		

Within the work program it has been defined, that all produced concretes should have a compressive strength between 60 and 120 MPa.

The produced specimens will be exposed due to the following types of attack in accordance to EN 206:

- Frost attack with and without de-icing agent
- Sulphate attack
- Chloride attack
- Acid attack
- Sea water attack
- Cyclic temperature attack

An overview about the accelerated test methods, which will be used within the project is included in the following table. Due to the lack of a standardisation for sulphate attack, the exposure has not been included in the laboratory test plan.

Table 3 – Overview of lab normal and accelerated test methods /1,2,3,6,7/

Test	Standard	Notes / Exceptions
Freeze thaw	A. CIF/CDF Draft of RILEM Standard	Beams 150 x 110 x 70 mm; test to 112 cycles or to 60% of initial UPV
	B. Borås slab test, Draft of RILEM Standard	test to 112 cycles or to 60% of initial UPV
Chloride Attack	A. CTH (NT BUILD 492) B. Penetration Profile (NT BUILD 443) C. Penetration Depth (Colorimetric test)	
Acid Attack	Immersion test with low pH SP/Aalborg test plan	150 x 150 x 50 mm slab
Cyclic Temperature Attack	A. FIB weather simulation B. Modified ASTM C666	A. Tested wet B. Tested dry, at 70% RH
Gas Permeability	CemBureau Method, as found in Mat. & Str., 1989, V. 22, p. 250	
Shrinkage	A. ASTM C157 B. RILEM TC107-CSP Draft Recommendations	Both autogenous and drying
Compression Strength	EN 12390-2 and -3	7, 28 and 56 days

The changes in the concrete structure of specimens tested in the field, will be continuously documented and compared with the results of the laboratory tests. Certainly, climate parameters will be recorded too. An overview of structural investigations and studies is given next.

Investigations:

- Mercury porosimetry with Carlo Erba equipment
- N_2 adsorption
- EDX (X-Ray)
- SEM/ESEM
- XDR
- Analysis of thin sections (polarised microscope)
- Carbonation depth determination (CEN CR 12793)
- Visual analysis

Studies/ Analysis:

- Changes in the concrete microstructure, effects on microstructure
- Effects on mesostructure (transition aggregates – matrix, interface transition zone)
- Chloride/moisture transport coefficients
- Surface scaling → resistance
- Internal damage analysis → resistance
- Corrosion rates
- Chloride/moisture profiles
- Strength testing parameters
- Transport mechanisms and phenomena (water/ chemical agents)
- Study of the pore size distribution
  - Analysis of changes during attack

- Study of air pore structure
- Investigations of air pore stability (fresh concrete)

o Changing of the chemical resistance under the exposure sites
o Study of phase distribution- transformation i.e. stability

3.4. Task 4 - Life-time analysis

The study of the data from the laboratory and field test as well as from the cores from real structures will lead to the identification of deterioration models. On one side the results can be presented as the following example shows.

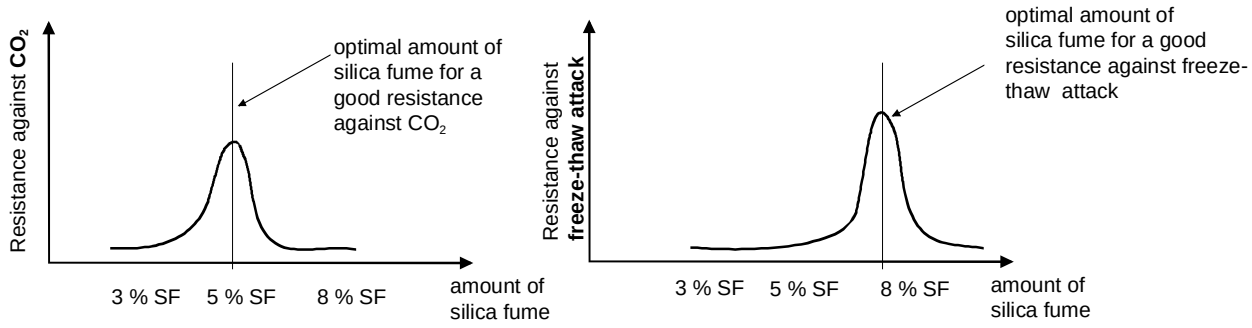

Fig. 1: Presentation of results – example

On the other side the evaluation of the received results of task 3 can be presented as demonstrated in illustration 2.

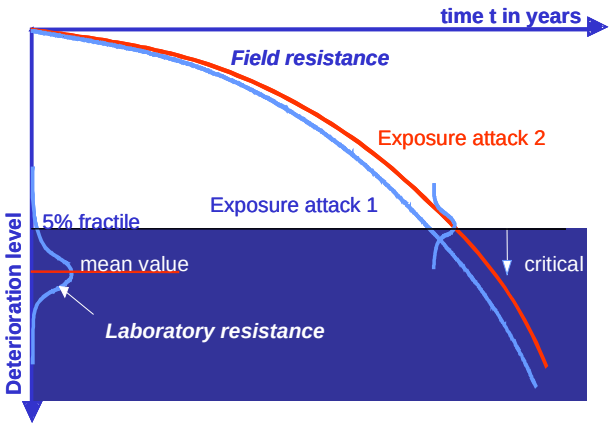

Fig.2: Illustration of field and laboratory test results

In the end, these results can be included in a recommendation for suppliers and consumers with regard to the application of additives and admixtures for HPC and their consequences concerning life-time of members under environmental attacks.

4. CONCLUSIONS

The project will help to optimise the structure of HPC, particularly with regard to improving durability. Here, all partners will add their national experience with this special kind of concrete as well as from normal concrete. The development of a European database concerning the

application and testing of HPC points out furthermore, national differences and leads to a unified comparison. Later on the results of this project should be a part of European standardisation efforts for HPC. Therefore, a manual will be developed in the last stage of the project, which is planned to be published subsequently. In the end of the project a workshop will be organised for the dissemination of these results. Beyond the project duration the partners will further study the in-service structures as well as the outdoor specimens in order to verify the developed degradation models.
An overview of results is also listed below:

- Accepted methodologies for life-time prediction will document *changes of the properties of HPC* under the exposure classes of the European standardisation EN 206 with dependence on time
- Overview of essential degradation aspects and understanding of *deterioration mechanisms* $\rightarrow$ projection to the behaviour during service
- *Service-life data* of HPC constructions
- Progressive use of industrial by-products and improvement of the durability of concrete with lower life change costs $\rightarrow$ *Innovative economical and ecological concrete design concept*
- Concrete with an excellent resistance against severe environmental conditions can be developed in the future (less scaling, high freeze thaw and cyclic durability, high resistance against de-icing chemicals, sulphate and less corrosion)
- A European *quality control system* can be developed

The results of this project are interesting for both consumers as well as suppliers and help to avoid damages and costs for redevelopment. Due to this fact, the use of HPC becomes more efficient and takes into consideration ecological as well as economical aspects.

REFERENCES

1. *RILEM:* Draft recommendation for the freeze-thaw resistance of concrete. CIF- and Slab-test for the determination of the internal damage of concrete, Materials and Structures, November 2001
2. *RILEM:* Draft recommendation for the freeze-thaw resistance of concrete. Tests with water (CIF) or with sodium chloride solution (CDF). Materials and Structures, Vol. 28, 1995.
3. *RILEM:* Draft recommendations for test methods for the freeze-thaw resistance of concrete. Slab Test and Cube Test. Materials and Structures, Vol. 28, 1995.
4. *RILEM*: Final Report CIB W80/RILEM TC 71-PSL 1987. Prediction of service life of building materials and components. Materials and Structures 20(1987)115. Pp. 55-72
5. Guide For Service Life Design of Buildings. ISO/CD 15686-1. ISO TC 59/SC14 Draft 3:1997.
6. *Tang, L., Nilsson, L-O.:* Transport of ions, Chapter 9.6 & 9.8 in: Performance Criteria for Concrete Durability, State-of-the-Art Report by RILEM Technical Committee TC 116-PCD, RILEM Report 12, ed. J. Kropp and H.K. Hilsdorf, Chapman & Hall, 1995.
7. *ASTM C1012* "Length change of hydraulic-cement mortars exposed to a sulphate solution", Annual book of ASTM standards, Vol. 04.01.

RELATED PROJECTS

1. *"Probabilistic Performance Based Durability Design of Concrete Structures"*
2. *"The Residual Service Life of Concrete Structures"* within the program Brite-EuRam (contract BREU-CT91-0591).
3. RILEM TC FHP: *"Predicting the frost resistance of high-performance concrete structures exposed to numerous freezing and thawing cycles"*
4. RILEM TC IDC 176 "*Internal Damage of concrete due to frost attack"*
5. *CEN TC51/WG12/TG4 "Freeze/thaw resistance of concrete*. The project *"Standard methods for testing the resistance of concrete to freezing and thawing" (MAT 1-CT 94-0055)* in the program Measurements and Testing.
6. *SUPERPLAST* "Design and function of novel polymeric admixtures for more durable high-performance concrete" *G1RD-CT-2000*
7. *LIFECON "Life-cycle Management of Concrete Infrastructures for Improved Sustainability", G1RD-CT-2000-00378*

Durability of Resource Saving “Green” Types of Concrete

M.Sc. Marianne Tange Jepsen, B.Sc. Dorthe Mathiesen,
and Centre Manager, M.Sc. Christian Munch-Petersen
Concrete Centre, Danish Technological Institute
Taastrup, Denmark
Chief Concrete Technologist, Ph.D. Dirch Bager
Cement and Concrete Laboratory, Aalborg Portland
Aalborg, Denmark

This paper was originally presented at the *fib*-Symposium

“Concrete and Environment”

Berlin 3 – 5 October 2001.

Durability of Resource Saving “Green” Types of Concrete

M.Sc. Marianne Tange Jepsen, B.Sc. Dorthe Mathiesen,
and Centre Manager, M.Sc. Christian Munch-Petersen
Concrete Centre, Danish Technological Institute
Taastrup, Denmark
Chief Concrete Technologist, Ph.D. Dirch Bager
Cement and Concrete Laboratory, Aalborg Portland
Aalborg, Denmark

Summary

One of the impediments for the use of resource saving "green" types of concrete on a larger scale is the lack of documentation of durability properties. The Danish Centre for Resource Saving Concrete has carried out durability investigations to encourage the use of green concrete. This article presents the results of an investigation of frost resistance, carbonation and chloride ingress for five types of green concrete. The investigation shows that the tested types of green concrete can be evaluated using the same accept criteria as for ordinary types of concrete. Some of the residual products lower the effect of the chemical additives, e.g. the air entraining agent, and therefore it can be difficult to obtain an air void structure with sufficient fineness to ensure frost resistance. However, it seems possible to produce green concrete, which is just as durable as ordinary concrete.

Introduction

In Denmark, a Centre for Resource Saving Concrete Structures was formed in 1998. The aim is to gain more knowledge about environment-friendly – so-called “green” - types of concrete and to develop technical solutions, so green concrete can be used in modern building technology. Fulfilment of the objectives of the centre calls for different kinds of expertise. Therefore, the centre involves partners from all sectors related to concrete production, i.e. cement and aggregate producers, a contractor, a ready mix plant, a consultant and a building owner besides Danish Technological Institute and the two technical universities in Denmark.

The ways to sustainable concrete design are manifold. The Centre aims for

- concrete with minimal clinker content
- concrete with green types of cement and binders
- concrete with inorganic residual products
- operation and maintenance technology for green concrete structures
- green structural solutions and structural solutions for green concrete

The centre has initiated five development projects corresponding to the five targets. The three first mentioned all imply changes of the traditional concrete mix design. Investigation of different concrete mix designs has been carried out in different phases: The first phase consisted of a screening of more than 30 different mix designs. Among these, the most promising mix designs were selected for a comprehensive test programme in the second phase. The results presented in this article originate from this second phase, from investigations of the durability of five green types of concrete intended for use in aggressive environment.

In the year 2001 the practical use of green concrete and green structural solutions will be demonstrated, when the results of the development projects are incorporated in a highway overpass project.

Environmental goals and intentions

The Centre for ressource saving concrete has laid down a list of environmental goals:

- CO_2 emission caused by concrete production must be reduced by at least 30%.

- The concrete must consist of at least 20% residual products, used at aggregates.
- The concrete industry's own residual products must be used in concrete production
- New types of residual products, previously landfilled or disposed of in other ways, must be used in concrete production
- CO_2-neutral, waste-derived fuels must replace at least 10% of the fossil fuels in cement production.

The Centre defines "green" concrete as concrete which satisfies one or more of the environmental goals. Moreover, a green type of concrete has to meet all of the environmental intentions listed below:

- avoid the use of materials which contain substances on the Danish Environmental Protection Agency's list of unwanted materials
- do not reduce the recycling ability of green concrete compared to conventional concrete (today, 95% of the concrete is reused)
- do not increase the content of hazardous substances in discharge water from concrete production

The environmental aspects of the project is described in greater detail in [1].

Test programme

Objectives

Depending on the environmental action the concrete will be subjected to most concrete codes state demands on e.g. maximum w/c ratio, minimum strength and minimum filler content (see for example DS 481 [2]). We know by experience that these requirements will lead to dense and durable concrete structures. But how do we know that these requirements are sufficient for types of concrete differing from conventional concrete, e.g. green types of concrete, where we have very limited experience? Therefore, in order to encourage the use of green types of concrete, one important task is to provide documentation of their durability properties and to prove that they have adequate service lives.

A number of standard test methods have been developed to test concrete resistance against specific deterioration mechanisms, e.g. salt surface scaling and chloride ingress. When testing new types of concrete using standard test procedures prepared for conventional concrete, one may face two problems:

- The test results approve non-durable concrete or disqualify durable concrete, because the accept-criteria are not adjusted to the present type of concrete.
- The standard tests do not uncover new durability problems introduced with new types of concrete, because the standard tests only relate to deterioration mechanisms relevant for conventional concrete.

The chemical composition of the green constituents in the concretes in this study has been thoroughly examined. In the light of this examination, it is believed that the concretes tabled in the next paragraph will not present any new durability aspects, so therefore this investigation is focused on the classical durability issues of frost resistance, chloride ingress, and carbonation.

The standard test procedures chosen are

Frost resistance: Surface scaling according to a modified SS 13 72 44 (Borås method) [3], and air void analysis according to DS/EN480-1 [4].

Carbonation: NT-BUILD 357 [5].

Chloride ingress: CTH-method [6].

All these methods prescribe testing of time dependent properties at fixed deadlines, e.g. 28 days after casting. However, in the preliminary testing of green concretes it has been observed

that the development of strength for some of the green types of concrete deviate from strength development of conventional concrete, and it is most likely that the development of other properties will deviate too. For this reason, measurements of surface scaling and chloride diffusion coefficient have been carried out at more than one concrete age.

Concrete mix designs

The investigation includes five green types of concrete. In addition, a reference concrete, *AR*, is included in the test programme. *AR* is a normal Danish concrete intended for aggressive environment. *AR* is produced with extra low alkali, highly sulphate resistant cement, a moderate fly ash content as well of a moderate content of silica fume. It fulfils the Danish code DS 481 [2] and the specification for concrete work of the Danish Road Directorate [7].

The five green types of concretes are:

A0 Concrete with low alkali, moderate sulphate resistant cement. Change of cement type lowers the energy consumption of cement production. The same cement type is used for *A1* and *A3*. A0 fulfils DS481, but not the specification of the Danish Road Directorate.

A1 Concrete with a high amount of fly ash (40% of powder b.w.)

A3 Concrete with sewage sludge incineration ash instead of ordinary fly ash

A5 Concrete with concrete slurry

A6 Concrete with stone dust

The compressive strengths of the green types of concrete are all comparable to the strength of *AR*. The concrete mix designs are listed in Table 1.

*Table **Fejl! Ukendt argument for parameter.**: Mix design for the tested concretes (according to the batch report from the ready mix plant). All constitutents are noted by weight [kg/m^3].*

Constituent	**Description**	**AR**	**A0**	**A1**	**A3**	**A5**	**A6**
Cement	Aalborg Portland LASR cement (CEM I 42.5 HS/EA)	287.6	-	-	-	-	-
	Aalborg Portland RAPID® cement (CEM I 52.5 MS/LA)	-	286.5	188.6	277.0	-	-
	Cementa ANL cement (CEM I 42.5 HS/LA)	-	-	-	-	398.0	397.2
Ordinary fly ash	Danaske B1	33.7	32.3	137.4	-	-	-
Silica fume	Elkem	17.4	17.0	17.8	17.0	-	-
Residual product	Fly ash/sewage plant	-	-	-	34.7	-	-
	Concrete slurry (weight of dry matter)	-	-	-	-	14.6	-
	Stone dust 0/2						462
Water		149.0	155.4	131.7	143.3	147.9	150.0
Plastizicer	Conplast 212	2.39	2.50	2.42	2.23	-	
	Peramin V	-	-	-	-	-	1.98
Super plastizicer	Conplast SP 605	-	-	3.40	3.18	-	-
	Peramin F	-	-	-	-	3,95	-
	CEM 92M	-	-	-	-	-	6.78
Air-entraing	Conplast 316 AEA 1:5	1.01	0.73	0.50	0.31	-	-

admixture	HPa	-	-	-	-	0,12	0,15
Sand	0/4 A, Nr. Haldne	621	629	646	640	-	-
	0/8 Östervang					832	457
Coarse aggregate	4/8 A, Uddevalla	244	245	251	249	-	-
	8/16 A, Uddevalla	855	858	871	865	-	-
	8/16 Östervang					200	197
	16/25 Östervang					718	693

AR, A0, A1, and *A3* is produced by a Danish ready mix plant, whereas *A5* and *A6* is produced by a Swedish concrete producer.

The above mentioned concretes present a mix of different ways to lower the environmental impact of concrete production. Substitution of cement with fly ash (*A1)* is the traditional way to minimise the clinker content. *A0*, *A1*, and *A3* are produced with a green type of cement, where 9% of the fuel for cement production comes from renewable resources. *A3*, *A5*, and *A6* introduce new residual products in concrete production, *A5* and A6 from the concrete industry itself, *A3* from other industries. An evaluation of the environmental goals is given in Table 2.

*Table **Fejl! Ukendt argument for parameter.**: Evaluation of environmental goals.*

Environmental goal	**A0**	**A1**	**A3**	**A5**	**A6**
• CO_2 reduction	27% (3)	52% 3	29% (3)		
• Residual products as aggregates					3
• Residual products from the concrete industry				3	3
• Residual products from other sources			3		
• Waste-derived fuels	9% (3)	9% (3)	9% (3)		

A0 is accepted as a green type of concrete; though it does not fulfil any of the goals, it is close to fulfilling two of the five goals.

Resistance against frost deterioration

Results

The test method used is an accelerated frost-thaw test according to SS 13 72 44, except each 7th frost-thaw cycle is replaced by 24 hours at constant temperature (20°C), which enables registration of ultrasound transmission time and dilation of the test specimens [3].

The measurements of scaling are shown in Figure 1.

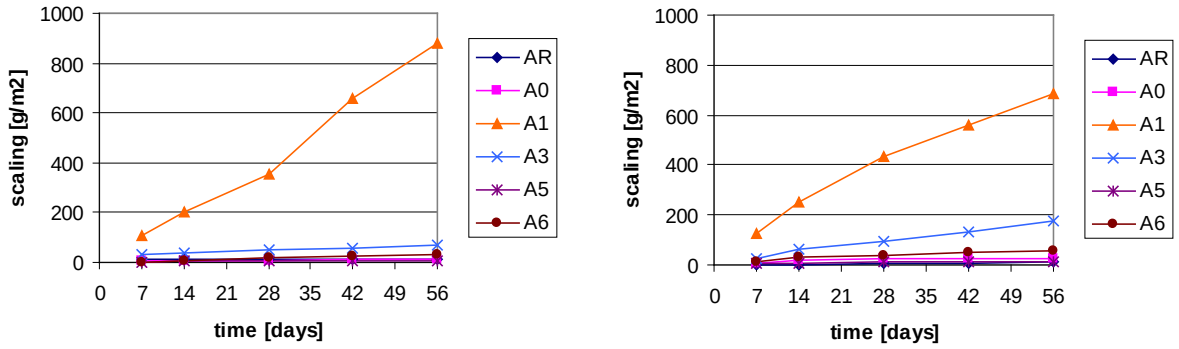

*Figure **Fejl! Ukendt argument for parameter.**: Results of surface scaling test according to SS 13 72 44 (modified). Left:Exposure to frost-thaw cycles started 31 days after casting*

(standard procedure). Right: Exposure to frost-thaw cycles started 59 days after casting.

The concretes were also subjected to an air void analysis according to DS/EN480-1, see Table 1.

*Table **Fejl! Ukendt argument for parameter.**: Results of air void analysis*

		AR	A0	A1	A3	A5	A6
Air content in hardened concrete	[vol-%]	6.18	5.86	5.23	6.44	4.04	3.94
Paste content	[vol-%]	26.1	27.0	26.3	25.6	28.2	27.1
Powers spacing factor	[mm]	0.13	0.18	0.33	0.30	0.17	0.35
Volume of micro air voids (diameter < 300 μm)	[vol-%]	3.00	2.25	0.84	0.83	2.03	0.72

Comments

Normally the salt scaling test is performed in a way that the exposure to frost-thaw cycles starts 31 days after casting. In this case, the accept criterion according to DS481 is that at least one of the following two requirements has to be fulfilled:

- The scaling after 56 freeze-thaw cycles is less than 0.2 kg/m^2
- The scaling after 56 freeze-thaw cycles is less than 0.5 kg/m^2 and the proportion between the amount scaled of after 56 cycles and the amount scaled of after 28 cycles is less than 2.

As can be seen in Figure 1, all concretes except *A1* (concrete with high fly ash content) can be accepted.

A1 probably fails due to the high spacing factor. According to the Danish concrete code, the spacing factor of a concrete, which is not subjected to a frost-thaw test, must not exceed 0.20 mm. If *A1* had fulfilled this requirement, it would probably also show sufficient frost resistance. A review of relevant litterature shows that it is possible to make frost resistant concrete with high fly ash contents if the fineness of the air void system is adequate (see e.g. [8]).

A6 has an even higher spacing factor than *A1*, though nearly no scaling was observed. At first sight this seems contradictory, but observations made by Pigeon can explain this [9]: Pigeon showed that the critical spacing factor is not a fixed quantity valid for all types of concrete. The critical spacing factor is lower, the denser the concrete is. In addition to fly ash, *A1* also contains silica fume, and *A1* is expected to be denser than *A6* without silica fume. For this reason the critical spacing factor of *A1* may be lower than 0.33, whereas the critical spacing factor of *A6* is higher than 0.35.

Effect of age of concrete, when the scaling test is performed

According to the standardised test procedure of the scaling test, the concrete is exposed to frost action for the first time 31 days after casting. In this study, a similar test has been run, where the age of the test specimens was 59 days, before they were exposed to frost. The results are shown in Figure 1 (to the right).

A comparison of results shows that the scaling of *A1* is reduced, when the concrete age is increased before frost action. However, the scaling of *A1* is still not satisfactory.

For *A3* a slight increase of scaling is observed at the later age. For the rest of the concretes, the amount of scaling is more or less unchanged. For all concretes except *A1* it is difficult to draw conclusions about the time dependent development of frost resistance, because it is not possible to detect a significant change, when the scaling in both tests were low.

Inner damage

Parallel to the scaling test, the test specimens were inspected by measuring ultra sound transmission time and dilation to reveal if any inner damage had occurred. However, the changes in ultrasound transmission time and the length changes were small, so there is no sign of inner deterioration.

Carbonation

Method

35 days after casting, the test specimens are placed in a climate chamber with a CO_2 enriched atmosphere (3% CO_2, 60% RH). The carbonation depth is measured 4, 8, and 12 weeks after the specimens have been placed in the chamber (the carbonation depth is made visible by means of phenolphthalein, according to NT-BUILD 357).

Results

The results (mean values of carbonation depth) are shown in Figure 2.

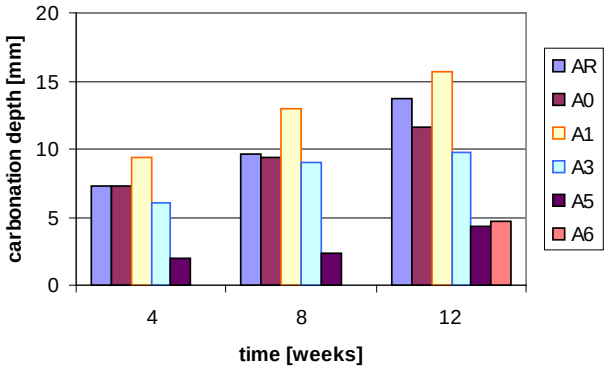

*Figure **Fejl! Ukendt argument for parameter.**: Carbonation depths measured according to NT-BUILD 357.*

Comments

The carbonation depths of *A0* and *A3* are at about the same level as the carbonation depth of the reference concrete *AR*. The carbonation is more pronounced for *A1* and less pronounced for *A5* and *A6*.

Calcium hydroxide, $Ca(OH)_2$, is formed during cement hydration, and because of the high alkalinity of calcium hydroxide, the presence of calcium hydroxide will ensure a high pH-value in the concrete. The pH-value is roughly constant, as long as calcium hydroxide is present, no matter the content of calcium hydroxide.

During the carbonation process, calcium hydroxide reacts with carbon dioxide, CO_2, from the atmosphere. When all calcium hydroxide in an area has reacted, the pH-value in the area decreases. If two types of concrete have different initial contents of calcium hydroxide, the one with the lowest content will be most sensitive to carbonation, because the carbonation front will travel faster. That means that the initial content of calcium hydroxide in hardened concrete expresses a kind of carbonation potential.

The initial content of calcium hydroxide has been calculated for the six types of concrete in this study by calculating the amount of calcium hydroxide formed during cement hydration and correcting the result by the amount of calcium hydroxide consumed during a pouzzolanic reaction with fly ash or silica fume. The calculation shows that the initial content of calcium hydroxide is about the same for *AR*, *A0*, and *A3* (~30 kg/m^3 concrete). The amount of fly ash

in *A1* is so high that it can eliminate all the calcium hydroxide. For *A5* and *A6* the initial content of calcium hydroxide is higher than that of the reference *AR* (~110 kg/m^3). These results indicate that *A1* will be more sensitive to carbonation than *AR*, *A0*, and *A3*, whereas *A5* and *A6* will be far less sensitive. This agrees very well with the experimental findings, though in *A1* there is still an amount of calcium hydroxide left after the puzzolanic reaction, which can be observed because there is still an area with high pH-value in front of the carbonated area.

It is important to notice that the difference in carbonation potential between *AR* and *A5* and *A6* does not come from the green elements in *A5* and *A6* (concrete slurry and stone dust, respectively). According to the explanation given above, the difference is due to differences in Danish and Swedish concrete practice: Swedish concrete has a higher cement content and contains no puzzolans, and therefore it will in general be more resistant to carbonation than Danish concrete.

Chloride ingress

Test Method

For this part of the project, a rapid chloride migration test method was used [6]. The method, which is developed at Chalmers University of Technology, is known as *the CTH-method*, but it is also an Nordtest standard (NT-BUILD 492). This test method was considered the most advantageous for the purpose in this project for the following reasons:

- Most other rapid test methods (i.e. AASHTO T277) measure the charge passing the specimen when a voltage is applied over it. The charge is very dependent on the ion content in the pore solution, not only the chloride ions. The ion composition in the pore solution may vary a lot from one green type of concrete to another, because of e.g. the residual products used, and therefore a comparison of results would be difficult. Using the CTH-method, the chloride diffusion coefficient is evaluated from a measurement of chloride penetration depth. That is, the result is based on a direct measurement of chloride ions present in the sample.
- Ponding tests (e.g. NT-BUILD 443) register the chloride profile after exposure to a salt solution. The test period is often several months, which means that the registered resistance against chloride ingress is a kind of average resistance during the test period. In contrast, the test period of the CTH-method is limited to some hours, which enables measurement of the resistance against chloride ingress at a certain age.
- In general, the CTH-method is theoretically clear, experimentally simple, and it has shown good repeatability.

Results

For each type of concrete, the chloride diffusion coefficient is measured 28 days, 3 months and 1 year after casting. The measured chloride diffusion coefficients are shown in Figure 3.

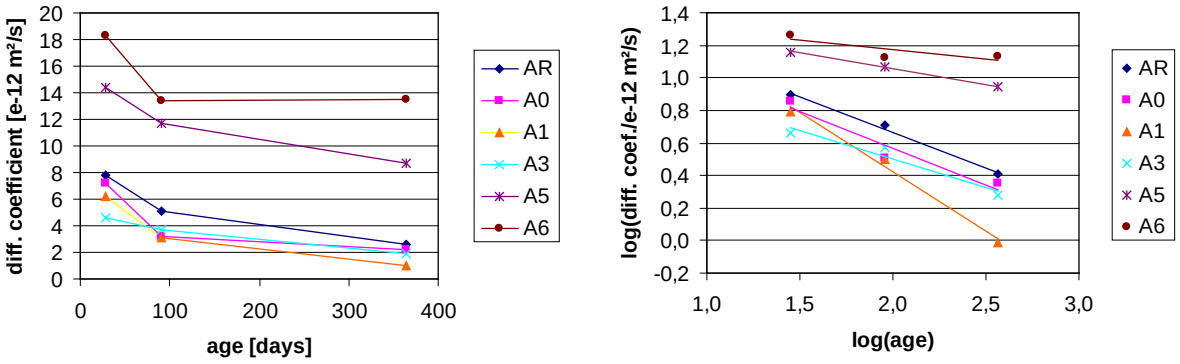

*Figure **Fejl! Ukendt argument for parameter.**: Left: Chloride diffusion coefficients measured with the CTH-method at different concrete ages. Right: Same data, pressented in logarithmic mapping.*

Comments

Time dependent diffusion coefficient

When the measured values are mapped in a system of co-ordinates with logarithmic axes (see Figure 3, to the right), the chloride diffusion coefficient as a function of time can be approximated with a straight line. This means, that the time dependency can be described by the following formula (suggested by Tang and Nilsson [10]):

$$D(t) = a \cdot t^{-b} \quad (1)$$

where

- t is the concrete age (days after cating)
- a and b are constants evaluated by regression. In a physical interpretation of the formula, a is the chloride diffusion coefficient one day after casting, whereas b expresses how fast the chloride diffusion coefficient is changing.

The a- and b-values for the six different types of concrete are listed in Table 4.

*Table **Fejl! Ukendt argument for parameter.**: a- and b-values for the tested types of concrete.*

	AR	A0	A1	A3	A5	A6
a	34.3	29.5	74.8	15.9	27.9	25.15
b	0.435	0.452	0.728	0.350	0.196	0.114

It can be observed in Figure 3 (and deduced from the figures in Table 4) that at all times chloride diffusion coefficients of *A0* and *A3* are at the same level as the diffusion coefficient of *AR* or even a little bit lower.

28 days after casting, the chloride diffusion coefficient of *A1* is at the same level as *AR*. But the reduction of the diffusion coefficient of *A1* is quicker, resulting in a diffusion coefficient of *A1* of less than 50% of the diffusion coefficient of the reference concrete one year after casting. The explanation of the very good chloride resistance is probably an increased chloride binding caused by the high fly ash content.

The diffusion coefficients of *A5* and *A6* are from the beginning of the test series (28 days after casting) at a higher level than the diffusion coefficients measured for the rest of the concretes. The development of the chloride diffusion coefficient is also slower. However, a check up on the development of the chloride diffusion coefficient of a normal Swedish concrete which was not originally a part of the test programme gave a result similar to the results of *A5* and *A6*. Just like in the case of carbonation, the differences between on the one hand *AR* and on the other hand *A5* and *A6* are not due to the green initiatives (concrete slurry and stone dust). The reason for the differences is the general differences between Danish and Swedish concrete tradition, where concrete in Sweden is produced without fly ash and silica fume.

Accept criterion

In the Danish and Swedish concrete codes, no acceptance criteria are stated for the chloride diffusion coefficient. Tang Luping has given the following guidelines for the chloride diffusion coefficient D measured with the CTH-method 28 days after casting:

- $D<2\cdot10^{-12}$ m^2/s: Very good resistance against chloride ingress
- $D<8\cdot10^{-12}$ m^2/s: Good resistance against chloride ingress
- $D<16\cdot10^{-12}$ m^2/s: Moderate resistance against chloride ingress
- $D>16\cdot10^{-12}$ m^2/s: Not suitable for aggressive environment

According to these guidelines, *AR*, *A0*, *A1*, and *A3* show good resistance against chloride ingress, whereas *A5* shows moderate resistance and *A6* just exceeds $16 \cdot 10^{-12}$ m^2/s and therefore is characterised as being not suitable for aggressive environment.

For practical reasons, we need accept criteria at an early age (e.g. 28 days after casting), though the diffusion coefficient at a later stage, e.g. one year after casting, is more relevant for the chloride ingress during the whole service life of the structure. When stating limits for the chloride diffusion coefficient 28 days after casting, we assume a "normal" further development of the diffusivity. But as it was demonstrated in the previous paragraph, the time dependency of the chloride diffusion coefficient may vary quite a lot.

Conclusion

In the study, the durability of five different types of green concrete and a reference concrete were investigated as regards frost action, carbonation, and chloride ingress. The five green types of concrete represent different green strategies, i.e. concrete with minimal clinker content, concrete with green cement and binder, and concrete with inorganic residual products.

All concretes except concrete with high fly ash content showed good frost resistance. The concrete with high fly ash content failed because the air void system was too coarse. Concerning frost resistance, nothing in the test results indicate that we cannot use the normal test procedures and acceptance criteria when testing green concrete.

A high content of fly ash also makes the concrete vulnerable to carbonation. It is possible to roughly forecast the susceptibility to carbonation by calculating the amount of calcium hydroxide in the hardened concrete.

The green types of concrete showed just as good resistance against chloride ingress as ordinary concrete. However, the study also made it clear that it is difficult to put forth strict limits for the chloride diffusion coefficient at an early concrete age (e.g. 28 days after casting), because green changes in the mix design may influence the development in time of the chloride diffusivity.

Acknowledgement

The following companies and educational and research institutions participate in the Centre for Resource Saving Concrete Structures:

Aalborg Portland A/S, Unicon Beton A/S, COWI Consulting Engineers and Planners AS, Højgaard & Schultz a/s, AB Sydsten, the Concrete Centre (Danish Technological Institute), Department of Buildings and Energy (the Technical University of Denmark), Department of Building Technology and Structural Engineering (Aalborg University), and the Danish Road Directorate.

The Centre is co-financed by the Danish Agency for Industry and Trade. The ongoing work of the centre will be terminated by the end of 2002.

References

[1] DAMTOFT, J.S., GLAVIND, M., and MUNCH-PETERSEN, C., "Danish Centre for Green Concrete", accepted for publication in proceedings from CANMET/ACI International Symposium on Sustainable Development of Cement and Concrete, San Fransisco, September 2001.

[2] DS 481, "Concrete - Materials", 1st ed. (in Danish: "Beton – Materialer"), Danish Standards Association, Copenhagen, 1999.

[3] LUPING, T., "Modified Slab Test. Test Method for the Freeze-Thaw resistance of Concrete – Scaling and Cracking", SP, Borås, 1999.

[4] DS/EN 480-1, "Admixtures for concrete, motar and grout – Test methods – Part 11: Determination of air void characteristics in hardened concrete", Danish Standards Association, Copenhagen, 1999.

[5] NT-BUILD 357, “Concrete, repairing materials and protective coating: Carbonation resistance”, NORDTEST, Espoo, 1989.
[6] “Evaluation of the Rapid Test Method for Measuring the Chloride Diffusion Coefficients of Concrete. Appendix 1: The CTH Rapid Test, version used in round robin test of the Nordtest project No. 1388-98”, SP Rapport 1998:42, SP, Borås, 1998.
[7] “Directions for construction of concrete bridges” (in Danish: “Udbuds- og anlægsforskrifter. Betonbroer. Almindelig arbejdsbeskrivelse), Danish Road directorate, Copenhagen, 2000.
[8] MALHOTRA, V. M., and RAMEZANIANPOUR, A. A., “Fly ash in concrete”, 2nd ed., CANMET, Ottawa, 1994.
[9] PIGEON, M., “La durabilité au gel du béton”, *Materials and Structures*, Vol. 22, No. 127, pp. 3-14.
[10] TANG, L., and NILSSON, L.-O., “Chloride diffusivity in high strength concrete at different ages”, Nordic Concrete Research, Publication No. 11, pp. 162-171.

Durability of high performance concrete containing fly ash and silica fume

Marco Friebert
Civil Engineer, Ph.D.-Student
Bauhaus-University of Weimar
F. A. Finger-Institute for Building Material Science
Coudraystr. 11
99421 Weimar (Germany)
E-mail: marco.friebert@bauing.uni-weimar.de

ABSTRACT

Studies on frost resistance and resistance against sulphuric acid corrosion of practice-oriented HPC and SCC were made. Porosity and hydrate phases were analysed by means of MIP, ESEM and thin section microscopy. Only the pore size distribution appeared no direct relations to the durability of HPC and SCC. The SCC showed an sufficient frost resistance after 90 days, but as for the HPC, after 28 days. For the HPC, the addition of silica fume did not effectively improve its resistance against sulphuric acid corrosion, the age of the concrete was more important.

Key words: fly ash, silica fume, frost resistance, sulphuric acid corrosion, high performance concrete, self compacting concrete

1 INTRODUCTION

The demands on the products of the concrete industry have been rising constantly in the last decades. A newly promising development which is based on novel concrete admixtures is the production of High Performance Concrete (HPC), because the high strength concrete shows a better durability through his high impermeability than standard concrete. A further development in concrete technology is Self Compacting Concrete (SCC). Due to its outstanding workability (no external compaction necessary), new perspectives for concrete industrie will be opend.

To produce HPC additives (superplasticiser) and admixtures (fly ash, silica fume) are used. As for normal cement concrete the hydration is basically finished after 28 days, for HPC the hydration continues after 28 days because of the mineral admixtures (fly ash). This leads to a further strength increase and impermeability of the binder matrix. As industrial by-products fly ash and silica fume contain pozzolanic characteristics, they consume portlandite which represents a weak spot in the concrete structure. Furthermore the use of fly ash is capable to lower the cement content of the concrete. This has economical and technological advantages.

An essential characteristic which is required for concrete is the frost resistance. The test of the frost resistance by means of CIF-test [1] represents good, to determine the resistance against physical attack. The characteristic values determined during the CIF-test provide not only statements for the structure, but also essential mechanical properties.

Concrete, which have contact with aggressive mediums, must also show a high structure impermeability. The use of HPC is demanded in the worksheet ATV M 168 [2] and in the Austrian standard [3] in specific cases of application. An "acid-resistant" HPC of the strength class B 85 with fly ash and silica fume was used to build a cooling tower of a power plant [4].

In this work, the influence of the binder combination and the test time on the durability of HPC was discussed. The frost resistance and the resistance against attack of sulphuric acid pH 2 both laboratory produced specimens and precast concrete manufactured in a precast plant were examined for this purpose. Additionally, analytical methods as Mercury Intrusion Porosimetry (MIP), Environmental Scanning Electron Microscope (ESEM) and thin section microscopy were carried out.

2 EXPERIMENTAL

2.1 Materials

In this work two kinds of portland cements made in Germany were used. C1 is an ordinary portland cement, CEM I 42,5 R and C2 is a sulphat-resistant portland cement, CEM I 42,5 R-HS, (according to DIN EN 197-1 [5]). A siliceouse fly ash (FA) was used. The silica fume (SF) was used as a slurry with a water content of 50 M.-%. The chemical compositions and important physical properties of the raw materials were given in Table 1.

Table1 - Properties of the material

	Unit	C1	C2	FA	SF
Material	-	CEM I 42,5 R	CEM I 42,5 R-HS	Fly ash	Silica slurry
Density	g/cm³	3,11	3,18	2,24	1,4
Specific surface (Blaine)	cm²/g	4780	4117	3140	-
d_m	µm	11,7	16,4	49,2	-
d_{50}	µm	8,3	8,8	23,2	-
Water demand	%	31,0	25,1	24,4	-
N.-eq.	%	0,85	0,65	3,17	0,59
C_3S	%	56	56,4	-	-
C_2S	%	13	16,9	-	-
C_3A	%	8,9	1,9	-	-
$C_2(A,F)$	%	7,2	16,1	-	-

Superplasticiser P (polycarboxylate-ether) was used for the SCC, superplasticiser N (naphthalene-based) for the HPC. The reference concrete were made with plasticiser L (lignosulfonate) and superplasticiser MN (naphthalene- and melamine-based). The aggregate was a quartzitic, round river sand/gravel with a density of 2,63 g/cm³.

2.2 Mixture proportions

The mix design and important values of concrete were shown in Table 2. Three SCC (SCC1 – 3) in accordance with the methods of Okamura [6] and one reference concrete (RC- KP) with plastic consistence (F2 according to DIN 1045-2 [7]) were produced. SCC3 has a higher content of aggregate than SCC1 and SCC2, so the water content of SCC3 must be higher to reach the given consistence. Auberg [1] showed that concrete without air voids with a w/c-ratio < 0,50 appeared a small reduction of the elastic modulus (< 30 %) after 56 Freeze-Thaw-Cycles, when the w/c-ratio > 0,55, the reduction of the elastic modulus was very high.

Two different cements (C1 and C2) were used for the HPC, to discuss the effect of the sort of cement on the durability of concrete. These concrete were all very stiff and had the consistence of C0 (according to DIN 1045-2 [7]). HPC-C1 and HPC-C2 had a lower w/c-ratio than the reference concrete RC-KS. HPC-C1+S and HPC-C2+S had also silica fume as admixture.

Table 2 - Mix design and important values

Constituents	Unit	RC-KP	SCC 1	SCC 2	SCC 3	RC-KS	HPC-C1	HPC-C1+S	HPC-C2	HPC-C2+S
Aggregates		1812	1512	1535	1665	1770	1799	1768	1799	1768
Cement (C1)		320	380	360	311	340	350	350	-	-
Cement (C2)		-	-	-	-	-	-	-	350	350
Fly ash (FA)		80	200	216	163	100	100	100	100	100
Silica fume (SF) dry	kg/m³	-	28,5	27	23,3	-	-	26,3	-	26,3
Water (W) *		161	186	180	178	141	129	126	126	124
Superplasticiser (P)		-	9,30	9,00	7,00	-	-	-	-	-
Superplasticiser (N)		-	-	-	-	-	11,10	5,33	5,34	3,00
Plasticiser (L)		-	-	-	-	1,53	-	-	-	-
Superplasticiser (MN)		5,60	-	-	-	-	-	-	-	-
Density (calculated)	kg/m³	2373	2308	2320	2342	2353	2383	2372	2377	2370
W/C	-	0,50	0,49	0,50	0,57	0,41	0,37	0,36	0,36	0,36
W/(C+0,4FA+2SF)	-	0,46	0,36	0,36	0,42	0,37	0,33	0,28	0,32	0,28
W/(C+FA+SF)	-	0,40	0,31	0,30	0,36	0,32	0,29	0,26	0,28	0,26
SFA/C	-	0,25	0,53	0,60	0,52	0,29	0,29	0,29	0,29	0,29
SFA/(C+SFA+SF)	-	0,20	0,33	0,36	0,33	0,23	0,22	0,21	0,22	0,21
SF/C	-	-	0,075	0,075	0,075	-	-	0,075	-	0,075
SF/(C+SFA+SF)	-	-	0,047	0,045	0,047	-	-	0,055	-	0,055
Strength class	-	C 35/45	C 60/75	C 60/75	C 55/67	C 45/55	C 60/75	C 60/75	C 60/75	C 70/85
Air	%	1,8	2,0	1,5	1,1	3,1	2,4	3,1	2,8	3,0
Consistence	-	F2	SCC	SCC	SCC	C0	C0	C0	C0	C0

* including the water of the silica slurry and the water of the (super)plasticizer

2.3 Frost resistance

The frost resistance was estimated by the CIF-test according to Setzer/Auberg [1], except that the most specimens was prismatic (80 * 80 * 250 mm³). Only the sample SCC2 82d was a cylinder in a diameter of 100 mm and a height of 75 mm, which was drilled from a precast element. Table 3 provided the values of all concrete.

Table 3 - Characteristic values of the CIF-test

	relative E_{dyn} in % after FTC					Water absorption in g/m²	
	0	14	28	42	56	Capillary suction	CIF-test
RC-KP 28d	100	94	63	49	38	1120	3610
SCC1 28d	100	98	93	41	30 *	470	3930
SCC2 28d	100	96	90	41	25 *	460	3890
SCC3 28d	100	94	73	16	29	520	5050
SCC2 82d	100	104	102	100	91	484	2725
RC-KS 28d	100	97	100	97	93	640	1660
HPC-C1 28d	100	98	96	98	100	450	870
HPC-C2 28d	100	98	93	95	96	520	1030
HPC-C2+S 28d	100	97	99	97	94	450	988
HPC-C1+S 28d	100	98	102	98	94	440	830

* 52 FTC

Figure 1 showed the reduction of the elastic modulus of some concrete due to CIF-test. Neither the HPC nor the reference concrete showed a significant reduction of the elastic modulus. That means the frost resistance remains very high. The SCC and the reference concrete showed a poor frost resistance after 28 days. Only the sample of SCC2 82d showed a desirable frost resistance because of the longer hydration of the binder. The measurement of resonance frequency for the SCC indicated a higher internal deterioration (rel. E_{dyn} ~ 10 %) of the concrete.

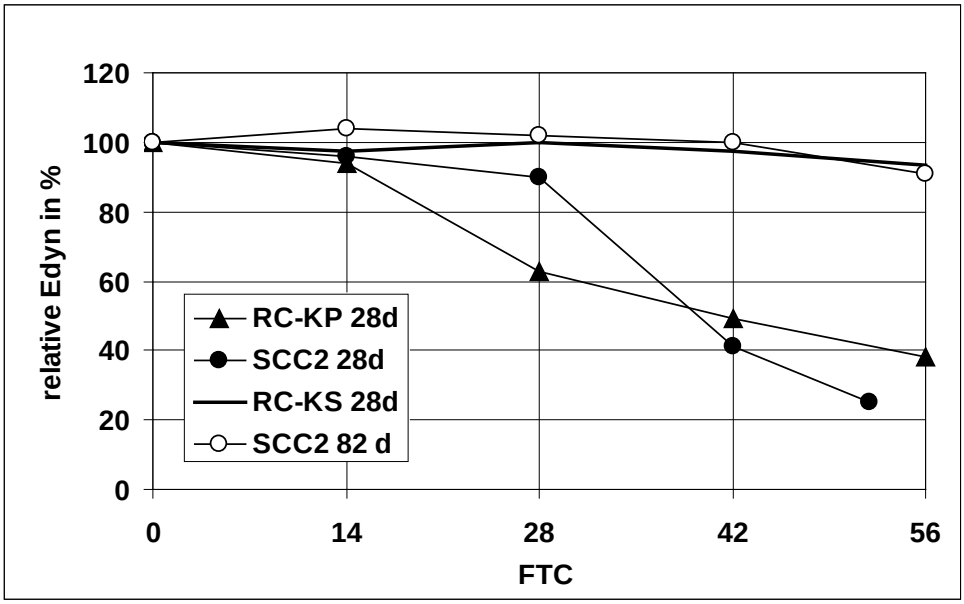

Figure 1 - Reduction of relative E_{dyn} by CIF-test (ultrasonic velocity)

The values of the water absorption supported those results (fig. 2). While the HPC and the reference concrete RC-KS showed only a small increase of water absorption, all SCC displayed a progressive water absorption. The water absorption of the reference concrete RC-KP is also high, but not progressive. Although series SCC2 82d had no high reduction in elastic modulus, the water absorption of it was also very high. Moreover, the sample of SCC2 82d showed after the CIF-test many microcracks on its surface.

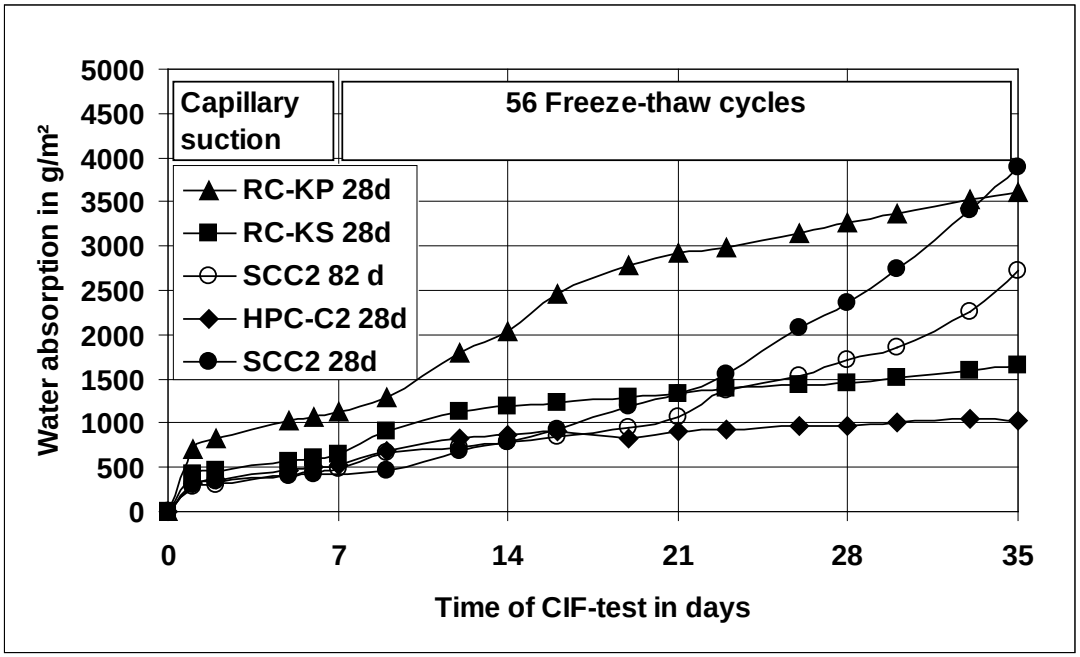

Figure 2 - Water absorption of the concrete by CIF-test

Figure 3 shows a thin section of the sample of series SCC2 28d after the CIF-test. There were many microcracks. The interface transition zone between aggregate and matrix are often destroyed (fig. 4), particulary in the areas employing the bigger aggregates. No new hydrate phases appeared in the microcracks. The ESEM analysis of the concrete after CIF-test showed a lot of new hydrate phases inside the most microcracks (fig. 5 and fig. 6). The identification of these hydrates was not sure, probably C-S-H and AFt.

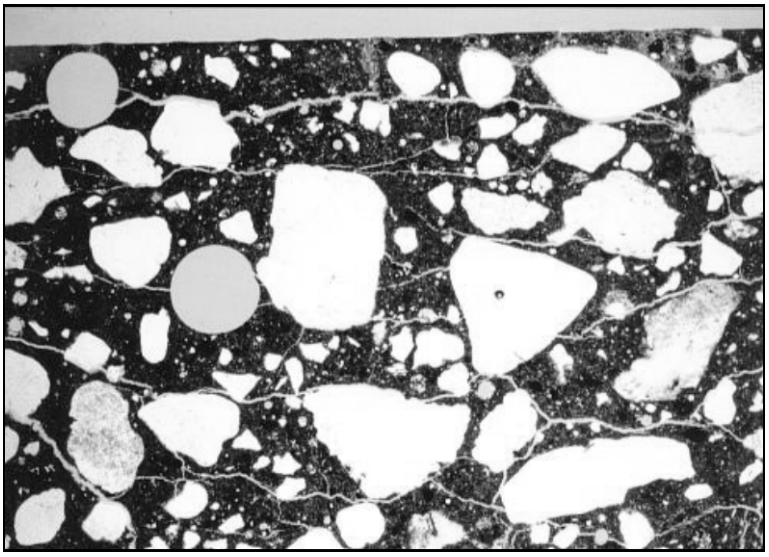

Figure 3 - Thin section microscopy of SCC2 28d after frost (30×)

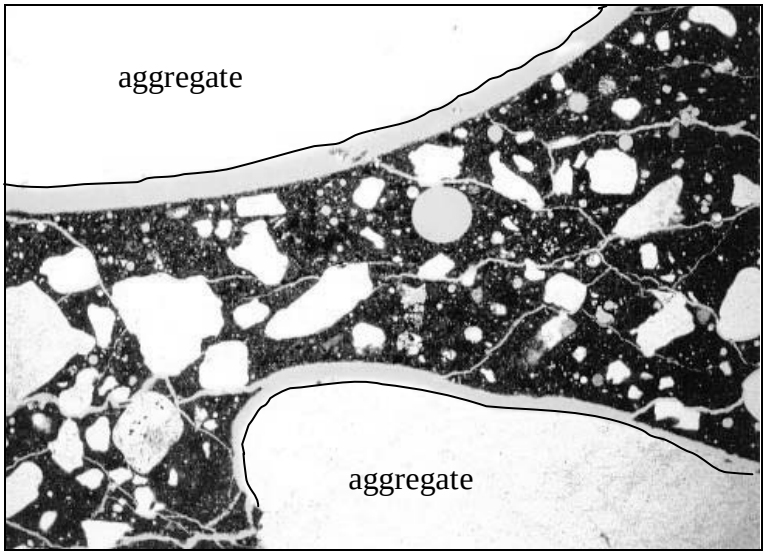

Figure 4 - Thin section microscopy of SCC2 28d after frost (120×)

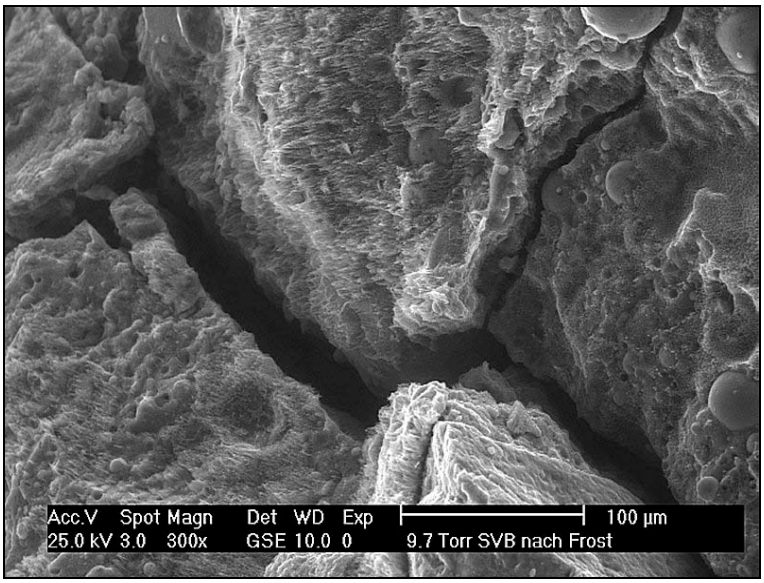

Figure 5 - Electron microscopy of SCC3 28d after frost (300×)

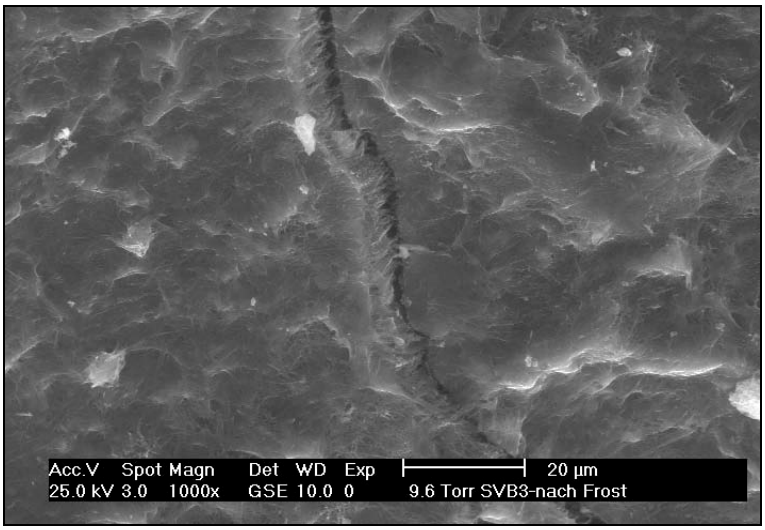

Figure 6 - Electron microscopy of SCC3 28d after frost (1000×)

MIP analysis of the samples before CIF-test was made on the mortars obtained from the concrete. The porosity measured by this method was not the real porosity but its possible to estimate the frost resistance (pores > 0,01 µm important). Figure 7 shows the pore size of HPC and the reference concrete before the CIF-test. The pore size of SCC2 28d before and after the test at different ages were also shown. The HPC with silica fume have a lower capillary porosity. For SCC2, the capillary porosity decreased with the increasing of age. The values of the porosity of the SCC were higher than the values of the other concrete series because of the higher amount of binder in concrete.

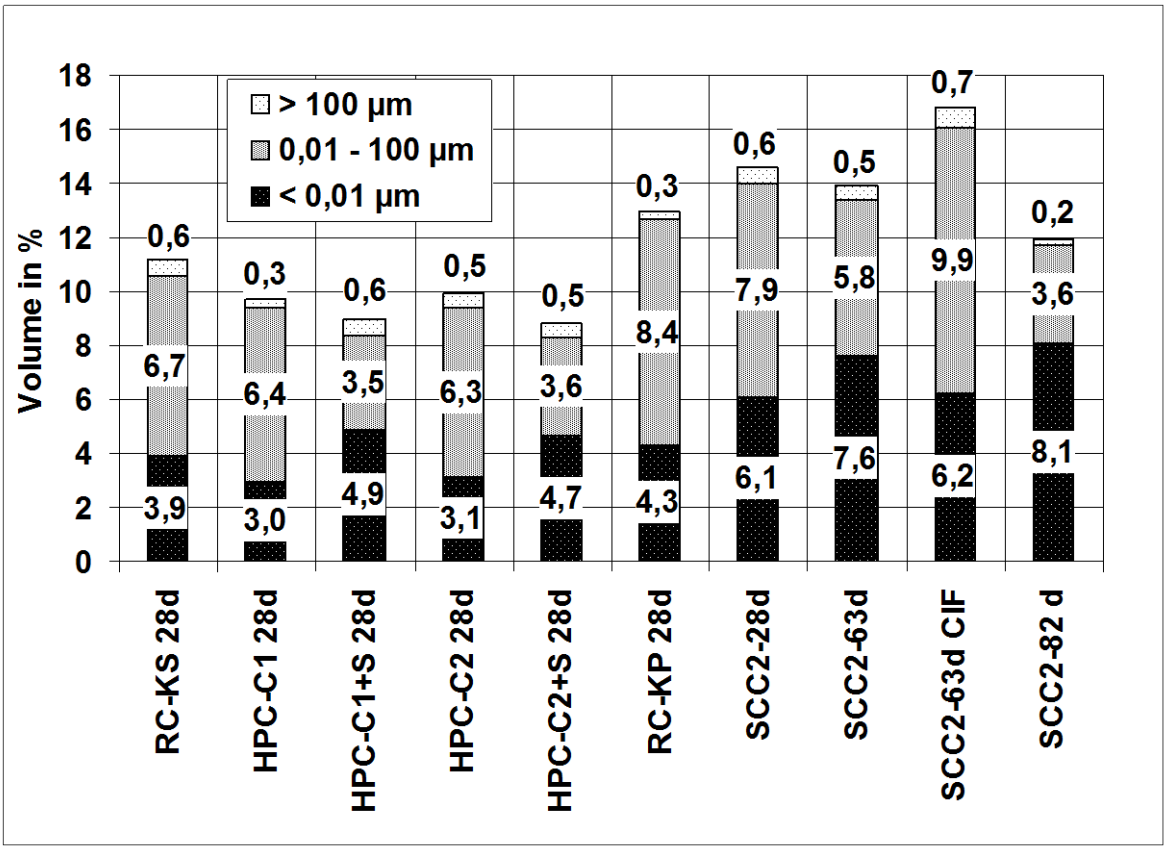

Figure 7 - Pore sizes of the concrete

The pore size distribution in fig. 8 shows the reduced pore radius by the pozzolanic reaction of the fly ash in SCC2. After 82 days of hydration the pores size distribution of the SCC is similar to the HPC. The pore radius of the HPC was significant reduced by the use of silica fume (HPC-C1 28d via HPC-C1+S 28d).

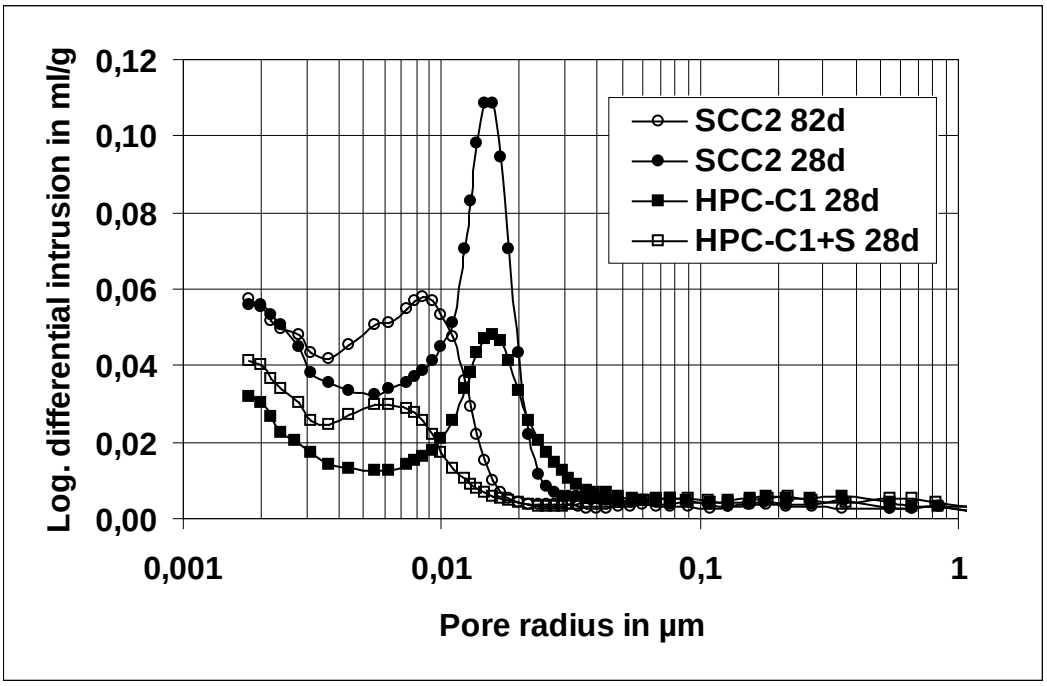

Figure 8 - Pore size distibution befor CIF-test

The pore size distribution ranging from 0,1 µm - 100 µm after CIF-test shows a higher porosity, probably due to microcracks (fig. 9). After 63 days of hydration without CIF-test the microstructure of SCC2 is also denser (SCC2 28d via SCC2 63d).

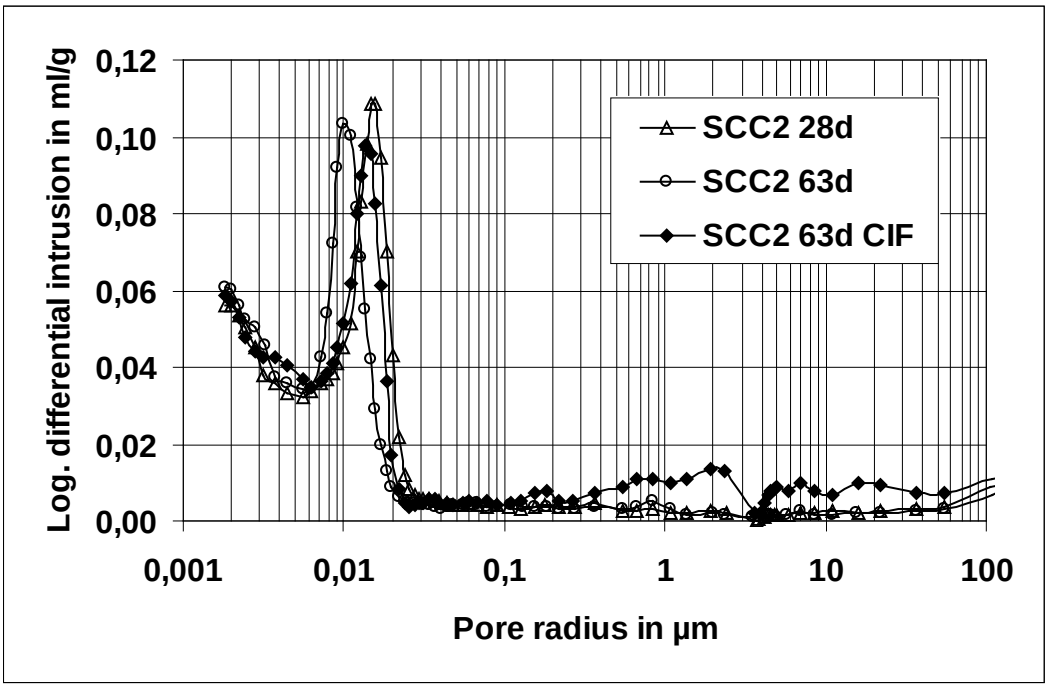

Figure 9 - Changes in pore size distribution through CIF-test

2.4 Sulphuric acid corrosion

To test the resistance against sulphuric acid corrosion of the concrete, the method proposed by Kaempfer and Berndt [8] was used. Cores drilled from the concrete (diameter/heigh: 80 mm/80 mm or 100 mm/100 mm) were immersed in a sulphuric acid with pH 2 for 35 days. Once a week the samples were immersed for 1 day in water and the destroyed surfaces were eliminated by an ultrasonic bath.

Figure 10 shows the mass loss of the surface. The HPC shows a higher mass loss than the reference concrete at an age of 30 days. A comparison between the HPC without silica fume and with silica fume shows only an small improvement through the silica fume. In comparsion with the concrete with normal portland cement the concrete with sulphate-resistant portland cement showed a considerably worse durability. At an age of the concrete of more than 100 days both the reference concrete and the HPC showed a better durability on the same level. The SCC and the reference concrete belonging to showed after 30 days a high level of durability. The durability also improves with increasing age.

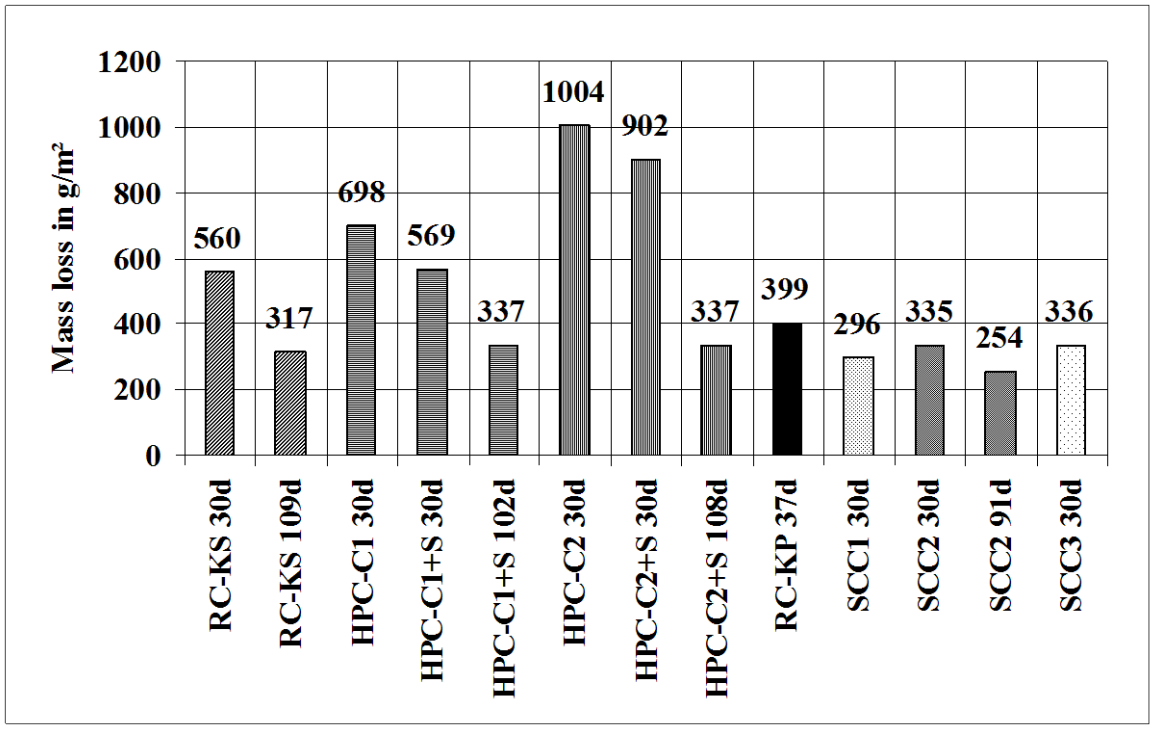

Figure 10 - Mass loss of the concrete under attack of sulphuric acid pH 2

3 CONCLUSION

All concrete showed a dense structure, which was improved by the application of silica fume and with increasing age. Nevertheless, although some concrete showed approximately a similar pore size distribution (SCC2 28d via HPC-C1 28d), their durability appeared different considerably. However the size of the pores are responsible for the transportation processes in the concrete.

The acid resistance of the concrete improves considerably with increasing age. The influence of the silica fume and the cement type are subordinated. The frost resistance of the investigated HPC is estimated to be very good. Due to the increased fly ash amount for the SCC a later age is recommended for CIF-test.

In conclusion, it has been found that the testing age of concrete with pozzolanic admixtures plays an important role. For the SCC with mostly very high amounts of fly ash, a sufficient frost resistance after 28 days is not always guaranteed. In future studies on durability, the mechanisms of the structure formation (pore size distribution, hydrate phase) is supposed to be investigated.

REFERENCES

1. Auberg, R., "Zuverlässige Prüfung des Frost- und Frost-Tausalz-Widerstands von Beton mit dem CDF- und CIF-Test," Dissertation, Universität-Gesamthochschule Essen, 1998 (in German)
2. Abwassertechnische Vereinigung e.V., "ATV Merkblatt M 168 - Korrosion von Abwasseranlagen-Abwasserableitung," Juli 1998, 39 S. (in German)
3. ÖNORM B 5017 (Entwurf), "Hochleistungsbeton im Siedlungswasserbau (HL-SW-Beton); Herstellung, Verwendung und Gütenachweis," Österreichisches Normungsinstitut, Wien, August 1997 (in German)
4. Hüttl, R.; Hillemeier, B., "Hochleistungsbeton - Beispiel Säureresistenz," Betonwerk + Fertigteil-Technik, 01/2000, S.52-60 (in German)
5. DIN EN 197-1, "Zement - Teil 1: Zusammensetzung, Anforderungen und Konformitätskriterien von Normalzement," Beuth-Verlag, Berlin, Februar 2001 (in German)
6. Okamura, H.; Ozawa, K., "Mix Design for Self-Compacting Concrete," Concrete Library of JSCE No. 25, Jun. 1995, S. 107-120
7. DIN 1045-2, "Tragwerke aus Beton, Stahlbeton und Spannbeton - Teil 2: Beton; Festlegung, Eigenschaften, Herstellung und Konformität," Beuth-Verlag, Berlin, Juli 2001 (in German)
8. Kaempfer, W.; Berndt, M., "Estimation of service life of concrete pipes in sewer networks," In Durability of Building Materials and Components 8 (Volume 1), 1999, S. 36-45

Utilisation of By-products as Filler in Concrete.

Helena Moosberg Bustnes
Tekn. Lic., Researcher
Swedish Cement and Concrete Research Institute
100 44 Stockholm, Sweden
E-mail: helena.moosberg@cbi.se

Björn Lagerblad
Ph.D., Senior Researcher
Swedish Cement and Concrete Research Institute
100 44 Stockholm, Sweden
E-mail: bjorn.lagerblad@cbi.se

ABSTRACT

To be able to promote the use of by-products as fillers in concrete the effect of filler on concrete has to be examined. This investigation has been made in order to gain knowledge of how inert fine particulate materials influence concrete properties, so that the by-products can be utilsed in similar ways. Use of by-products requires a screening procedure that will reliable determine their impact on concrete. A test procedure was developed.

Key words: concrete properties, by-products, filler, heat of hydration, compressive strength, expansion, shrinkage.

1. INTRODUCTION

The production of 1 tonne of cement releases about 800 kg of carbon dioxide into the atmosphere. It is also costly in terms of fossil fuels and coal, since it consumes between 5 and 10 GJ/tonne cement. The burning of clinker consumes non-renewable resources. It would be positive for the environment in many ways if the production of cement were decreased. At the same time, a lot of by-products are produced every day by the mineral and metallurgical industries. Much of these materials are deposited. The iron and steelmaking industries in Sweden produced 1,170,000 tonnes of slag during 1999, approximately half of it was utilised in some way and the rest deposited. The tailings from the mineral-producing concentrator plants in Sweden during 1999 exceeded 20,000,000 tonnes, most of it was deposited. The incitement from the industry to find uses for by-products has risen since the Swedish government has decided to introduce a deposition fee; the lowest amount will be SEK 250 per tonne deposited material.

Use of waste materials as a substitute for natural raw materials in the construction industry may help to conserve natural resources, and at the same time reduce the environmental hazards arising from the disposal of some waste materials. However, to be able to successfully utilise a waste material it must be an economically competitive substitute for the natural raw material that is commonly used. This includes the costs of processing and transportation. The material must

also be suitable for the planned purpose, i.e., its stability and durability over the expected life span must be ensured in the context of the particular building application.

2. BACKGROUND

Fillers are natural or artificial (industrial) inorganic mineral materials. They can be inert or chemically reactive, i.e., have latent hydraulic or puzzolanic properties. Due to their small size, the fillers can be regarded either as part of the aggregate or the paste. Fillers that are chemically inert can still have a catalytic effect on the cement hydration by fostering nucleation, densifying and homogenising the cement paste, or a physical effect on the properties of the fresh and hardened concrete. This phenomenon is referred to as the filler effect.

Large quantities of filler are needed in the production of modern concrete types. Self-compacting concrete is a self-levelling concrete that is able to completely fill formwork, even with very congested reinforcement, without any vibration. The market for this type of concrete is expanding, since it has better properties than ordinary concrete and it reduces building costs. The principle is to use large amounts of fine material to reduce the friction between the aggregates.

Fillers are usually inexpensive, especially if they are by-products; consequently, they can be used to manufacture cheaper concrete. However, cost reduction is no longer the only, or even the most important, consideration for using fillers in concrete. Fillers can be used to increase or to decrease the density; to change the concrete properties; for example, strength and rheology, and to add colour to concrete.

With a better knowledge of the behaviour of fine particles in fillers, new cement-based materials can be developed or customised to meet the requirements of a specific application. High-strength cement can be made by improved particle packing, rather than excessive cement content, and self-compacting concrete can be made with fine particles fillers. By-products that are used as fillers can thus be recycled into concrete

Part of the project is to change the properties of concrete, both in the fresh and hardened state, by addition of finely ground particles. The particles may be used as filler, cement replacement or to modify the particle size distribution of the aggregates. If the effects of fine particle addition on concrete properties were better known, concrete with improved and/or desirable properties could be custom-made to fulfil specified requirements, for instance self-compacting concrete or high-strength concrete. Certain environmental and economic benefits may also accrue from the use of fine particles.

The influence of filler on concrete properties was examined. Quartz was chosen as filler since it can be considered an inert material. Fillers interact with the cement in several ways. They may be chemically inert but can still indirectly influence the chemical structure of the cement paste and concrete in a positive way. Fillers can also replace cement and be used to improve rheological properties, which in turn will influence the properties of the hardened concrete.

The quartz fillers used in the experiments had different particle sizes and were added to the concrete in different amounts. The obtained knowledge of how quartz filler behave may be used on other types of filler with different origin, i.e., by-products.

To be able to utilise by-products as filler materials the effect of specific products on the properties of concrete has to be evaluated. It is thus important to find reliable evaluation methods that both can be used and also produces results within a reasonable timeframe, since a by-products reaction in the cement system can not be predicted by its chemical analysis. Materials can have the same chemical components but still react in different ways, and it is therefore imperative that materials with desirable properties can be separated from materials with undesirable ones. The largest potential use for the by-products are as filler for self-compacting concrete or to minimise the use of cement in ordinary concrete.

3. FILLERS FUNCTION

Addition of fine particles, i.e., particles with a maximum size of 125 microns, can affect the concrete in three ways: On the physical level – filler effect, when the added particles fill the intergranular voids between cement particles and thus improves the compactness of the concrete, on the surface chemical level – when the added particles enhance hydration by acting as nucleation sites and becomes an integrated part of the cement paste, on the chemical level – a puzzolanic effect, when the particles reacts with calcium hydroxide and forms cement gel.

4. EXPERIMENTAL

Details of the experiments and the results can be found in [1].

4.1 Inert filler

Three commercial quartz products, M300, M500, M6000 (from SIBELCO SA) and a by-product (quartz) from the mineral processing industry are used in this investigation. M6000 is a cristobalite, which is a polymorph of quartz, i.e. the same chemistry but a different structure. It is also a chemically inert material in a short time perspective, but it will have a puzzolanic effect in concrete after a long period of time. The fillers used in the experiments had different particle sizes and were added to the concrete in different amounts.

The effect of replacing cement with filler is the same as if the water/cement-ratio was raised. Concrete strength is dependent on the w/c-ratio, which in this case provides a suitable basis for comparison. In Figure 1 the relationship between w/c-ratio and compressive strength at 28 days is plotted together with the curve for standard concrete [2]. The concrete with filler addition shows a slightly steeper decrease in strength than the standard concrete.

The experimental starting-point is an ordinary concrete recipe with 433 kg Portland cement (CEM I) per cubic meter and a water/cement ratio of 0.48 without addition of filler material. To be able to mix the components properly, especially after the filler addition, it is necessary to add a superplasticizer. A naphtalene-based poly-condensate was chosen. The quantities of water and aggregates were kept constant while parts of the cement was replaced with filler (10, 20…50 volume percent, of the cement volume).

The experiments, where aggregates was replaced with filler (shown in Figure 1), shows that the more filler that replaced aggregates the higher strength were obtained. The results are similar for

the 260 and 216-kilo cement levels. When the w/c-ratio was increased from 0.81 to 0.96 for the concrete with 260-kg cement was the decrease in compressive strength significant (the quarts-curve). This decrease is due to the looser particle packing that is the result of an increased amount of water.

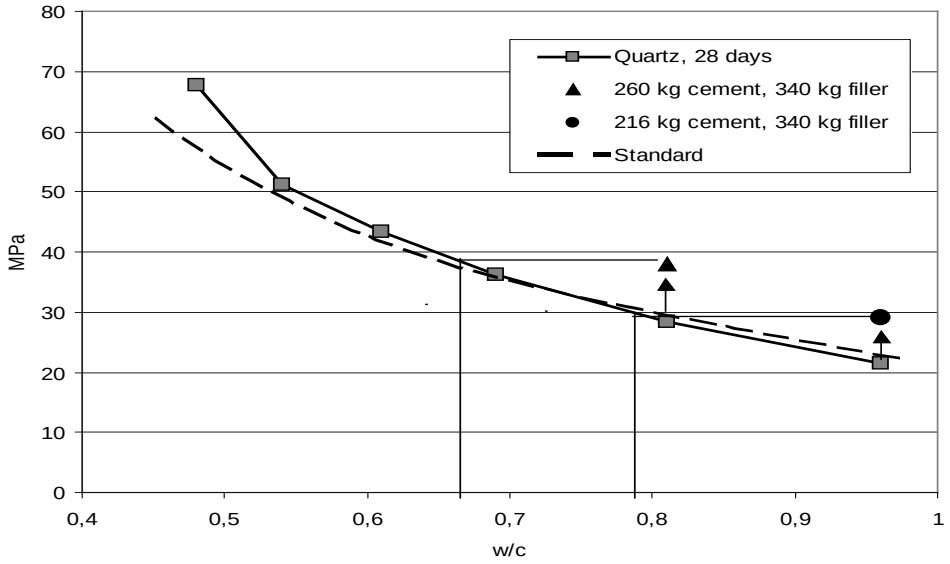

Figure 1: The relation between w/c-ratio and compressive strength at 28 days for a standard concrete and concrete with filler (quartz) addition. The obtained strength after extra filler addition at w/c-ratio 0.81 and 0.96 are marked in the diagram.

Concrete with 260 kg cement, 340 kg filler and a w/c-ratio of 0.81 has 9.6 MPa higher compressive strength than the concrete without filler. This compressive strength correlates to a w/c-ratio of 0.67. The compressive strength for the concrete with 216 kg cement, 340 kg filler and a w/c-ratio of 0.96 is 5.1 MPa higher then the ordinary concrete. This value corresponds to a w/c-ratio of 0.79. This extrapolation of strength and w/s-ratio, in Figure 1, shows that it is possible to raise the w/c-ratio without losing strength.

Table 1 (I) shows the effect of different amounts of filler added to concrete with 260 kg cement. The amounts of added filler are 0, 86, 172 and 300 kg. The figures shows that the strength increases with the increase in filler addition. Unfortunately, the superplasticizer that is needed to disperse cement and filler and give the concrete proper viscosity acts as a retarding agent when added in higher dosages. This phenomenon influences the early strength negatively, but not the long-term strength. The 7-day strength for the concrete with 300 kg filler is lower than it should be, but the 28-day strength is back to the expected level.

The effect of the particle size distribution of the filler on concrete strength is shown in Table 1 (II). Concrete with 260 kg cement was mixed with 300 kg of filler with different particle sizes. Quartz and M300 have the same particle size as cement, d50 is 12 and 14 microns, respectively, while M500 is slightly smaller and can be considered ultra-fine filler with a d50 of 4 microns. M6000 is significantly smaller than cement with a d50 of 2.2 microns. Quartz and M300 have the same strength development, while the addition of M500 and M6000 increases the strength significantly.

Table 1: Compressive strength for concrete: the effect of different amounts of filler (I) and the effect of filler with different particle sizes (II)

I	260 kg cement	w/c = 0.81
Filler kg	7 days MPa	28 days MPa
0	20.8	25.7
86	22.2	27.0
172	24.8	29.4
300	25.1	30.4

II	260 kg cement	w/c = 0.81
Filler 300 kg	7 days MPa	28 days MPa
Quartz	25.1	30.4
M300	24.2	29.7
M500	30.3	37.9
M6000	30.4	44.4

The rheology experiments were performed to show the importance of fine particles on mortar strength and their influence on the fresh mortar rheology. Figure 2 shows that the fine mortars yield stress increases as the amount of fine quartz filler that replaces the base filler increases. When the total particle system gets finer, the water demand increases, leaving less water available for the suspension liquid phase, and thus increasing the shear resistance. A relatively finer particle system also results in shorter inter-particle distances, increasing particle-to-particle friction while shearing, and also the ability of structural build up at rest. Consequently, the replacement of coarser particles has a minor influence on yield stress and shear resistance. Addition of superplasticizer to the mixture with fine filler decreases the yield stress. (Yield stress is the stress corresponding to the transition from elastic to plastic deformation.)

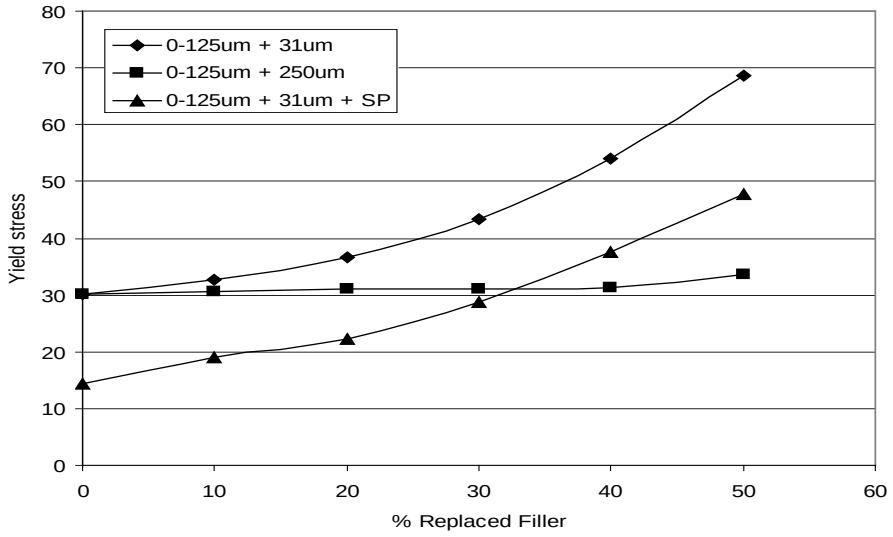

Figure 2: Yield stress versus percent replaced filler. 0-125 µm is the base filler, which is replaced with the fractions 0-31µm and 125-250µm respective. Superplasticizer (SP) is used in one experimental series.

The prisms that contained the finer material had higher compressive strength than the ones with coarse particles. Addition of superplasticizer enhances the performance of the fine filler even more, see Figure 3.

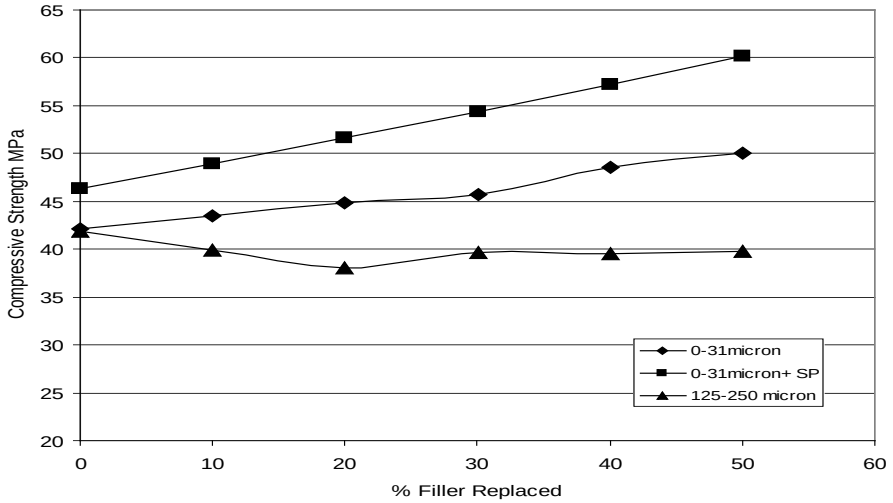

Figure 3: Compressive strength versus percent replaced filler. 0-125 µm is the base filler, which is replaced with the fractions 0-31µm and 125-250µm respective. SP is added in one experimental series.

Viscosity is the property of a material describing the increase in deformation resistance (shear stress, Pa) due to an increased rate of deformation (shear rate, s^{-1}). Measurements of viscosity show similarities in yield stress (Figure 2). Figure 4 shows how the viscosity changes with the amounts of fine and coarse fillers that replace the base filler. The curve that shows the results from the replacement with coarse filler can be estimated with a straight line. Replacement with fine filler increases the viscosity. This is due to the decrease in distance between the particles caused by the fines (the total amount of particles increases). Addition of superplasticizer to the fine filler mortar decreases the viscosity.

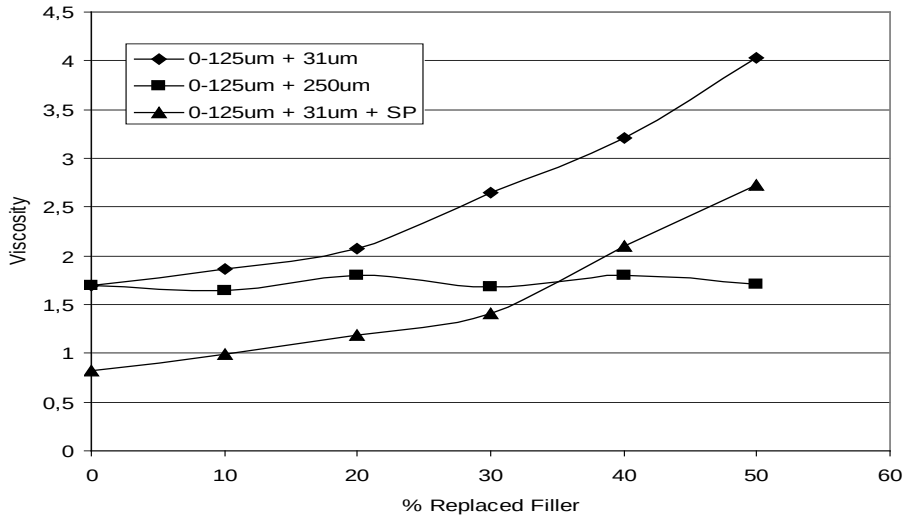

Figure 4: Viscosity versus percent replaced base filler.

The addition of superplasticizer improves particle packing by dispersing the fine particles, and thus increases the strength.

4.2 Development of a test method.

A test procedure consisting of simple, reliable experimental methods was developed. The choice of properties and methods is based on the knowledge of how a concrete should be designed to suit the concrete producers and users.

The reaction of Portland cement with water is an exothermic process. Depending on temperature, water/cement ratio, particle size and composition, the intensity of heat liberated varies with time. Measurements of the heat development provide information on the rate of hydration, and also how added materials influence it. Addition of by-products/fillers may change the cement hydration in different ways, either positively or negatively. The added materials may cause the hydration to accelerate or retard, to increase or decrease the individual peaks, and even affect the total heat development.

Material characteristics, such as the particle size distribution, particle shape, surface texture and the nature of the material influence the properties of fresh concrete mixtures more than hardened concrete. Compared to smooth and rounded particles, rough textured, angular, and elongated particles require more cement paste to produce workable concrete mixtures. Flaky particles, for example mica, have a larger water demand than spherical particles. Calcium oxide reacts with water and will thus lower the amount of free water in the mixture, thus lowering the flowability. Chemical reactions between the particles and the cement paste may also cause the particles to dissolve, thereby creating a rougher surface.

Strength development of concrete is dependent on the water/cement ratio and the characteristics of the cement, such as particle size distribution and clinker composition, as well as the amount of admixtures and fillers. The curing conditions, time, temperature and RH are also important.

The effect of additives may vary and can influence the strength in different ways. If the strength of a mixture is higher than the reference after one day, the added material is accelerating the hydration; if the strength is lower, the material is acting as a retarding agent. When the material affects the seven-day strength it functions as a binder. If there is a prominent increase in the long-term strength, the material can be considered a puzzolan or latent hydraulic. Strength measurements combined with calorimetric data show that materials with a strong initial heat peak have a negative influence on the early strength of the concrete. Materials with a low initial heat peak but a high total heat development indicate a latent hydraulic/puzzolanic effect. Inert materials can with advantage be used as aggregates or filler. Inert filler may also contribute to a higher strength, since the increased amount of fine material gives the paste better homogeneity. Internal structural damages, such as cracks and pores, will decrease in size because of the added filler and thus have a positive effect on the concrete properties. There is a correlation between compressive- and flexural strength, but since the effect of the by-products on concrete strength were unknown, determining the flexural strength was also an important consideration.

It is essential that cement paste, once it has set, does not undergo a large change of volume, and that material used as filler or aggregate in concrete does not cause high shrinkage or expansion, since that will affect the final properties of the concrete. Shrinkage depends on the amount of water that can evaporate from the paste: the higher the w/s ratio, the greater the shrinkage. It can also result from the withdrawal of water from the capillary pores by the hydration of unhydrated cement, self-desiccation, or the presence of water-absorbing (swelling) clay or materials that behave in a similar way. Expansion and cracking, leading to loss of strength, elasticity, and

durability of concrete can result from the swelling of water-absorbing material or chemical reactions between the cement gel and compounds that may be present in the by-product, such as free lime, magnesium oxide or calcium sulphate

Scanning electron microscopy can be used both to evaluate the shape of the particles and to verify results.

The chosen test methods are:

- Chemical- and XRD analysis of the by-product.
- Isothermal calorimetry measurements – shows the heat of hydration in fresh concrete and thus also the effect of the added by-products. The amount (volume percent) of by-product that replaces cement does not affect the results, as long as all material mixes in the experimental series have the same proportions, since the heat curve is presented as mW/g cement. Addition of superplasticizer would affect the measured heat of hydration and is therefore not recommended.
- Flowability – a rheology test that depends on material characteristics.
- Strength measurements – the compressive and flexural strength shows the influence of the by-products on the strength development.
- Shrinkage- and expansion measurements – shows how the durability is affected.
- Scanning Electron Microscopy – shows the microstructure of the hardened concrete.

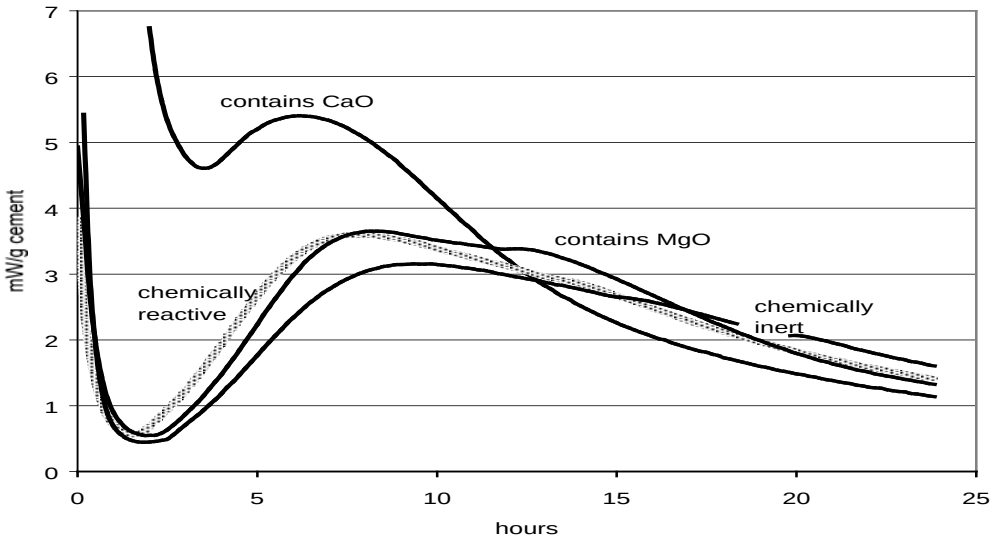

Figure 5: Examples of heat development curves for concretes that contain 45 volume percent of different types of by-products. The cement used is a standard Portland cement from Sweden (CEM I 42.5R).

The heat development curve (Figure 5) of materials containing calcium oxide (free lime) shows one peak and an extremely high initial heat development, the total heat development is however low. This is due to the hydration of the free lime, which will cause an early heat development when it reacts in the cement paste. The result is that cement hydration will be disturbed and thus affect the concrete properties. Both the early- and long term strength are affected. Magnesium oxide does not affect the heat development or the short term strength, it will though affect the long term strength. Chemically reactive materials compared to inert materials have a higher, or

similar heat development curve. Reactive/Puzzolanic materials usually affects the long term strength and can not be pinpointed only by their heat development.

Table 2: Examples of how the results vary with the chemical content in the by-product.

By-product	Shrinkage	Expansion	Strength [MPa]			Total Heat
	91 days [‰]	91 days [‰]	Compressive 28 days	Compressive 91 days	Flexural 28 days	[mW/g cem.]
Containing reactive CaO	1.82	0.25	12.9	14.4	3.1	183.02
Containing Reactive MgO	1.50	0.30	22.1	21.2	4.8	329.69
Chemically Inert	0.56	0.06	17.4	20.6	4.8	195.37
Chemically Reactive	0.59	0.08	29.1	29.1	5.6	205.12

Table 2 shows that the compressive strength development for a material that contain magnesium oxide is initially positive, but it ceases (after the 28 day measurement) and the strength decreases or slows down. The slow hydration of magnesium oxide to brucite, that has a larger volume, causes the expansion, and thus the decrease in strength. If the by-product contains calcium oxide the strength development will be positive but on much lower level and the shrinkage and expansion will be higher compared with an inert material.

The results from the shrinkage- and expansion measurements shows clearly that materials containing calcium oxide and/or slowly hydrating magnesium oxide tend to have a detrimental influence on concrete durability.

Materials that are mainly or fully amorphous usually acts as inert or chemically reactive fillers when mixed into concrete.

5. CONCLUSIONS

The addition of fillers affects the concrete structure. Cement pastes containing fine particles have a denser and more homogenous structure than pastes without filler, i.e., filler addition improves particle packing and reduces the wall effect. The use of superplasticizers is necessary for achieving the best dispersion of the filler. The homogeneity of the pastes that contain the finest fillers may also be a result of the particles acting as nucleation sites, and thus improving hydration. Ultra fine particles will not only improve the particle packing but also become an integrated part of the cement paste.

Based on the results, the conclusion can be drawn that an improved particle packing in the concrete leads to a higher strength without an increase in cement content. Several of the by-products generated by the mineral and metallurgical industries can therefore be recycled into concrete to bring about improvements in strength, durability and rheology.

Addition of industrial by-products to concrete may not only be a viable means of using materials that would otherwise be deposited; it may also improve certain properties in the concrete. Even if a filler is inert, it may give the concrete a higher strength; not by chemical reaction, but by the added amount of fine material in the paste. The homogeneity will increase, and thus give the

concrete better properties on the whole. In an environmental context, this phenomenon may be turned to advantage and it may also make it possible to use less cement without loss of material strength.

The developed test procedure, i.e., the combination of test methods and chemical analyses and x-ray diffraction (XRD) measurements of the by-products, provides a good means of screening by-products, and makes it possible to predict their behaviour in concrete and their influence on concrete properties. These methods reveal early chemical reactions, indicate if the material has a puzzolanic/latent hydraulic effect and predict the influence on concrete durability.

REFERENCES

1. Moosberg, H. (2000), Utilisation of Chemically Inert or Puzzolanic Particles to Modify Concrete Properties and Save Cement. *Licentiate Thesis 2000:53*, ISSN: 1402-1757, Luleå University of Technology.

2. *Betonghandbok: Material* , (Reference book on Concrete: Material) (1994) Solna, Sweden, AB Svensk Byggtjänst.

Gasification Residues - a Challenge to Make Durable & Environmentally Friendly Concrete

Erika Holt
Research Scientist
VTT Building and Transport
The Technical Research Centre of Finland
P.O. Box 1805
02044 VTT, FINLAND
E-mail: erika.holt@vtt.fi

Paula Raivio
Research Scientist
VTT Building and Transport
The Technical Research Centre of Finland
P.O. Box 1805
02044 VTT, FINLAND
E-mail: paula.raivio@vtt.fi

ABSTRACT

New concepts for dealing with recycled materials and biofuels are being explored. Development work has been done for years to gasify this type of wastes. The produced gas is cleaned from the solid residues that are cement-sizes dusts. They exhibit pozzolanic reactivity which varies according to the source fuel. Unfortunately, the residues can also contain harmful compounds which limit their use. If applicable building materials are found in which the residues can be utilised it would mean a significant advantage for further introduction of gasification techniques in modern societies.

The properties of six gasification residues were studied for their suitability in compacted concrete.

Key words: gasification; by-product; composition; environment; compacted concrete; factory tests

1. INTRODUCTION

Industrial processes and power generation increasingly produce wastes and by-products that are partly utilised in building material production and earth construction. Yet, large amounts of wastes are deposited in landfills. Many of these wastes and by-products contain harmful elements or compounds that pose risks on the living organisms and the environment. It may be more beneficial to bind the harmful constituents of the by-products within building materials

rather than to pile the by-products in landfills which are more or less exposed to external weather conditions. As concrete is produced in huge quantities and for diverse products in every country it should be possible to find suitable concrete products that could also incorporate problematic wastes. Concrete developers are able to provide a valuable contribution to the industrial world and to the environment if they could develop qualified building materials that also utilise problematic constituents.

With the recent introduction in Finland of new production plants to gasify waste and generate energy, there will be more residue by-products (or wastes) which need proper disposal. In the past few years the concrete industry has accepted certain by-products, such as silica fume and fly ash, to their products. In some cases the by-product is actually improving the concrete properties, while in other cases the by-product is merely a replacement of more expensive materials like cement or filler placed in the concrete to save costs required for other disposal methods.

The types of concrete products that can accept by-products are highly dependent on the by-product's chemical composition, reactivity and grain size distribution. Before a by-product can be used, these chemical and physical properties of the by-product need to be verified. By-products can be added to the concrete in two different ways: replacing fine aggregate or cement. Replacing cement is the more economic choice of the two since cement is the most expensive ingredient in concrete. Some precautions must be taken when adding by-products to concrete products due to their chemical reactivity. By-products containing chlorides are avoided in concrete which contains steel (re-bar) or concrete that is at risk of leaching.

Another concern is that as electric utilities are upgraded to low-NO_x burners, by-product residue often has a higher carbon content. The higher carbon ash can affect concrete products as it adheres to air-entraining admixtures, causing a decrease in the volume of entrained air. (1)

A final set of criteria which may have to be met when using the by-product residues is the European standards for fly ash. (2) These standards include various limitations, especially regarding the amount of certain compounds that can be present, such as < 5% carbon, < 0.1% chlorides and < 1.0 % free lime. According to research already concluded on the current residues (3), all of these three compounds have been exceeded in some aspect.

In this research, concrete applications for the by-product substitutions were selected which would not be greatly affected by the chemical composition of the residue. For this reason, paving stones were chosen which are manufactured by compacting dry-concrete into a mould, similar to roller compacted concrete. Dry-concrete means the concrete has a low paste content, usually with a lower binder content than traditional concrete. With a lower paste and water content the concrete can not be self-consolidated by vibration and therefore requires alternative compaction methods.

Gasification Process

The gasification process was designed to dispose bio- and recycled fuels that are difficult to burn with conventional techniques due to harmful compounds. Gasification occurs at around the temperature of 900°C in a reducing environment. The residues in the product gas are collected with the cyclone and the filters and the purified gas is burned together with coal, oil or natural gas. Development of gasification techniques has been carried out since the late 1970s at VTT Energy in Finland. (4) One of the goals during the development work has been to find utilisation areas for the residues in the building industry and to avoid landfill disposal. Plans have been

made to build the first commercial-scale gasification power plant with a gas cleaning unit near Helsinki, Finland in the next years.

The composition of the cyclone and filter dusts is highly dependent on the gasified fuel and other process additives. It has been noted that the dusts often show pozzolanic reactivity. This led to the idea of utilizing the gasification residue in the manufacture of various concrete products. The dusts also can include abundant amounts of chlorine that is harmful for moulds and re-bar of some concrete. The purpose of the tests in this research was to determine if the gasification residues could be incorporated to compacted concrete for a savings in material costs. Preliminary laboratory tests were done prior to full-scale factory tests to evaluate how the compacted concrete products were affected by the gasification residue addition.

2. MATERIALS

Six gasification residue samples from various pilot or demonstration gasifications plants were provided in this investigation, as shown in Table 1 with their basic properties. Besides elemental and inorganic carbon, the residues also contained organic carbon in tars, some of which may cause risks to living organisms. Luckily the elemental carbon seemed to act as activated carbon and tightly bound the tars. The specific surface area is an indicator of how much water is required in the mixture to coat all particle surfaces and insure adequate workability.

The particle size distributions of the six residues and the reference cement, as measured by a Sedigraph 5100 machine, are shown in Figure 1. The first residue, FW-BA, had a grain size more similar to fine aggregate while the other residues had size fractions resembling cement grains. Note that 99.5% of FW-BA residue was retained on the 63 µm sieve or greater, so Figure 1 only shows the size distribution of the finer particles. From the grain size distribution we see that most of the residues were slightly coarser than the rapid hardening cement (CEM IIA 42.5R).

Table 1 – Residue Properties. BA = bottom ash. CD = cyclone dust. FD = filter dust. (3)

Residue	Gasifier Fuel	Density (g/cm^3)	Specific Surface (m^2/kg)	Carbon content (elemental + organic) %	Mineral Composition
Cement	-	3.12	440	-	-
FW-BA	straw	2.59	510	1.4	quartz, pyroxene, feldspar, amorphous
FW-CD	straw	2.28	680	25.8	sylvite (KCl), lime, calcite, amorphous
SK FD	wood	2.44	640	46.0	periclase (MgO), calcite, amorphous
ENE 99/21-FD	wood	2.32	2130	40.3	calcite, lime
ENE 99/24-FD	paper/plastic pellet	2.54	1310	11.3	calcite, lime, sylvite, halite (NaCl), metallic aluminium
ENE 99/24-CD	paper/plastic pellet	2.68	630	8.1	lime, metallic aluminium, calcite, quartz

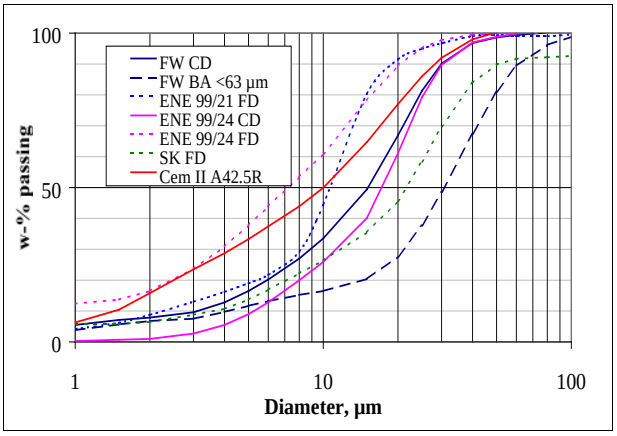

Figure 1 – Grain size distribution of residues and reference cement. (3)

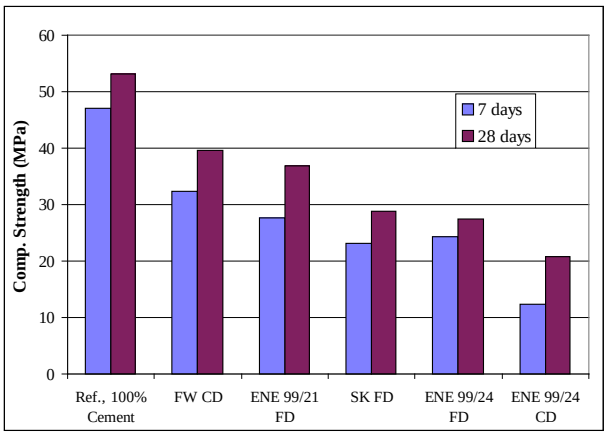

Figure 2 – Pozzolanic behavior of gasification residues.

None of these residues can be considered for use in the cement manufacturing process or in reinforced castable concrete because of their high chlorine content. Excess chlorine would accelerate the rusting of steel reinforcement bars that are often placed in structural concrete applications. High carbon content may also have a negative effect on admixtures. For these reasons compacted concrete paving stones were selected as a possible application for the residue substitutions. The residues do have a pozzolanic reaction, providing strength, similar to cement. This is demonstrated in Figure 2, where 25% of the cement is replaced with residue and tested in compressive strength.

The next sections detail the test results from concrete made with the residue FW-CD, which had the greatest pozzolanicity. This residue was characterised by the highest amount of water-soluble compounds of the studied residues, at approximately 17 w-% (mainly as sylvite, KCl). The straw-derived FW-CD residue contained negligible amount of heavy metals, least of the studied residues, and it probably does not pose a risk to the environment. It is expected that the water-soluble chlorides would be leached from the paving stones into the ground during their service life. Currently there are no limitations for chloride leaching amounts in Finland or elsewhere in Europe, but in the future limitations may be given.

The cement used was rapid hardening cement from Finnsementti Oy in Finland. Aggregates consisted of clean natural granite, with a maximum size of 10 mm and a gradation as given in Table 2. Clean cool tap water was used for mixing and no admixtures were used.

Table 2 – Aggregate Gradation

Size (mm)	% Passing
0.125	4.6
0.25	14.0
0.5	22.3
1	35.1
2	47.8
4	67.4
8	94.3
16	100.0

Table 3 – Performance Required Properties (5)

Test	Requirement
Tensile Strength (28 d)	> 3.6 MPa
Water Absorption	< 6 %
Mass Loss After Freeze-Thaw (28 cycles)	< 1.0 kg/m^2

3. EXPERIMENTAL PROGRAM

The test program included doing laboratory tests to establish the amount of FW-CD residue which could be added to the compacted concrete, followed by multiple property tests on a few selected mixtures to evaluate their performance. After laboratory tests the initial information was applied to a field test at a paving block factory, Lakan Betoni Oy in Joensuu, Finland. The factory tests used the FW-CD residue to replace cement at 2 levels. Some small trials were done in the factory before making the full scale (200 liter) mixtures.

3.1 Laboratory Mixing, Compacting and Curing Procedures

Laboratory tests were done with the residue replacing the cement at 5, 10 and 25% by weight. The materials were mixed in a 5-litre Hobart mixer for 2 minutes and then compacted in 2000 g portions in an ICT-100R machine to simulate paving block manufacturing. The ICT ("Intensive Compaction Tester", Figure 3) is used for testing the compactability of granular materials, like no-slump concrete or other similar materials. The ICT compacts the sample with a shear-compaction principle, using shear movement and pressure to get closely packed particles. (6) Compacted paving blocks are manufactured in a similar method with vibration and pressure to achieve the high-density concrete.

Figure 3 – ICT machine to simulate paving block manufacturing in a laboratory.

During compaction with the ICT, each samples' height, weight and shear values were logged on a computer at various cycle intervals. From this data it was possible to evaluate the workability and density with time for each specimen and thus determine which samples had better properties. The density corresponded to the expected porosity and strength of the samples. The final weight was an indicator of over-compaction if too much of the sample mass was lost, due to excess slurry being pressed out of the mould and too low porosity.

In some cases the ICT machine was set to compact the samples until a target density was achieved, regardless of the number of cycles. The fewer cycles that were required was an indicator of improved workability of the mixtures. In this way it was also possible to ensure that all samples had similar porosities, which is necessary for freeze-thaw resistance comparisons.

Compacted samples had dimensions of 100 mm in diameter and 100 to 110 mm in height. Immediately after compaction the samples were extruded from the moulds, weighed and labeled before moving to the curing rooms. The compacted cylinders were stored at 100% RH and 20 °C until further testing. Prior to testing all cylinders were top sliced to a height of 100 mm to make similar specimen size.

3.2 Factory Mixing, Compacting and Curing Procedures

Factory tests included using the residue replacing cement at 10 and 15% by weight. A few early trials were done in the factory to ensure proper material proportions and water amounts for the residue addition. The early factory trials included hand mixing 1 liter mixes for ICT machine compaction. The next set of early factory trials included mixing 30 liters in a pan mixer for 3 minutes. This set had 1 plate of paving blocks compacted in the large factory compactor. The ICT machine was also utilised in the early factory tests.

The main set of factory tests was done in the factory mixer with 200 liters of concrete. It was automatically placed by conveyors and mechanically compacted on the paving stone machine. Residue was added directly to the mixer with the other dry ingredients. Compaction took place approximately 5 minutes after water addition. 14 paving stones were compacted per tray, at 2.5 seconds per tray. Figures 4 and 5 show the compaction machine and final product on the conveyors.

Figure 4 – Compaction of paving stones.

Figure 5 – Tray of paving stones moving out of compaction machine in factory.

After compaction, the paving stones or ICT samples were stored at 100% RH for the first day. Paving stone samples were then transported back to VTT's laboratory for future testing. Samples were then stored at 20ºC and either 100% or 70% RH depending on the specified tests.

3.3 Required Performance Tests

As earlier mentioned, compacted concrete paving blocks were a viable concrete application for the by-product residues. The physical and mechanical properties that must be met for paving blocks are given in Table 3 as specified by the draft European standards. (5) Other properties such as abrasion resistance and slip/skid resistance would be unaffected by the residue substitution and were untested. Color and texture changes in the concrete product are allowed,

as long as they are as expected. In these tests in all cases the residue substitution resulted in samples with a darker (nearly black) appearance.

In preliminary laboratory tests, the split tensile test was done on 2 samples at 28 and 56 days. An additional 3 split tensile tests were done on the samples that had undergone the freeze-thaw test to determine if they had lost much strength during the test, though this was not required by the freeze-thaw test method.

After the factory tests flexural strength tests were done at 1, 7 and 28 days on the paving stones to assess the tensile properties. The freeze-thaw test with de-icing salt was done in accordance to the Swedish Borås test method, where the samples are wrapped in insulating rubber with only the top surface exposed to a 3% NaCl solution. The samples went through 28 cycles of 24 hours each of freezing and thawing (+24 to -16 °C) after which time the mass lost was measured.

Water absorption was done by submerging oven dried samples which were in a water bath. The weight change was measured daily until the change was < 0.1 % per day. Many times additional compression strength tests were done on samples to be used as an estimate of tensile strength.

4. LABORATORY TEST RESULTS AND EVALUATION

The results presented in the following sections are only for the basic reference concrete and for the concrete containing the Danish straw-derived residue, FW-CD.

4.1 Initial Laboratory Trials

Initial laboratory trials were done to investigate workability, density, porosity and strength with the residues. Ideal properties include high density (corresponding to high strength) and a porosity of 30-50 l/m^3 to provide adequate freeze-thaw resistance.

With the addition of the residue the following properties were seen during production and subsequent testing:

- Increased residue addition demanded more water to have the sample workability.
- Residue could be squeezed out of the samples with excess water/slurry if over-compacted.
- Concrete samples were darker with increased residue addition.
- Strength and density remained equal or decreased with residue addition.

It was possible to add up to 25% residue (the maximum amount tested) to the compacted concrete, though this reduced strength and 10% appeared to be near the maximum amount of residue which could be added without drastic side-affects. It was also possible to substitute residue for either cement or fine aggregate in the concrete. Replacing cement is more economically beneficial as long as the residue is reactive enough to provide strength similar to the cement bonding reactions.

4.2 Primary Laboratory Tests

From the preliminary tests a sample design including 10% residue was chosen for further full-scale tests. The sample had residue replacing cement. An additional reference basic mixture was

also made. The materials and mixing processes followed the same procedure as earlier described and the laboratory tests included those specified in the draft European standards (5) for paving blocks. The specimens were compacted different amounts of time (varies cycles in the machine) to achieve equivalent densities with a target porosity of 50 l/m^3 (5% air).

12 test specimens of each mixture were compacted with the mix design, average densities and air content presented in Table 4. The water-to-cement ratio had to be increased when including the residues due to the increased water demand from the larger surface area of the small residue particles.

Table 4 – Average Compacted Properties of Laboratory Primary Tests

Concrete	w/c	Density (kg/m^3)		Porosity	Cycles
		Target	Actual	(l/m^3)	Required
Basic	0.26	2410	2400	53	51
10% FW-CD	0.32	2360	2350	53	42

The results from the ICT compaction process are shown in Figure 6 over the cycle intervals. The amount of cycles required to achieve the target density and porosity indicated the workability of the mixture. The workability of the mixtures is influenced by the size of the residue particles and their ability to pack tightly. The FW-CD residue is coarser than cement (from sedigraph, Figure 1) and thus required less work (cycles) to reach the required density and porosity. Therefore, in field applications the addition of some residues could be beneficial as it would require less effort to compact samples, saving on time and energy cost.

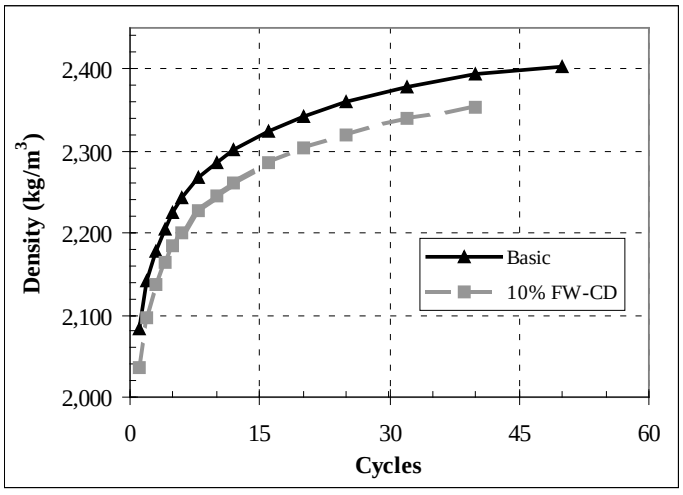

Figure 6 – ICT results showing amount of cycles needed to reach target densities. Fewer cycles represents improved workability.

After curing the compacted samples had various tests applied as described earlier. The later age laboratory test results are shown in Tables 5 and 6.

Table 5 – Strength Test Results at 28 days of Laboratory Primary Tests

Residue	Strength (MPa)		
	$Compressive_{cyl100}$	$Compressive_{cube150*}$	Tensile
Required	-	-	> 3.6
Basic	42.8	45.0	5.4
10% FW-CD	44.1	46.4	4.7

*Note: Converted from the measured "$Compressive_{cyl100}$" according to Beton-Bogen (7).

Table 6 – Weathering Test Results of Laboratory Primary Tests

Residue	Mass Loss with Freeze-Thaw (kg/m^2)	Absorption (%)
Required	< 1.0	< 6
Basic	0.0	4.1
10% FW-CD	0.3	5.4

From these results we see the residue tested met all the requirements for its use in compacted concrete paving blocks. There was actually a compressive strength increase as FW-CD residue was added as cement. This is a great benefit, since the water-to-cement ratios for the mixture was increased (usually resulting in decreased strength) compared to the reference mixture. Therefore it is shown that the residue has good benefits in the paving stones, as it is performing better than the reference mixture. The residue samples had a slight decrease in tensile strength compared to the reference concrete but it was < 15% and still far above the required strength.

The absorption of the samples was under the required 6%, though the residue concretes absorbed more water than the reference mixture. The residues' carbon content and higher specific surface are likely responsible for the higher absorption of the residue concretes.

In the freezing-thawing tests the samples were well within the range of allowable mass loss. The concrete containing the residue did have a greater mass loss than the reference concrete but still much lower than the limit. An extra non-required tensile test comparison was done on the samples that had underwent the freeze-thaw tests to see if there was a drastic reduction in strength following the severe environmental exposure. These strength values are presented in Table 7 and show that the strength was reduced quite a bit after the freeze-thaw test. This could be a concern for the FW-CD residue, as there was a 35% reduction in strength as well as a distinct mass loss. The strength reduction is probably due to the high content of water-soluble compounds (approx. 17%) in the FW-CD residue.

Table 7 – Change in Split Tensile Strength After Freeze-Thaw Tests

	Split Tensile Strength		Strength
	Before (MPa)	After (MPa)	Change (%)
Basic	5.4	4.7	13
FW-CD	4.7	3.0	35

5. RESULTS OF FIELD TESTS

The FW-CD residue obtained from Foster-Wheeler's pilot gasification plant was also used in further factory field tests. This residue was chosen because it had the best pozzolanic reactivity (see Figure 2). The factory tests at Lakan Betoni Oy also had 2 parts: some small preliminary

trials and then the primary factory tests. The factory trials were done with residue added at 10% and 15% by cement replacement.

Table 8 shows the mix designs for the primary factory tests, where the cementitious material amount was held at 350 kg/m^3 for all tests. The aggregate and water amounts were adjusted with the residue addition to provide adequate workability and comparable compaction times to get equivalent densities of the final product.

Table 8 – Mixture Proportions for Factory Tests
(Lab = Preliminary, 40 liters; Factory = Primary, 200 liters)

	Basic Mix	10% Mix	15% Mix
Residue (%)	0	10	15
Cement (kg/m^3)	350	315	297.5
FW-CD Residue (kg/m^3)	0	35	52.5
Actual Water (kg/m^3)	63	107.5	117.5
Aggregate (kg/m^3)	1910	1835	1800
Water/Binder Ratio	0.18	0.31	0.34
Agg/Binder Ratio	5.46	5.24	5.14

5.1 Preliminary Factory Tests (40 liters)

The preliminary factory tests were done on a small scale to verify how much the aggregate and water amounts should be adjusted. They showed that the aggregate gradation of field materials was different and would require less water than the initial VTT laboratory tests. The compaction showed that the masses were slightly drier than desired and the later tests confirmed this hypothesis. The tensile strengths were lower and the moisture absorption was too high, likely due to the excess pores when the proper compaction was not achieved.

5.2 Primary Factory Tests (200 liters)

The main tests done in the factory again had 10 and 15% FW-CD residue replacing cement. Both mixtures appeared good and had adequate compaction in the large factory machine. Factory staff commented that both mixtures looked “normal” and could be applicable in the field. The ICT machine was also used to compact a small sample from each concrete batch made in the factory. Additional compression and flexural strength tests on paving stones were done at the age of 7 and 28 days in VTT’s testing laboratory.

The hardened concrete test data is presented in Table 9. It must be noted (*) that the 1 day compressive strength was done on an ICT cylinder while all other strength tests were performed on paving stones.

Table 9. Strengths of Paving Stones in Factory Tests (Note: ICT cylinder)*

	Time (d)	Basic Mix	10% Mix	15% Mix
Compressive Strength (MPa)	1 *	24.1	21.9	20.7
	7	37.9	40.2	38.9
	28	44.3	39.8	43.2
Flexural Strength (MPa)	1	5.1	4.3	4.3
	7	6.3	6.1	6.4
	28	6.5	6.3	6.4
Density (kg/m^3)		2219	2197	2234
Absorption (%)	7	5.0	5.3	5.7
Void Content (%)		17.7	13.9	14.4
Frost Resistance (kg/m^2 lost)	28 cycles	0.2	1.2	1.6
Freeze-Thaw Resistance (Relative Ultrasound)	28 cycles	0	-0.01	0.00

The results show that strength improved with aging from 1 to 7 to 28 days. The addition of both 10% and 15% residue had no detrimental effects even though it replaced the ”binding” cement. Lower strength at the age of 1 day for the residue concretes was expected, since the pozzolanic behaviour of the residues is slower than cement. At the age of 7 days, the compressive strength was greater in the residue concretes compared to the basic mixture. By 28 days the variation in strengths is less than 10% and acceptable. The flexural strength was about equivalent at 7 and 28 days in the residue mixes compared to the basic mixture.

A high density was desired for all paving stones, since the density corresponds to strength. All paving stones had a similar density of approximately 2200 kg/m^3. It was good to see there was no loss of density with the residue addition, which has a lower density compared to cement.

The absorption of the paving stones was tested to ensure they would not uptake excessive amounts of water. The results presented in Table 9 show both factory mixtures had absorption values below the limit of 6% as specified. The mixtures with residue had higher absorption than the reference mixture but not too excessive.

Frost scaling resistance was tested using the Swedish Borås method (SS 13 72 44) after the paving stones had aged to 28 days. A standard freeze-thaw test was also done to assess internal frost resistance. After the freeze-thaw testing the mass loss was measured, which should be under 1.0 kg/m^2 after 28 cycles of freezing. The results showed both mixtures containing residue had mass loss values over the limit, whereas the reference sample was well within the limit. This lack of frost scaling resistance is likely due to over-compaction of the paving stones. With the addition of the fine residue the smaller pores are filled in the mass and do not provide adequate space for freezing. This was confirmed by measuring the paving stones percentage of air voids. As seen in Table 9, the air void content was lower for the residue containing paving stones. In future work this would need to be improved to provide adequate frost resistance. Additional tests by a standard freeze-thaw test (SFS 5447) showed no drastic reduction in the ultrasonic pulse velocity measurements after 28 cycles of exposure. The recommended limit is a reduction in the relative ultrasound of less than 0.33, which all test mixtures met.

The final color of the paving stones with the residue addition was of great importance to the factory. Currently they use an expensive pigment to provide the black color to the paving stones. If this could be eliminated with the use of the gasification residue it would be very useful to the

factory production as well as the residue disposal aspects. The black in the residue is a result of the carbon, which will not bleach with sun exposure or aging. Figures 7 and 8 show the variation in color of the paving stones with the addition of 10 and 15% residue compared to the reference concrete. The color was not as dark as the factory staff would have liked and it would take a high percentage of residue addition to get a truly black paving stone. It may be possible that the pigment amount could be reduced with using the residue.

a. b.

Figure 7 – Comparison of black hue for reference (a) and 15% residue addition (b) in factory paving stones.

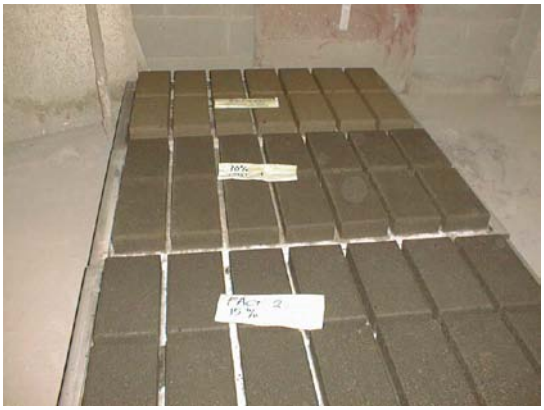

Figure 8 – Comparison of the three different paving stone colors (from back: 0, 10 and 15% residue).

6. CONCLUSIONS

Residue by-products resulting from gasifying waste materials can be suitably placed in concrete. Due to their chemical composition it is necessary to limit their use to non-structural applications where they will not aid corrosion of steel reinforcing. For this reason the application of paving blocks made from compacted concrete was chosen. The addition of the residues provided a dark or black color to the paving stones which could be to a great advantage and should be marketed for field applications.

The residue particle size is similar to very fine aggregate or cement. Replacing cement is the more economic choice since the cement is the most costly item in paving block production. The residues have some pozzolanic reactive behavior but not as strong as basic cement binder. For this reason the residue substitution could not exceed 25%. The substitution amount of 10% seemed more viable and still resulted in the darker colored concrete.

In the preliminary laboratory test series it was determined that using FW-CD residues had no harmful changes to the strength or weathering properties of the concrete. The tensile strength, mass loss after freeze-thaw tests and absorption were all well within the allowable limits proposed by the draft European standards for paving blocks (5). The compressive strength was increased when adding the residue as cement, even though the water amount was increased. The strength benefit of the residues could result from their reactivity and small particle size and this advantage should be marketed.

At the Lakan Betoni Oy paving stone factory the FW-CD residue derived from straw was added to the paving stones at 10 and 15% by weight to replace cement. The mixtures were workable and could be compacted to similar densities as the reference mixture. The compressive strength, flexural strength and absorption were again within the limits. Resistance to freezing and thawing

needs to be improved by optimizing the production and material proportions. There were no complications when applying the preliminary laboratory tests to full-scale production in a factory. This application of gasification residues to concrete paving stones may show future success and could be used as a viable method for by-product disposal. The use of residues is also beneficial to the factory, as it can greatly reduce their material costs when residue replaces the cement.

REFERENCES

1. The 1997 International Ash Utilization Symposium, Preface, Fuel, (1999).
2. Fly Ash for Concrete -- Definitions, Requirements and Quality Control, European Standard EN 450, 1995.
3. P. Raivio, Internal Report RTE36-IR-20/1999, p. 23, Technical Research Centre of Finland, 1999.
4. E. Kurkela, A. Moilanen, and M. Nieminen, in Power Production from Biomass III - Gasification and Pyrolysis R&D&D for Industry Eds. K. Sipilä and M. Korhonen, Finland, 213 (1999) .
5. Concrete Paving Blocks, draft European Standard prEN 1338, 1996.
6. Intensive Compaction Tester, Operating Instructions, model ICT-100R/RB, Invelop Oy, 1997.
7. Beton-Bogen. Aalborg Portland/CtO. 2'nd edition 1985 (In Danish).

Durability of Fibre Reinforced Concrete Structures Exposed to Mechanical and Environmental Load

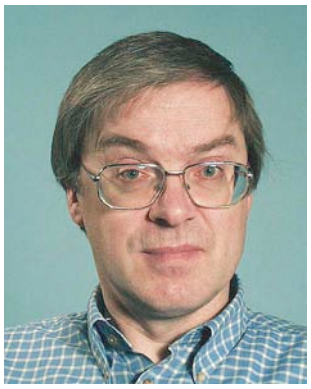

Ernst Jan de Place Hansen*
Ph.D., Senior Researcher
Danish Building and Urban Research
P.O.Box 119, DK-2970 Hørsholm, Denmark
E-mail: ejp@by-og-byg.dk

Kurt Kielsgaard Hansen
Ph.D., Associate Professor
Dept. of Civil Engineering, Technical University of Denmark
Building 118, Brovej, 2800-Kgs. Lyngby, Denmark
E-mail: kkh@byg.dtu.dk

ABSTRACT

Durability studies are carried out by subjecting fibre reinforced concrete (FRC) beams to combined mechanical and environmental load. The mechanical load is retained while the beams are exposed to a chloride solution or pure water. The test programme involves four different concrete qualities. Both steel fibres and polypropylene fibres are used as well as main reinforcement. Uncracked FRC-beams and beams without fibres are used as reference. This paper gives an overview of the main results from the durability tests and summarizes the discussions and the conclusions regarding the effect of fibres, cracks and concrete quality on the durability of FRC-structures.

Key words: concrete, fibre, durability, cracks

1. INTRODUCTION

Fibre reinforcement has been introduced in concrete to improve the fracture toughness. The improvement of the fracture toughness is related to the ability of the fibres to arrest cracks and to minimize the extent of cracking and the crack width. Since durability is related to ingress of substances such as water and chloride this change of crack pattern is expected to improve the durability compared with plain concrete. Although FRC has been studied for several years, the main part of the research has involved mechanical properties.

The purpose of the durability tests performed in this project is to indicate whether FRC exposed to a combination of mechanical and environmental load is less or more durable than concrete without fibres. Secondly, it is the aim to identify important mechanisms for the effect of the fibres on the durability.

* The first author was employed at the Technical University of Denmark when this research was made.

In the laboratory, degradation mechanisms are normally treated separately, and in most cases, no mechanical load is involved when materials are tested for durability. However, natural exposure of concrete structures consists of a combined mechanical and environmental load (e.g. water, chlorides and freeze-thaw). Therefore, in this project, specimens are subjected to a combined load. Durability tests are combined with studies of the pore structure, fire tests and full scale tests. An overview of the test programme is given in [1].

2. MATERIALS

Except for fire tests (Section 3.2), three different concrete mixes, relating to three different environmental classes, are tested [2], [3], refer to Table 1. M = moderate environmental class, A = aggressive, SA = more severe than A. All concretes contain fly ash and silica fume. Water/powder ratio: 0.52 (M), 0.44 (A), 0.38 (SA). Aggregates are rounded (class M) or crushed rock (class A and SA). All concretes are air entrained, 2.5 - 4% air for class SA concrete, 6 - 9% air for class A and M concrete. The concretes contain differing amounts of plastizicers to maintain acceptable workability. The mixes are chosen to represent mixes made in Denmark today.

The 28 days compressive strength of the concrete mixes is based on 100/200 mm cylinders (wet cured), f_{cyl100}. For comparison, the compressive strength is recalculated from 100/200 mm cylinders to 150 mm cubes (wet cured), $f_{cube150}$. Both f_{cyl100} and $f_{cube150}$ is given in Table 1, for class M, A and SA respectively.

Table 1 - Concrete mixes without fibres, plastizicers and air entrainment. Durability tests.

Materials [kg/m^3]	Class M	Class A	Class SA
Equivalent water/cement ratio [1]	0.52	0.44	0.38
Cement (CEM I, ASTM Type III)	240	-	-
Cement (CEM I, ASTM Type V)	-	298	285
Fly ash	65	65	60
- Fly ash [% of cement / binder]	27 / 21	22 / 18	21 / 17
Silica fume - slurry [2]	15.5	15.5	24
- Silica fume [% of cement / binder]	3.3 / 2.6	2.7 / 2.2	4.2 / 3.4
Water	142	140	115
Fine aggregate 0-4 mm	774	702	758
Coarse aggregate 4-8 mm	319	340	-
Coarse aggregate 8-16 mm	649	680	535
Coarse aggregate 16-25 mm	-	-	565
f_{cyl100} [MPa]	31.6	41.6	54.6
$f_{cube150}$ [MPa] [3]	36.7	48.2	63.3

Note:
[1]: The amount of water included in the plastizers and air entrainment is disregarded.
[2]: The silica fume - slurry consists of about 50% water.
[3]: Converted from the measured f_{cyl100} according to the introduction in the proceedings.

Fixed amounts of three different types of fibres are used, 1.0 % by volume of polypropylene fibres (PP), 0.4% by volume of steel fibres with hooked ends (ZP) or 0.066% by volume of polypropylene fibres (CS) especially designed for control of cracking due to plastic shrinkage. The following combinations of concrete mixes and fibres are studied: M-0, M-PP, M-ZP, A-ZP, SA-0,

SA-CS, SA-PP and SA-ZP. 0 refers to concrete without fibres. Uncracked beams and beams without fibres are used as reference. The values for the compressive strength given in Table 1 is representative for all the studied combinations of mixes and fibres.

3. TEST SET-UP AND EXPOSURE CONDITIONS

3.1 Durability tests

Beams with dimensions 100x200x1150 mm are used as specimens. A test set-up has been developed to permit beams to be subjected to combined mechanical and environmental load as described in [4]. The beams are subjected to 4-point bending, resulting in transverse cracks on the centre part of the beam as indicated on Figure 1.

The beams contain main reinforcement, rebar size 8 mm, cover depth 30-35 mm (tension side), 12-15 mm (compression side), respectively. The amount of load is determined as the amount required to produce predetermined levels of crack width immediately after loading. Two levels of crack widths are involved; 0.05-0.1 mm and 0.15-0.35 mm in order to investigate the importance of crack widths on the durability, especially when exposed to chlorides. The surface crack pattern immediately after loading is characterized using video-scanning and digital image analysis. The crack width of each crack is measured in 5-9 positions along the crack.

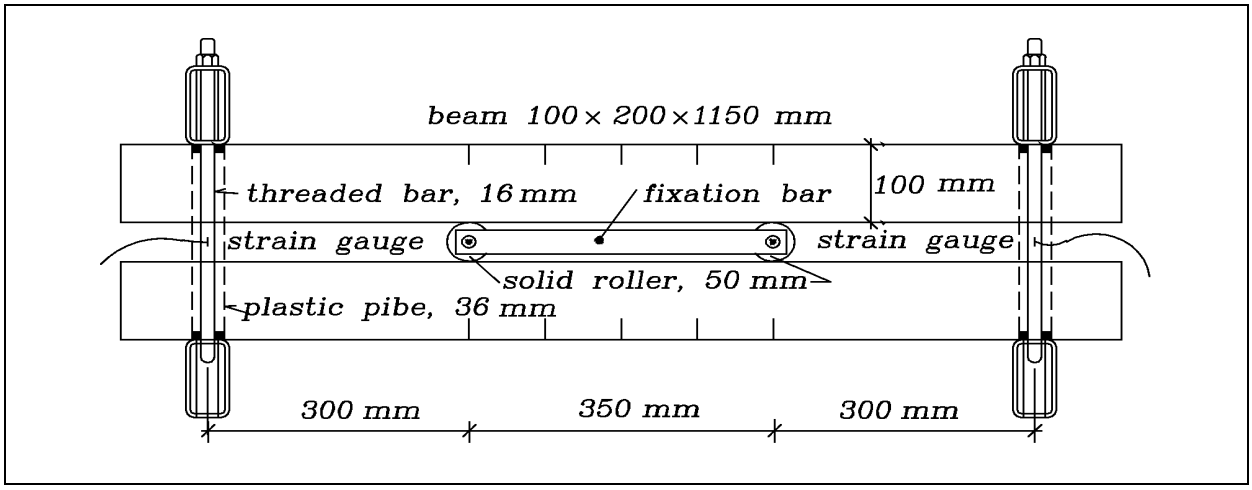

Figure 1 - Test set-up to precrack specimens for durability testing (cracks are indicated). The fixation bar is removed before loading.

Several test methods are applied to simulate environmental load, including exposure to water or water vapour [5], [6], [7], chlorides [8], [9] and freeze-thaw with de-icing salt [3], [10]. A test set-up has been developed for in-situ water uptake [4]. Two methods are applied to characterize the chloride content qualitatively, the UV-test and Electron Probe Micro Analysis (EPMA) [11], [12]. They are compared with traditional chloride profile measurements performed with a commercial kit, Germann's Rapid Chloride Test (RCT) [8]. Beams are exposed for chlorides for 7 or 13 months. When downsizing beams for measurement of chloride content, the main reinforcement and the steel fibres are inspected for signs of corrosion. Thin section analysis is applied on specimens exposed to chlorides or freeze-thaw. The pore size distribution of the concretes is determined. Test methods are described further in [2], [3], [4], [13], [14].

3.2 Fire tests

Fire resistance of high performance FRC-structures with a water/powder ratio 0.32 (including 7% of micro silica) and either 0.5% by volume of PP-fibres, 1% by volume of ZP-fibres or 0.066% by volume of CS-fibres is investigated at Dept. of Building Technology and Structural Engineering, University of Aalborg. The purpose of these tests is to investigate the influence of fibres on the fire resistance of concrete and the influence of fibres on explosive scaling at heating. Especially two hypotheses are to be confirmed or rejected: 1) whether fibres are able to refine the crack system and improve the toughness/tensile strength, 2) whether the PP-fibres leave small canals through which the water vapour can disappear when they melt. The properties during fire exposure are tested 1) by determination of the fracture toughness of beams heated to 400°C, 2) by heating mechanically loaded beams to 400°C and 600°C and thereafter increase the load until failure, 3) by exposing mechanically loaded beams to a Danish standard fire test for 60 min. In this test the temperature of the fire chamber follows a $\log_{10}$ curve by which the temperature reaches 950°C after 60 min. The beams contains main reinforcement. Also compressive strength of cylinders heated to 400°C or exposed to a Danish standard fire test is determined [14], [15].

3.3 Full-scale tests

At a full-scale test field outside Ølstykke six lanes of concrete has been cast in October 1997 [16]. The lanes are made of class SA concrete with about 6% of air and with different combinations of ZP- and CS-fibres (1.0% by volume, 0.066-0.132% by volume respectively). During the first year after casting moisture profiles are determined in term of water content and RH on cored cylinders. Other cored cylinders are exposed to freeze-thaw in the laboratory. These results are compared with the frost resistance of SA-concrete cast in the laboratory.

4. TEST RESULTS

A short presentation of the main results is given below with focus on the chloride exposure. A presentation and discussion of the test results in general is found in [14]. Refer also to [2], [3], [4], [13] and [15] for detailed discussions. Main discussions and conclusions from [14] are given in Section 5 and 6.

4.1 Durability tests

In general, the exposure of concrete specimens to environmental load shows the importance of 0.05-0.35 mm wide cracks on the penetration of water and chlorides. As an example beams exposed to chlorides for 13 months are shown in Figures 2 and 3. After exposure the beams are unloaded and a silver nitrate solution is sprayed on sawn concrete surfaces perpendicular to the surface exposed to chlorides. After a few minutes of UV-exposure areas containing free chlorides change in colour to blue or grey while the rest remain brown in colour. The boundary between these areas is marked on Figures 2 and 3 as well as the mechanically induced cracks.

Figure 2 - Chloride exposed specimen after UV-test. Concrete SA-ZP. Exposure time 13 months. Load level 3.6 kNm. The beam contains 7 mechanically induced cracks, crack width between 0.07 and 0.28 mm (one crack is not included on Figure 2). Overall average crack width 0.17 mm. Beam size in vertical direction 100 mm. Thick, mostly horizontal lines indicate the boundary found by the UV-test. Thinner, vertical lines indicate the visible, mechanically induced cracks.

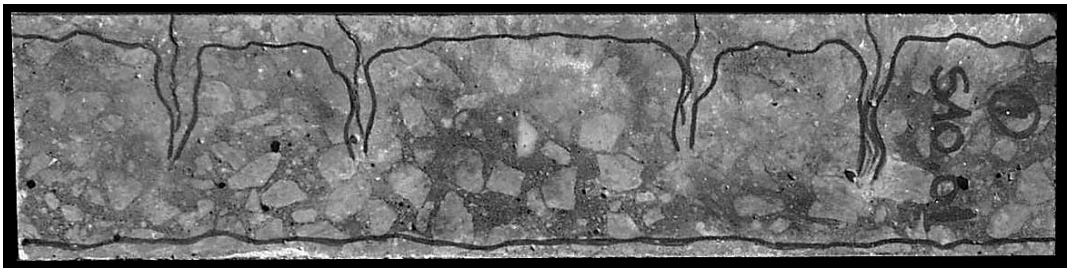

Figure 3 - Chloride exposed specimen after UV-test. Concrete SA-0. Exposure time 13 months. Load level 2.0 kNm. The beam contains 4 mechanically induced cracks, crack width between 0.21 and 0.32 mm. Overall average crack width 0.27 mm. Beam size in vertical direction 100 mm. Added lines: see Figure 2.

The depth of penetration is seen to be much larger around cracks than in areas without visible cracks. Notice also, that when 0.4% by volume of ZP-fibres are added to the SA-concrete, the concrete can be exposed mechanically to 80% higher level without increasing the depth of penetration as shown in [2]. This means that the addition of fibres because of the effect on the mechanical properties also improves the durability.

EPMA is applied on 25x25 mm samples sawn from the beam in Figure 2 perpendicular to the original chloride exposed surface. Figures 4 and 5 show the result of mapping for chlorides on these samples. In Figure 4 the top edge equals the originally exposed surface, while the area in Figure 5 is positioned about 50 mm from the exposed surface. Figure 4 represents an area without visible cracks while Figure 5 represents an area around a mechanically induced crack. The crack in Figure 5 is highlighted in Figure 6.

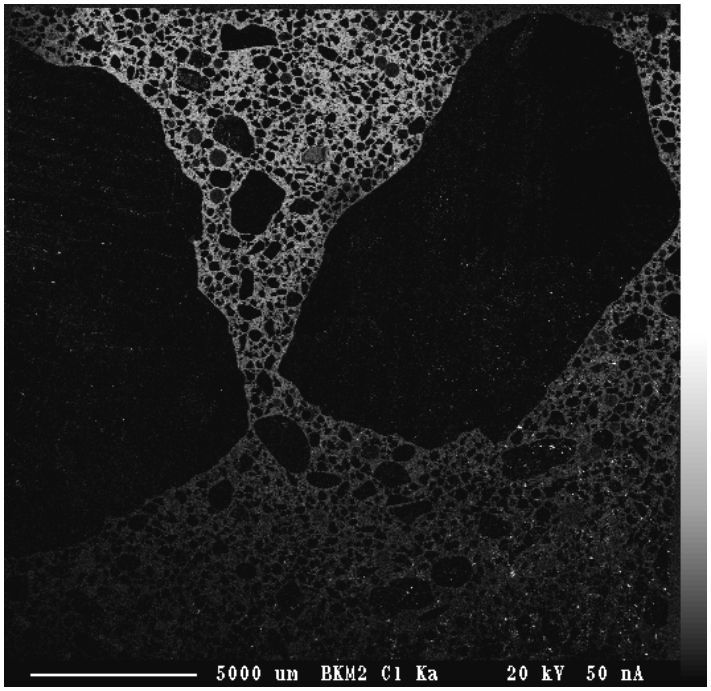

Figure 4 - Detail of chloride exposed specimen in Figure 2, area without visible cracks. Mapping for chlorides by means of EPMA. Concrete SA-ZP. Top edge corresponds to originally exposed surface.

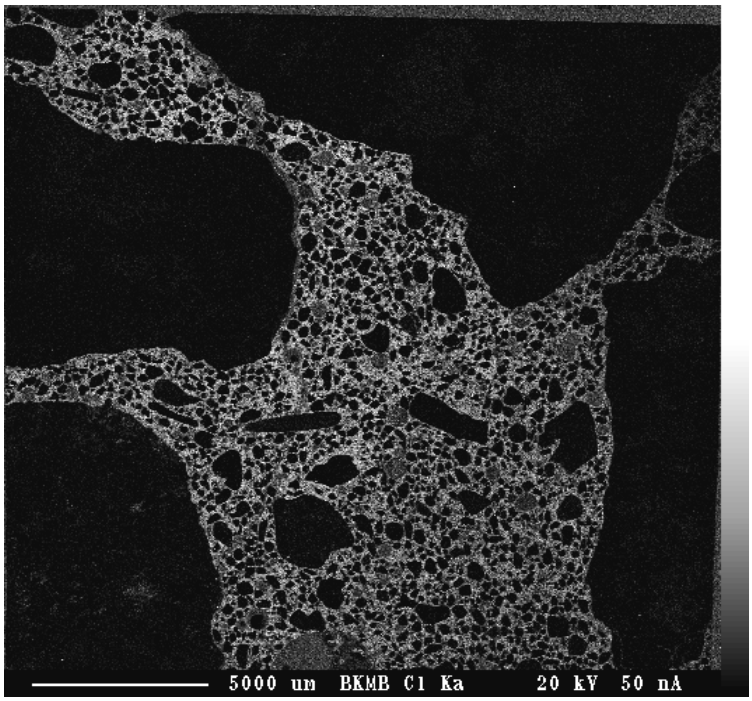

Figure 5 - Detail of chloride exposed specimen in Figure 2, area with mechanically induced crack (see also Figure 6). Mapping for chlorides by means of EPMA. Concrete SA-ZP. Centre of the samples is positioned about 50 mm from the exposed surface.

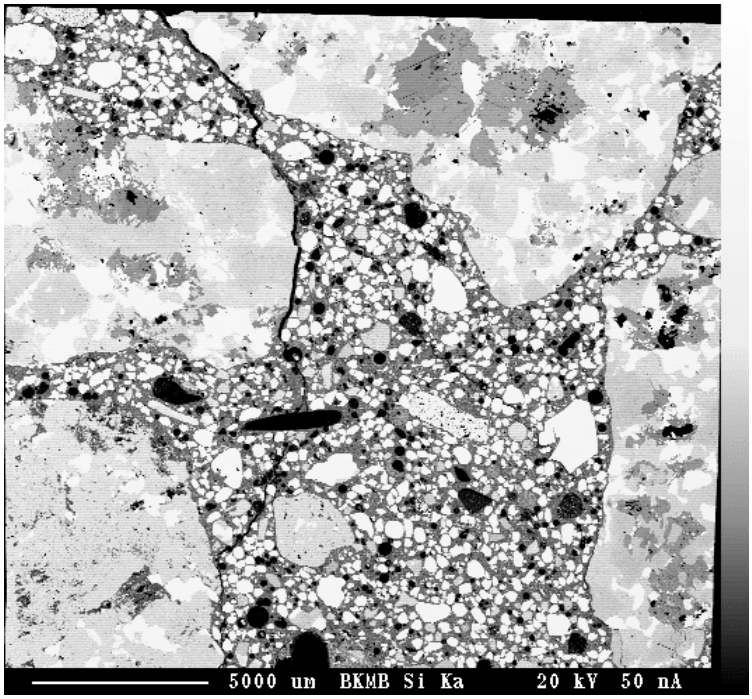

Figure 6 - Same detail as Figure 5. Mapping for silicon. This accentuates the position of the crack; it runs from top to bottom in the left side of figure. The dark spot in the centre of the figure shaped as the cross section of a wing of an aeroplane is a steel fibre.

Both samples include aggregate with grain size about 10-15 mm. While Figure 4 shows a decreasing chloride content from the top edge the chloride content is high in all parts of the cement paste in Figure 5. The crack in Figure 5 acts as an extra surface from which the chlorides penetrate into the concrete.

Addition of fibres to concrete cannot replace air entrainment to secure freeze-thaw de-icing salt resistance. The performed tests indicate that FRC-structures need about 6% air in the fresh state to withstand freeze-thaw exposure. The laboratory mixed class SA concretes contained considerably less air than expected, especially when PP-fibres were added. The results therefore emphasize the need for a critical evaluation of the mix design and the mixing methods when designing FRC-structures, [3], [13].

4.2 Fire tests

Specimens stored at laboratory climate before heating to 400°C showed that the addition of PP- or ZP-fibres increases the residual strength by 5-10%, [14], [15]. Some of the specimens failed at 250°C because of spalling. Therefore, the rest of the specimens were stored at 80°C until the loss of moisture in 24 hours was below 0.1% by weight. Plane section analysis show that all the concretes are fully cracked after exposure to a standard fire test with or without fibres. This indicate that the rate of heating during the fire tests is to high to differentiate between the different concretes and thereby evaluating whether fibres have any effect on the fire resistance of high performance concrete. The temperature in the centre of the beams and at the surface reached 400°C and 800°C respectively after 40 min. The standard fire test reduced the compressive strength by 75%.

5. DISCUSSION

The following discussion is based on the presentation of test results in [14].

5.1 Cracks and durability

The importance of cracks on the durability of the tested concretes seems to depend on the type of degradation. While penetration of chlorides and moisture uptake is markedly increased around mechanically induced cracks [2], [4], the existence of cracks does not seem to affect the amount of scaling during freeze-thaw tests [3]. The fact that degradation related to freeze-thaw in combination with de-icing salt primarily is a surface degradation could explain this.

The depth of penetration of chlorides is several times higher around 0.05-0.35 mm wide cracks than in uncracked area. It seems that the crack depth, the concrete quality and the time of exposure are more important for the chloride penetration than the crack width is. It has not been possible to confirm or disprove the existence of a lower limit below which no chloride penetration is measured in a crack. Even at 0.05 mm the crack affects the chloride penetration considerably. With 0.05-0.35 mm wide cracks no correspondence seems to exist between crack width and chloride content around the cracks [2]. Since chlorides penetrate into concrete along with water, the depth of penetration is an indication of the penetration of water as well as chlorides into concrete.

A difference in the density of micro cracks in areas of specimens in tension and areas in compression while exposed for chlorides is shown by thin section analysis [14]. This explains observations of different depths of penetration of chlorides between tension and compression side of specimens; 1.5-2 times higher in tension side. Although a total content of chlorides up to 1.5% by weight of concrete is detected around main reinforcement only very little amount of corrosion of main reinforcement is seen.

5.2 Effect of fibres and concrete quality on the durability

Generally, fibres have a positive effect on the durability because the crack pattern is characterized by less continuous and less deep cracks compared with concrete without fibres. This effect is seen even when FRC-structures are loaded to a higher load level than concrete without fibres, cf. Figures 2 and 3.

When mechanically loaded the effect of fibres on the durability is increased with the concrete quality. A 40-80% higher mechanical load can be accepted when using concrete with water/powder ratio 0.38 without increasing the crack depth and the depth of chloride penetration. The load can only be increased 10-15% when using concrete with water/powder ratio 0.52 [2].

Visual inspection indicates that steel fibres only corrode if they are in direct contact with the surface exposed to chlorides [14]. Fibres are defined as being corroded when a discolourization is seen. The amount of corrosion, i.e. the reduction in diameter of the fibres is not studied. Whether fibres in contact with the surface of a visible, mechanically induced crack are corroded (discolourized) is not studied in detail because the size of the cracks limits the availability for

inspection. On the other hand, no effect of eventual corrosion on the mechanical behaviour during the chloride exposure (expressed as a reduction in load level) is observed.

Addition of fibres does not affect the water uptake of concrete. Freeze-thaw and chloride exposure tests indicate that 0.4% by volume of steel fibres are more effective than 1.0% by volume of PP-fibres in relation to withstand scaling or chloride penetration [2], [3], [4]. This corresponds with the fact that the addition of PP-fibres makes it harder to obtain a satisfying air content in relation to frost resistance and that the PP-fibres have a negative effect on the workability of the concrete.

Thin section analysis show that fibres in general are well mixed into the concrete [3]. No special arrangements are made during casting of steel fibre reinforced concrete compared to concrete without fibres. When casting concrete with PP-fibres, the fibres are mixed with moist sand prior to the concrete mixing. Addition of fibres do not change the importance of a good concrete quality, a certain amount of air entrainment and a suitable thickness of the concrete cover to secure the concrete durability.

The performed fire tests cannot be used to confirm or disprove two hypotheses concerning the effect of fibre reinforcement on the fire resistance of concrete, especially whether they can reduce the explosive spalling of high performance concrete.

6. CONCLUSIONS

Based on the performed tests the conclusions for the project are as follows, as given in [14]:

- Cracks (0.05-0.35 mm at surface) increase the penetration of chlorides and water heavily. The cracks act as motorways for the ions from the concrete surface into the concrete.

- It has not been possible to confirm or disprove the existence of a lower limit of crack width at the concrete surface below which no chloride or water penetration is measured in a crack.

- Crack depth, concrete quality and duration of exposure are more important for the penetration than the crack width.

- Formation of micro cracks in the tension zone can explain the differences in depth of penetration in areas without visible, mechanically induced cracks; 1.5-2 times higher in the tension side.

- Steel fibres seem only to be corroding if they are in contact with the exposed surface.

- Only very little amount of corrosion of main steel reinforcement is seen although very high contents of chlorides is detected around main reinforcement.

- The lower the water/cement ratio the more effective are the fibres in relation to improving the durability of the tested concretes.

- Thin section analysis show that fibres in general are well mixed into the concrete.

- Freeze-thaw tests show that a higher amount of air entrainment is needed to maintain a satisfactory amount of air (6-7% by volume) when fibres are added.

- Addition of fibres does not change the importance of a good concrete quality and a suitable thickness of the concrete cover to ensure the durability.

7. ACKNOWLEDGEMENTS

Thin section analysis is performed by Rambøll in Virum, freeze-thaw test at The Concrete Centre at the Technological Institute in Taastrup and fire tests at the University of Aalborg. Electron Probe Micro Analysis is performed at Dept. of Chemistry, University of Aberdeen, Scotland. The present work is part of the research project *Design Methods for Fibre Reinforced Concrete* funded by the Materials Technology Development Programme, MUP2, under the supervision of the Danish Council of Technology, the Danish Technical Research Council and the Danish Natural Science Research Council.

REFERENCES

1. Hansen, E.J. de Place and Hansen, K.K., "Durability of fibre reinforced concrete structures". *Proceedings*, Nordic Concrete Res. Meeting, Espoo, Finland 1996 (Norsk Betongforening, Oslo, Norway 1996), pp.277-278.
2. Hansen, E.J. de Place, Ekman T. and Hansen, K.K., "Durability of fibre reinforced concrete structures exposed to chlorides". *Proceedings*, 8th International Conference on Durability of Building Materials and Components, Vancouver, Canada, May 30-June 3, 1999. Vol.1. (M.A.Lacasse, D.J.Vanier, ed., NRC Res. Press, Ottawa, 1999), pp.280-289.
3. Hansen, E.J. de Place, "Frost resistance of fibre reinforced concrete structures". *Proceedings*, 3rd Nordic Research Seminar on Frost Resistance. Lund, Sweden, Aug 31 - Sep 1, 1999. (Report TVBM-3087, Div. of Building Materials, Lund Inst. of Technology), pp.19-27.
4. Hansen, E.J. de Place and Nielsen, L., "Durability of cracked fibre reinforced concrete structures". In 'Advanced Design for Concrete Structures. Symp. held at Chalmers University of Technology, Göteborg, June 12-14, 1997. (A publication of Int. Center for Numerical Methods in Eng. (CIMNE), Barcelona 1997, Gylltoft, Engström, Nilsson, Wiberg and Åhman (Eds.)), pp.145-152.
5. Fagerlund G., 'The critical degree of saturation method of assessing the freeze/thaw resistance of concrete". *Materials and Structures*, Vol.10, No.58, 1977, pp.217-253.
6. BS 1881, "Methods of testing concrete. Part 5. Methods of testing hardened concrete for other than strength". British Standards Inst., London. 1970, pp.27-35.
7. Thorsen T., ""Inverted-cup" method". In 'Building Physics in the Nordic Countries'. Symposium and day of Building Physics in Lund, Sweden, August 24-27, 1987. (Document D13:1988, Swedish Council of Building Research, Stockholm 1988), pp.380-385.
8. Germann Instruments, "In-situ Test Systems for Durability, Inspection & Repair of Reinforced Concrete Structures". Catalogue IST-98. Germann Instruments A/S In-Situ Test Systems, Copenhagen, Denmark, 1998.
9. "Standard Test Method for Electrical Indication of Concrete's Ability to Resist Chloride Ion Penetration". ASTM C 1202-91, Feb 1992. American Society for Testing and Materials. (Annual book of ASTM standards, vol.04.02).

10. SS 13 72 44, "Testing of concrete - hardened concrete - Scaling at freezing" (in Swedish). SS 13 72 44 (Swedish Standard), 3.edition. Standardiseringen i Sverige, 1999.
11. Schöppel K., Dorner H. und Letsch, "Nachweis freier Chlorionen auf Beton-oberflachen mit dem UV-Verfahren". *Betonwerk und Fertigteil-Technik*, Vol.54, No.11, 1988, pp.80-85.
12. Jensen, O.M., "Chloride ingress in cement paste and mortar measured by Electron Probe Micro Analysis". *Series R* No 51. Dept. of Structural Engineering and Materials, Technical University of Denmark. Lyngby 1998. 60 pp.
13. Hansen, E.J. de Place, "Durability of cracked fibre reinforced concrete exposed to freeze-thaw and de-icing salt". *Proceedings*, Construction and Environment. CIB World Building Congress 1998, Gävle, Sweden, 7-12 June. (Int. Council for Building Research Studies and Documentation (CIB), Rotterdam 1998 (CD-ROM and abstract folder)). 8 pp.
14. Hansen, E.J. de Place, "Durability of fibre reinforced concrete structures. Experimental investigations" (in Danish). *Series R* No 63. Dept. of Structural Engineering and Materials, Technical University of Denmark. Lyngby 1999. viii + 128 pp.
15. Christensen, F.A. and Hansen, F.T., "MUP2 Durability. Fire tests" (in Danish). Dept. of Building Technology and Structural Engineering, University of Aalborg, Denmark. 2nd ed. 1999. 11 pp + appendices.
16. Olesen, J.F., "FRC Slabs on Grade, Full-Scale Tests". Dept. of Structural Engineering and Materials, Technical University of Denmark. Lyngby 1999.

Predicting concrete durability by using artificial neural network

Marianne Tange Jepsen
M.Sc.
Concrete Centre, Danish Technological Institute
Gregersensvej, P.O. Box 141, DK-2630 Taastrup
E-mail: marianne.t.jepsen@teknologisk.dk

ABSTRACT
A neural network was designed to investigate the influence of different parameters on the salt frost resistance of concrete. The analysis shows that the most significant parameters are the water/binder ratio and the total air content. The mix composition also has some influence on the frost resistance, i.e. fly ash tends to undermine the frost resistance, whereas silica fume improves the frost resistance. Surprisingly, no relation was found between frost resistance and spacing factor, but the neural network ascribes some importance to the specific surface of the air void structure. However, the neural network analysis is uncertain and should be followed by a statistical analysis to test the significance of the findings.

Key words: Artificial neural network, frost resistance, spacing factor, mix design.

1. INTRODUCTION

Concrete has been used as a construction material for more than a century. During this period of time, the concrete has undergone a continuous development, e.g. the growing use of secondary cementitious materials in the binding phase. Concrete with properties comparable to the properties of today's concrete has only been produced for a short time span, i.e. a couple of decades.

Today, it is not unusual to prescribe service lives of concrete structures up to 100 years even for heavily exposed structures. However, the durability of the concrete cannot be proved sufficiently by referring to experience, because experience with the actual material is limited to a much shorter period. Therefore, there is an urgent need for modelling concrete durability.

1.1 General considerations pertaining modelling

Most often, modelling implies evolution of either a physical or a mathematical model.

Models based on the laws of nature
A model of a process based on the laws of nature will have to take into account all the important aspects, e.g. physical, chemical and thermodynamic aspects. Subsequently, a model based on the laws of nature is called a physical model.

In the case of frost deterioration of concrete, the physical model will have to cover at least phase transition, moisture transport, changes in the concentration of soluble salts in the pore solution, and freezing point depression in narrow pores. The physical mechanisms take place simultaneously, and they interact – meaning interactions which also have to be modelled.

Firstly, the physical model itself may be a simplification not accounting for all mechanisms. Secondly, a physical model includes a number of physical parameters describing relevant physical properties of the system (pore size distribution, diffusivity, etc.), and the determination of the parameters is always associated with some uncertainty. The overall result may be a model which shows the relevant characteristics, when conditions are changed (e.g. less ice formation when the concentration of soluble salts is increased), but the actual predictions may be so uncertain that the model is useless for practical application.

Mathematical models
The mathematical model consists of a mathematical function fitted to a number of measured data. Unlike the physical model, the mathematical model is a purely empirical model. However, the choice of function may of course be inspired by physical phenomena, so in reality there is a grey area between physical and mathematical modelling.

One problem with the mathematical model is to identify the most suitable function. Often this is a matter of trial and error, where one guesses a function and then tests how well it works. Another problem is that it is difficult to generalise. It can always be questioned whether the results of the model are valid for other conditions than those present during the measurements where the fundamental data were obtained. For example, it can be questioned whether the results are valid for other concrete mix designs than those experimentally tested.

1.2 The second best way – artificial neural network

Artificial neural network (or simply neural network) offers an alternative to mathematical modelling. The idea of the neural network is to present it with input data as well as the right answer, and it will *learn* the relation between input and output. Subsequently, the *trained* network can be used to predict the outcome of other sets of input, where the answer is unknown. (For further explanation of the neural network technique, the reader is referred to one of the many introductory textbooks on the subject, e.g. [1] or [2].)

Being based on empirical data, the neural network has the same weakness as the mathematical model. The validity of predictions is limited to cases comparable to cases, where the input data were collected. But the advantage over the mathematical model is that the human programmer making the model doesn't have to declare every action of the program, i.e. state the correct function from the beginning. When using neural network applications for problem solving, one needs to understand the problem to such a level that one can choose the relevant parameters as input. But when the network is trained, one can learn more about the problem by studying the way the network generalises. In a way, the neural network summarises the experience hidden in the input-output relation.

The neural network has been called *the second best way to do just about anything* [1]. The best way is of course to attain a full understanding of the problem and then find the right formula or

optimum algorithm for the particular problem. However, this may not always be possible, and it leaves plenty of problems to be solved by the second best approach.

2. PROBLEM: ESTIMATION OF CRITICAL SPACING FACTOR

The purpose of this article is to try out the neural network approach on a specific problem. It is chosen to use a neural network to estimate the critical spacing factor for a certain concrete composition. Some background information on the problem is stated below (sections 2.1-2.3) along with a plan of action (section 2.4).

2.1 Powers spacing factor

T. C. Powers was among the first to put forth the *hydraulic pressure hypothesis*, i.e. a theory which explains how hydraulic pressure is generated in concrete, when growing ice crystals displace unfrozen water, causing water to flow to unfrozen parts of the body [3]. The pressure build-up depends on the distance from the growing ice crystal to a free surface, where the excess water can be expelled. According to this theory, air entrainment protects concrete against frost deterioration by introducing free surfaces in the concrete and thereby reducing the flow distance and the hydraulic pressure.

Powers defined the critical thickness as the maximum thickness of a body, where the distance to the nearest escape boundary is still sufficiently short to avoid frost damage. Later, Powers spacing factor was formulated as a measure of the maximum flow distance in the paste matrix. Mathematically, Powers spacing factor is equivalent to the maximum half distance between air voids.

2.2 Previous observations of critical values of the spacing factor

Determination of the critical spacing factor requires a lot of experimental work, as it is necessary to test a lot of concrete mixtures, where only the air void structure differs, to lay down the boundary between durable and non-durable concrete. The critical spacing factor depends on the test condition under which it is obtained, e.g. the test result is influenced by cooling rate, surrounding medium etc. But test results produced by Pigeon et al. [4] shows that the critical spacing factor also depends on the actual type of concrete, see figure 1 and table 1, where the results are reproduced.

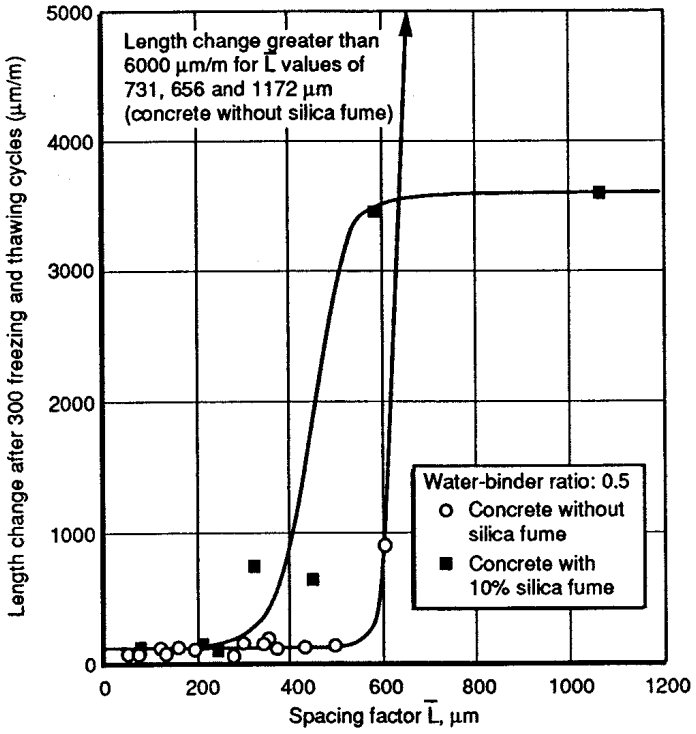

*Figure **Fejl! Ukendt argument for parameter.** – Examples of relations between spacing factor and length change after 300 freeze/thaw cycles (ASTM C 666 procedure A), here for an ordinary Portland cement concrete and the same concrete made with silica fume as partial cement replacement (after [4]).*

*Table **Fejl! Ukendt argument for parameter.** – Critical spacing factors (µm) obtained for various types of concretes subjected to 300 freeze/thaw cycles in water (ASTM C 666 procedure A), after [4].*

Water/binder ratio	Type 10	Type 10 + SF	Type 30 + SF
0.50	500	250	-
0.50 (SP)	500	200	-
0.30 (SP)	400	300	>800
0.25 (SP)	750	-	>800

Type 10: normal Portland cement
Type 30: high early strength Portland cement
SF: silica fume
SP: super plasticizer

If one leaves the high strength concrete out of account, i.e. concrete with cement type 30 or water/binder ratio < 0.30 where the amount of freezable water is neglectible, the summary of results in table 1 indicates that the critical spacing factor is smaller the denser the concrete. For example for water/binder ratio 0.50, the critical spacing factor is 500 µm for the pure Portland cement concrete, whereas it is only half this value, 250 µm, when the binder phase also contains silica fume. According to the hydraulic pressure hypothesis, this is because silica fume lowers the flow rate and thereby hinders the moisture transport to the air voids. Then the distance between air voids needs to be lowered to prevent a deleterious pressure build-up.

However, in the ASTM C 666 procedure A the test specimen is surrounded by pure water, and the test is used to investigate if freeze/thaw cycles cause inner damage. It is not evident that the results can be applied in the case of salt frost scaling. When combined salt and frost action causes surface scaling, transport of outer salt solution into the specimen is an important issue. A very dense concrete produced by means of silica fume will delay moisture transport into the surface layer. Even though the critical spacing factor is lower, the dense concrete may show less scaling than a less dense concrete with higher critical spacing factor.

2.3 Adequacy of the Danish concrete standard

According to the Danish concrete standard DS 481 [5], concrete exposed to salt and frost action, i.e. concrete of environmental class A (aggressive) and E (extra aggressive), has to be frost resistant. In addition to minimum and maximum limits on for example total air content and equivalent water/cement ratio, the concrete has to fulfil at least one of the following two requirements:

- The concrete spacing factor must be smaller than 0.20 mm
- The concrete must be classified *good* after an accelerated freeze/thaw test conforming to SS 13 72 44 [6]. This means that m_{56}, the accumulated scaling after 56 freeze/thaw cycles, is less than 0.20 kg/m^2, or m_{56} is less than 0.50 kg/m^2 and at the same time m_{56}/m_{28} is less than 2.

It is less expensive to make an air void analysis and calculate the spacing factor than to perform an accelerated freeze/thaw test, for which reason the first mentioned criteria is most often used. But in the light of the discussion in section 2.2, the question is if it is adequate to use the same limit value (0.20 mm) for all types of concrete, or if this value ought to depend on the actual mix design? This question is relevant, because ideally, the standard should provide the same safety level, no matter the composition of the concrete. The question will be investigated by means of a neural network.

2.4 Plan of action

The aim of this project is to study to which extend the critical spacing factor is dependent on mix composition. The plan of the project includes the following phases:

- First a neural network is built, which takes mix design details (fly ash content, water/binder ratio, etc.) and results of air void analysis (spacing factor) as input variables and predicts the scaling after 56 freeze/thaw cycles in a standard SS 13 72 44 test.
- Then the trained network is used for analysis. The network is used to determine the critical spacing factor for certain mix compositions: For each composition the scaling is predicted for varying spacing factors. The critical spacing factor is the spacing factor resulting in an amount of scaling which corresponds to the limit between acceptable and unacceptable frost resistance. For the sake of simplicity this limit is set to 0.50 kg/m^2, i.e. the demand on m_{56}/m_{28} is left out of account.
- Finally, by comparing the critical spacing factors of different mix designs, it is possible to judge if DS 481 provides the same safety level for all mix compositions.

3. BUILDING A NEURAL NETWORK

The neural network analysis is performed by using a commercial software package, *BrainMaker*, from California Scientific Software [7]. BrainMaker is not a very sophisticated program, but it is easy to use and can carry out all necessary functions to build a plain neural network.

3.1 Input data

To train a neural network, it is necessary to have a large number of data sets of high quality. It was difficult to collect the necessary number of data sets, because as mentioned in section 2.3, it is common practice either to prove the air void structure or to measure the scaling in an accelerated test, but not both. This means that only seldom both results are known for concrete for normal construction purposes. Instead the data collected originate from research and development projects in Denmark, Norway and Sweden, e.g. from testing of concrete for large civil structures or the preceding laboratory investigations of concrete before a field test.

The data collected for each concrete are:

- mix design details: cement type and content of cement, water, fly ash, and silica fume
- air content in fresh concrete
- result of air void analysis: total air content, specific surface, and spacing factor
- scaling after 56 freeze/thaw cycles according to SS 13 72 44

Then it is also possible to use derived data in the analysis such as water/binder ratio or equivalent water/cement ratio ($(w/c)_{eq} = \frac{w}{c+0.5FA+2SF}$).

In all, data are collected for 123 different types of concrete. They cover a wide range of different mix compositions, e.g. 1-, 2-, and 3-powder combinations. For about 40% of the concretes, the scaling after 56 cycles exceeds 0.50 kg/m^2 (it is important that the network is trained with data from both good and bad quality concretes, if it is going to learn to tell the difference). The data and their span of equivalent water/cement ratio and spacing factor are shown in figure 2.

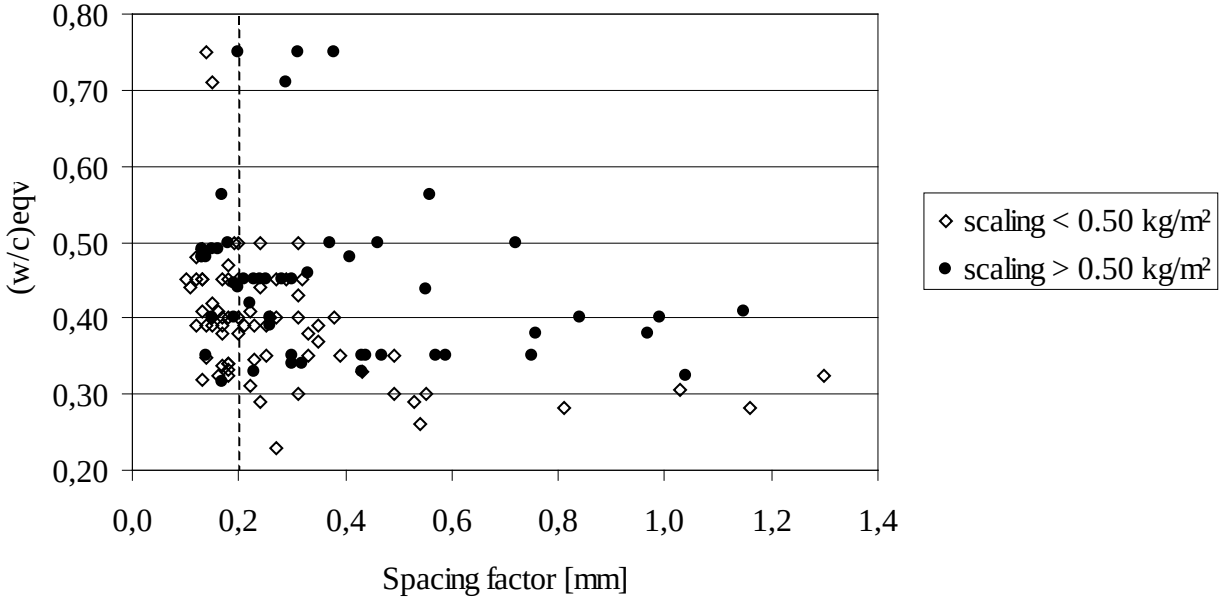

*Figure **Fejl! Ukendt argument for parameter.** – Presentation of the 123 types of concrete in the study; their spacing factor, equivalent water/cement ratio and ranking of scaling after 56 freeze/thaw cycles in a SS 13 72 44 test.*

3.2 Network architecture

The network consists of neurons in layers, each neuron being linked to a number of neurons in the subsequent layer. The training consists in adjusting the way a signal is processed in each connection, when the signal passes through the network. A large network with many connections demands a high number of data sets for training, whereas a smaller network can be trained satisfactorily with proportionally fewer data sets. The data set available allows for a network size of the order of 20 connections.

It is a matter of trial and error to find the network architecture, which provides the most reliable predictions. Different neural networks were trained:

- 2- and 3-layer networks, i.e. networks with 1 and 2 hidden layers, respectively
- networks with 2, 3, and 4 hidden neurons
- networks with different combinations of input variables

The data presented in section 4 is for a network like the one shown in figure 3. Of all the tested networks, this network turned out to be the one which made the most accurate predictions.

In the network presented in figure 3, the output is *ln(scaling)* instead of *scaling*, because this substitution improves the predictions for scaling in the range of 0-1.0 kg/m^2. The accuracy for higher scaling values is considered less important, e.g. it is not important if the scaling is 3 or 5 kg/m^2 as in both cases the scaling is unacceptable.

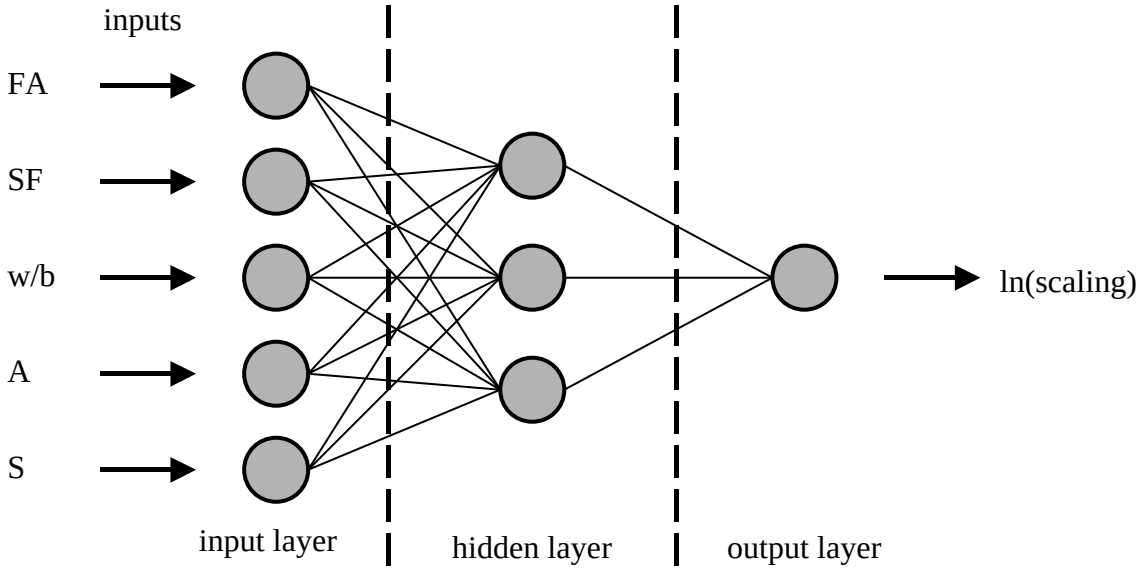

*Figure **Fejl! Ukendt argument for parameter.** – A 2-layer network with 3 hidden neurons. FA: fly ash content [% of powder weight], SF: silica fume content [% of powder weight], w/b: water/binder ratio, A: total air content [% of concrete volume], S: specific surface [mm^{-1}].*

4. RESULTS

4.1 General

To test the network, it is presented to a number of input data sets which have not been used during training. Then the predictions of the network can be compared to the real values. Such a comparison is illustrated in figure 4. In the figure, the axes correspond to *ln(scaling)–ln(0.50)*. In this way of mapping the quadrants classify the predictions:

- 1st quadrant: The network correctly predicts scaling larger than 0.50 kg/m^2 after 56 cycles.
- 2nd quadrant: The network predicts scaling larger than 0.50 kg/m^2 and rejects the concrete, though the actual scaling is acceptable.
- 3rd quadrant: The network correctly predicts scaling less than 0.50 kg/m^2 after 56 cycles.
- 4th quadrant: The network predicts scaling less than 0.50 kg/m^2, though the actual scaling is larger than the accept limit.

Points in 2nd and 4th quadrant show the cases, where the network misjudges the situation and either rejects acceptable concrete (scaling < 0.50 kg/m^2), or accepts concrete which should have been rejected (scaling > 0.50 kg/m^2).

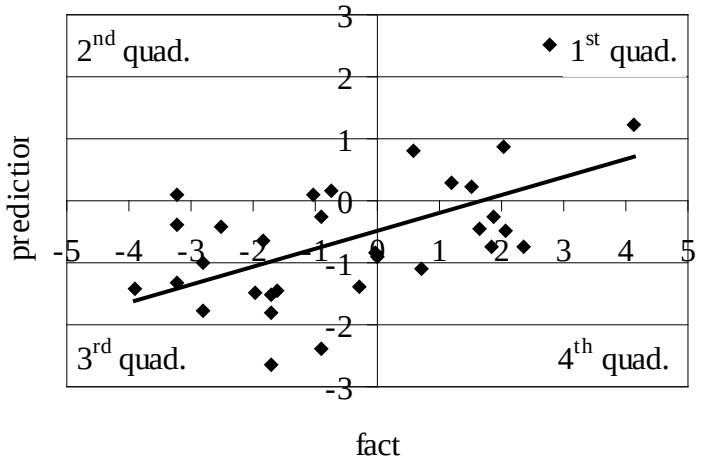

*Figure **Fejl! Ukendt argument for parameter.** – Real values of scaling after 56 freeze/thaw cycles (fact) versus values predicted by the network. Note the axes! ln(scaling)-ln(0.50).*

In general, the network has difficulties in predicting extreme values, both high and low scaling. The network also tends to be a little bit optimistic. This can be realised by observing the regression line, which passes below origo, and by comparing the number of points in 2nd and 4th quadrant, respectively.

It is possible to look into the inner logic of the trained network by making predictions, where one variable is varied at the time. This is done in the following two sections.

4.2 The significance of mix design

Predictions made with varying contents of fly ash and silica fume are shown in figure 5, whereas predictions with varying w/b ratio are shown in figure 6. Interpretations are to be made from the slope of the curve, not from the actual vertical location, as it can be manipulated by changing the default values of the rest of the parameters.

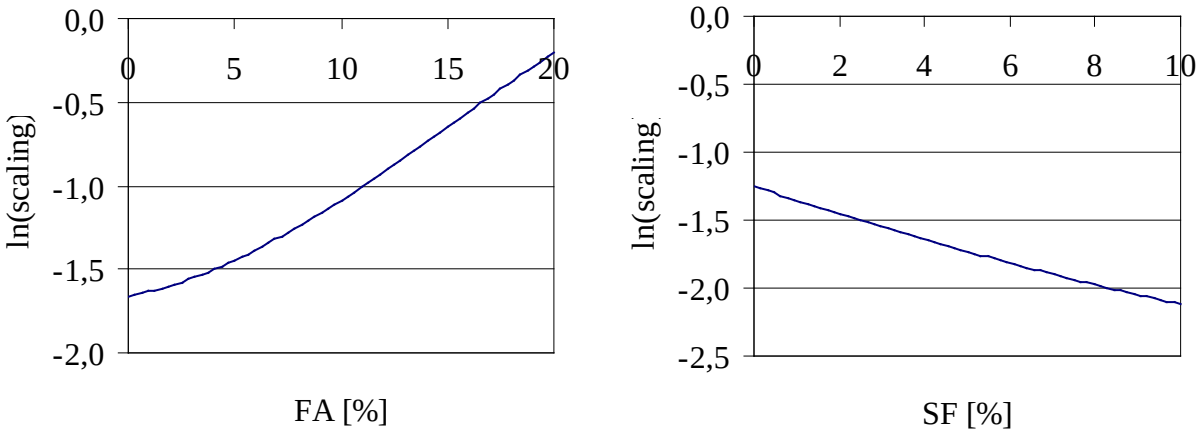

*Figure **Fejl! Ukendt argument for parameter.** - Left: predictions made with varying fly ash content (FA). Right: predictions made with varying silica fume content (SF). Default values: FA=4.0%, SF=2.5%, w/b=0.40, A=4.0%, S=23 mm^{-1}.*

Figure 5 shows that fly ash has a negative effect on frost resistance, whereas silica fume has a positive effect. A probable explanation, which at least partly can account for these effects, is that fly ash doesn't contribute as much to the strength as cement and silica fume. The effects of fly ash and silica fume are reduced if the network is trained with the equivalent water/cement ratio as input variable instead of the water/binder ratio. As regards silica fume, the results are contradictory to the results of Pigeon et al. presented in section 2.2, because when silica fume lowers the critical spacing factor, a decrease of frost resistance was to be expected.

However, neither fly ash nor silica fume has the same importance as the water/binder ratio, see figure 6.

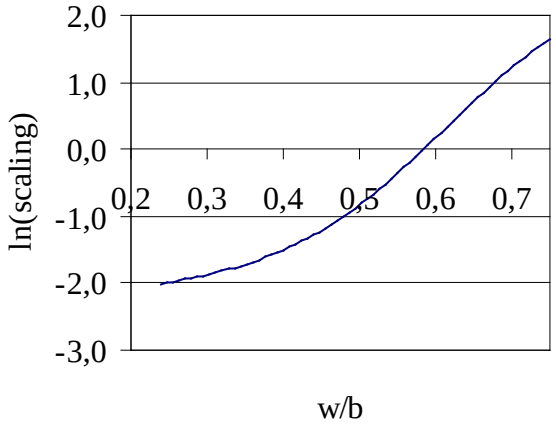

*Figure **Fejl! Ukendt argument for parameter.** – Predictions made with varying w/b ratios. Default values: FA=4.0%, SF=2.5%, A=4.0%, S=23 mm^{-1}.*

4.3 The significance of air void structure

Predictions made with varying air void parameters are shown in figure 7. The network ascribes more weight to the total air content than to the specific surface. In this context it is appropriate to mention that it was tried to train a network with spacing factor as input variable instead of specific surface. But the spacing factor more than anything seemed to confuse the network. Irrespective of the network architecture, training did not improve the network, i.e. the error of the trained network was at the same level as the error of the untrained network. For this reason it has not been possible to determine a critical spacing factor for various mix compositions.

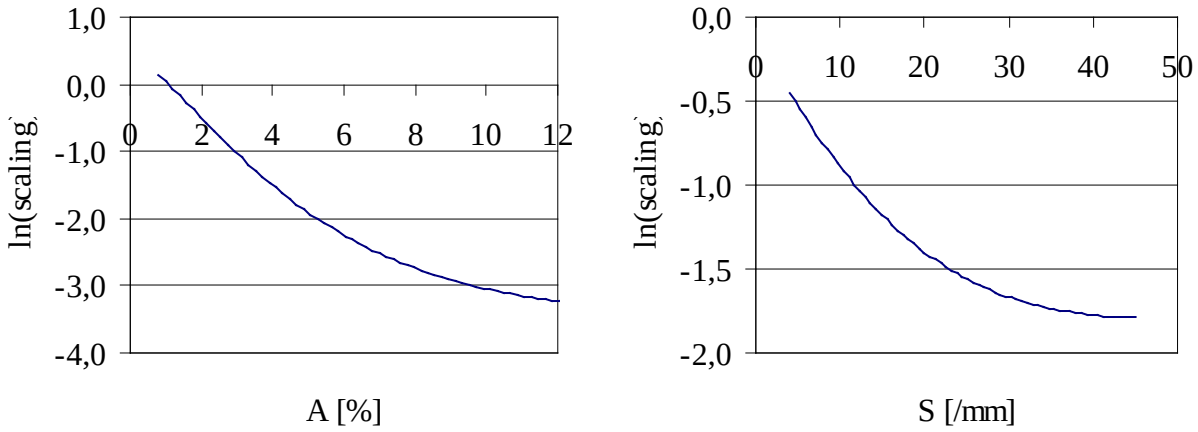

*Figure **Fejl! Ukendt argument for parameter.** – Left: predictions made with varying air content A. Right: predictions made with varying specific surface S. Default values: FA=4.0%, SF=2.5%, w/b=0.40, A=4.0%, S=23 mm^{-1}.*

5. DISCUSSION AND CONCLUSION

A neural network was designed to investigate the influence of different parameters on the salt frost resistance of concrete. The analysis shows that the most significant parameters are the water/binder ratio and the total air content. The mix composition also has some influence on the frost resistance, i.e. fly ash tends to undermine the frost resistance whereas silica fume improves the frost resistance. Surprisingly, no relation was found between frost resistance and spacing factor, but the neural network ascribes some importance to the specific surface of the air void structure.

DS 481 states maximum equivalent water/binder ratios and minimum air content for concretes exposed to combined salt and frost action. These provisions offer some degree of protection against frost deterioration. DS 481 is based on experience which tells that, combined with demands on spacing factor, concretes complying with the standard will be frost resistant.

The neural network analysis calls attention to two areas. Firstly, the spacing factor may not be the best parameter to characterise the air void structure. More work should be done to find an air void parameter which correlates better with the actual frost resistance. Secondly, the actual mix composition (powder combination) should be taken into account. However, the neural network analysis is subjected to a rather large uncertainty. The neural network approach is a suitable tool for introductory investigations, but the investigation should be followed by a thorough, statistical analysis to test if the findings are significant.

REFERENCES

1. Hertz, J., Krogh, A., and Palmer, R. G., “Introduction to the theory of neural computation”, Addison-Wesley Publishing Company, New York, 1991.
2. Skapura, D. M., “Building Neural Networks”, ACM Press (Addison-Wesley Publishing Company), New York, 1996.

3. Powers, T. C., "Basic considerations pertaining to freezing-and-thawing tests", PCA Bulletin 58, Proceedings of the American Society for Testing Materials, Pa. Vol. 55, Philadelphia, 1955.
4. Pigeon, M., Pleau, R., and Aïtcin, P. C., "Freeze-thaw durability of concrete with and without silica fume in ASTM 666 C (Procedure A) test method: Internal cracking versus scaling", *Cement, Concrete, and Aggregates*, Vol. 8, pp. 76-85, 1986.
5. DS 481: "Concrete – Materials", Danish Standards Association, 1999.
6. SS 13 72 44: "Concrete Testing – Hardened concrete – Scaling at freezing", Swedish Standards Institution, 1995.
7. "BrainMaker. User's Guide and Reference Manual", 7th edition, California Scientific Software, Nevada City, 1998.

ACKNOWLEDGEMENT

This investigation would have been impossible if it had not been for colleagues all over Scandinavia, who helped collecting relevant training data for the neural network.

Studies on chloride penetration into concrete in marine environments – project description and preliminary results

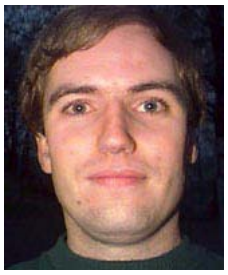

Anders Lindvall
Ph.D.-student
Department of Building Materials
Chalmers University of Technology
SE-412 96 Göteborg
E-mail: lindvall@bm.chalmers.se

ABSTRACT

Concrete specimens, made from the same concrete composition, are exposed at twelve different marine submerged exposure locations around the world. The purpose of the study is to get a quantitative measure of how different environments influence the chloride penetration. Specimens are also exposed in the marine tidal zone and the road environment. Parallel with the field exposure, specimens are exposed in the laboratory in two salinities and temperatures. The chloride penetration is determined as chloride penetration profiles, which also are curve-fitted to the error-function solution of Fick's second law. The severity of the exposure environment is expressed as a chloride load that is determined by integrating the area under each profile. Additionally chloride binding isotherms are established for the exposed concrete. The exposure conditions are documented as the chemical composition and temperature of the seawater. In this paper a description of the project is given and some preliminary results presented.

Key words: Marine exposure, Chloride penetration, Swedish Sulphate Resistant Portland Cement (CEM I 42.5 BV/SR/LA), Submerged zone, Tidal zone, Environmental actions.

1. INTRODUCTION

1.1 General

The service life of marine reinforced concrete structure is to large extent influenced by the occurrence of reinforcement corrosion. Reinforcement corrosion in a marine environment is usually initiated by chloride ions penetrating into the concrete and after a certain time exceeding a critical concentration, the so-called threshold level, at the reinforcement. The chloride penetration into the concrete is a function of the environment for the location of the (future)

structure, the concrete composition and the execution during construction. The environmental conditions in a marine environment can be expressed as a function of the water temperature, chemical composition of the seawater, the position to the water-surface, tidal actions and characteristics of splash and spray from waves. However, it should be pointed out that the extent of reinforcement corrosion is also dependent on the availability of oxygen and galvanic contact in the concrete.

The process of reinforcement corrosion is normally divided into an initiation period, during which chlorides are penetrating into the concrete and initiating corrosion, and a propagation period, during which the reinforcement is actively corroding, [7]. To predict the chloride penetration into a concrete structure mathematical prediction models are used. There are two types of mathematical prediction models: (i) Physical models based on transport theories and (ii) Empirical models based on observations of response from structures. Both these types of models require information about boundary and initial conditions and data to validate predictions. These data usually consist of measured chloride penetration profiles for different concrete compositions, types of execution and exposure conditions. However, reliable data are scarce, which makes it hard to quantify the boundary and initial conditions in the models.

With the new performance based design methodologies that are developed, e.g. DuraCrete [1], this becomes even more important, since fairly large amounts of reliable data are needed for statistical quantifications. Usually these quantifications are made with parameters evaluated by curve-fitting of measured chloride penetration profiles. Thus there is a need for quality data in the form of measured chloride penetration profiles for different concrete compositions, types of execution and exposure conditions.

There are fairly large amounts of data available on how different concrete compositions and types of execution influence the chloride penetration, e.g. [2] and [3]. However, data on the environmental influence are scarce – usually one concrete composition is exposed only in one or in some rare cases in two exposure environments. In [4] some concrete compositions are exposed both on the Swedish west coast, at the Träslövsläge field station, and the Swedish east coast, at the site of the Öland-bridge. Some of the concrete composition described in [2] and [3] have been exposed in both marine and road environments. The lack of data makes it hard to only compare how different environments influence the chloride penetration into concrete, since effects from concrete composition and curing also will be included in comparisons between different environments.

1.2 Exposure programme

Based on the facts mentioned above, there is a need for quality data that show the differences in chloride penetration into concrete exposed in different environments, without effects from concrete composition and execution during construction. An expose programme has been started, where concrete specimens made from one single concrete composition are exposed, to clarify and investigate these differences. The exposure programme is divided into a field exposure, where the specimens are exposed at different marine locations around the world, and a laboratory exposure. After a certain time the specimens will be analysed by means of profile grinding and potentiometric titration to determine the chloride penetration. The exposure conditions at the exposure locations will be determined as chemical composition and temperature of the seawater. In this paper the exposure programme will be described and some of the preliminary results will be presented and discussed.

1.3 Objective and scope

The objective of the field exposure is to quantify the differences between different exposure environments, concerning chloride penetration. Concrete specimens, made from the same concrete composition, have been exposed at twelve different locations around the world. The exposure locations have been chosen in such way that they represent typical environments where marine reinforced concrete structures are built.

The objective of the laboratory exposure is to compare chloride penetration into concrete under different environmental conditions (chemical compositions of seawater and water temperatures) Additionally chloride-binding isotherms are established for the examined concrete compositions, where the relationship between the content of bound, free and total chlorides in the concrete is given. Since the total chloride content is analysed when the chloride penetration profiles are determined and the free chlorides initiate corrosion, the information provided by the chloride binding isotherms is vital to predict the risk of chloride induced reinforcement corrosion.

2. BACKGROUND

2.1 Prediction of service life for reinforced concrete structures

Degradation of concrete, due to chloride induced reinforcement corrosion, can be divided into two periods, [7]: **initiation**, during which chloride ions penetrate into the reinforcement and initiate reinforcement corrosion, and **propagation**, during which the reinforcement is actively corroding. There are two principal approaches for predictions of service life for reinforced concrete structures affected by problems related to chloride induced reinforcement corrosion: only consider the initiation period, which is a conservative approach, or to consider both the initiation and propagation periods. In this paper only the initiation period, due to chloride ingress, will be considered.

An example of a mathematical prediction model for chloride penetration into concrete is the DuraCrete chloride-model, which is an empirical model. The principals of the models is given in [5]. In this model only the time for initiation of reinforcement corrosion is considered. The model is presented in (1)

$$C_x = C_{SN} \cdot \left[1 - erf \frac{x}{2 \cdot \sqrt{D_a(t) \cdot t}} \right] \quad (1)$$

where:
C_x: the chloride concentration at a certain penetration depth. [weight-% per binder]
C_{SN}: the surface chloride concentration. [weight-% per binder]
x: the chloride penetration depth. [m]
t: the exposure time. [s]
$D_a(t)$: the apparent diffusion coefficient for chlorides, see (2). [m^2/s]

$$D_a(t) = D_a(t_0) \cdot \left(\frac{t_0}{t} \right)^n = k_c \cdot k_e \cdot k_t \cdot D_0 \cdot \left(\frac{t_0}{t} \right)^n \quad (2)$$

where:
k_c: constant parameter that considers the influence from execution conditions. [-]
k_e: constant parameter that considers the influence from environment. [-]
k_t: constant parameter that considers the influence from test-method. [-]
D_0: chloride diffusion coefficient determined at standardised conditions. [m^2/s]
t_0: reference time, at which D_0 is measured. [s]
n: age factor that describes the decrease of D_a with time. [-]

The apparent diffusion coefficient for chloride, $D_a(t)$, is determined by curve-fitting of measured chloride penetration profiles to the error-function solution to Fick's second law. The factors k_e and n describe how different environments influence the diffusion coefficient for chlorides determined under standardised conditions, D_0 at the reference time, t_0.

2.2 Environmental actions

The first idea of starting an exposure programme, like the one described in this paper, came up during the DuraCrete-project, described in [1]. In a part of this project a statistical quantification of the environmental parameters in the DuraCrete chloride ingress model, see (1), was done. A database was established within the project to get enough data for the statistical quantification. The data put in the database were mainly found in literature but some data were also produced within the DuraCrete-project. The result from the quantification showed on large statistical uncertainties. It was especially hard to find data that show how similar concrete compositions cured under similar conditions behave in different environments. The complete procedure for the statistical quantification in the DuraCrete-project and the final results from the quantification are presented in [5].

In this paper concrete specimens exposed in marine environments are described. Depending on the position towards the surface of the water the marine exposure environment can be divided into the following four zones, [6]:

- **Submerged zone**. The submerged zone is below the surface of the water. The surface of a concrete structure in the submerged zone is constantly exposed to seawater.
- **Tidal zone**. The tidal zone is limited by the extent of the tidal actions. The surface of a concrete structure in the tidal zone is cyclical exposed to seawater.
- **Splash zone**. The splash zone is limited by the extent of splash from breaking waves, above the tidal zone. The surface of a concrete structure in the splash zone is randomly exposed to seawater.
- **Atmospheric zone**. The atmospheric zone is limited by the extent of spray from breaking waves, above the splash zone. The surface of a concrete structure in the atmospheric zone is randomly exposed to spray from breaking waves.

In the exposure programme described in this paper, the concrete specimens have been exposed in the submerged zone at all locations except one, where also the tidal zone has been included. Additionally four specimens have been exposed along a thaw-salted road. The submerged zone has been chosen to get a well-defined exposure, where only the chemical composition of the seawater and the water-temperature varies between the locations. In the other zones also other parameters, e.g. position towards the surface of the water and the road surface, will significantly influence the achieved chloride penetration.

3. MATERIAL AND SPECIMENS

The concrete composition used in the exposure programme is given in table 1.

Table 1 – The concrete composition used in the exposure programme.

Material	Amount (kg/m^3)	Density (kg/m^3)	Volume proportion (-)
Cement (CEM I 42.5 BV/SR/LA)	450	3105	0.143
Sand 0-8 mm	938	2650	0.354
Stone 8-16 mm	745	1650	0.281
Water	180	1000	0.180
Air*	-	-	0.045

CEM I 42.5 BV/SR/LA – Swedish SRPC (Sulphate Resistant Portland Cement – Anläggnings-cement Portland Degerhamn)

* : The air content in the concrete is regulated by adding AEA (Cementa L 14) – dosage 0.030 weight-% of cement-weight.

The exposure programme is divided into two exposure periods. The first exposure period started in the summer of 2000 and the second exposure period started in the summer of 2001. The specimens used in the first exposure period have been made from concrete mixed at two occasions, with 120 litres of concrete mixed at each occasion. The specimens used in the second exposure period have been made from concrete mixed at five different occasions, with 45 litres of concrete mixed at each occasion.

To minimise the effects from variations in the constituent materials the cement used in the first six castings came from the same delivery from the cement factory. The seventh casting has been made with cement from another delivery. Furthermore the aggregates used in all castings have been taken from the same delivery. The mixing-water used in all castings has been normal tap water. The air-entraining agent has been taken from the same bottle for all castings.

Two types of specimens have been used, measuring 75x150x150 mm and 150x150x150 mm. The small specimens are exposed for around one year and the larger specimens are exposed for a longer period. In the first round of exposure only the small specimens have been included and in the second period of exposure also the larger specimens have been included.

The concrete specimens have been casted in moulds, used to cast standard-cubes measuring 150x150x150 mm, without the partition walls. This means that beams, 150x150x470 mm (each partition wall is approximately 10 mm thick), have been casted. After casting the concrete has been cured for three days in the moulds, before de-moulding, and then wrapped in plastic in a constant-room (+20ºC and 60%RH) to an age of at least 28 days. After the curing the concrete beams have been sawed to specimens. The sawing has been made with a water-cooled diamond saw and then the specimens have been stored in a constant-room (+20ºC and 60%RH), under a plastic cover to prevent drying, before exposure. During the transport to each exposure locations the specimens have been wrapped in plastic to prevent drying.

4. EXPOSURE PROGRAMME

The exposure programme is, as mentioned earlier, divided into two exposure periods. In the first exposure period specimens, 75x150x150 mm, have been exposed at twelve locations around the

world and in the laboratory of Building Materials at Chalmers University of Technology. In the second exposure period two sizes of specimens, 75x150x150 mm and 150x150x150 mm, have been exposed on some of locations used in the first exposure period. To minimize effects from variations in concrete compositions between the specimens, a randomisation process has been used where the specimens exposed at each location have been taken from different beams. Five specimens are exposed at each location to achieve enough data to evaluate statistical uncertainties both within each exposure location and between different exposure locations.

The first exposure period started between August 2000 and January 2001 and was finished approximately one year later. The second exposure period started in August 2001 and was still in progress when this paper was finalised. During both exposure-periods the surfaces of the specimens have not been cleaned from marine growth until the specimens have been picked up.

4.1 Field exposure

The concrete specimens are exposed at twelve locations around the world. Information about each exposure location is given in the following listing (each location is listed with name of the closest town, country and name of the ocean/sea):

- **Banyuls sur Mer**, France. Mediterranean. During the first exposure period ten small specimens have been exposed in an aquarium (water taken from 8 m depth in the sea) and at sea (depth 24.5 m) – five specimens at each location. The exposure started in August 2000 and was finished in August 2001. During the second exposure period ten specimens are exposed in the aquarium and at sea – four small and one large specimen at each location. The exposure started in August 2001.
- **Cascais**, Portugal. Atlantic Ocean. During the first exposure period ten small specimens have been exposed in an old lobster farm at a depth of approximately 1 m. The exposure started in August 2000 and was finished in August 2001. During the second exposure period three large and five small specimens are exposed. The exposure started in August 2001. The difference between low and high tide is some 1 m at the exposure location.
- **Dubai**, United Arab Emirate. Persian Gulf. During the first exposure period five small specimens have been exposed in a harbour at a depth of approximately 1 m. The exposure started in late October 2000 and was finished in November 2001.
- **Hirtshals**, Denmark. North Sea. During the first exposure period five small specimens have been exposed in a harbour at a depth of approximately 1 m. Unfortunately three specimens disappeared during the exposure. The exposure started in September 2000 and finished in October 2001. During the second exposure period four small specimens are exposed. The second exposure period started in October 2001. The difference between low and high tide is some 0.30 m at the exposure location.
- **Hvalfjördur**, Iceland. Atlantic Ocean. During the first exposure period five small specimens have been exposed in a harbour at a depth of approximately 1 m. The exposure started in September 2000 and was finished in September 2001.
- **Källahamn**, Sweden. Baltic Sea. During the first exposure period five small specimens have been exposed in the sea at a depth of approximately 1 m. The exposure started in September 2000 and was finished in September 2001.
- **Kjøpsvik**, Norway. Atlantic Ocean. During the first exposure period five small specimens have been exposed in a harbour at a depth of approximately 1 m. The exposure started in late October 2000 and was finished in November 2001. During the second exposure period five specimens have been exposed. The exposure started in early November 2001. The difference between low and high tide is approximately 2.5 m at the exposure location.

- **La Rochelle**, France. Bay of Biscay/Atlantic Ocean. During the first exposure period ten small specimens have been exposed in two harbours – five of the specimens have been hanging from a floating pontoon at a depth of approximately 1 m and the other five specimens have been exposed in the tidal zone. The exposure started in August 2000 and was finished in August 2001. During the second exposure period six small and two large specimens are exposed in the tidal zone and five small specimens hanging from the floating pontoon. The exposure started in August 2001. The difference between low and high tide at the exposure locations is approximately 2 m.
- **Oosterschelde damm**, Netherlands. English Channel/North Sea. During the first exposure period five small specimens have been exposed in a harbour hanging from a floating pontoon at approximately 1 m depth. The exposure started in late August 2000 and was finished in September 2001. During the second exposure period five small specimens are exposed. The exposure started in September 2001. The difference between low and high tide is approximately 2 m at the exposure location.
- **Skanör**, Sweden. Öresund. During the first round of exposure five small specimens have been exposed at a depth of approximately 1 m. The exposure started in August 2000 and was finished in late August 2001.
- **Hobart**, Australia. Pacific Ocean. During the first exposure period five small specimens have been exposed at a depth of approximately 1 m. The exposure started in late January 2001. Unfortunately two specimens have disappeared during the exposure.
- **Träslövsläge**, Sweden. Kattegat. During the first exposure period nine specimens have been exposed at a depth of approximately 0.5 m. The exposure started in September 2000 and finished in early October 2001. In December 2000 three additional small specimens were submerged at the exposure site. During the second exposure period two large and four small specimens are exposed. The exposure started in early October 2001.

Apart from the exposure locations described above, additional exposure locations are planned in the south of Italy at two different locations, where ten small specimens are planned to be included. Parallel with the marine exposure four small specimens are exposed in a road environment at the Rv40 field station outside Borås to compared the chloride penetration in marine and road environments.

Ten of the exposure locations are situated in Europe. The exposure locations are shown on a map, where each location is marked with a circle, see figure 1.

Figure 1 – Exposure locations in Europe. Map downloaded from [12].

4.2 Laboratory exposure

Parallel with the field exposure some small concrete specimens are exposed in NaCl-solutions in the laboratory. The specimens are exposed in solutions with two chloride-contents, 8.3 g NaCl and 33 g NaCl per litre water, and two temperatures, +7ºC and +20ºC. The exposure-solutions have been chosen so they represent the water in the Baltic Sea (8.3 g NaCl/l) and the Atlantic Ocean (33 g NaCl/l). The pH in the exposure-solutions has been continuously measured and when it has exceeded 11 the exposure solution has been changed. Until now (January 2002) the exposure solution, with the requirement of pH-regulation, has been changed once a week or every second week. The exposure in the laboratory started in February 2001 and will continue until February 2002.

Additionally chloride-binding isotherms are determined for the concrete composition in the exposure programmes, giving the relationship between free and total chloride-content. The chloride binding isotherms give the relation between the amounts of total, free and bound chlorides in the concrete. This information is of interest since it is only the free chlorides that are transported into the concrete and initiate reinforcement corrosion. The method used to determine

the chloride penetration profiles, determine the total amount of chlorides in the concrete, which means that the information from the chloride binding isotherms is vital to predict the risk of chloride induced reinforcement corrosion.

5. ANALYSIS

5.1 Chloride penetration

The chloride penetration is determined as chloride penetration profiles where the quotient of chloride and calcium content is given as a function of depth. To get a well-defined surface, without any effects from the type of mould etc, only chloride penetration through the sawed surfaces on the specimens have been studied. Since the specimens are sawed from beams almost all specimens have two exposure surfaces. The exposure time has been approximately one year for the small specimens and longer time-period for the larger specimens.

After the exposure has finished the exposed specimens have been cleaned from possible marine growth and transported to the laboratory. Before the transport the specimens have been dried in the air, to let surface-water dry away, and then packed in plastic-bags, which have been sealed, to prevent uncontrolled drying and an adverse transport of chlorides during the transport.

When the concrete specimens have arrived to the laboratory, cores (diameter 75 mm) have been drilled from the centre of each sawed surface, see figure 2 (left). Powder-samples have been collected from the cores in depth-intervals from the exposure surface by means of thorough profile grinding. The profile grinding has been done in a modified turning-lathe equipped with a drilling machine and a diamond-drill. The principal appearance of the equipment is shown in figure 2 (right). The core is fastened in the chuck of the turning-lathe, which is rotating, and the powder is grinded from the specimen with the drill that is rotating in the same direction compared to the chuck. The drill is mounted non-centric compared to the core, so the complete cross-section of the core will be grinded. The depth-intervals increase with increasing depth from the surface, i.e. small intervals in the surface-near region (0-10 mm) and larger intervals further in from the surface. The depth of each interval is measured with an accuracy of 0.5 mm. The powder-samples from the profile grinding have been dried in +105ºC and finally stored in airtight boxes before analysis for chloride and calcium content.

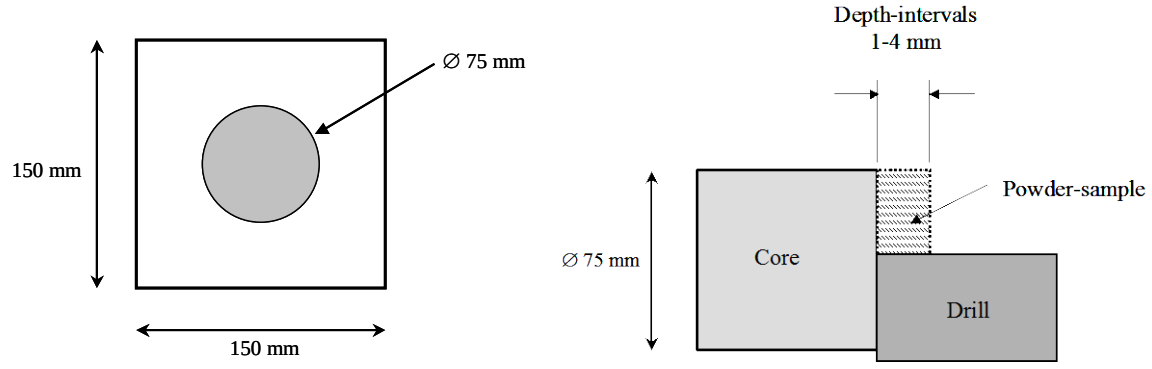

Figure 2 – Position for cores are drilled from the concrete specimens (left) and profile grinding of the cores (right).

The chloride-content in each powder-sample is determined principally in accordance with AASHTO T260 [8], except that the sample size is about 1 g to facilitate parallel calcium

analysis. The calcium content is determined in order to estimate the binder content in each sample. Since the aggregates used in the concrete contains in principle no calcium the measured calcium content can be correlated to the binder content. The procedure to determine the chloride- and calcium-content in each powder-sample is further described in [9].

5.2 Chloride binding isotherms

Chloride binding isotherms, i.e. relationship between the content of free, bound and total amount of chlorides in the concrete, are established for the concrete composition used in the exposure programme. The chloride binding is determined for different chloride-contents and temperatures of the exposure solution. The following two methods are used:

- **Total-free chloride relationship**. The total and free chloride content is determined on concrete disks exposed in NaCl-solutions with known chloride-contents and at different temperatures. The free chloride content is known from the solution and the total chloride content in the disks is determined when equilibrium is reached. The total chloride content in the disks is determined with profile-grinding and potentiometric titration.
- **Bound-free chloride relationship**. The total and bound chloride content is determined by putting crushed concrete in a certain amount of NaCl-solution. The concentration of free chlorides is the achieved concentration in the storage solution when equilibrium is reached. The bound chlorides can be evaluated from the decrease in chloride concentration in the storage solution.

The procedures to determine the chloride binding isotherms are further described in [10].

5.3 Chemical composition of seawater

Water-samples have been taken from all exposure locations to determine the chemical composition of the seawater. The chemical composition of the seawater at all the exposure locations has been determined in terms of chloride content, pH and content of alkali metals and sulphates. Additionally the water-temperatures at the exposure locations have been investigated.

The chloride content of the seawater is determined with potentiometric titration with silver nitrate, $AgNO_3$ as titration solution. The pH is determined with an electrical pH-gauge, the content of alkali metals is determined with an ICP-MS and the sulphate-content is determined with wet-chemical analysis.

6. RESULTS

6.1 Chloride penetration profiles

The chloride penetration into the concrete specimens has been determined as chloride penetration profiles, where the quotient between chloride and calcium content at different depths are presented. With this procedure variations in aggregate-content between the powder-samples can be minimised. All sawed surfaces on the specimens have been investigated, which means that chloride penetration through at least one surface on each specimen has been studied. For most specimens the chloride penetration has been determined through two surfaces. At least five

specimens have been exposed at each exposure location and since the specimens are exposed at twelve different locations the exposure programme will result in at least 100 chloride penetration profiles.

The chloride penetration profiles are curve-fitted to the error-function solution of Fick's second law. Each chloride penetration profile has been divided into an outer convection zone and an inner diffusion zone. The curve fitting is only done to the inner diffusion-zone, where the coefficient of correlation, R, exceeds 0.95. The curve fitting results in an apparent diffusion coefficient, D_a, an apparent surface chloride concentration, C_{sa}, a thickness of the convection zone, x_c, and a surface chloride concentration for the diffusion-zone, C_{sc}. The procedure for the curve fitting is further described in [11].

The severity of the exposure environments has been determined as a chloride load. The chloride load is determined as the area under each chloride penetration profile, to get a measure of the amount chlorides that has penetrated into the concrete.

When this paper was finalised only few chloride penetration profiles from some of the exposure locations in the exposure programme were available. In figure 3a the analysed chloride penetration profiles are presented. The amounts of chlorides that have penetrated into the concrete, i.e. the chloride load, have been determined by integrating the area below each penetration profile. The amounts of chlorides that have penetrated into the concrete are presented in figure 3b.

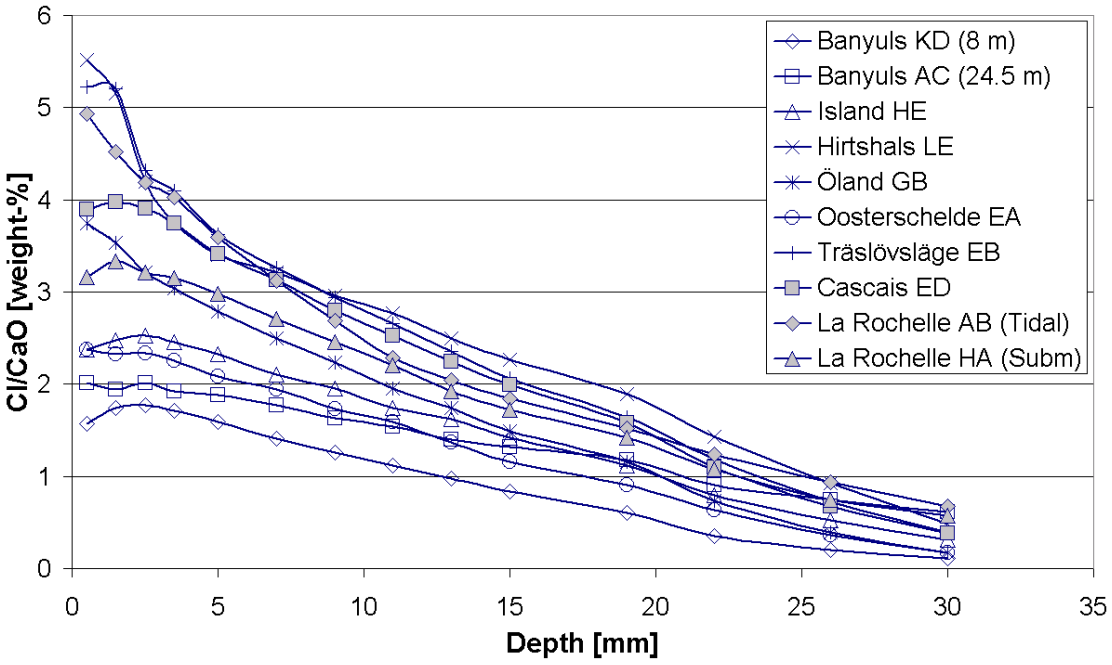

Figure 3a – Chloride penetration profiles in the concrete specimens exposed at some of the locations in the exposure programme.

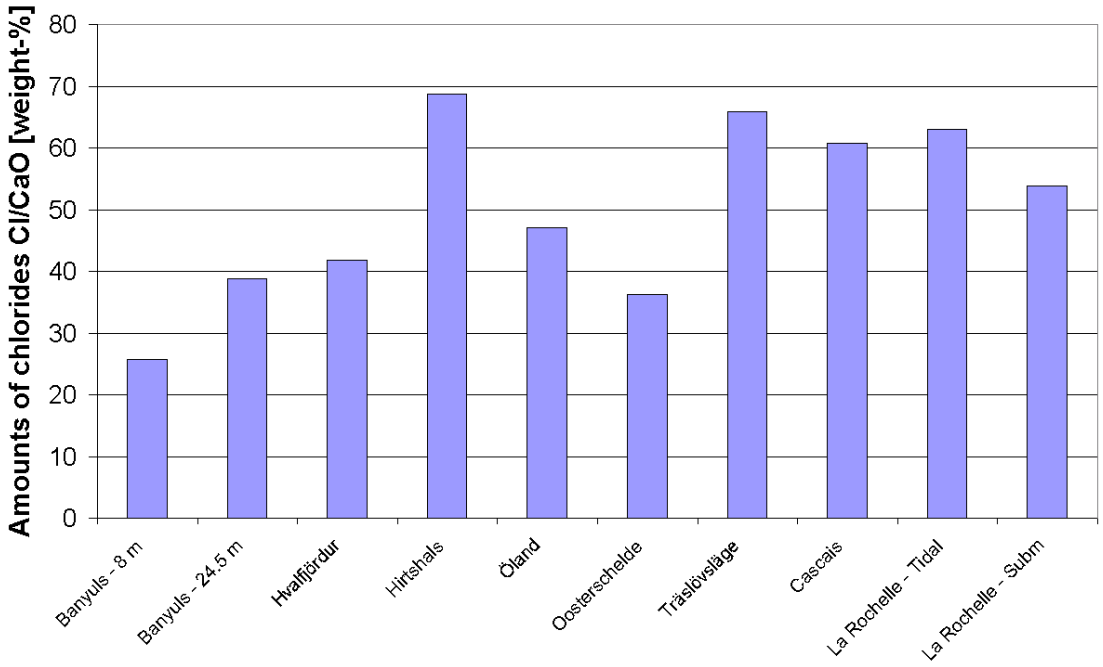

Figure 3b – Amounts of chlorides that have penetrated into the concrete specimens exposed at some of the locations in the exposure programme.

From figure 3a and 3b it can be seen that the chloride penetration profile from Hirtshals has the highest chloride concentrations and the profiles from Banyuls sur Mer (index KD – 8 meters depth) has the lowest chloride concentrations. Possible explanations for the variations in chloride penetration are differences in the salinity of the exposure water at the different exposure locations and temperature effects on the chloride binding, where the binding capacity increases with increasing temperature.

The chloride penetration profiles have been established with the total amount chlorides in the concrete specimens, i.e. both bound and free chlorides. Thus a high chloride concentration could occur due to the increase of bound chlorides in the concrete. This does not necessarily mean that the risk for reinforcement corrosion is high, since only the free chlorides initiate corrosion. Thus to get a complete picture of the chloride penetration information about the chloride bindings isotherms, for different salinities and temperatures, is required.

6.2 Chloride binding isotherms

When this paper was finalised, in January 2002, no chloride binding isotherms were available for the exposed concrete composition.

6.3 Chemical composition of seawater

When this paper was finalised (January 2002) only preliminary results are available on the chemical composition of the seawater. In figure 4 some of the measured chloride contents in the seawater are presented. The different columns represent analysis of the chloride content in water-samples taken at different times.

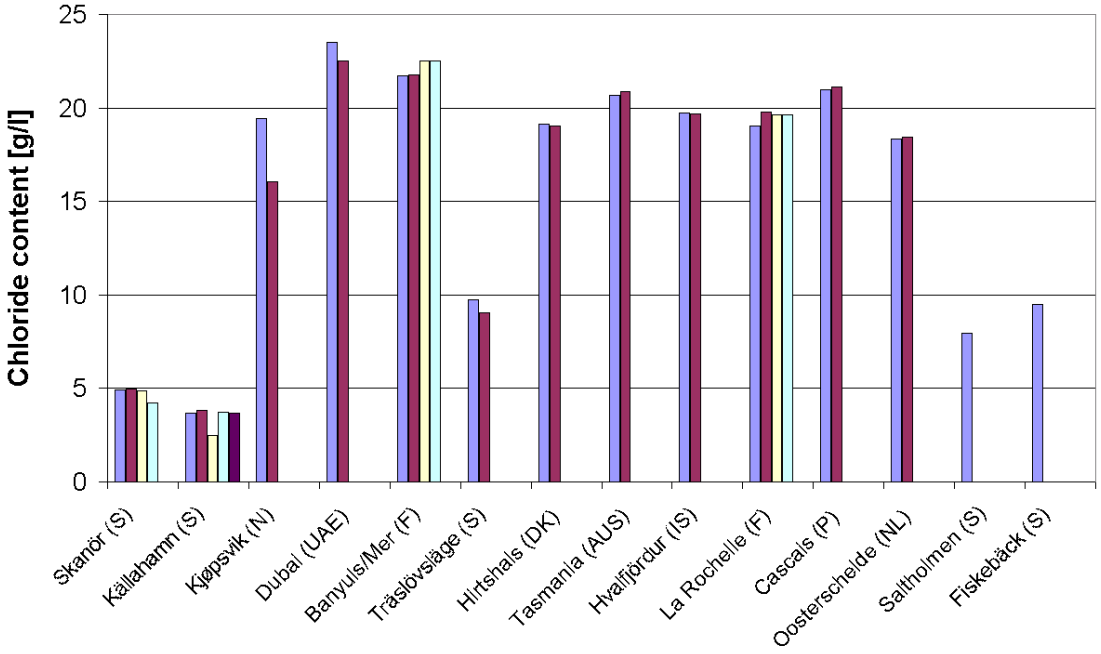

Figure 4 – Measured variations in chloride content at the exposure locations.

However, it should be noticed that there is a relationship between the water-temperature and the salinity[1], see figure 5 (based on data from the submerged exposure location in La Rochelle). Since the water-temperature varies over the year, this means that the measured chloride content only gives a picture of the state at the time for sampling.

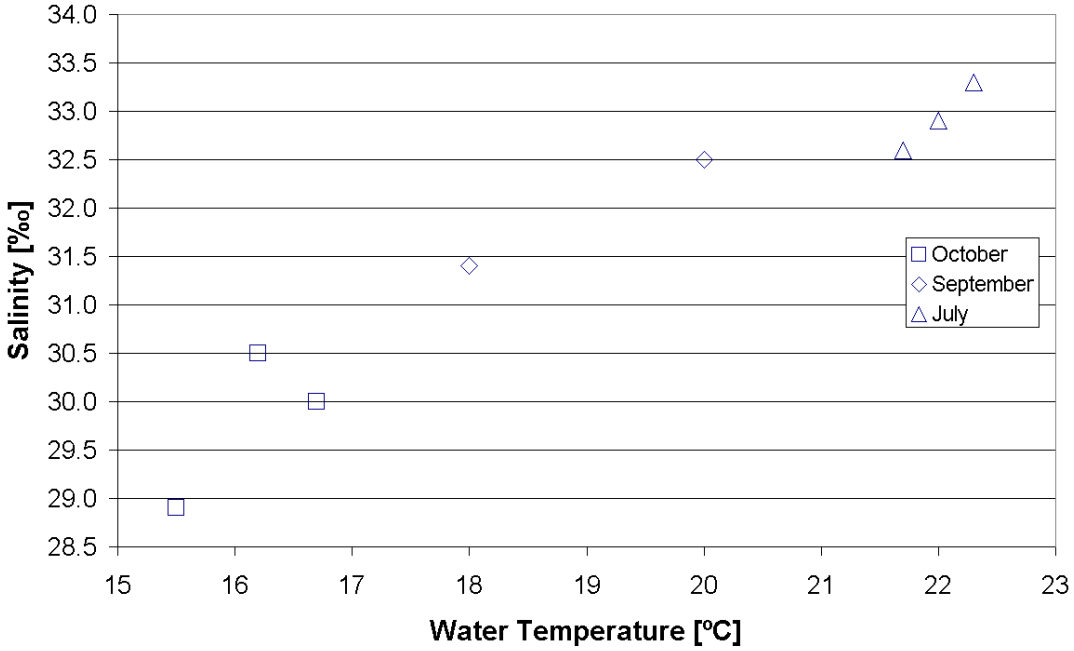

Figure 5 – Example of correlation between the water-temperature and the chloride content in La Rochelle.

[1] The salinity is equal to the total salt-content in the water, i.e. both chlorides and other substances (Na, K etc.)

The results from the analysis of the chemical composition of the seawater are going to be correlated with the measured chloride penetration profiles. This is done to make it possible to predict the chloride penetration with knowledge about the chemical composition of the exposure solution.

7. ACKNOWLEDGES

The author wants to acknowledge the following persons who have made this project possible with their kind help and assistance.

- **Banyuls sur Mer**, France. Dr Antoine Grémare & Laurent Zudaire. Observatoire Oceanologique de Banyuls-sur-Mer, Laboratoire ARAGO, Banyuls sur Mer.
- **Kjøpsvik**, Norway. Anders Bergvik & Erling Kristensen, NORCEM, Kjøpsvik.
- **Cascais**, Portugal. Dr. Arlindo Goncalves, Manuel Vieira & Angela Machado. Laboratório de Engenharia Civil (LNEC), Lissabon.
- **Dubai**, United Arab Emirate. Tor H Sandgren & Odd Moe, Gulf Agency Co., Dubai.
- **Hirtshals**, Denmark. Dr. Dirch Bager, Aalborg Portland, Aalborg.
- **Hvalfjördur**, Iceland. Techn. Lic. Jon Möller, ISTAK, Reykjavik.
- **Källahamn**, Sweden. Erik Mattson, Göteborg.
- **La Rochelle**, France. Prof. Karim Aït-Mokhtar & Dr. Olivier Poupard, Laboratoire d´Etude des Phénomènes de Transfert Appliqués au Bâtiment (LEPTAB), Universite de La Rochelle, La Rochelle.
- **Oosterschelde damm**, Netherlands. Eddie van de Ketterij & Joost Gulikers, Rijkswaterstaat (RWS), Amsterdam.
- **Skanör**, Sweden. Prof. Lars-Olof Nilsson, Department of Building Materials, Chalmers University of Technology, Göteborg.
- **Tasmania**, Australia. Rod McGee, Department of Infrastructure, Hobart Tasmania.

REFERENCES

1. DuraCrete, “General Guidelines for Durability Design and Redesign”, Document BE95-1347/R15, The European Union – Brite EuRam III, Contract BRPR-CT95-0132, Project BE95-1347, CUR, Gouda, 2001.
2. Utgenannt, P., “Field Exposure Site at Highway Rv30. List of specimens and tests up till autumn 1998” (in Swedish), BTB report 12, SP Building Technology, Borås, 1998.
3. Andersen, A., Hjelm, S., Janz, M., Johannesson, B., Pettersson, K., Sandberg, P., Sørensen, H., Tang, L. & Woltze, K., ”Total chloride profiles in uncracked concrete exposed at Träslövsläge marine field station – Raw data from 1992 to 1997”, Report TVBM-7126, Division of Building Materials, Lund Institute of Technology, Lund, 1998.
4. Tang, L., “Chloride penetration profiles and diffusivity in concrete under different exposure conditions”. Publication P-97:3, Department of Building Materials, Chalmers University of Technology, Göteborg, 1997. 53 pp.
5. DuraCrete, “Statistical quantification of the variables in the Limit State Functions”, Document BE95-1347/R9, The European Union – Brite EuRam III, Contract BRPR-CT95-0132, Project BE95-1347, CUR, Gouda, 2000. 130 pp.
6. CEB – Comité Euro International du Béton, “Durable Concrete Structures”, Bulletin 182, Comité Euro-International du Béton (CEB), Lausanne, 1989.
7. Tuuti, K., “Corrosion of steel in concrete”, *fo 4.82*, CBI Research, Stockholm, 1982.
8. AASHTO, “Standard Method of Sampling and Testing for Total Chloride Ion in Concrete and Concrete Raw Materials”, American Association of State Highway and Transportation Officials, Designation: T 260-84, Washington, 1984.
9. Luping, T. & Andersen, A. “Chloride ingress data from five years field exposure in a Swedish marine environment”, *Proceedings*, 2nd International RILEM Workshop on Testing and Modelling the Chloride Ingress into Concrete, Paris, September 2000, 2000, pp. 105-119.
10. Tang, L., “Chloride Transport in Concrete – Measurement and Prediction”. Publication P-96:6, Department of Building Materials, Chalmers University of Technology, Göteborg, 1996. 88 pp.
11. Nilsson, L.-O., Andersen, A., Luping, T. & Utgenannt, P. “Chloride ingress data from field exposure in a Swedish road enviroment”, *Proceedings*, 2nd International RILEM Workshop on Testing and Modelling the Chloride Ingress into Concrete, Paris, September 2000, 2000, pp. 69-83.
12. Map showing exposure locations downloaded from “http://www.lib.utexas.edu/maps/”

The durability of white Portland cement to chloride and sea water attack

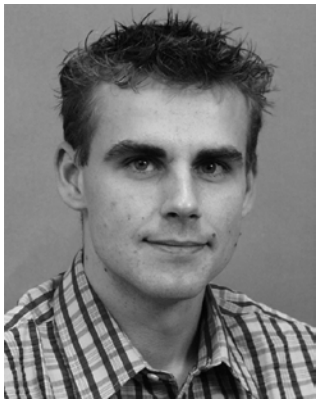

Erik Pram Nielsen
M.Sc., Industrial Ph.D. student
Research and Development Centre, Aalborg Portland A/S
Rørdalsvej 44, P.O. Box 165, DK-9100 Aalborg
E-mail: epn@aalborg-portland.dk

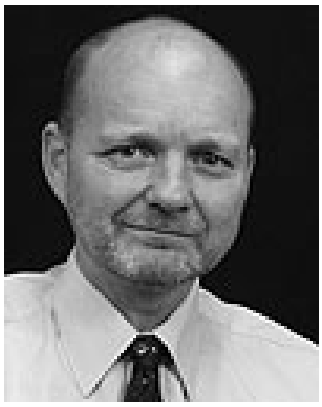

Duncan Herfort
M.Sc., Scientific Manager
Research and Development Centre, Aalborg Portland A/S
Rørdalsvej 44, P.O. Box 165, DK-9100 Aalborg
E-mail: dhe@aalborg-portland.dk

Mette Geiker
M.Sc., Ph.D., Associate Professor
BYG•DTU, Technical University of Denmark
Brovej, Building 118, DK-2800 Kgs. Lyngby
E-mail: mge@byg.dtu.dk

ABSTRACT

A PhD-project is described which is designed to test the hypothesis that white Portland cement significantly improves the durability of concrete to selected types of attack, including chlorides which is the main focus of the study. This hypothesis is mainly based on the premise that white Portland cement results in a lower porosity and permeability than can be achieved with conventional grey Portland cements. In order to test this hypothesis the rate of chloride ingress and sulfate attack over a range of composition is studied, particularly with regard to the aluminate content which plays a major role in binding both chlorides and sulfates.

Key words: white Portland cement, chlorides, durability, phase rule.

1. INTRODUCTION

Durability concerns play a major role in the design of reinforced concrete structures in aggressive environments, for example where de-icing salts are used or in marine environments.

It is generally agreed that when chlorides penetrate into concrete they become partially fixed by the hydrate phases by one or more processes collectively referred to as binding. The mechanisms are still not entirely clear [1] but it is assumed that it is mainly the aluminium-bearing hydration products that react chemically with the chloride ions and form Friedel's salt or solid solutions which include Friedel's salt. Competition for the aluminates by the sulfate and

carbonate ions will affect the capacity of the system to bind chlorides. The very high specific surface area of the C-S-H phase is often believed to substantially contribute to binding through physical absorption, although evidence that it plays little or no role is also convincing [2]. Binding is also influenced by temperature [1].

Some authors have found good agreement between experimental data and theoretical models which assume that the binding of chloride ions occurs spontaneously [3], whilst others have measured periods of up to a week before chloride binding in Ordinary Portland Cement pastes reaches equilibrium [4], with the rate of diffusion depending on the experimental conditions in question. Since binding is a key factor in controlling the rate of ingress, this topic is in need of thorough investigation.

Among existing models, a numerical routine developed at Chalmers University [5] predicts the rate of diffusion-based ingress of chloride ions in fully saturated material by taking into account the interaction with other ions in the transport process. The effect of the microstructural development and moisture content on transport is not included in this model.

One of the parameters relevant for service life design and reassessment of concrete structures which has not been fully addressed, is the effect of the degree of saturation and the state of moisture on the ingress of chlorides into reinforced concrete structures. Except in fully submerged parts of marine structures, concrete is rarely completely saturated when exposed to chlorides or other deteriorating agents.

Some empirical models (e.g. [9]), which include the degree of saturation, are available. A theoretical approach was proposed in [6,7], where the diffusion coefficients of ions were calculated by combining the composite theory [3] with Powers' model for the phase composition [8]. A similar approach has recently been proposed, but without distinguishing between the rate of diffusion in the capillary and 'gel' pores [12,13], and without taking into account the microstructural changes due to reactions within the system. Compared to an earlier empirical model, which includes the effect of relative humidity on the rate of diffusion [9], better agreement between experimental and theoretical results have been obtained by [6,7]. The method still needs verification, and further development is needed to improve the model for percolation through the capillary pores, and to increase the field of application for different cement types.

Preliminary investigations at Aalborg Portland predict non-pozzolanic systems based on white Portland cement to have a significantly lower capillary porosity (after all of the cement has reacted) than comparable systems containing grey cement; and assuming that pore distributions and connectivity remain unaffected, to have lower permeability. At equal porosity, the sulfate resistance of white Portland cement from Aalborg Portland is expected to be significantly greater than that of most grey sulfate resisting cements owing to its lower Al_2O_3 content, of only 1.9%. The low alkali content of white Portland cement, which is generally in the region of 0.2 $Na_2O_{,equivalent}$, can be safely assumed to involve lower risks of both alkali aggregate reaction, and delayed ettringite formation from heat curing or excessive heat of hydration.

Areas which could suggest poorer durability of concrete produced from white Portland cement include excessive heat of hydration, since most white Portland cements are rapid hardening, and may facilitate early age cracking, and lower chloride binding due to lower Al_2O_3 contents, particularly of the white Portland cement from Aalborg Portland's plant in Denmark. An obvious solution to this would be to add an Al_2O_3 rich pozzolan such as granulated blast furnace slag which, apart from increasing chloride binding and lowering the heat of hydration, is predicted to further reduce permeability as a result of lower capillary porosities. The effect of silica fume, on the other hand, is less clear. Although it clearly reduces capillary porosity, its

effect on chloride binding is open to debate. According to models which rely solely on the binding of the aluminate bearing hydrate phases [10], silica fume should have no effect despite several reports to the contrary such as in [11]. Our explanation for silica fume's apparent effect is that, at levels of replacement sufficiently high for all portlandite to be exhausted, higher ratios of Si/Ca result in the C-S-H phase which can then accommodate higher levels of alkali by adsorption. This in turn results in lower concentrations of both alkalis and chloride in the pore solution.

2. MODELS

The aim of the project is to develop a model for diffusion based ingress of chloride ions in presence of sulfate, carbonate and alkali ions to be used for service life prediction. Different degrees of saturation are to be included to the model. The service life prediction model will result from the combination of two separate models, i.e. phase equilibria and ingress, as described below.

2.1 Phase Equilibria and microstructure

The model will be based on the hydrate phase assemblages, and the relative contents of phases within the assemblages, calculated from the chemical composition of the anhydrous cementitious constituents plus water. The calculations will assume thermodynamically stable or metastable equilibrium, and therefore strict observance with the phase rule. As a first approximation, the model will assume invariant assemblages at constant temperature (and pressure), containing the maximum number of phases, i.e. where the number of phases is equal to the number of chemical components.

The relative contents of phases in weight % within the system can be calculated by solving 'n' equations for 'n' unknowns, where 'n' is the number of components and phases. This can be performed on a 'n x n' matrix where the determinant corresponds to the chemical composition of the system and the known chemical compositions of the phases are entered into the matrix. The result can be recalculated to volume % from the phase densities. Account will then be taken of the possibility of solid solution of phases such as Friedel's salt with the other AFm phases, and variable alkali contents, both of which would introduce degrees of freedom which among other things allow variability in the concentration of free chlorides in the pore solution. The above calculations will be used to determine the relative contents of all phases with increasing additions of chlorides, sulfates and alkalis in addition to the theoretical capillary porosity. An attempt will also be made to model the permeability of the cement matrix based on the size and spatial distribution of pores calculated from the distributions of the anhydrous material at different water/cement ratios.

2.2 Kinetic model

In addition to the phase equilibria model kinetic variables responsible for diffusion will also be taken into account. This will primarily involve modelling the relationship between the rate of ingress and porosity, pore size distribution and the extent of physical adsorption, e.g. at the surface of the C-S-H phase. A "multi-species" approach, as the described in [5], will be used for simulating the diffusion of ions within the pore solution.

2.3 Combined model

A combined model will be obtained by combining the phase equilibria and kinetic models to determine the effective diffusion coefficient in the cement matrix, i.e. by combining the intrinsic diffusion coefficients of free chloride ions through the capillary and 'gel' pores, and the distribution of chlorides between the hydrate phases and the pore solution as a function of the mineralogical composition. Finally, the effect of different degrees of saturation will be included towards the end of the project by applying the model proposed in [6,7].

3. EXPERIMENTAL

The experimental procedure designed to test the above models will essentially involve testing of paste specimens covering a range of compositions listed below:

Low-alumina white PC (4.5% C_3A) + GBFS (0, 30%) + SF (0,10,30%)
High-alumina white PC (12%C_3A)
Ordinary PC + GBFS (0, 30%).

The three cements are EN 197-1 CEM I 52.5 N.
The pastes will be prepared at a high water cement ratio to allow rapid reaction before subsequent exposure: water cement ratios of 0.70 and 0.45 are used for microstructure and transport, respectively.

3.1 Paste mineralogy

Once hydration has essentially gone to completion, the paste specimens will be immersed in solutions of $CaCl_2$ and $MgSO_4$ at three different levels of alkali-concentration, over a range of concentrations allowing progressively higher degrees of reaction or binding to take place (i.e. Cl binding isotherms etc.). Once equilibrium is obtained, the mineral phases in the paste will be identified by a combination of EPMA and XRD analysis, whilst the pore solution will be analysed by ICP (Inductively Coupled Plasma Atomic Emission Spectrometry) and AA (Atomic Absorption) for all major components, by analysing the above solutions after removal of the paste specimens. The experimental set-up for the exposure of specimens is shown in fig.1.

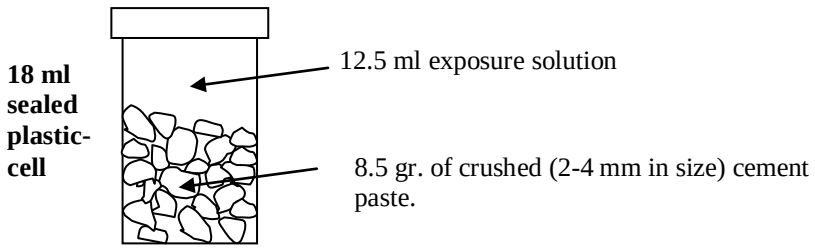

Figure 1: Experimental set-up for the chloride binding-isotherms.

3.2 Paste porosity

The capillary porosity, air content, pore size distribution and water sorption isotherms of pastes with similar compositions will be determined by vacuum- and pressure saturation, low-temperature microcalorimetry and RH-conditioning (RH ranging from 11% to 98%), respectively, at lower water cement ratios than those used above for the mineralogical analysis, i.e. 0.45.

3.3 Ingress of ions

A series of tests on mortars and/or pastes will be performed with the primary goal of verifying the combined model; i.e. by determining rates of ingress, particularly of chlorides, as a function of the two sets of variables, i.e. mineralogy and paste porosity.
The water powder ratio for the samples will be 0.45. Similar procedures will be carried out in order to determine the rate of sulfate diffusion and the phase development, in addition to seawater where the combined diffusion of both chlorides and sulfate are involved.

3.4 In-situ testing

A series of large concrete slabs will be placed in a marine exposure site on the west coast of Jutland to study the performance of the concrete when exposed to real-life conditions and to verify and further develop the service life model. This study will, of course, extend beyond the completion date for the PhD project described here. The concrete compositions chosen will allow the effect of different alumina and silica contents to be studied at the same porosity and the effect of variable porosity to be studied at the same alumina and silica contents.

REFERENCES

1. O.M.Jensen, M.S.H. Korzen, H.J.Jakobsen and J.Skibsted, Influence of Cement Paste Constitution and Temperature on Chloride Binding in Cement Paste. Advances in Concrete Research 12 No.2, April 2000.
2. Lambert, P., Page, C.L. and Short, N.R., Pore solution chemistry of the hydrated system Tricalcium silicate/Sodium chloride/water. Cement and Concrete Research, Vol.15, 1985.
3. O.M.Jensen, Chloride Ingress in Cement Paste and Mortar Measured by Electron Probe Micro Analysis, Dept. of Structural Engineering and Materials, Technical University of Denmark. Series R No. 51, 1999.
4. Tang L. and L.-O.Nilsson, Chloride Binding Capacity and Binding Isotherms of OPC Pastes and Mortars, Cement and Concrete Research, Vol.23, 1993.
5. Olivier Truc, Prediction of Chloride Penetration into Saturated Concrete- Multi-Species Approach. Ph.D thesis at the Department of Building Materials, Chalmers University of Technology, Göteborg, Sweden 2000.
6. E.P.Nielsen, Transport Mechanisms in Cementitious Materials. MSc thesis, BYG·DTU, April 2001.

7. E.P.Nielsen and M.Geiker, Transport of Moisture and Chlorides in partially Saturated Cementitious Material, submitted for publication in Cement and Concrete Research.

8. T.C.Powers and T.L.Brownyard, Studies of physical properties of hardened portland cement paste. Jour. Amer. Concr. Inst., Vol. 43 or Portland Cem. Ass. Bull. No. 22, 1946-47)

9. A.V.Saetta, R.V.Scotta, and R.Vitalini, Analysis of Chloride Diffusion into Partially Saturated Concrete. ACI Materials Journal, Vol.90, M47. Sept-Oct 1993.

10. U.A.Birnin-Yauri and F.P.Glasser, Friedel's salt, Ca2Al(OH)6(Cl,OH).2H2O: Its solid solution and their role in chloride binding, Cement and Concrete Research, Vol.28, No.12, pp.1713-1723, 1998

11. T.Yamato, M.Soeda and Y Emoto, Chemical resistance of concrete containing condensed silica fume. In:Proceedings of the 3rd International Congress on fly ash, silica fume, slag, and natural pozzolans in concrete, Trondheim, 1989. ACI Special publication 114;vol.Iipp.897-913.

12. T.Ishida, An integrated computational system of mass/energy generation, transport and mechanics of materials and structures, PhD thesis, University of Tokyo, 1999 (in Japanese), referred to in [12].

13. K.Maekawa and T.Ishida, Service life evaluation and durability design system for self-compacting concrete. In Proceedings of 2nd International Symposium on self-compacting concrete, Tokyo, 2001. Edt. by K.Ozawa and M.Ouchi.